HOST-PARASITE INTERACTIONS DURING ABOMASAL PARASITISM AND POTENTIAL ROLES FOR ES PRODUCTS

A thesis presented in partial fulfilment
of the requirements for the degree of
DOCTOR OF PHILOSOPHY

at

Massey University,
Palmerston North,
New Zealand

WIEBKE BÜRING

2009

Table of Contents

Abstract

Parasite excretory/secretory (ES) products are believed to play a role in the initiation of the host response to the abomasal parasites *Haemonchus contortus* and *Teladorsagia circumcincta*. Both parasites inhibit and cause loss of the acid-producing parietal cells. Three days after transplantation of adult *T. circumcincta* into parasite-naive sheep, a subpopulation of their parietal cells no longer expressed the proton pump β-subunit, but still stained for Transforming Growth Factor-α, suggesting loss of the proton pump preceded cell death. To investigate the ability of parasites to modify the function of mammalian cells *in vitro*, HeLa, AGS and CaCo-2 cells were exposed to ES products. ES products vacuolated all three cells, causing the development of large numbers of small vacuoles, which differed in appearance from those produced by *Helicobacter pylori* bacterial toxin VacA or ammonia. The vacuoles were unlike those which develop in parietal cells in the parasitised abomasum. Neither lipids nor prostaglandins appeared to play a role in vacuolation and the vacuolating factor *in vitro* is likely to be a protein because of its heat and acid lability. Vacuolation occurred within one hour and was partially reversible. ES products were also able to cause cytoskeletal rearrangement and detachment of HeLa cells, similar processes to those caused by bacterial pathogens, which also disrupt tight junctions in mammalian cells. *H. contortus* ES products also disrupted tight junctions of CaCo-2 cell monolayers, a model cell system used for these studies. The increased epithelial permeability was associated with structural rearrangements of the tight junction proteins occludin and ZO-1. This could explain protein loss and back-diffusion of pepsinogen into the blood, a marker of abomasal parasitism. Cell detachment and disruption of cell-cell adhesion in parasitised sheep may inhibit acid production by parietal cells, which cannot function when separated from adjacent cells. Increased permeability of the surface epithelium would allow parasite ES products to penetrate the mucosal barrier, causing further damage. This could also allow inhibition of parietal cells deeper in the abomasal glands and also allowing adult parasites living in the gastric lumen to modulate host immunity to enhance their survival.

Acknowledgements

Below is a list of persons/institutions (in alphabetical order), who crossed my path during my PhD and to whom I am very grateful, whether it be for inspiring and motivational discussions, administrative support, financial support, or teaching skills beyond the PhD:

Katharina Hillrichs, Van Hoang, Mike Hogan, Peter Jessop, Veronika Kristova, Arturo Luque, Meat and Wool New Zealand, Kevin Pedley, David Simcock, Heather Simpson, Lois Taylor and Lisa Walker.

Special thanks to:

- David Simcock and Katharina Hillrichs for the help with all sheep-related issues, e.g. infections
- Mike Hogan (IVABS, Pathobiology) for euthanasing the sheep
- Lisa Walker and Kevin Pedley for the help with the CaCo-2 cell experiments
- Michelle McGrath (IFNHH, Animal Nutrition and Physiology) for providing the plate reader for the cell proliferation assay
- Leiza Turnbull (IFNHH, Animal Nutrition and Physiology) for freeze-drying samples
- the histopathology lab, especially Pat Davey and Mary Gaddam, for processing tissue and cutting tissue samples

Ethical requirements applicable to this study have been approved as required by Massey University (ethical authorisations: MU 03/139 and 06/117).

Finally, I would like to thank Lars, my family and friends for their continuous support, understanding and love.

List of Figures

List of Tables

List of Abbreviations

#	Number
$[Ca^{2+}]_i$	Intracellular Ca^{2+} concentration
$[cAMP]_i$	Intracellular cAMP concentration
~	Approximately
µg	Microgram
µl	Microlitre
µm	Micrometre
µM	Micromolar
1D	1-dimensional
2D	2-dimensional
3T3	Fibroblasts isolated from mouse embryo
7H6	Tight junction associated antigen
A. caninum	*Ancylostoma caninum*
AA	Aminoacid
Ac	*A. caninum*
ACase	Adenylate cyclase
ACh	Acetylcholine
ADP	Adenosine diphosphate
AEBSF	4-(2-Aminoethyl)-benzenesulfonyl fluoride
AF-6	ALL-1 fusion partner from chromosome 6, also called afadin
AGS	Human gastric adenocarcinoma cell line derived from the stomach
Akt	Serine-threonine protein kinase
Amot	Angiomotin
AP	Adaptor protein
aPKC	Atypical protein kinase C
APR	Aspartic protease
AQ	Aquaporin

AR	Amphiregulin
ASH1	Absent, small, or homeotic-like (Drosophila), transcription factor
ASIP	Atypical PKC isotype specific interacting protein
ATP	Adenosin triphosphate
ATPase	Enzyme that can bind and hydrolyse ATP to ADP and P_i
B. malayi	*Brugia malayi*
Bcl	B cell lymphoma
biotin-XX	Biotinylated
BN-PAGE	Blue native-polyacrylamide gel electrophoresis
BSA	Bovine serum albumin
BSL	*Bandieraea simplicifolia* lectin
C1q	Complement component 1, subcomponent q
Ca^{2+}	Calcium ion
$CaCl_2$	Calcium chloride
CaCo-2	Human epithelial colonic adenocarcinoma cell line
CagA	*H. pylori* virulence factor encoded by cytotoxin-associated gene A
CaM	Calmodulin
CAM	Cell adhesion molecule
CaMK	Calmodulin kinase
cAMP	Adenosine 3', 5'-cyclic monophosphate
CAR	Coxsackie virus and adenovirus receptor
CaSR	Calcium-sensing receptor
CBL	Cathepsin B-like cystein protease
CCK	Cholecystokinin
CCK_B	Cholecystokinin B/gastrin receptor
CD95	Cluster of differentiation, added numbers are standing for distinct Antigens, death receptor, also called Fas, TNF receptor superfamily, member 6
Cdc42	Cell division cycle 42, small GTPase, belonging to the subfamiliy of Rho GTPases, superfamily Ras GTPases
cDNA	Complementary DNA
CEM	Complete essential medium

CGRP	Calcitonin gene-related peptide
CHO	Chinese hamster ovary epithelial cell line
Cl^-	Chloride ion
cm	Centimetre
cm^2	Square centimetre
CMC	Critical micelle concentration
Conc.	Concentration
CO_2	Carbon dioxide
CP	Cysteine protease
CRP	C-reactive protein
Ct	Control
d	Day
D. pteronyssinus	*Dermatophagoides pteronyssinus*
D10	DMEM medium with 10% FBS
DAG	Diacylglycerol
DBA	*Dolichos biflorus* agglutinin (horse gram)
Der p 1	Allergen 1 from *D. pteronyssinus*
DLG	Discs-large protein in *Drosophila*
DMEM	Dulbecco's modified eagle medium
DMSO	Dimethyl sulfoxide
DNA	Desoxyribonucleinacid
E. caproni	*Echinostoma caproni*
E. coli	*Escherichia coli*
E. histolytica	*Entamoeba histolytica*
e.p.g.	Eggs per gram
EC	Enterochromaffin
E-cadherin	Cadherin in epithelial cells
ECL	Enterochromaffin-like
ECL1	Extracellular loop 1 of claudin
EDTA	Ethylenediaminetetraacetic acid
EEA1	Early endosome antigen 1
EGF	Epidermal growth factor

ERK	Extracellular signal-regulated protein kinase
ES	Excretory/Secretory (products)
ESAM	Endothelial cell selective adhesion molecule
EVOM	Epithelial volt-ohm meter
F. hepatica	*Fasciola hepatica*
F12-Hams	Originally developed to support growth of several clones of Chinese hamster ovary (CHO) cells
F-actin	Filamentous actin, filaments can be dissociated in their globular subunits (G-Actin)
FAK	Focal adhesion kinase
Fas	Death receptor, also called CD95, TNF receptor superfamily, member 6
FBS	Fetal bovine serum
FEC	Faecal egg count
g	Gram
g	Gravitational force
G protein	Guanine nucleotide binding protein
GAP	GTPase activating proteins
Gd^{3+}	Gadolinium ion
GDH	Glutamate dehydrogenase
GEF	Guanine nucleotide exchange factor
GEF-H1	Guanine nucleotide exchange factor H1
Gi	Guanine nucleotide binding protein, inhibitory
GIP	Gastric inhibitory peptide
Gq	Guanine nucleotide binding protein, q polypeptide, regulating PLC
GRP	Gastrin-releasing peptide
Gs	Guanine nucleotide binding protein, stimulatory
GTP	Guanosine triphosphate
GTPase	Enzyme that can bind and hydrolyse GTP to GDP (guanosine diphosphate) and P_i (inorganic phosphate)
h	Hour
H&E	Hematoxylin and eosin
H. contortus	*Haemonchus contortus*

H. pylori	*Helicobacter pylori*
H.c.	*Haemonchus contortus* infected
H^+	Hydrogen ion/proton
H^+/K^+-ATPase	Hydrogen/Potassium-ATPase, proton pump
H11	Hidden antigen of *H. contortus*
H_2/H_3	Histamine receptor
H_2CO_3	Carbonic acid
H_2O	Water
Hb	Hemoglobin
HB-EGF	Heparin binding-epidermal growth factor-like growth factor
HBSS	Hank's balanced salt solution
HCl	Hydrochloric acid
HCO_3^-	Hydrogen carbonate/bicarbonate ion
HDC	Histidine decarboxylase
HeLa cells	Derived from Henrietta Lacks, cell line of her cervical cancer
Hep2 cells	Originally thought to be derived from human epidermoid larynx carcinoma but actually derived via HeLa cell contamination
HES5	Hairy and enhancer-of-split homologue, basic helix-loop-helix protein
H-gal-GP	*Haemonchus* galactose-containing glycoprotein complex
HGF	Hepatocyte growth factor
HAT29-D4	Human colon adenocarcinoma cell line HAT 29, D4 is a clonal cell line of these
IEC-6	Epithelilal cell line from newborn rat intestine
IFN-γ	Interferon-γ
Ig	Immunglobuline
IgA1 protease	Secreted protease from *Neisseria gonorrhoeae* which inactivates human IgA1
IGF	Insulin-like growth factor
IgG_1	Immunglobulin G subclass 1
IL	Interleukin
ILK	Integrin linked kinase
INT407	Intestinal epithelial cell line from human embryo

IP_3	Inositol 1,4,5-triphosphate
IPEC-1	Intestinal epithelial cell line from neonatal piglet
IRD-98	Epithelial cell line from rat fetus intestine
I$\varkappa$B	Inhibitor of NF$\varkappa$B
JAM	Junctional adhesion molecule
JEAP	Junction enriched and associated protein, Angiomotin-like protein 1
K^+	Potassium ion
KCL	Potassium chloride
kDa	Kilodalton
kg	Kilogram
KGF	Keratinocyte growth factor
KH_2PO_4	Potassium dihydrogen phosphate
l	Litre
$L/L_1/L_3/L_4$	Larva/first stage larva/third stage larva/fourth stage larva
LAMP1	Lysosome-associated membrane protein 1
Lasp-1	Includes a LIM domain (*Lin*11, *Isl*-1, and *Mec*-3) in the NH_2-terminal region followed by two actin-binding repeats (R1, R2), and an Src homology 3 (SH3) domain in the COOH-terminal region
LEA	*Lycopersicon esculentum* agglutinin
LIM	Domain including *Lin*11, *Isl*-1, and *Mec*-3
M	Molar
M_3	Muscarinic acetylcholine receptor
MAGI	Membrane-associated guanyl kinase inverted proteins
MAPK	Mitogen-activated protein kinase
MASCOT	MAGI-associated coiled-coil tight junction protein, Angiomotin-like protein 2
max.	Maximum
MDCK	Madin-Darby canine kidney epithelial cell line
MEM	Minimum essential medium
MEP	Metalloprotease
mg	Milligram
Mg^{2+}	Magnesium ion

MIDAS	Metal ion dependent adhesion site
min	Minute
ml	Millilitre
MLC	Myosin light chain
MLCK	Myosin light chain kinase
mM	Millimolar
mm	Millimetre
mm^2	Square millimetre
MMP	Matrix metalloprotease
Mn^{2+}	Manganese ion
m-Numb	Mammalian Numb (notch inhibitor)
mOsM	Milliosmol
mRNA	Messenger ribonucleic acid
MUPP-1	Multi PDZ domain protein 1
MW	Molecular weight
n	Number/quantity
N. americanus	*Necator americanus*
N. brasiliensis	*Nippostrongylus brasiliensis*
Na^+	Sodium ion
Na^+/K^+-ATPase	Sodium/Potassium pump
Na_2HPO_4	Disodium hydrogen orthophosphate
NaCl	Sodium chloride
$NaHCO_3$	Sodium bicarbonate
NaOCl	Sodium hypochlorite
NaOH	Sodiumhydroxide
neg.	Negative
NF$\varkappa$B	Nuclear factor $\varkappa$B
ng	Nanogram
NH_4Cl	Ammonium chloride
nm	Nanometre
No.	Number

Notch	Transmembrane receptor, notch gene discovered in *Drosophila melanogaster* with notches in their wings
NR	Neutral Red
O. leptospicularis	*Ostertagia leptospicularis*
O. ostertagi	*Ostertagia ostertagi*
O. sinensis	*Ovomermis sinensis*
O. volvulus	*Onchocerca volvulus*
OH^-	Hydroxide ion
OMV	Outer membrane vesicles
p	Passage
p	Probability
p.i.	Past infection
p120CAS	p120 catenin isoform
p130CAS	v-Crk (oncogene product of avian sarcoma virus CT10) associated tyrosine kinase substrate
p120ctn	Catenin in adherens junctions
PACAP	Pituitary adenylyl cyclase-activating peptide
PALS-1	Protein associated with Lin-7
PAR	Partitioning defective protein (interacting partner aPKC)
PAR	Protease activated receptor
PATJ	PALS-1 associated tight junction
PBS	Phosphate buffered saline
PC	Parietal cell
PDZ	Binding domain first described in the proteins PSD-95, DLG and ZO-1
PEPI	Parasite pepsinogen-like aspartic protease
PG	Prostaglandin
P_i	Inorganic phosphate
PI3	Phosphatidylinositol 3
PKA	Protein kinase A
PKC	Protein kinase C
PLC	Phospholipase C
PNA	Peanut agglutinin

pos.	Positive
PP	Pancreatic polypeptide
PP2A	Protein phosphatase 2A
Proteinase K	Broad specifity serine protease from *Engyodontium album*, it was called Proteinase K because it is able to digest native keratin
PSD-95	Post-synaptic density protein 95
PSN	Penicillin-Streptomycin-Neomycin
PTEN	Phosphatase and tensin homologue
PYK2	Protein tyrosin kinase 2, FAK homologue
PYY	Peptide YY
Rab	Rab family of small G proteins, role in vesicular transport
Rac	Ras-related C3 botulinum toxin substrate, small GTPase, belonging to the subfamiliy of Rho GTPases, superfamily Ras GTPases
Rap	Small GTPase, belonging to the superfamily of Ras GTP
Ras	Small GTPases, from rat sarcoma
RCA	*Ricinus communis* agglutinin
Reg	Regenerating gene product
Rf	Retention factor
Rho	Ras homologue gene family
RhoA	Ras homologue gene family, member A, small GTPase, belonging to the subfamiliy of Rho GTPases, superfamily Ras GTPases
RIC	Epithelial cell line from adult rabbit intestine
Rich-1	Cdc42 GAP
RNA	Ribonucleic acid
rpm	Rounds per minute
RPTPβ	Receptor protein tyrosine phosphatase beta
RT	Room temperature
s	Second
S. mansoni	*Schistosoma mansoni*
Sat	Secreted auototransporter toxin
SBA	Soybean agglutinin
SDS	Sodium dodecylsulfate

SDS-PAGE	Sodium dodecylsulfate-polyacrylamide gel electrophoresis
Serpin	Serine protease inhibitor
SH	Sheath
SH3	Src homology region 3
SMC	Surface mucous cell
SNARE	Soluble N-ethylmaleimide-sensitive factor attachment protein
SOD	Superoxide dismutase
SPATE	Serine protease autotransporters of *Enterobacteriaceae*
spp.	Species pluralis
SS	Somatostatin
SS2	Somatostatin receptor
STA	*Solanum tuberosum* agglutinin
T. brucei	*Trypanosoma brucei*
T. circumcincta	*Teladorsagia circumcincta*
T. colubriformis	*Trichostrongylus colubriformis*
T. cruzi	*Trypanosoma cruzi*
T. muris	*Trichuris muris*
T. spiralis	*Trichinella spiralis*
T. suis	*Trichuris suis*
T. vitrinus	*Trichostrongylus vitrinus*
T75	Tissue/cell culture flask 75cm^2
TEER	Transepithelial resistance
TEMED	N,N,N',N'-Tetramethylethylenediamine
TFF	Trefoil factor
TGF	Transforming growth factor
Tiam-1	T-lymphoma invasion and metastasis, Rac specific GEF
TJ	Tight junction
TLC	Thin-layer chromatography
TNF	Tumor necrosis factor
tPA	Tissue type plasminogen activator
tSNARE	SNARE protein on the target membrane
Tuba	Cdc42 specific GEF

Tyr	Tyrosine
UEA	*Ulex europaeus* agglutinin (gorse)
uPA	Urokinase plasminogen activator
UV	Ultraviolet
V	Volt
v/v	Volume per volume
VacA	Vacuolating cytotoxin from *H. pylori*
VAMP	Vesicle-associated membrane protein
VASP	Vasodilator stimulated phosphoprotein
Vero cells	Kidney epithelial cells from African green monkey, Vero derived from "Verda Reno", meaning "green" and "kidney" in esperanto
VIP	Vasoactive intestinal peptide
VMAT-2	Vesicular monoamine transporter of subtype 2
vSNARE	SNARE protein on the vesicle membrane
V-type ATPase	Vacuolar-type ATPase
w/v	Weight per volume
Yes	Tyrosine kinase
ZAK	Sterile alpha motif and leucine zipper containing kinase AZK, which is also known as ZAK
ZO	Zonula occludens
ZONAB	ZO-1 associated nucleic acid binding protein
Ω	Ohm, SI unit for electric resistance

Introduction

Infections with gastrointestinal nematodes, particularly trichostrongylids, in domestic ruminants are an important economic burden worldwide (Holmes, 1985; Fox, 1997; Miller and Horohov, 2006). A major factor in the pathogenesis of abomasal parasitism of sheep (McLeay *et al.*, 1973; Anderson *et al.*, 1976) and cattle (Fox *et al.*, 1989a; b) is a depression in voluntary food intake (anorexia) that leads to decreased weight gain (Holmes, 1985; 1993; Parkins and Holmes, 1989) as well as diarrhoea, malabsorption (Koski and Scott, 2001) and increased protein loss due to a more permeable epithelium, which all in turn increases susceptibility to infection (van Houtert and Sykes, 1996; Scrimshaw and SanGiovanni, 1997). In particular, infections with the blood-feeding nematode *Haemonchus contortus* are concerning, as they additionally cause considerable anaemia in infected animals (Parkins and Holmes, 1989). Adding to the production loss are costs for anthelmintics, veterinary care and death of infected animals. Around 29% of the animal health market are anti-parasitic drugs, worth US$5.2 billion in 2007 (International Federation for Animal Health, 2007).

Parasite control relies on anthelmintic treatment, although alternative strategies also exist to cope with increasing anthelmintic resistance, including grazing management, breeding management, nutrition supplementation, use of plants containing natural antheltmintics and vaccine development (Coop and Kyriazakis, 1999; Newton and Munn, 1999; Koski and Scott, 2001; 2003; Bakker *et al.*, 2004; Miller and Horohov, 2006; Pomroy and Adlington, 2006). Anthelmintic resistance is widespread, even multiple drug resistant parasites have been reported worldwide (Kaplan, 2004; Wolstenholme *et al.*, 2004; von Samson-Himmelstjerna, 2006; Kaminski *et al.*, 2009). Although a new class of anthelmintics has been recently discovered and monepantel as the first component was launched earlier this year (Kaminski *et al.*, 2008; 2009), there is still need for the improvement of already existing alternative strategies and the development of new ones.

An alternative control method would be an antiparasitic vaccine. Attention has focused on using antigens present in the excretory/secretory (ES) products, as these are often recognised by immune animals (Schallig and Leeuwen, 1997; Schallig *et al.*, 1997; Bakker *et al.*, 2004) and may also be a source of ongoing antigenic stimulation to maintain immunity. ES products contain numerous proteins and glycoproteins with functions including depression of host immunity and probably also in initiating the host immune response and pathology.

The role of parasite ES products in abomasal pathophysiology and histopathology has been previously examined (Rhoads and Fetterer, 1996; Scott and McKellar, 1998; Lawton *et al.*, 2002; Merkelbach *et al.*, 2002; Haag *et al.*, 2005; Huber *et al.*, 2005; Przemeck *et al.*, 2005), but it is still unclear whether ES products act at least in part directly on abomasal cells or also indirectly through the inflammatory response. The aim of this study was to further investigate the host-parasite interactions with the main focus on the role of ES products. Particular interest was on the effects on parietal cells leading to impaired acid secretion. Tissue samples of infected and control animals were used as well as different cell lines as model systems.

Chapter 1

LITERATURE REVIEW

1.1 Parasitic Abomasal Nematodes of Sheep

The abomasal nematodes *Haemonchus contortus* and *Teladorsagia circumcincta* (previously *Ostertagia circumcincta*) are members of the subfamilies Haemonchinae and Ostertagiinae, respectively, which belong to the family Trichostrongylidae, superfamily Trichostrongyloidea, order Strongylida, (Anderson, 2000). The superfamily was initially classified on the basis of morphology (Durette-Desset *et al.*, 1999), which may vary within a species with experimental conditions (Suarez *et al.*, 1995), but this has not always been consistent with results obtained from molecular markers (Lichtenfels *et al.*, 1997; Chilton *et al.*, 2006) and interbreeding experiments (Suarez and Cabaret, 1992).

The superfamily contains many parasites of the gastrointestinal tract, as well as other organs, of a broad range of hosts, including all terrestrial vertebrates. Trichostrongyloidea are an extremely diverse group of parasites of mammals, especially bats, rodents and ruminants. Their buccal capsule is usually reduced in size and lips and corona radiata (a series of leaf-like structures of the labial region) are rudimentary or absent. For blood

Facing page 2

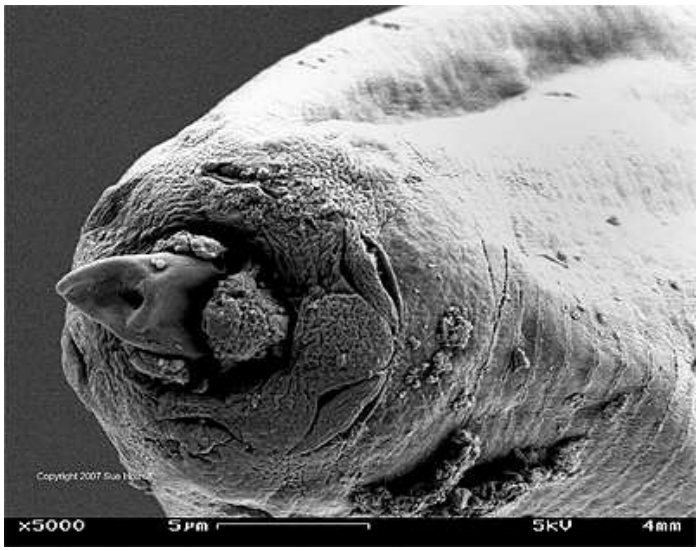

Figure 1.1: Anterior morphology of *H. contortus*. The scanning electron micrograph shows the dorsal lancet. (Kaplan, 2008)

Figure 1.2: Adult *H. contortus* - female. Note the barber's pole appearance (white ovaries/red intestine).

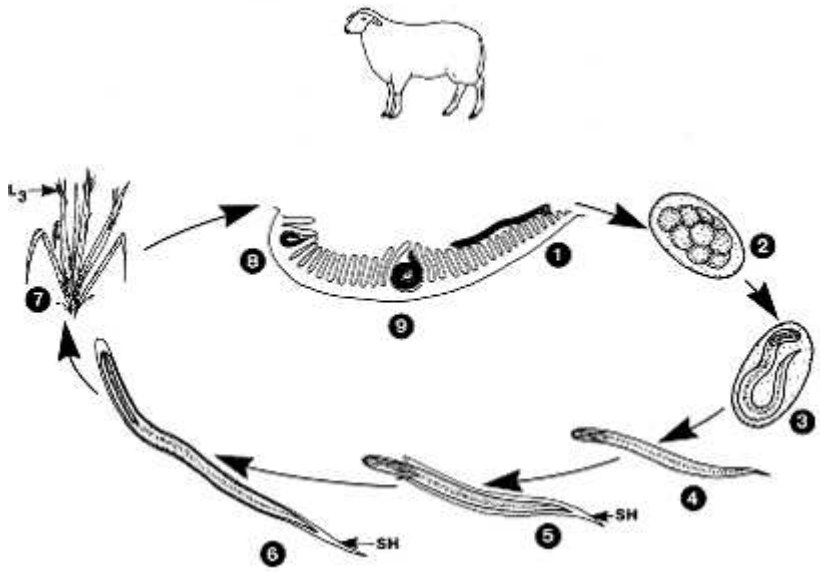

Figure 1.3: Generalised life cycle of Trichostrongylidae. **1** Adults live in the lumen of the abomasum, **2** eggs are passed in the faeces of the host, **3-7** development of larvae (L) in the external environment. **8-9** L_3 of *Haemonchus* and *Teladorsagia* are ingested by the host following parasitism of the abomasum. (modified after Mehlhorn, 2001)

sucking species, such as *H. contortus*, the buccal capsule may be equipped with teeth or a lancet, which allows access to blood after puncturing the abomasal mucosa (Figure 1.1) (Bowman, 2003).

Members of the genus *Haemonchus* parasitise the abomasum of ungulates, including sheep, goats, cattle, bison and deer. *H. contortus* is a blood-sucking parasite, which is commonly called the barber's pole, twisted stomach or wire worm due to the appearance of female worms, in which the white ovaries wind spirally around the red intestine (Figure 1.2). Adult female worms are up to 30mm in length. Male worms are uniformly red and up to 20mm long.

Hosts for the genus *Teladorsagia* include cattle, sheep, goats and holarctic cervidae. *T. circumcincta*, also commonly called the brown stomach worm, is a small parasite of sheep and goats. Adult female worms are usually not longer than 14mm and males 10mm. Molecular studies have shown that *T. circumcincta*, *Teladorsagia davtiana* and *Teladorsagia trifurcata* are all morphs of *T. circumcincta* and not separate species (Stevenson *et al.*, 1996).

1.1.1 Life Cycle of Abomasal Nematodes

A generalised life cycle of Trichostrongylidae is shown in Figure 1.3. Fertilised eggs are passed in the faeces of the host and the embryo inside develops in the external environment to the first stage larva (L_1). After hatching, the L_1 moults to the second and third stage larvae. The third stage (L_3) is the infective stage, which does not feed. This stage retains the surface cuticle of the second stage as the sheath. The nematode cuticle is a critical structure, which acts as a hydroskeleton, maintains postembryonic body shape and permits motility and elasticity. It also represents the first site of contact with the host immune response in parasitic species. The L_3 are ingested by the host and exsheath in the rumen to become the parasitic third stage. Exsheathing is initiated by host gut factors (may include components of the bicarbonate buffer system) followed by secretion of an exsheathing fluid from the parasite (Sommerville, 1957; Rogers and Somerville, 1963; 1968). The exsheathed L_3 migrate to the abomasum, where they invade the gastric glands

Facing page 3

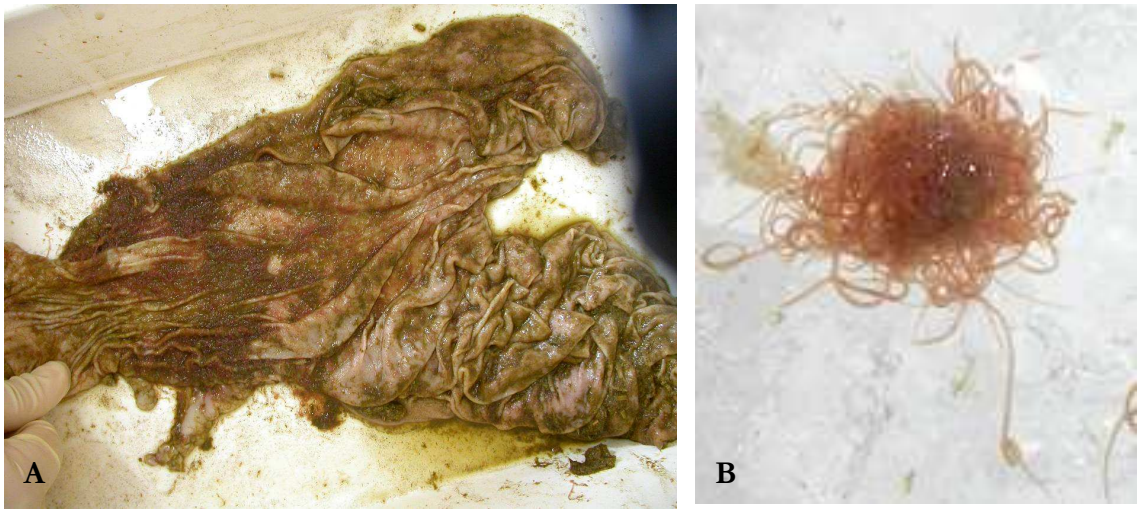

Figure 1.4: Sheep abomasum and adult *H. contortus* 21d p.i. A. Sheep abomasum at d21 of *H. contortus* infection after removal of the abomasal contents with numerous adult worms attached to the mucus, B. Aggregated adult worms removed from the abomasum.

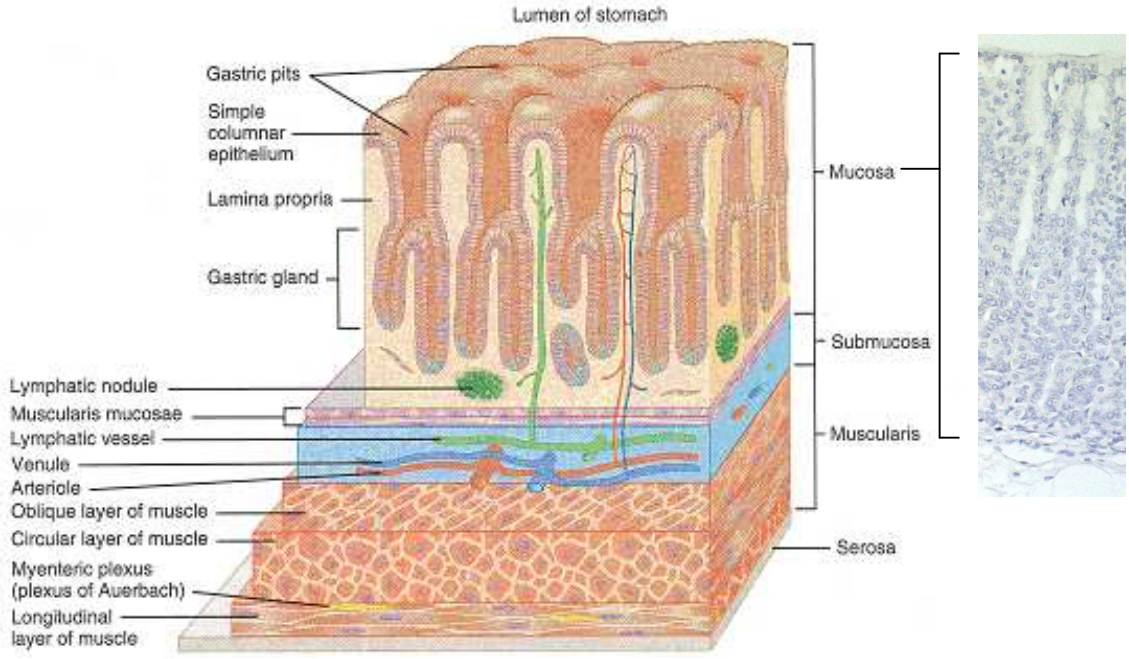

Figure 1.5: Layers of the gastric wall (schematic, human stomach) and tunica mucosa (tissue section, sheep fundus). (human stomach, schematic, Tortora and Grabowski, 1996)

and pits of the fundic and pyloric region. There, the larvae cause nodules and swellings containing one or sometimes more larvae (Sommerville, 1953; 1954). The L_3 moult to L_4 in the glands and, depending on the species and host factors, emerge as L_4 or immature adults. Worms may be found free in the abomasum or in the mucus (Figure 1.4). Generally, *T. circumcincta* emerge into the lumen after development for 5-6 days (Armour *et al.*, 1966; 1981; Anderson *et al.*, 1976; Lawton *et al.*, 1996) and *H. contortus* after 2-4 days (Christie, 1970; Nicholls *et al.*, 1987; 1988; Simpson *et al.*, 1997), although the size of the infective dose (Dunsmore, 1960; Elliott, 1974a, b; Durham and Elliott, 1976), the existing presence of adult worms in the infected abomasum (Michel, 1971) and the immune status of the host (Michel, 1970; Stear *et al.*, 1995) all influence the rate of development of the larvae.

In many trichostrongylids, the phenomenon of arrest or inhibition during development in the definitive host is very common, especially in ruminants (Michel, 1974; Gibbs, 1986). This allows them to survive in the arrested stage without feeding during periods when external conditions, such as winter in temperate regions, are unsuitable for the development, survival and transmission of the larval stages (Anderson *et al.*, 1965; Blitz and Gibbs, 1972a, b; Michel, 1974).

Effects of abomasal parasitism include the disruption of the secretory activity of the abomasum, protein loss across the epithelium and changes in the cell composition of the glands. Pathological changes will be discussed later (1.3) after the structure and function of the abomasum are described (1.2).

1.2 Structure and Function of the Abomasum

The abomasum, the fourth chamber of the ruminant stomach after the fore-stomachs rumen, reticulum and omasum, functions in a similar manner to the monogastric stomach. It can be divided into two distinct areas: the fundus (upper part) characterised by folds and the antrum by rugae. The gastric wall consists of four layers, from the lumen outward: the tunica mucosa, the tella submucosa, the tunica muscularis and the tunica serosa (Figure 1.5). The tunica mucosa is made up of three layers: lamina epithelialis mucosae, the

connective tissue lamina propria mucosae and lamina muscularis mucosae. The lamina propria mucosae contains the densely packed tubular glands that open into pits on the surface of the stomach (Liebich, 1993).

There are two types of glands in the mucosa of the abomasum. The glands of the fundus are the acid producing glands (Hersey and Sachs, 1995) which also secrete pepsinogen (Hirschowitz, 1989; Samloff, 1989), bicarbonate, mucins (Garner *et al.*, 1984) and intrinsic factor (necessary for the absorption of vitamin B_{12}) (McKay and McLeay, 1981; Lorenz and Gordon, 1993). The antrum has pyloric glands which secrete mucus, the hormone gastrin and small amounts of pepsinogen (Walsh, 1988; Dockray and Gregory, 1989).

1.2.1 Pyloric Glands

The pyloric glands in the antrum usually consist of a pit, an isthmus and a gland, although some glands are branched with more than one gland per pit (Lee, 1985). The pits are typically very long, ending in short glands. Pyloric glands contain mostly mucous cells (also called gland cells) which secrete mucus and in addition endocrine cells, mainly G cells, which secrete gastrin (Creutzfeld *et al.*, 1971; Walsh, 1988; Dockray *et al.*, 1996) and the neighbouring D cells which secrete somatostatin (SS) (Larssson *et al.*, 1979; Larsson, 2000). There are also small numbers of serotonin-secreting enterochromaffin (EC) cells, which are located at the base of the glands (Bordi *et al.*, 2000). EC cells are more frequent in the proximal antral mucosa and rare near the pylorus (Bordi *et al.*, 2000). Histamine-secreting mast cells are also present in the antrum (Schubert and Makhlouf, 1996).

1.2.1.1 The G Cell and Gastrin Secretion

G cells are mainly located in the basal part of the glands in sheep, as in other mammals (Kapur, 1982; Černý *et al.*, 1991; Scott *et al.*, 1998b; Bordi *et al.*, 2000). The peptide hormone gastrin is secreted by G cells in the antral glands and to a lesser extent by the duodenum of sheep (Reynolds *et al.*, 1991; Simpson *et al.*, 1993). Gastrin regulates

Facing page 5

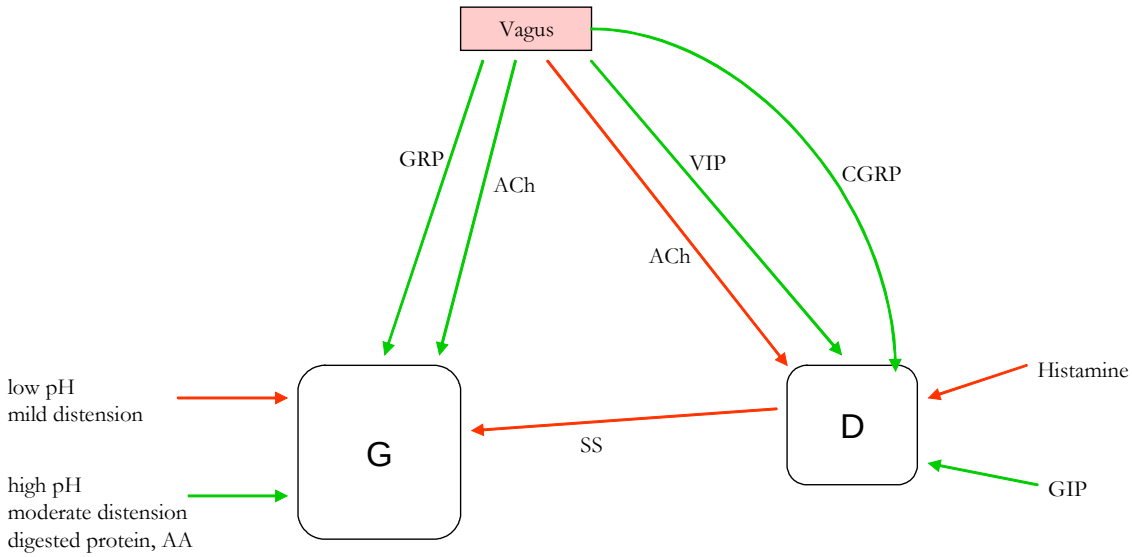

Figure 1.6: Regulation of gastrin secretion. In general, acid feedback plays an important role in regulating gastrin secretion. When the pH is raised, gastrin secretion is increased. The vagus nerve mediates the central nervous control of gastrin secretion, either acting directly on the G cell or by modulating SS secretion from the D cell. Green arrows: stimulation; red arrows: inhibition; AA: aminoacids; GRP: gastrin-releasing peptide; ACh: acetylcholine; VIP: vasoactive intestinal peptide; CGRP: calcitonin gene-related peptide; GIP: gastric inhibitory peptide; SS: somatostatin.

numerous complex cellular functions that include growth, proliferation, apoptosis, migration and secretion (Stepan *et al.*, 2004) (see also 1.2.2.3.3.2 and 1.2.4.3.1).

The mechanisms that regulate gastrin secretion are shown in Figure 1.6. The sight, smell and taste of food increase the secretion of gastrin (Dockray and Tracy, 1980a, b; Hirschowitz and Fong, 1990), as do also moderate gastric distension (Debas *et al.*, 1975; Schiller *et al.*, 1980) and breakdown products of proteins (Richardson *et al.*, 1976; Strunz *et al.*, 1978, Saffouri *et al.*, 1984; Schubert *et al.*, 1992), whereas lowering of the gastric pH (Becker *et al.*, 1973; Saffouri *et al.*, 1984; Konturek *et al.*, 1995) and mild distension (Schubert and Makhlouf, 1993) inhibit gastrin secretion. In general, acid feedback plays the most important role in regulating gastrin secretion. When the pH is raised, gastrin secretion is increased. In sheep, alkalisation of the abomasal contents and restricted once-daily feeding also stimulated gastrin secretion (Reynolds *et al.*, 1991).

The interaction of chemicals and extrinsic and intramural nerves control the secretion of gastrin. Effectors act either directly on the G cell or by modulating secretion of the G cell inhibitor SS from D cells (Larsson *et al.*, 1979; Buchan *et al.*, 1985). *In vitro*, gastrin secretion by ovine antral tissue is also stimulated via muscarinic receptors (Lawton et al, 2000). Schubert *et al.* (1992), Weigert *et al.* (1994) and Zeng *et al.* (1996) have also shown a direct stimulation of the G cell. Alternatively, many studies observed an increased gastrin secretion in response to cholinergic stimulation via the indirect pathway of concentration-dependent SS inhibition (Saffouri *et al.*, 1980; DuVal *et al.*, 1981; Richelsen *et al.*, 1983; Wolfe *et al.*, 1983). The main mediator of cephalic activation of gastrin secretion is the vagus nerve (Dockray and Tracy, 1980a, b; Hirschowitz and Fong, 1990). Vagal stimulation mainly acts on the G cell through direct effects of gastrin-releasing peptide (GRP) (Schubert *et al.*, 1985; Weigert *et al.*, 1993; Debas and Carjaval, 1994), but also via inhibitory cholinergic neurons on the D cell which reduce SS secretion (Debas and Carjaval, 1994). Cholinergic neurons are recruited progressively by increased distension to increase gastrin secretion and reduce SS secretion, whereas vasoactive-intestinal peptide (VIP) neurons, recruited by mild distension of the rat stomach, act to stimulate SS secretion (Schubert and Makhlouf, 1993). SS secretion is also increased through gastric-inhibitory peptide (GIP), a structural analogue of secretin (Wolfe and Reel, 1986). Lawton *et al.* (2000) have shown that these principal neural pathways controlling gastrin and SS secretion are also active in the

Facing page 6

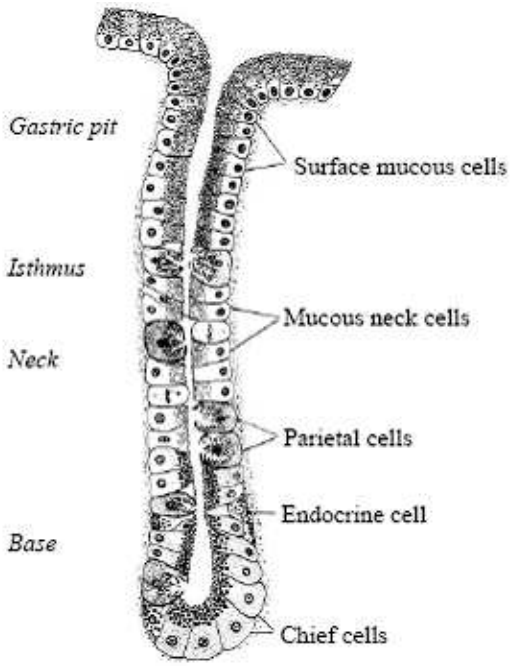

Figure 1.7: Gastric gland of the fundus (schematic). The pit is lined by pit cells/surface mucous cells, the isthmus by immature precursors, the neck by mucous neck cells, and the base by chief cells and endocrine cells. Parietal cells are scattered through the gland. (modified after Boron *et al.*, 1994)

Table 1.1: Activators and inhibitors of pepsinogen secretion.

Activators	Inhibitors
➢ Acetylcholine (Ach) ➢ Cholecystokinin (CCK) ➢ Gastrin ➢ Histamine ➢ Gastrin-releasing peptide (GRP)	➢ Secretin ➢ Vasoactive intestinal peptide (VIP) ➢ Pancreatic polypeptide (PP) ➢ Neuropeptide Y ➢ Gastric inhibitory peptide (GIP) ➢ Peptide YY (PYY) ➢ Somatostatin (SS)

sheep abomasum, but probably play a minor role in comparison with chemically mediated pathways.

1.2.2 Fundic Glands

Fundic glands consist of short pits opening into long glands; occasionally one pit opens into more than one gland. The whole gland is made up of four regions (Figure 1.7): (1) the pit is lined by pit cells/surface mucous cells; (2) the isthmus (containing immature precursor cells); (3) the neck (containing mucous neck cells) and (4) the base (containing zymogenic/chief cells). Parietal cells, also called oxyntic cells (*oxyntos*, to make acid), are scattered through the neck and base (Karam, 1999; Karam *et al.*, 2003). Surface mucous and mucous neck cells secrete mucus, parietal cells produce gastric acid (HCl) and zymogenic cells produce pepsinogen (Karam *et al.*, 2003). Endocrine cells in the fundus include Enterochromaffin-like (ECL) cells (histamine secretion), D cells (SS secretion) and EC cells (serotonin secretion) (Bordi *et al.*, 2000).

1.2.2.1 Zymogenic Cells and Pepsinogen Secretion

Pepsinogen is the inactive precursor (zymogen) of pepsin, an aspartic protease, which degrades protein into peptides. An acidic pH allows the autocatalytic conversion of pepsinogen to pepsin. Pepsinogen is stored as granules in chief cells and mucous neck cells in the ovine fundic epithelium and in the bovine fundus also in surface mucous cells (Yamada *et al.*, 1988; Cybulski and Andren, 1990; Scott *et al.*, 1998c; 1999). After stimulation, pepsinogen is biphasically released into the gland lumen (an initial peak is followed by sustained secretion for a prolonged time) (Hirschowitz *et al.*, 1984; Hersey, 1989). In general, pepsinogen secretion is regulated by agents which stimulate either intracellular levels of adenosine 3', 5'-cyclic monophosphate $[cAMP]_i$ or intracellular calcium $[Ca^{2+}]_i$. The main activators and inhibitors of pepsinogen secretion are shown in Table 1.1.

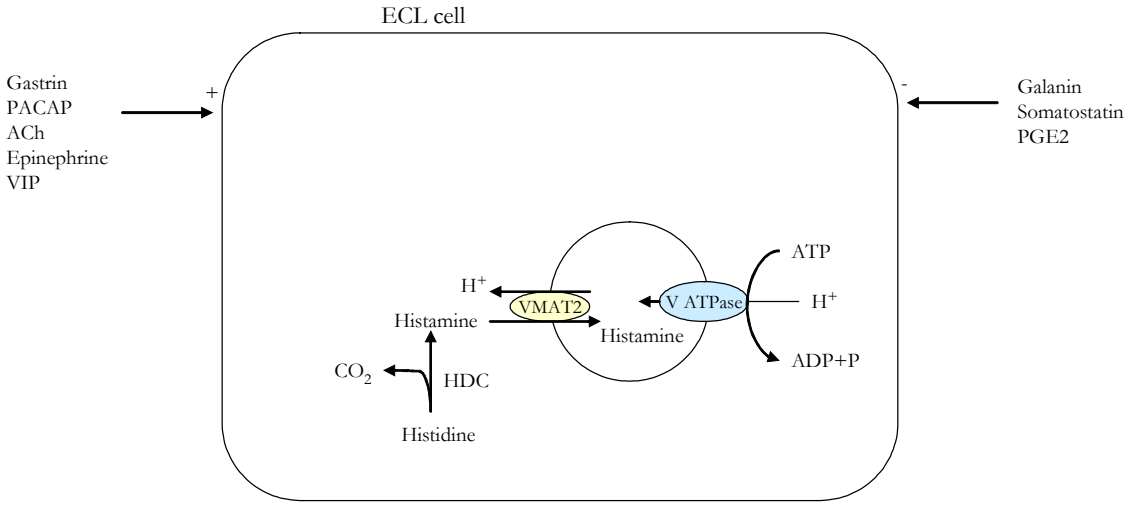

Figure 1.8: Regulation of histamine secretion and scheme of histamine synthesis by the ECL cell. The stimulants (+) and inhibitors (-) of histamine synthesis, storage and secretion, as well as ECL cell proliferation, are shown together with the mechanism of histamine synthesis. Histidine is decarboxylated by HDC and stored in secretory vesicles via V-type ATPase and VMAT-2. ECL cell: enterochromaffin-like cell; PACAP: pituitary adenylyl cyclase-activating peptide; ACh: acetylcholine; VIP: vasoactive intestinal peptide; PGE2: prostaglandin E_2; HDC: histidine decarboxylase; VMAT2: vesicular monoamine transporter; V ATPase: vacuolar-type ATPase.

1.2.2.2 The ECL Cell and Histamine Secretion

The ECL cell, the predominant endocrine cell in the fundus, is typically located in the lower third of the gastric glands (Bordi *et al.*, 2000; Yao and Forte, 2003). ECL cells secrete histamine, the most important stimulant of gastric acid secretion in humans and most animals (Hersey and Sachs, 1995) (see 1.2.2.3.3 and 1.2.2.3.3.1). Histidine is decarboxylated by histidine decarboxylase (HDC) to histamine (Viguera *et al.*, 1994; Dockray *et al.*, 1996), which is stored in secretory vesicles via V (vacuolar)-type ATPases and vesicular monoamine transporters of subtype 2 (VMAT-2) (De Giorgio *et al.*, 1996; Prinz *et al.*, 1999; Watson *et al.*, 2001). Protons are transported across the vesicular membrane by V-type ATPases which acidify the contents of the vesicle (Forgac, 1999; Nishi and Forgac, 2002), leading to concentration of histamine in these compartments by the action of VMAT-2 (Figure 1.8). Exocytosis of histamine follows two patterns: histamine is either immediately released from secretory vesicles after calcium entry (within minutes) or there is a delayed secretion following gastrin-induced *de novo* synthesis via HDC (Prinz *et al.*, 1999).

1.2.2.3 The Parietal Cell and Acid Secretion

Parietal cells are large (~25μm), pyramidal shaped cells (Ito, 1981), but tend to be more round towards the lumen (Karam *et al.*, 1997). Several studies have shown regional morphological differences among parietal cells (Karam *et al.*, 1997). Isthmus and neck parietal cells are young and appear to migrate actively and rapidly towards the base compared to basal parietal cells that are old and less metabolically active. Coulton and Firth (1983) and Karam *et al.* (1997) suggested that the function of parietal cells depends in part on their position along the gland. Parietal cells differ in their acid secretory activity: at the base of the gland parietal cells appear to be less acid producing than in the middle or upper parts (Coulton and Firth, 1983), but may have a different function, such as playing a role in the maintenance of the zymogenic cell population (Karam *et al.*, 1997) (see also 1.2.4.2).

The parietal cell has two distinctive, characteristic membrane systems: (1) a specialised luminal plasma membrane, the intracellular canaliculus, which is lined by numerous microvilli and is the site of gastric acid secretion and (2) an extensive cytoplasmic

Facing page 8

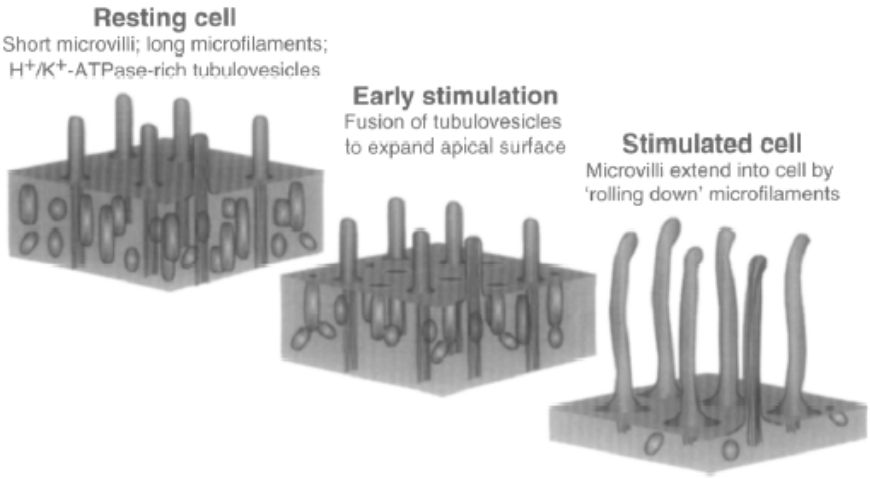

Figure 1.9: Scheme of the transformation of the parietal cell tubulovesicular membrane system into the intracellular canaliculus during acid secretion. The resting parietal cell has short microvilli and long microfilaments sticking into the cytoplasm. The tubulovesicular membrane system contains the H^+/K^+-ATPase. The transformation of the tubuolovesicular membrane system into the membrane of the intracellular canaliculus is shown from left to right. (Forte and Yao, 1996)

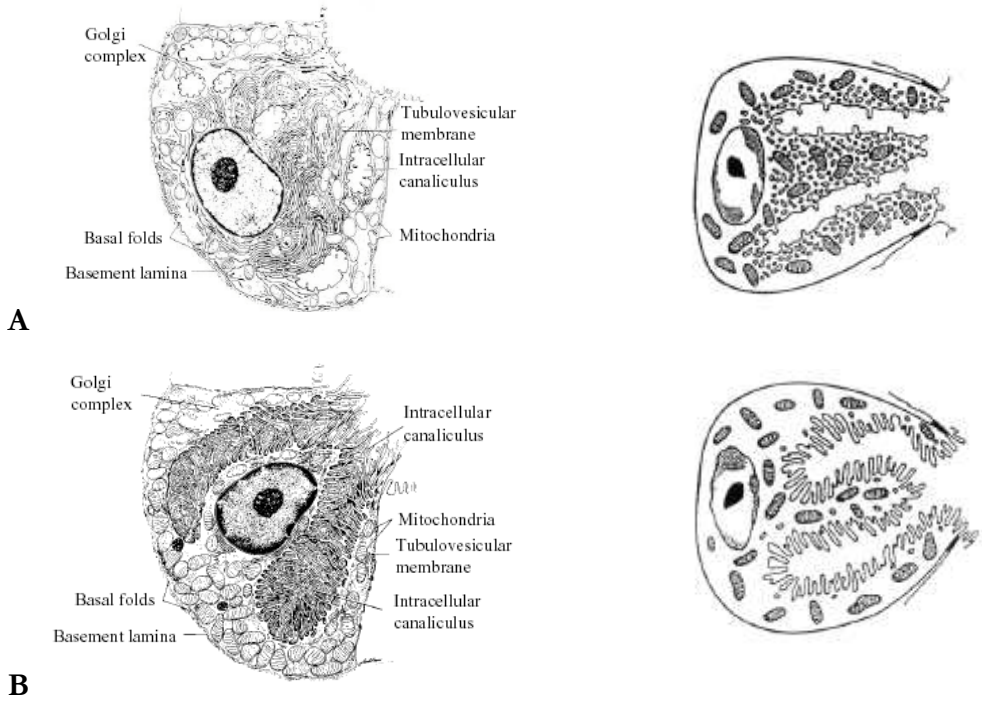

Figure 1.10: The parietal cell at rest and after stimulation (schematic). Drawing and schematic diagram of the unstimulated parietal cell (A.) and stimulated, acid-secreting parietal cell (B.). (left side modified after Boron *et al.*, 1994; right side Forte and Yao, 1996)

tubulovesicular membrane system (Ogata and Yamasaki, 2000). The tubulovesicular membrane system is rich in the gastric proton pump, the H^+/K^+-ATPase, which is responsible for gastric acid production (Ganser and Forte, 1973; Sachs *et al.*, 1976; Forte and Lee, 1977; Urushidani and Forte, 1987; Duman *et al.*, 2002).

The recruitment-recycling hypothesis is the currently accepted model describing acid secretion (Figure 1.9) (Forte and Yao, 1996; Ogata and Yamasaki, 2000). This model suggests that upon stimulation, the tubulovesicular system transforms into the membrane of the intracellular canaliculus. Ogata and Yamasaki (2000) showed connections between these two membrane systems in the resting and stimulated parietal cells and Duman *et al.* (2002) later reported that these connections are not permanent. The H^+/K^+-ATPase is selectively recycled into the tubulovesicular membrane system after inactivation. In the unstimulated parietal cell (Figure 1.10 A), the apical surface contains many short (0.2-0.5μm) microvilli, each with a system of underlying microfilaments (Forte and Yao, 1996). After stimulation (Figure 1.10 B), the intracellular canaliculus/cell surface membrane area increases (usually as elongated microvilli, (Forte and Yao, 1996)) simultaneously with a decrease in the tubulovesicular compartment, translocating the H^+/K^+-ATPase on the intracellular membrane to the apical membrane (Helander and Hirschowitz 1972; 1974; Ito and Schofield, 1974; Forte *et al.*, 1977; Vial *et al.*, 1985; Ito, 1987). Concomitant with the translocation, the permeability to potassium (K^+) and chloride (Cl^-) ions is increased, mainly in response to the rise in intracellular $[cAMP]_i$ (Urushidani and Forte, 1997; Akagi *et al.*, 2001).

In general, parietal cells are rich in mitochondria due to the high energy requirements for the functioning of the H^+/K^+-ATPase. Duman *et al.* (2002) demonstrated that mitochondria form an extensive reticular network with intermembrane connections throughout the cytoplasm, as occurs generally in eukaryotic cells and suggested to allow power transmission or signalling

1.2.2.3.1 H^+/K^+-ATPase, Cl^- Channels and K^+ Channels

Three membrane transporters, H^+/K^+-ATPase, K^+ channel and Cl^- channel, located in the

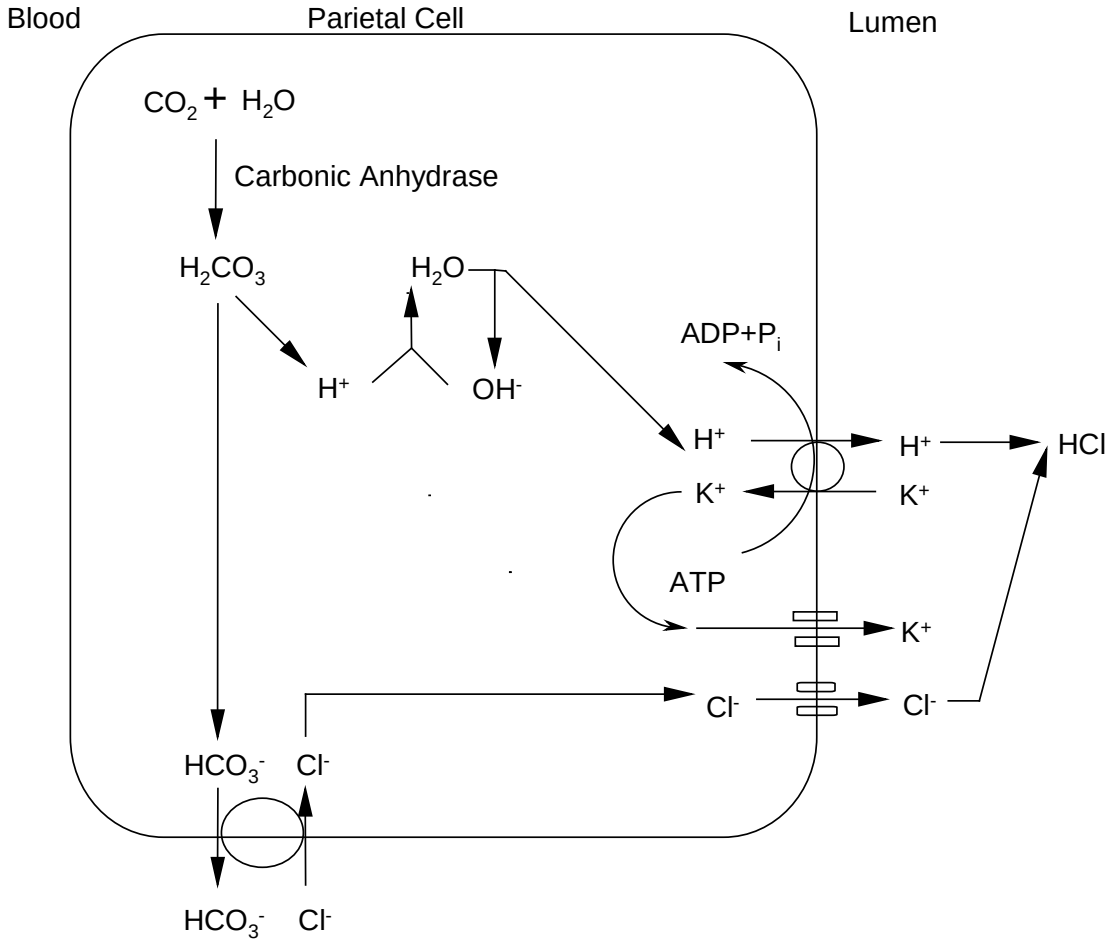

Figure 1.11: Mechanism of acid production by the parietal cell. The reaction catalysed by carbonic anhydrase provides H_2CO_3 that dissociates to HCO_3^- and H^+. Bicarbonate is exchanged for Cl^- and the proton for K^+ through the proton pump. All chemical formulae are in the list of abbreviations.

canalicular membranes, play important roles in gastric acid secretion (Boron *et al.*, 1994). The H^+/K^+-ATPase, which has been identified as the primary gastric proton pump by Ganser and Forte (1973), operates the final step of HCl production (Urushidani and Forte, 1997). This enzyme consists of an α- and β-subunit. The catalytic α-subunit, a multispanning membrane protein with most of its mass located in the cytoplasm (Shull and Lingrel, 1986; Tyagarajan *et al.*, 1996), is responsible for ATP-catalysed exchange of H^+ for K^+ (Thangarajah *et al.*, 2002). The β-subunit, which has a single transmembrane segment and 70% of its mass oriented in the extracellular space (Canfield *et al.*, 1990; Okamoto *et al.*, 1990; Shull, 1990), is highly glycosylated, which may play a protective role for the holoenzyme against acidic and peptic conditions (Chow and Forte, 1995; Thangarajah *et al.*, 2002). The glycosylation of the β-subunit (Klaassen *et al.*, 1997), as well as the three existing disulfide bonds (Chow *et al.*, 1992), influence the enzymatic activity (Thangarajah *et al.*, 2002). Further, the glycosylation is required for proper subunit folding and interaction and/or trafficking through the cell (Asano *et al.*, 2000). Biochemical studies suggest that the cytoskeletal proteins ankyrin and spectrin interact with the H^+/K^+-ATPase in the microsomal fraction of resting parietal cells and appear to relocate with the H^+/K^+-ATPase to the apical membrane of the secreting parietal cells (Smith *et al.*, 1993). It has been speculated that ankyrin and spectrin form a functional complex to stabilise H^+/K^+-ATPase at the apical membrane upon stimulation, but it is not clear if these proteins directly bind to H^+/K^+-ATPase or how this is regulated (Yao and Forte, 2003).

The K^+ channels mediate the efflux (recycling) of K^+ across the canalicular membrane, thereby providing sufficient luminal K^+ to support the action of the H^+/K^+-ATPase (Forte and Wolosin, 1987). The Cl^- channels mediate the efflux of Cl^- (Reenstra and Forte, 1990). Together, these three components allow the secretion of HCl from the cytoplasm into the lumen of the gastric gland (Boron *et al.*, 1994).

1.2.2.3.2 Mechanism of Acid Production

The mechanism of acid production is shown in Figure 1.11. Cytosolic carbonic anhydrase catalyses the reaction of water (H_2O) and carbon dioxide (CO_2) to hydrogen ion/proton (H^+) and hydrogen carbonate/bicarbonate ion (HCO^-_3) (Flemstrom, 1994). Dissociation of carbonic acid (H_2CO_3) provides the H^+ for the H^+/K^+-ATPase and the HCO_3^- is

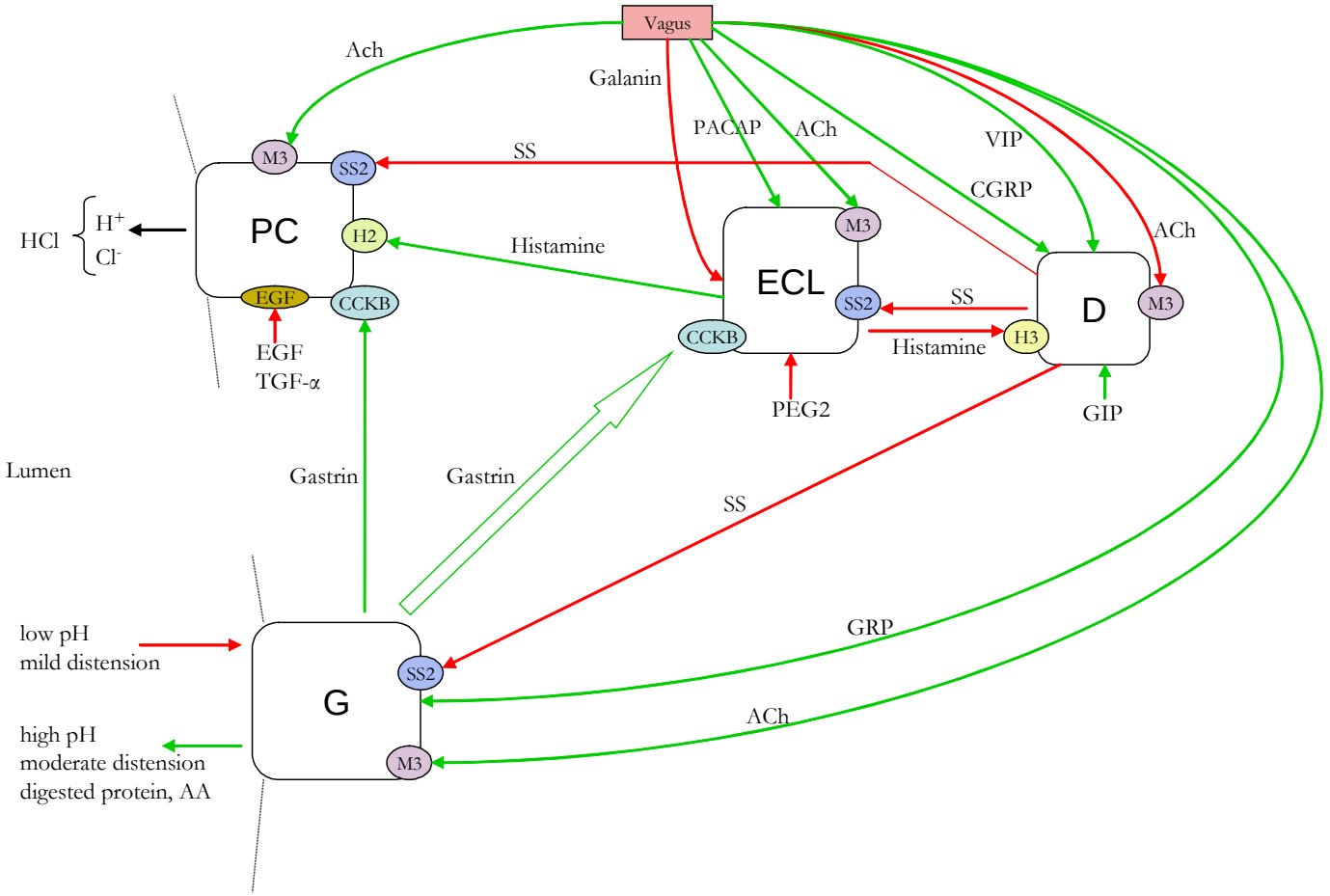

Figure 1.12: Overview of the principal pathways involved in the regulation of acid secretion. The factors that are involved in regulating acid secretion are shown, including gastrin regulating factors. Green arrows: stimulation; red arrows: inhibition. All abbreviations are in the list of abbreviations.

Facing page 10

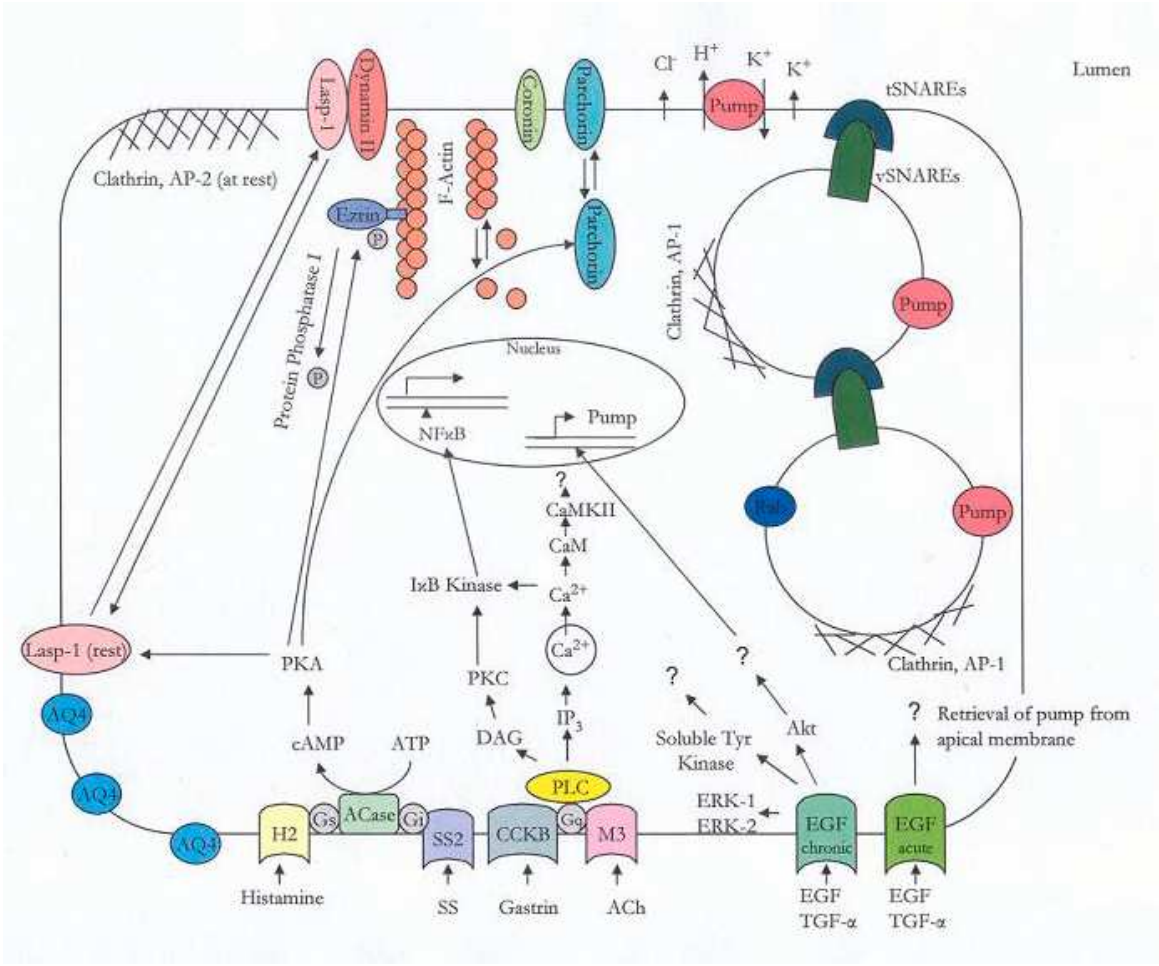

Figure 1.13: Intracellular pathways involved in acid secretion by parietal cells. The intracellular pathways in the parietal cell that finally lead to the secretion of gastric acid are shown, including receptors (H_2, M_3, CCK_B, SS_2, EGF), downstream effectors (Acase, PKA, PKC, PLC) and proteins involved in vesicular trafficking and cytoskeletal proteins (e.g. Rab, SNARE, clathrin, dynamin, coronin, F-actin). All abbreviations are in the list of abbreviations. (modified after Urushidani and Forte, 1997)

exchanged for a Cl^-, which is required for secretion of HCl across the apical membrane (Paradiso *et al.*, 1989; Flemstrom, 1994). The Cl^-/HCO_3^- exchange takes place on the basolateral membrane of the parietal cell; HCO_3^- is released into the extracellular fluid and diffuses into the blood causing a slight elevation of blood pH, a process which serves to maintain intracellular pH in the parietal cell (Hersey and Sachs, 1995). Basolateral Cl^-/HCO_3^- exchange in the parietal cell, as well as in mucous cells, is mediated by anion exchanger 2 (Cox *et al.*, 1996; Wang *et al.*, 1996; Jons and Drenckhahn, 1998; Rossmann *et al.*, 2001). K^+ and Cl^- diffuse via their channels into the canaliculi. H^+ are pumped out of the cell into the canaliculi in exchange for K^+ via the H^+/K^+-ATPase (Thangarajah *et al.*, 2002). Aquaporin 4 (AQ4) has been implicated in water transport from the interstitial fluid to the intracellular milieu to maintain cellular osmolarity and volume during acid secretion (Fujita *et al.*, 1999), although others have shown normal gastric function in AQ4 knockout mice (Wang *et al.*, 2000a).

1.2.2.3.3 Regulation of Acid Secretion

Acid production by parietal cells is stimulated and inhibited via paracrine, endocrine and neural pathways (Yao and Forte, 2003). An overview of the general pathways in the regulation of acid secretion is shown in Figure 1.12 and the intracellular pathways in parietal cells in Figure 1.13. The three main activating receptors on the basolateral membrane are (1) histamine H_2, (2) muscarinic acetylcholine M_3 and (3) gastrin/cholecystokinin CCK_B. The release of histamine mediates much of the action of gastrin, as gastrin is also a stimulant of the ECL cell (Urushidani and Forte, 1997). Stimulation of acid secretion typically involves an initial elevation of parietal cell $[Ca^{2+}]_i$ and/or $[cAMP]_i$, followed by activation of a cAMP-dependent protein kinase cascade (including protein kinase A (PKA)), protein kinase C (PKC), Ca^{2+}-calmodulin (CaM) kinase II, phophatidyinositol 3 (PI3) kinase and several other downstream kinases, which trigger the translocation and insertion of the H^+/K^+-ATPase into the apical plasma membrane targeting motif. The stimulation-mediated translocation of the H^+/K^+-ATPase from the cytoplasmic membrane compartment to the apical plasma membrane is mediated by a soluble *N*-ethylmaleimide-sensitive factor attachment protein (SNARE) protein complex and its regulatory proteins (Yao and Forte, 2003).

1.2.2.3.3.1 Histamine H_2 Receptors

Histamine plays a major role in the activation of acid secretion. The H_2 receptor couples to stimulatory G proteins (Gs; G protein: guanine nucleotide binding protein) to activate adenylate cyclase (ACase), which produces cAMP (Figure 1.13). Then, cAMP leads to the activation of the cAMP-dependent PKA (Urushidani and Forte, 1997). Activation of PKA initiates a cascade of phosphorylation events through the activation of other downstream effectors, including myosin light chain kinase (MLCK) (Akagi *et al.*, 2001), ezrin (Hanzel *et al.*, 1989; 1991; Okamoto and Forte, 2001), parchorin (Nishizawa *et al.*, 2000; Mizukawa *et al.*, 2002) and lasp-1(LIM and SH3 domain-containing protein-1) (Chew and Brown, 1987; Chew *et al.*, 2000).

The cytoskeletal-associated protein ezrin may integrate signalling pathways leading to the remodelling of the actin cytoskeleton (Hanzel *et al.*, 1989; 1991; Okamoto and Forte, 2001). Parchorin is a chloride intracellular channel recently implicated in Cl^- and water transport (Nishizawa *et al.*, 2000; Mizukawa *et al.*, 2002). Endogenous parietal cell parchorin is present in the cytosol and relocates to the apical plasma membrane upon histamine stimulation, simultaneous with the translocation of H^+/K^+-ATPase in response to stimulation (Yao and Forte, 2003). In total, these events trigger membrane and cytoskeletal rearrangements within the parietal cell resulting in the relocation of H^+/K^+-ATPase (Forte and Soll, 1989).

Lasp-1 is a phosphoprotein involved in cAMP-mediated activation of acid secretion. It is phosphorylated by PKA upon elevation of $[cAMP]_i$ in the pancreas and intestine as well as in the gastric mucosa (Chew and Brown, 1987). Immunostaining showed that lasp-1 was redistributed from the basolateral membrane to the apical canalicular membrane of parietal cells upon stimulation (Chew *et al.*, 2000). Yao and Forte (2003) suggested that the selective phosphorylation-dependent regulation of lasp-1 in filamentous (F)-actin-rich epithelial cells and the recruitment of lasp-1 to cellular regions associated with dynamic actin turnover may allow this protein to play an integral and specific role in the regulation of cytoskeletal/membrane-based cellular activities.

1.2.2.3.3.2 Gastrin CCK_B and Acetylcholine M_3 Receptors

In monogastric species, increased acid secretion is predominantly mediated by the different actions of increased gastrin levels (Blair *et al.*, 1987; Kovacs *et al.*, 1989). Gastrin acts either directly on parietal cells via CCK_B-type receptors or, mainly through the release of histamine from ECL cells (Chuang *et al.*, 1991; Håkanson *et al.*, 1994). Cholinergic agents, such as acetylcholine, released by postganglionic neurons of the enetric nervous system, act on muscarinic M_3 receptors to activate the parietal cell (Yao and Forte, 2003). Acetylcholine acts either directly on parietal cells or indirectly by releasing antral gastrin and fundic histamine, or additionally by inhibiting the release of SS (Hersey and Sachs, 1995) (Figure 1.12).

Both M_3 and CCK_B receptors couple to non-Gs/Gi ($G_{stimulatorry}/G_{inhibitory}$) systems, probably Gq (q polypeptide), to activate phospholipase C (PLC) (Figure 1.13). Binding of the agonists to their G protein coupled receptor activates PLC, which produces inositol 1,4,5-trisphosphate (IP_3) and diacylglycerol (DAG). IP_3 is responsible for releasing intracellular stored Ca^{2+} $[Ca^{2+}]_i$ (independent of extracellular Ca^{2+}, unless the stores are first depleted) and DAG for activation of PKC (Urushidani and Forte, 1997). The Ca^{2+} pathway itself cannot provide full activation of the secretory machinery, but is a potentiating factor for the cAMP pathway (Soll, 1982; Chiba *et al.*, 1989; Negulescu *et al.*, 1989; Li *et al.*, 1995). Athmann *et al.* (2000) have also shown that the increase in $[Ca^{2+}]_i$ in ECL cells precedes that in the adjacent parietal cells by 1-2s, whereas more distant parietal cells did not respond, suggesting that a paracrine stimulation of parietal cells by histamine was involved.

The role of PKC in cholinergic activation has been controversial: both inhibition and activation has been shown for both carbachol- and histamine-stimulated acid secretion (Anderson and Hanson, 1985; Beil *et al.*, 1987; Brown and Chew, 1987; Hanson and Hatt, 1989). Tsunoda *et al.* (1992) suggested that CaM kinase plays a role in parietal cell activation stimulated by the cholinergic pathway. Carbachol has also been shown to induce IκB (inhibitor of NFκB) kinase activity in canine parietal cells via Ca^{2+} and PKC (Todisco *et al.*, 1999). IκB kinase appears to be a key element in the signalling cascade that activates nuclear factor κB (NFκB) (DiDonato *et al.*, 1997), which is an important transcription factor and regulator for a variety of genes, including numerous cytokines, immunoreceptors, growth factors and transcription factors (Pahl, 1999).

Facing page 13

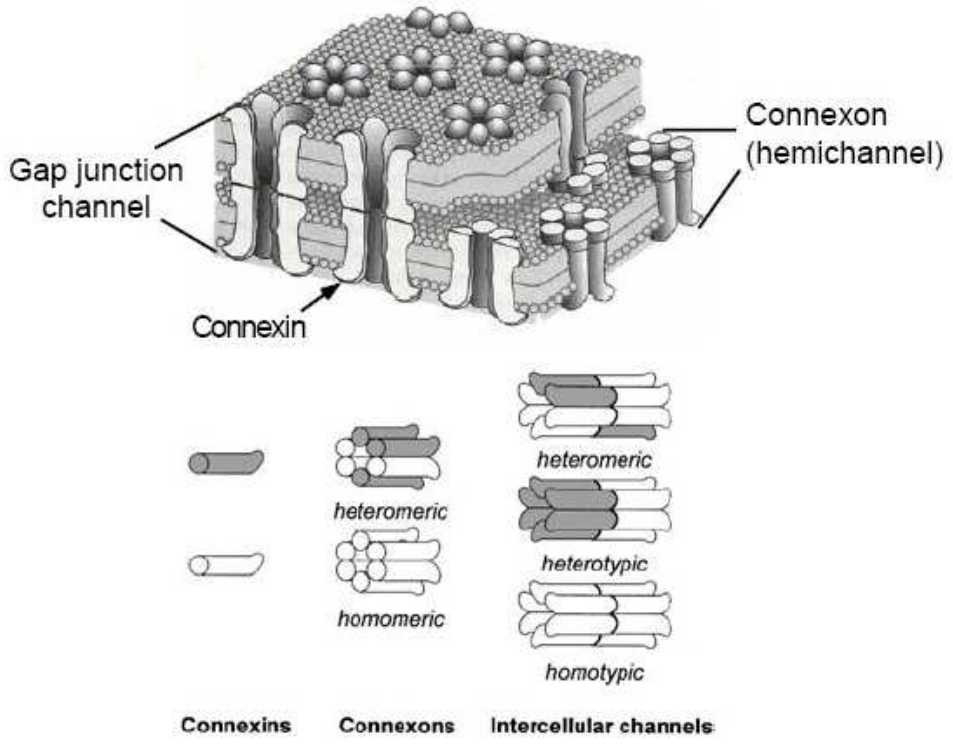

Figure 1.14: Components of the gap junction (schematic). Connexins can build either heteromeric or homomeric connexons, which form heteromeric, heterotypic or homotypic intercellular channels then. (Parker, 2006)

1.2.2.3.3.3 Calcium-Sensing Receptor

The calcium-sensing receptor (CaSR) has been identified not only in parathyroid gland and kidney, which maintain systemic extracellular Ca^{2+} homeostasis, but also in other tissues such as pancreas and gastrointestinal system, including in G cells, pit cells and parietal cells (Brown and MacLeod, 2001). In gastric parietal cells, the CaSR is expressed on the basolateral membrane and was proposed to play a role in acid secretion in addition to the three classic pathways (histamine, gastrin, acetylcholine) (Cheng *et al.*, 1999; Herbert *et al.*, 2004; Remy *et al.*, 2007). The CaSR is activated by Ca^{2+} and magnesium ions (Mg^{2+}), gadolinium ions (Gd^{3+}) and spermine (Dufner *et al.*, 2005). Activation of the CaSR induced an increase in $[Ca^{2+}]_i$ and modulated H^+/K^+-ATPase activity in both the absence and presence of histamine. However, it remains to be established whether the CaSR provides an independent pathway from the classic route *in vivo* (Dufner *et al.*, 2005). Remy *et al.* (2007) also showed the involvement of G proteins, PLC, PKC and extracellular signal-regulated protein kinases (ERK-1/-2). The signal cascades following CaSR activation could play a role in enhancing or modulating signals controlling gastric acid secretion.

1.2.2.3.3.4 Gap Junctional Channels

The processes involved in acid secretion require a synchronised activation of parietal cells along a gastric gland. This has been attributed to the use of the gap junctional channels (Radebold *et al.*, 2001). In general, gap junctions are a primary pathway for intercellular message transfer. Six transmembrane proteins (connexins) build a connexon, which forms the intercellular channel with the opposing connexon of the neighbouring cell (Alberts *et al.*, 1995) (Figure 1.14). Gap junctions allow the exchange of low-molecular weight metabolites, ions and signalling molecules such as cAMP, Ca^{2+} and IP_3 (Sáez *et al.*, 1993; Giaume and McCarthy, 1996). In rat gastric glands, Radebold *et al.* (2001) identified two gap junctional proteins: connexin 26, which is mainly found in the cytosol, and connexin 32, which appears to be distributed along the plasma membrane of parietal cells. They showed that parietal cells communicate with each other during gastrin or histamine stimulation, because of a sequential rise in Ca^{2+} in neighbouring cells. However, the source of Ca^{2+} (intracellular store, influx of extracellular Ca^{2+} or other pathways causing the

elevation of Ca^{2+} signal in the neighbouring parietal cells) and which molecules or second messengers move through the gap junctions remained unclear.

1.2.2.3.3.5 Inhibition of Acid Secretion

Acid secretion is mainly inhibited by SS, which is released from fundic D cells (Schusdziarra *et al.*, 1978; Schubert *et al.*, 1988). Sensory nerves containing calcitonin gene-related peptide (CGRP) act on the D cell to increase SS secretion (Ren *et al.*, 1992; Manela *et al.*, 1995). In addition to direct inhibitory effects of SS on parietal cells via their SS_2 receptors (Park *et al.*, 1987; Delvalle *et al.*, 1993), indirect effects of SS are the inhibition of gastrin secretion from antral G cells (Walsh, 1988; Beglinger *et al.*, 1992) and the inhibition of histamine secretion from fundic ECL cells (Athmann *et al.*, 2000; Chen *et al.*, 2000). The SS_2 receptors operate via G_i proteins to decrease the activity of adenylate cyclase.

Epidermal growth factor (EGF) and transforming growth factor-α (TGF-α) are also inhibitors of gastric acid secretion. Chew *et al.* (1994) suggested that EGF and TGF-α modulate parietal cell function by multiple signalling pathways during both chronic and acute exposure to these growth factors. Acute exposure led to an inhibition of histamine-induced acid secretion. Yao and Forte (2003) suggested that the inhibitory action of EGF and TGF-α on histamine-stimulated acid secretion acts by promoting the retrieval of H^+/K^+-ATPase from the apical plasma membrane. However, chronic exposure to EGF and TGF-α enhanced acid secretion suggested to be due to a soluble tyrosine kinase. EGF also activated ERK-1 and ERK-2, but this pathway has only a minimal role in the direct activation of gastric secretion (Chew *et al.*, 1994; Takeuchi *et al.*, 1997; 1999). Another element in the EGF activation cascade is the serine-threonine protein kinase Akt, which was reported to increase H^+/K^+-ATPase expression, at least in canine parietal cells (Todisco *et al.*, 2001).

1.2.3 Gastric Mucosal Barrier

The gastric mucosal barrier protects the mucosal lining in an acidic and proteolytic environment and against the entry of bacteria, toxins and luminal antigens or even parasite chemicals potentially present in gastric contents. The gastric mucosal barrier consists of secreted mucus and bicarbonate and the properties of the gastric epithelium (Werther, 2000). The formation of a tight epithelium with selectively permeable intercellular junctions between gastric epithelial cells and the rapid turnover of gastric surface epithelial cells, which are replaced every three days on average (Karam, 1999), contribute to maintaining mucosal integrity. The latter requires a precise balance between cell death and proliferation, which is described in 1.2.4.

1.2.3.1 Mucus and Bicarbonate

Surface mucous cells secrete both mucus and bicarbonate ions onto the epithelial surface to protect the epithelial cells lining the stomach against gastric acid and pepsin. The mucus layer acts as a diffusion barrier to hydrogen ions/protons, which may have a millionfold concentration gradient between the gastric lumen and blood. The mucus gel with its increased impermeability to protons, and the ability of bicarbonate to neutralise acid are the first line of defence to back-diffusing acid from the lumen into the blood stream (Kaunitz, 1999; Werther, 2000). In addition, the luminal surface of the mucus gel contains a hydrophobic layer of phospholipids, which provides further protection against the inward influx of protons or other damaging agents (Kaunitz, 1999; Werther, 2000). Secreted hydrochloric acid crosses the mucus layer by the process of viscous fingering, by which fluids of low viscosity pass through fluids of high viscosity without mixing. Due to the secretory pressure of the glands, the acid moves through these temporary channels in the mucus gel into the lumen (Fabry, 1990; Bhaskar *et al.*, 1992).

The mucus-bicarbonate barrier is believed to cover only the cells on the luminal surface of the stomach, as well as those in the more superficial regions of the gastric glands. There is no obvious mucus barrier covering the apical membranes of the parietal and chief cells

Facing page 16

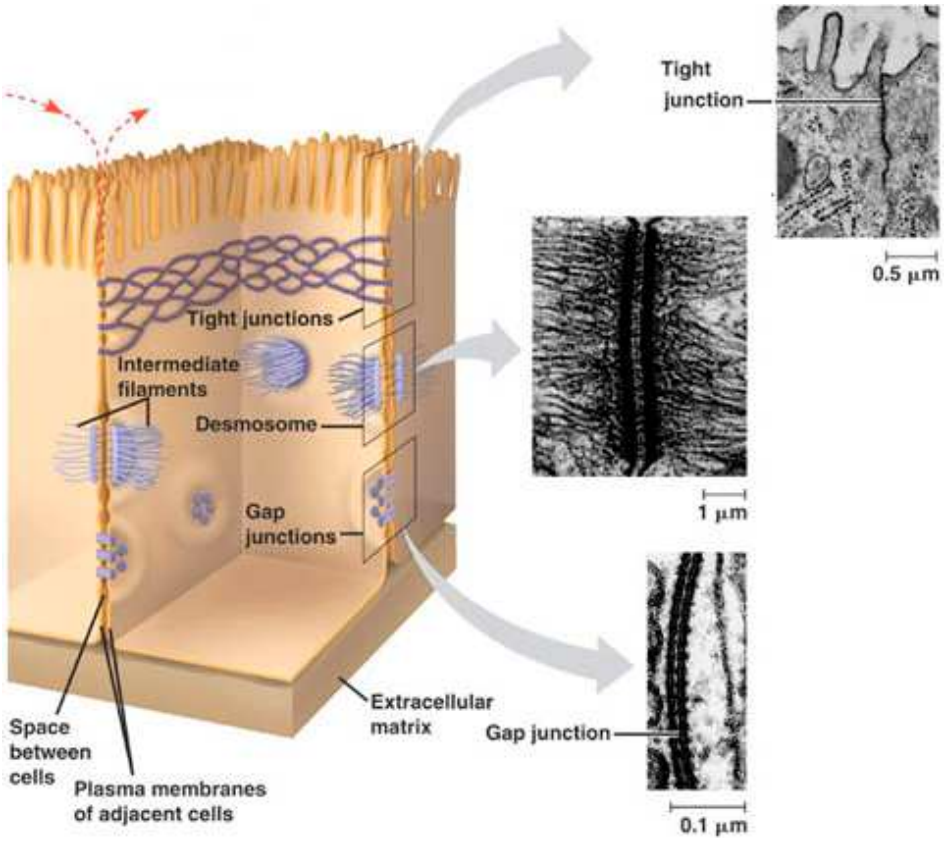

A

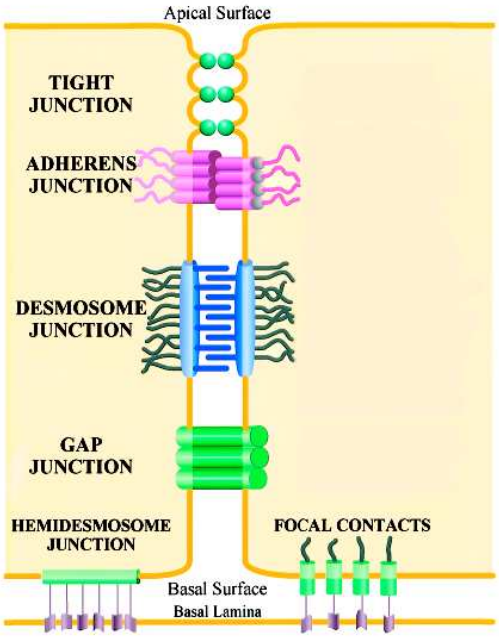

B

Figure 1.15: Overview of cell adhesion mechanisms. A. Cell-cell junctions, including details of tight junctions, desmosomes and gap junctions (Mallery, 2009), B. Cell-cell and cell-matrix adhesion mechnisms, including adherens junctions and the cell-matrix adhesion sites hemidesmosomes and focal contacts/focal adhesions (modified after Blonder *et al.*, 2004).

deeper in the gastric gland, however, the permeability to H^+ on the apical membranes of these cells is low (Boron *et al.*, 1994; Waisbren *et al.*, 1994). Exposure of the luminal surface of isolated perfused gastric glands to a pH as low as 1.4 resulted in no change in intracellular pH, whereas application of a solution of pH 6.4 to the basolateral surface resulted in rapid and substantial acidification (Boron *et al.*, 1994). In addition, the β-subunit of the H^+/K^+-ATPase is highly resistant to acidic and peptic conditions due to its glycosylation (Thangarajah *et al.*, 2002; Crothers *et al.*, 2004). Kurbel *et al.* (2001) proposed a model stating that a backflux of mucus might take place during gland relaxation and repeated gland contractions and relaxations would move mucus down to the gland base.

1.2.3.2 Properties of the Gastric Epithelium

Cells in multicellular organisms contact tightly and are able to interact specifically with each other. Cell-cell adhesion takes place through junctional adhesion mechanisms, including tight junctions, adherens junctions, desmosomes and gap junctions and cell adhesion molecules (CAM), including immunglobulin (Ig)-like CAMs, Ca^{2+}-dependent cadherins, integrins and selectins (Alberts *et al.*, 1995). In tissues, cells are embedded into the extracellular matrix, which consists of proteoglycans, collagen fibres and multiadhesive matrix proteins. Integrins play the major role in cell-matrix adhesion especially in focal adhesions and hemidesmosomes (Alberts *et al.*, 1995). Figure 1.15 gives an overview of both cell-cell and cell-matrix adhesion mechanisms. The cell junctions can also be divided into three groups according to their function: (1) selectively permeable barrier (tight junctions); (2) stability (adherens junctions and desmosomes for cell-cell adhesion and focal adhesions and hemidesmosomes for cell-matrix adhesion) and (3) communication (gap junctions).

1.2.3.2.1 Cell-Cell Adhesion

On the apical side of epithelial cells, a junctional complex is formed by tight junctions, adherens junctions and desmosomes (Tsukita *et al.*, 2001). Tight junctions are most important for the epithelial barrier and will be described in more detail in the next section

Facing page 17

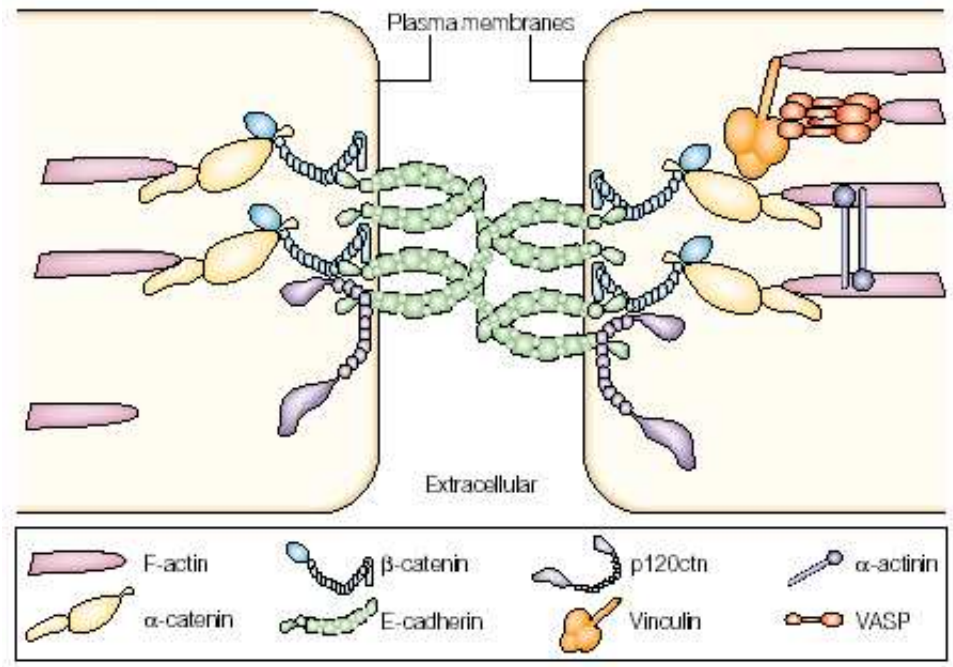

Figure 1.16: Schematic model of adherens junctions. p120ctn: catenin in adherens junctions; VASP: vasodilator-stimulated phosphoprotein. (Fuchs and Raghavan, 2002)

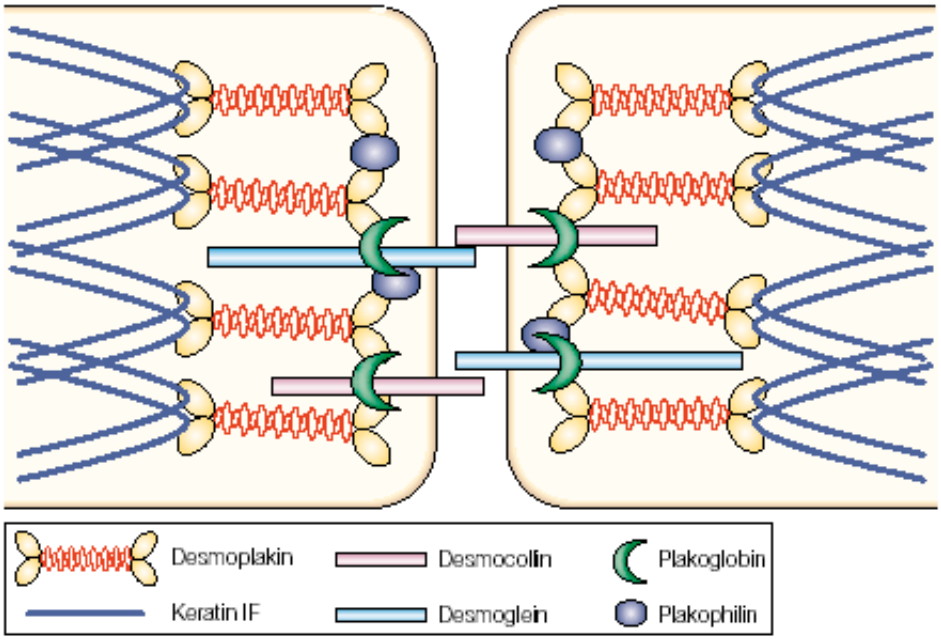

Figure 1.17: Schematic model of a desmosome. (Fuchs and Raghavan, 2002)

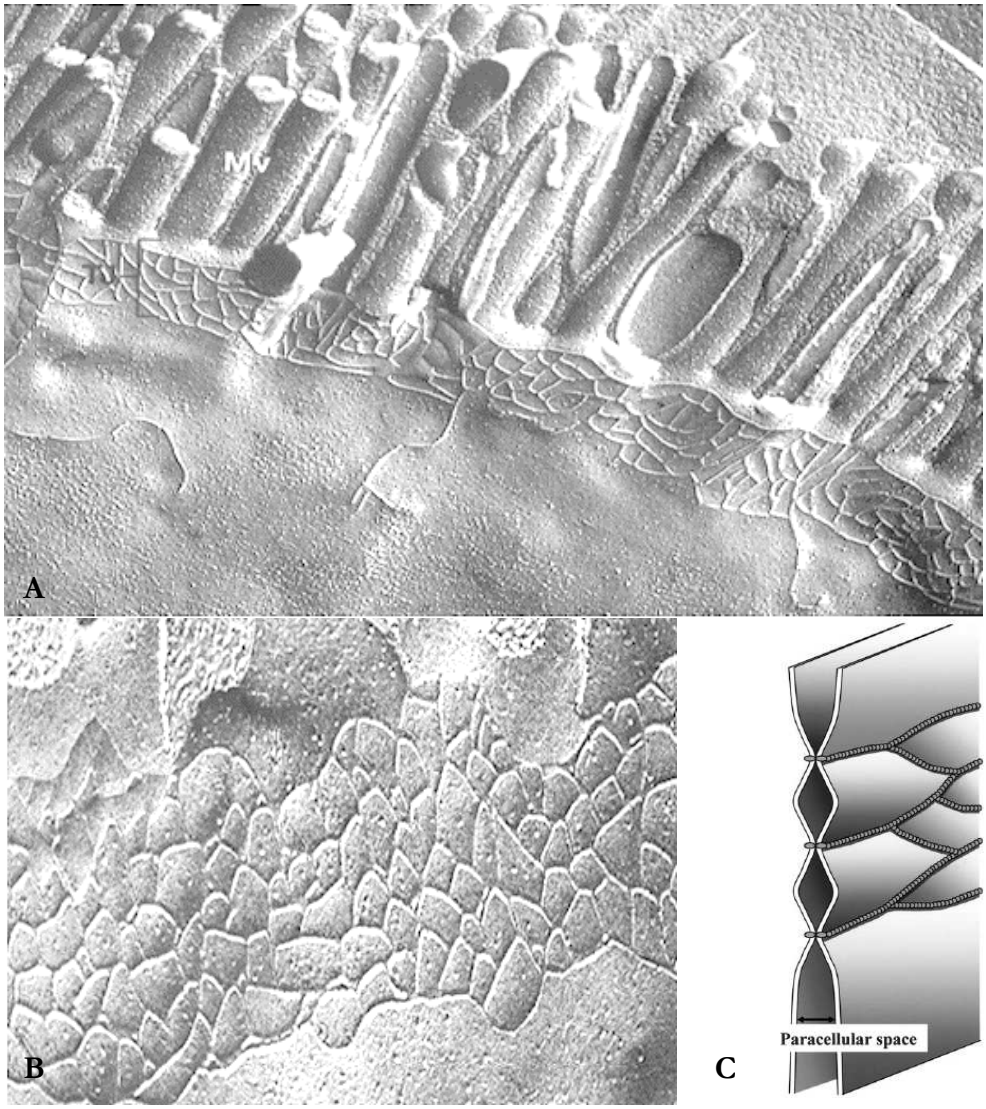

Figure 1.18: Freeze-fracture electron micrographs and schematic model of tight junction strands. A. The tight junction strand network can be seen on the apical side underneath the microvilli, B. Magnification of the tight junction strand network, C. Schematic illustration of the tight junction strand network. (A. and B. Wagner and Hossler, 2009, C. Sawada *et al.*, 2003)

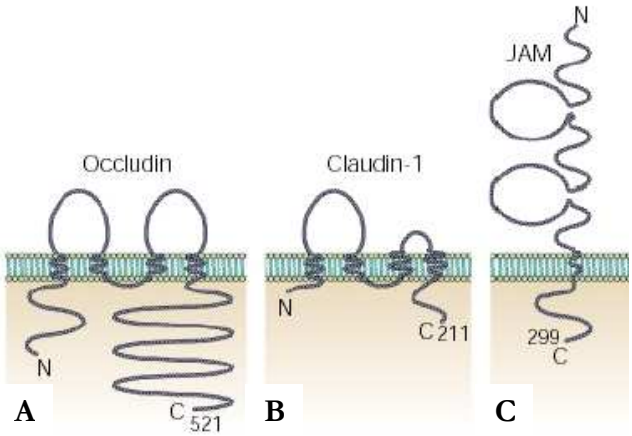

Figure 1.19: Transmembrane proteins of tight junctions. A. Occludin, B. Claudin-1, C. Junctional adhesion molecule (JAM). (Tsukita *et al.*, 2001)

(1.2.3.2.1.1). Adherens junctions form a continuous belt around cells, also called the adhesion belt, consisting of cadherins (Figure 1.16) (Alberts *et al.*, 1995). E-cadherin (cadherin in epithelial cells) binds to β-catenin in the cytoplasm, which in turn links through α-catenin to the actin cytoskeleton (Fuchs and Raghavan, 2002; Niessen, 2007). Another component is the nectin-afadin complex (Niessen, 2007). Desmosomal adhesion also takes place via cadherins: desmogleins and desmocollins are the desmosomal cadherin forms. The cytosolic desmosomal plaque proteins plakoglobin (similar to β-catenin), plakophilin and desmoplakin link the cadherins to keratin filaments (Figure 1.17) (Alberts *et al.*, 1995; Fuchs and Raghavan, 2002). Further desmosomes, which do not belong to the junctional complex, and gap junctions, which also play a role in signal transfer between adjacent cells during acid secretion (see also 1.2.2.3.3.4), are distributed sporadically.

1.2.3.2.1.1 Tight Junctions

Tight junctions serve as a selectively permeable barrier in the paracellular pathway, with ion and size selectivity and tightness varying with the tissue or cell type (Tsukita *et al.*, 2001; Clayburgh *et al.*, 2004). Tight junction strands also act as a "fence" between apical and basolateral membrane domains, which restricts diffusion of both phospholipids and membrane proteins within the outer leaflet of the membrane bilayer (Tsukita *et al.*, 2001; Köhler and Zahraoui, 2005).

Using freeze-fracture electron microscopy, tight junctions appear as continuous, complex network of fibrils, the tight junction strands (Figure 1.18). The number of strands varies as does the complexity of the network depending on the type of tissue (Tsukita *et al.*, 2001; Schneeberger and Lynch, 2004). Tight junction strands from adjacent cells form "paired" strands which contact in the intercellular space building the barrier (Tsukita *et al.*, 2001; Van Itallie and Anderson, 2004). The tight junction is formed by the transmembrane proteins occludin, members of the claudin family and junctional adhesion molecule (JAM) (Figure 1.19) (Tsukita *et al.*, 2001; Schneeberger and Lynch, 2004). The tight junction plaque formed on the cytosolic side contains numerous proteins, including Zonula occludens (ZO) proteins (ZO-1 to -3), which link to the cytoskeleton and also recruit regulatory

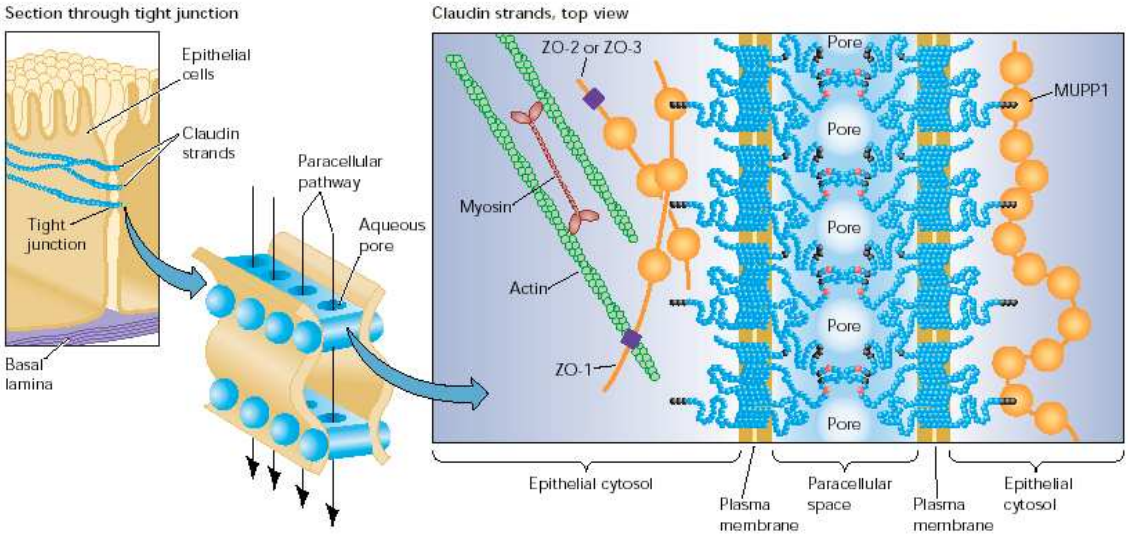

A

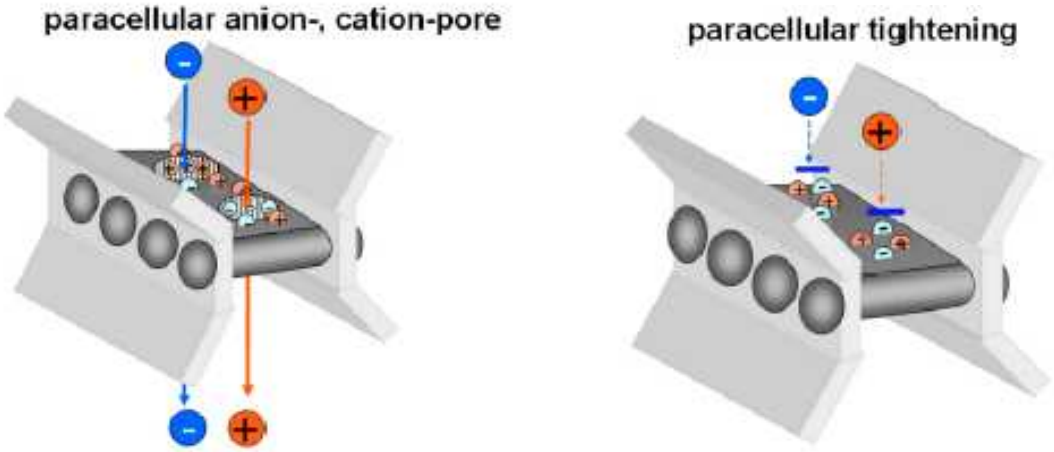

B

Figure 1.20: Model of tight junction pores formed by claudins. A. Extracellular charged residues in the first extracellular loop (ECL1) of claudins (red balls) form selective pores. ZO-1, -2, -3 Zonula occludens proteins, MUPP-1 Multi PDZ domain protein 1. (Van Itallie and Anderson, 2004), B. The pore is suggested to form by repulsion of equally charged residues in the ECL1 and the paracellular tightening by charge attraction of charged amino acids in the ECL1, both depending on distribution and facing of either equal or unequal charged residues. Claudin-2 (monovalent cations), -7 (Na^+), -10 (cations), -15 (Na^+) and -16 (mono- and divalent cations) were as pore forming identified (anion pores are not clarified yet) and claudin-4, -5, -8, -11, -14 and -19 as sealing claudins (selective paracellular cation permeability decrease). (Krause *et al.*, 2008)

proteins, thus regulating cell polarity, proliferation and differentiation (Schneeberger and Lynch, 2004; Köhler and Zahraoui, 2005).

Occludin (~60kDa) has four transmembrane domains, two extracellular loops separated by a short cytoplasmic loop and the carboxy-terminal and amino-terminal domain located in the cytoplasm. There are two isoforms of occludin, which are generated by alternative splicing (Muresan *et al.*, 2000). The function of occludin has not been completely clarified. It may be involved in the barrier and fence function, but tight junction strand formation is also possible without occludin (Tsukita and Furuse, 1999; Tsukita *et al.*, 2001; Schneeberger and Lynch, 2004).

Members of the claudin family (20-27kDa) also have four transmembrane domains, two extracellular loops of which the second one is shorter and compared to occludin short cytoplasmic carboxy-terminal and amino-terminal domains. So far, 23 members of the claudin family have been identified in humans (Hewitt *et al.*, 2006). The expression of the different claudins depends on the cell type, with more than two different claudins usually polymerising to form the tight junction strand (Tsukita *et al.*, 2001; Van Itallie and Anderson, 2004). Claudins have been suggested to build the strand backbone, with occludin being incorporated into claudin based strands (Tsukita *et al.*, 2001; Förster, 2008). The ion and size selectivity as well as variability in tightness are attributed to claudins (Van Itallie and Anderson, 2004; Schneeberger and Lynch, 2004; Niessen, 2007). Furthermore, it has been suggested that claudins form the tight junction pores (Figure 1.20). Charged residues on the extracellular loops influence the paracellular charge selectivity and tightness (Schneeberger and Lynch, 2004; Van Itallie and Anderson, 2004; Förster 2008; Krause *et al.*, 2008). On the carboxy-terminus, tight junction plaque proteins bind through the PDZ domain (named from their presence in the proteins PSD-95 (post-synaptic density protein 95), DLG (Discs-large protein in *Drosophila*) and ZO-1) (Schneeberger and Lynch, 2004; Van Itallie and Anderson, 2004).

JAM (~40kDa) has a single transmembrane domain, two extracellular Ig-like domains and a relatively short cytoplasmic carboxy-terminal domain. Four family members have been identified, all belonging to the IgG superfamily (Schneeberger and Lynch, 2004). Although, JAM has not been identified in tight junction strands (Tsukita *et al.*, 2001; Sawada *et al.*,

Facing page 19

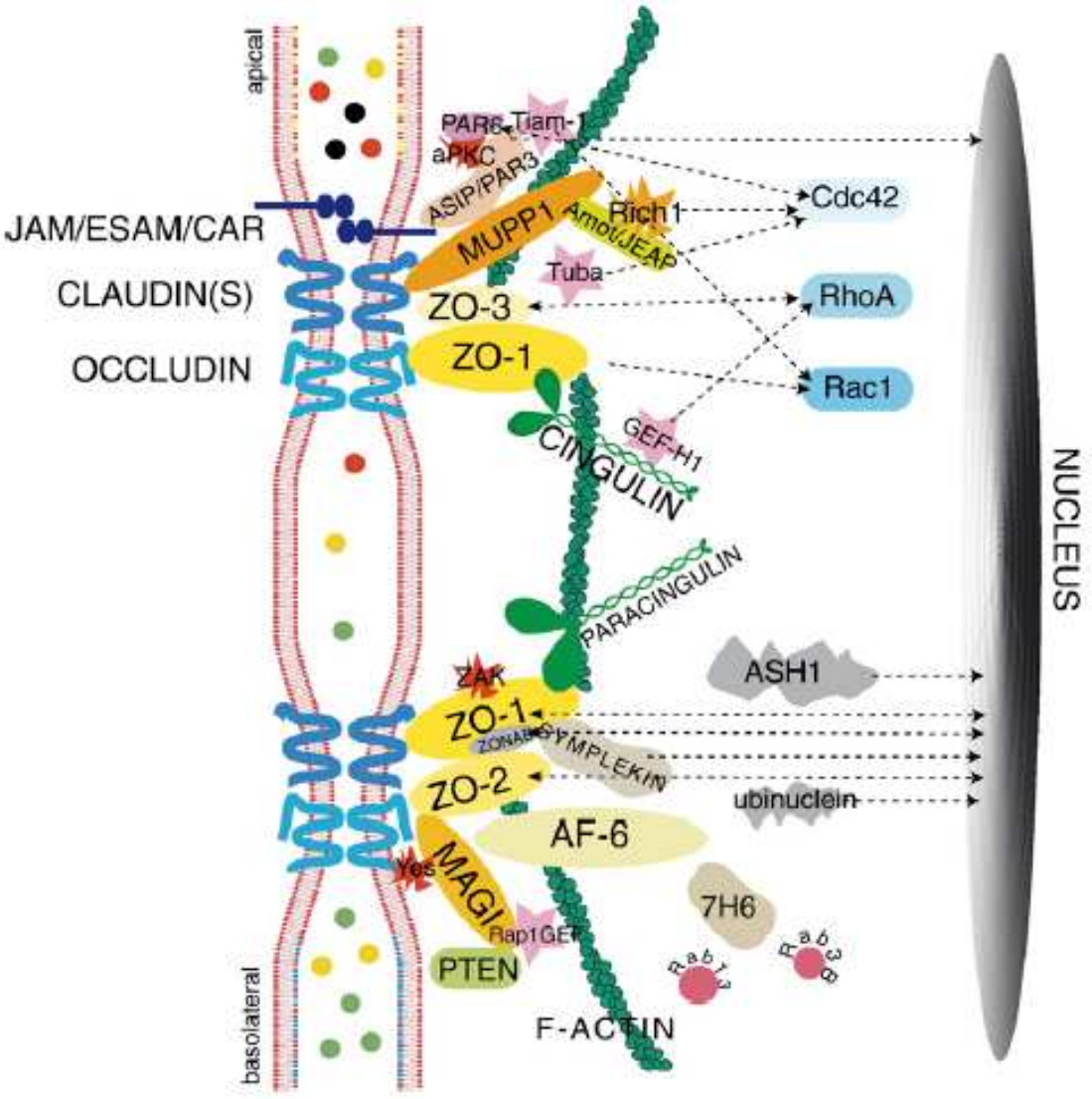

Figure 1.21: Tight junction model with associated tight junction plaque proteins. Shown are the transmembrane proteins occludin, claudin(s) and JAM and the tight junction plaque proteins, which have scaffolding as well as regulating functions. Kinases: red irregular shapes; GEFs: pink stars; membrane traffic regulators: red circles; plaque protein-signalling protein interaction: dotted arrows; proteins with dual nuclear-junctional localisation: arrows directed to the nucleus; all abbreviations are in the list of abbreviations. (Guillemot *et al.*, 2008)

Table 1.2: Possible functions of PDZ containing proteins of the tight junction plaque. ZO: Zonula occludens proteins; MAGI: membrane-associated guanyl kinase inverted proteins; AF-6: ALL-1 fusion partner from chromosome 6, also called afadin; MUPP-1: multi PDZ domain protein 1; PAR-3 and -6: partitioning defective proteins; PALS: protein associated with Lin-7; PATJ: PALS-1 associated tight junction protein.

Protein	Possible function(s)
ZO proteins	Involvement of polymerisation of claudins into tight junction strands, linking tight junction transmembrane proteins to the actin cytoskeleton, scaffolding function
MAGI proteins	Role in adhesion, but role in tight junctions unclear, possible scaffolding and signalling functions
AF-6/afadin	Role in epithelial morphogenesis by scaffolding, linking to the actin cytoskeleton and modulation of Ras/Rap1 signalling
MUPP1	Role in tight junctions unclear yet, possible scaffolding function
PAR3, PAR6	Role in regulation of cell polarity and tight junction assembly
PALS, PATJ	Role in regulation of cell polarity, possible involvement in later stages of tight junction assembly

(after Schneeberger and Lynch, 2004; Guillemot *et al.*, 2008)

Table 1.3: Non-PDZ containing proteins of the tight junction plaque, including interaction partners and possible functions. All abbreviations are in the list of abbreviations.

Protein	Interacting partner(s)	Possible function(s)
Cingulin	JAM, ZO-1, ZO-2 and ZO-3, GEF-H1 (RhoA regulator)	Crosslinking tight junction proteins to the actin cytoskeleton, RhoA dependent regulation of gene expression and cell proliferation
Paracingulin	maybe ZO-1	-
Symplekin	Co-localises with ZO-1, also present in nucleus, ZONAB	Processing of pre-mRNA and its polyadenylation
ZONAB	ZO-1	Transcription factor
Angiomotin family proteins (Amot, JEAP, MASCOT)	MAGI-1, Rich1 (Cdc42 GAP), PATJ, MUPP1	Involvement in tight junction integrity by regulating Cdc42 through Rich1, involvement in the regulation of morphogenetic cell movements
7H6	-	-
PP2A (phosphatase)	-	Regulation of aPKC, ZO-1, occludin and claudin-1 phosphorylation
aPKC	PAR3, PAR6	Serine/threonin kinase involved in regulation of cell polarity
Rab3b, Rab13	-	G protein, vesicle targeting to cell-cell adhesion sites
GEFs (Tiam1, GEF-H1, Tuba)	PAR3, cingulin, Cdc42	Tiam1 is an activator for Rac1, GEF-H1 down-regulates RhoA, Tuba regulates Cdc42
GAPs (among others Rich1)	Amot	Regulation of Cdc42 activity, in general control of small GTPases (Rho, Rac, Ccd42) activity

- not known

(after Tsukita *et al.*, 2001; Schneeberger and Lynch, 2004; Guillemot *et al.*, 2008)

2003; Förster, 2008) it can bind structural and signalling proteins of the tight junction plaque, in particular through the PDZ binding motif (Sawada *et al.*, 2003; Schneeberger and Lynch, 2004; Förster, 2008). JAM is believed to have a role in tight junction assembly and regulation of paracellular permeabilty (Schneeberger and Lynch, 2004; Förster, 2008).

Several tight junction plaque proteins are associated on the cytosolic side of the tight junction. They are divided into two major groups, the PDZ containing proteins and the non-PDZ containing proteins. PDZ-containing proteins interact through the PDZ domain with other PDZ proteins linking tight junction transmembrane proteins to the cytoskeleton, building a scaffolding network and recruiting signalling proteins to the tight junction plaque (Tsukita *et al.*, 2001; Guillemot *et al.*, 2008). The group of the ZO proteins (ZO-1 to -3) is at the centre of this protein interaction network. It has been suggested that the second group (non-PDZ proteins) plays an important role in the regulation of signalling processes (Förster, 2008; Guillemot *et al.*, 2008). Some of the tight junction plaque proteins and their interaction partners are summarised in Table 1.2 and 1.3 and a model of the tight junction is illustrated in Figure 1.21.

Tight junction regulation is complex and is mediated by phosphorylation. Phosphorylation mediators include PKCs (including atypical PKC (aPKC)), PKA, Rho (Ras homologue) GTPase family members (including RhoA, Rac1 and cdc42), MLCK and mitogen-activated protein kinase (MAPK) (Sawada *et al.*, 2003; Aktories and Barbieri, 2005; González-Mariscal *et al.*, 2008). In addition, tight junctions are highly dynamic and undergo continuous remodeling. Downregulation of junctional proteins is one factor, but rapid remodeling, both physiological and pathological, includes endocytosis (Ivanov *et al.*, 2005; Shen *et al.*, 2008; Yu and Turner, 2008). Shen *et al.* (2008) found that under physiological conditions, approximately 70% of occludin and ZO-1 and 24% of claudin were in a mobile fraction. Occludin and claudin were found to diffuse within the plasma membrane and ZO-1 to exchange with an intracellular pool.

The EGF receptor may also be involved in regulating paracellular permeability. Application of EGF to apical or basolateral surfaces of canine gastric monolayers was shown to rapidly decrease permeability, which was stable for hours in case of the apical exposure. As this

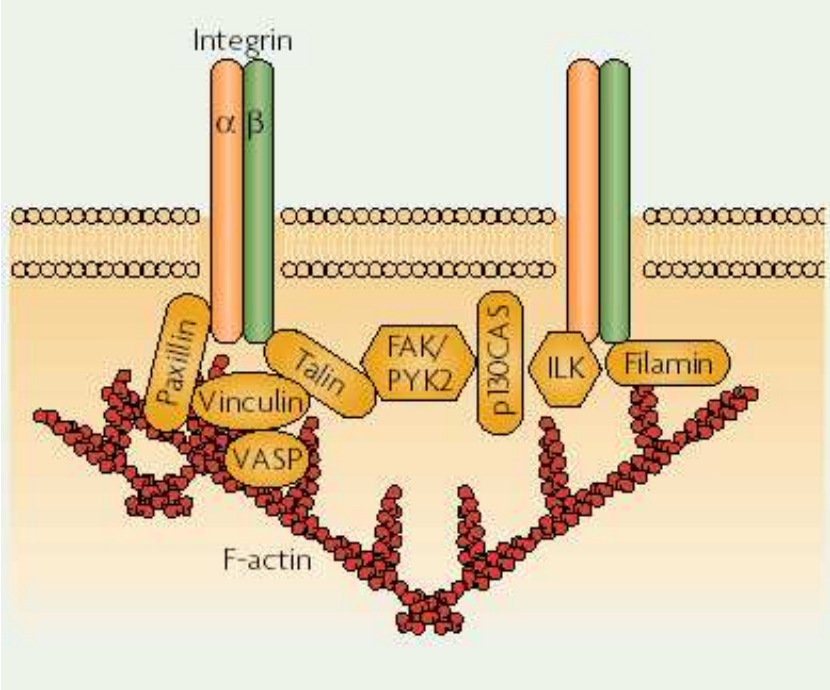

Figure 1.22: Schematic model of focal adhesions (focal contacts). VASP: vasodilator-stimulated phosphoprotein; FAK: focal adhesion kinase; PYK2: protein tyrosine kinase 2, FAK homologue; p130CAS: v-Crk associated tyrosine kinase substrate; ILK: integrin-linked kinase. (Billadeau *et al.*, 2007)

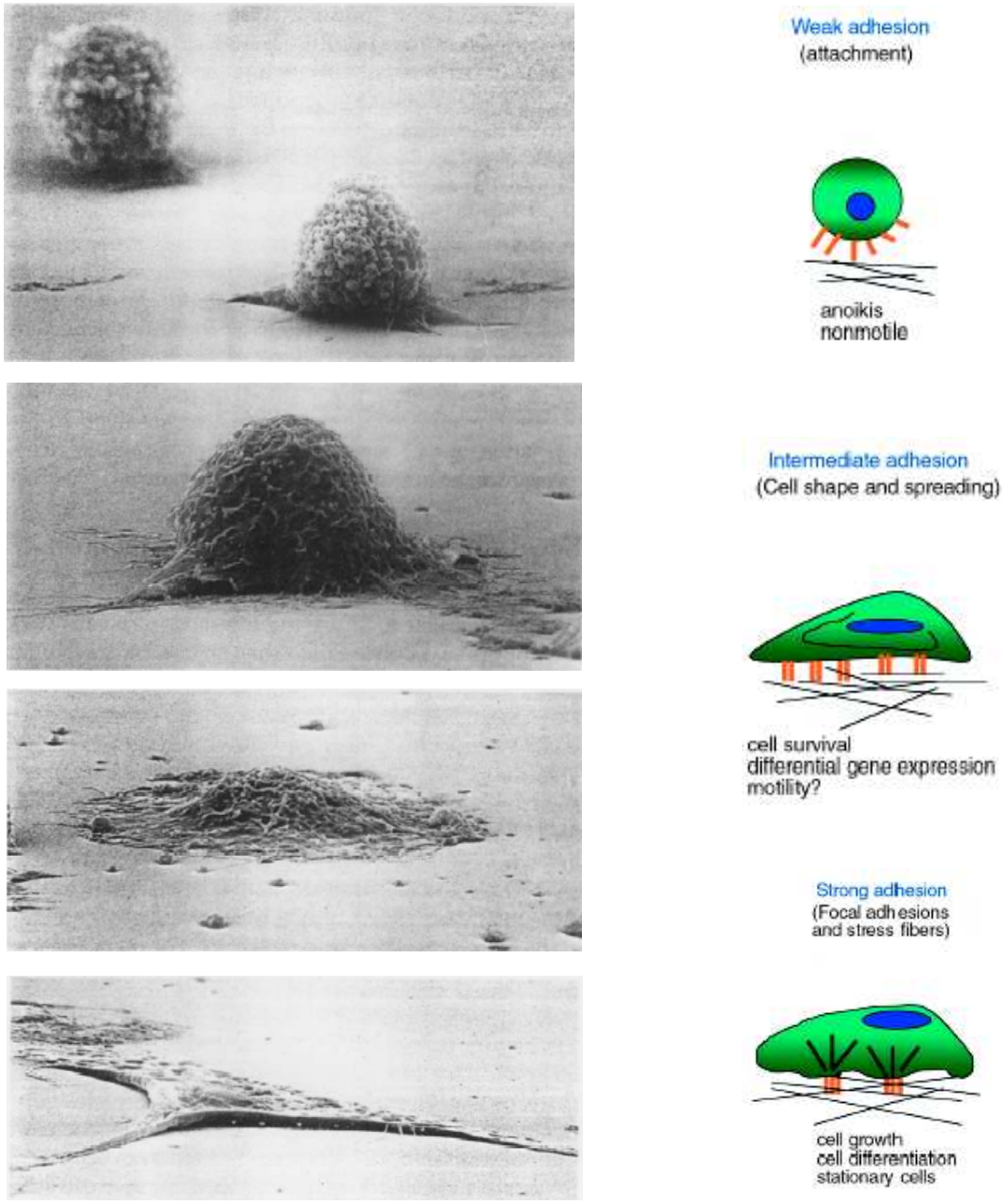

Figure 1.23: Stages of cell-matrix adhesion. Adhesion includes cell attachment, spreading and the formation of stress fibres and focal adhesions, with increasing adhesive strength shown from top to bottom (Left side, Deutzmann, 2008/2009, right side, modified after Murphy-Ullrich, 2001)

correlated with increased resistance to apical acidification it was suggested that the apical EGF receptor also plays a role in the gastric mucosal barrier (Chen *et al.*, 2001). In addition, hepatocyte growth factor (HGF) was recently shown to be involved in tight junction formation in chief cells *in vitro* (Tashima *et al.*, 2009). Without HGF, tight junctions were discontinuous and permeability was high.

1.2.3.2.2 Cell-Matrix Adhesion

The extracellular matrix not only provides a scaffold for the attachment of cells, but also mediates interactions of the cell with the extracellular environment. Intracellular signalling in response to cell-matrix adhesion regulates processes including cell survival, proliferation, differentiation and migration (Berrier and Yamada, 2007). Integrins are the major cell surface receptor family and are composed of α- and β-transmembrane subunits which associate in heterodimers (Harburger and Calderwood, 2009). Cells are attached to the matrix via integrin containing focal adhesions (also called focal contacts) (Figure 1.22) and hemidesmosomes.

Binding of extracellular matrix components activates integrin receptors, leading to the formation of integrin clusters and the recruitment of plaque proteins, such as focal adhesion kinase (FAK), talin, paxillin and vinculin. Following the signal cascade, the activation of Rho GTPase family members promotes the assembly of actin filaments (Clark and Brugge, 1995; Giancotti and Ruoslathi, 1999; Carragher and Frame, 2004). The formation of actin filaments and cell spreading increases the surface contact area, a state which is called intermediate adhesion (Figure 1.23) (Murphy-Ullrich, 2001). Actin filaments are reorganised into larger stress fibres leading to more integrin clustering (Giancotti and Ruoslathi, 1999; Murphy-Ullrich, 2001). Hemidesmosomes mainly anchor epithelial cells to the basal lamina. The cytosolic plaque links integrins to the ends of keratin filaments of the cytoskeleton (Alberts *et al.*, 1995).

1.2.4 Differentiation, Proliferation and Maintenance of Gastric Epithelial Cells

The normal maintenance of the gastric epithelium requires a precise balance between cell proliferation and cell death. Complex mechanisms regulate this balance and disturbances resulting in excessive cell loss, excessive cell proliferation or prolonged cellular life span can lead to atrophy and ulceration or hyperplasia respectively. In addition, epithelial cell regeneration and repair is associated with proliferation to counterbalance mucosal damage due to constant exposure to potentially injurious agents, including gastric acid, toxins and pathogenic bacteria.

1.2.4.1 Cell Death

Maintenance of the gut epithelium involves cell death, which is generally mediated by apoptosis under physiological conditions (von Herbay and Rudi, 2000). Pit and parietal cells at the luminal surface undergo autophagic (necrosis-like) cell death followed by extrusion into the gland lumen or apoptotic cell death followed by phagocytosis by neighbouring cells. Zymogenic and parietal cells at the gland base undergo degeneration with direct extrusion into the gland lumen or phagocytosis by neighbouring cells (Karam, 1999). In addition, parietal cells in the neck, but more frequently at the base, occasionally degenerate with extensive dissolution of canaliculi and intermitochondrial cytoplasm with the formation of vacuoles (Karam *et al.*, 2003). Macrophages may also be involved in the elimination of dead cells (Karam, 1999).

Regulation of apoptosis is complex and involves extracellular signalling through TGF-β and related peptides and the death receptor Fas/CD95 ligands, tumor necrosis factor-α (TNF-α) and related peptides. These apoptosis-activating factors act via binding to their receptors on their target cells. Within the cell, members of the Bcl-2 protein family, which include suppressors and promotors of apoptosis, are a major class of regulators (von Herbay and Rudi, 2000).

1.2.4.2 Proliferation

Gastric epithelial cells are renewed through mitosis of cells in the isthmus (Karam and Leblond, 1992; 1993a; Karam, 1995). In the pyloric antrum, the stem cells of the isthmus near the base of the glands give rise to mottled granule cells, which divide several times to produce mixed granule cells. These give rise to pre-pit and pre-neck/pre-gland cells, which develop into pit and gland cell lineages (Karam, 1999). In the fundus, stem cells of the isthmus at the base of the pits give rise to lineage precursor cells, which migrate bidirectionally from the isthmus either to the lumen or to the base of the gland and differentiate on the way to their final location (Karam, 1993; 1999; Karam and Leblond, 1993a-d; Karam *et al.*, 2003). The parietal cell is the only cell which can migrate in both directions, although in humans they migrate only downwards (Karam *et al.*, 2003). The precursor cells include pre-pit cells, which differentiate to surface mucous cells (Karam and Leblond, 1993a, b; Karam, 1999; Karam *et al.*, 2003), pre-neck cells, which differentiate to chief cells (Karam and Leblond, 1993a, c; Karam *et al.*, 2003), and pre-parietal cells, which differentiate to parietal cells (Karam, 1993; Karam *et al.*, 2003). Pre-parietal cells do not undergo mitosis at any stage through development. They are divided into three variants, developing from pre-parietal cell precursors, pre-pit cell precursors or pre-neck cell precursors (Karam, 1999). The average turnover times in mice for gastric epithelial cells are 3 days for pit cells, 194 days for chief cells and 54 days for parietal cells (Karam, 1999; Kirton *et al.*, 2002). In both oxyntic mucosa and antrum, the stem cells also give rise to the endocrine cells (Karam, 1999).

Studies have shown that parietal cells play an important role in maintaining normal proliferation and differentiation of the gastric epithelium. Inhibition of the secretory activity of parietal cells, either by inhibition of the H^+/K^+-ATPase by omeprazole (Karam and Forte, 1994) or inhibition of the H_2 receptors by ranitidine (Karam and Alexander, 2001), resulted in parietal cell degeneration, but also increased the production of pre-parietal cells. Li *et al.* (1996) demonstrated that the loss of parietal cells evoked by diphtheria toxin in transgenic mice affected gastric mucosal morphology resulting in mucosal hyperplasia and loss of neck and chief cells.

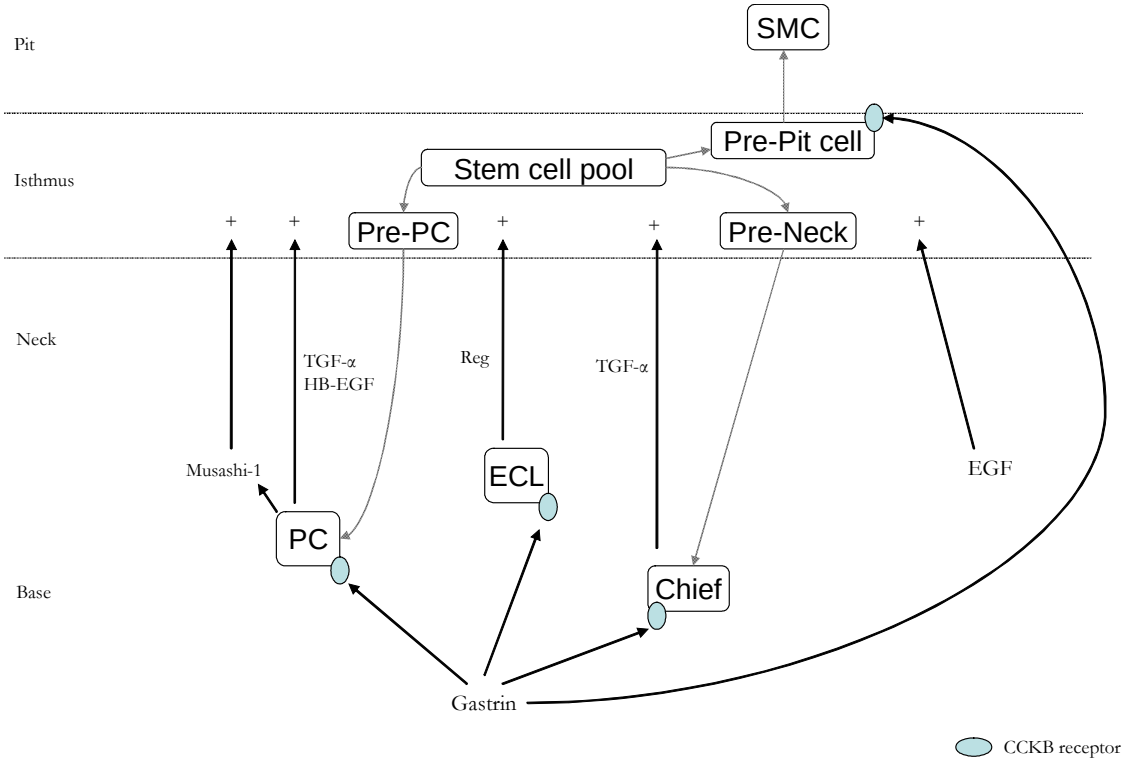

Figure 1.24: Overview of proliferation, differentiation and maintenance of gastric epithelial cells. Stem cells of the isthmus differentiate to SMC, PC, and chief cells, as well as ECL cells involving the different stimulating agents. SMC surface mucous cell, PC parietal cell, ECL enterochromaffin-like cell, EGF epidermal growth factor, TGF transforming growth factor, HB-EGF heparin binding-epidermal growth factor, Reg Regenerating gene product, CCKB cholecystokinin B/gastrin receptor, + stimulatory.

1.2.4.3 Trophic Agents

An overview of the principal factors involved in maintenance, growth and proliferation of gastric gland cells is presented in Figure 1.24. Other trophic factors for the gastrointestinal tract include the hedgehog proteins (sonic, desert and indian hedgehog) (Lees *et al.*, 2005; Parkin and Ingham, 2008) and trefoil factors (TFF), which are important in mucosal healing (Taupin and Podolsky, 2003).

1.2.4.3.1 Gastrin

Gastrin is potent in stimulating the growth of the gastric mucosa, predominantly in the fundus (von Herbay and Rudi, 2000), in addition to stimulating gastric acid secretion (Johnson, 1976; 1988; Wang and Dockray, 1999; Stepan *et al.*, 2004). Gastrin receptors interact with multiple GTP binding proteins, such as Ras, Rho and Cdc42, which regulate different protein kinase cascades including ERKs and Akt regulating cell proliferation and survival (Stepan *et al.*, 2004). It has been shown *in vivo* and *in vitro* that gastrin stimulates growth of the pit cell lineage by increasing the expression of the CCK_B receptor (Takeuchi *et al.*, 1980; Johnson, 1988; Nakajima *et al.*, 2002), that is also found on parietal, chief and ECL cells (Nakamura *et al.*, 1987; Tarasova *et al.*, 1996), leading to stimulation of growth by gastrin. Initially, gastrin was believed to act only indirectly as CCK_B receptors were not identified in precursor cells of the isthmus. However, Nakajima *et al.* (2002) demonstrated in a transgenic mouse model that expression of the CCK_B receptor could also be induced in pit precursors by hypergastrinaemia.

It was suggested that, because of the CCK_B receptor expression, gastrin-stimulated cell growth is mediated indirectly by parietal cells and/or ECL cells by expressing heparin binding-EGF-like growth factor (HB-EGF) and TGF-α and Reg, respectively (Nakajima *et al.*, 2002). HB-EGF is expressed in parietal cells (Murayama *et al.*, 1995) and gastrin-induced HB-EGF expression and secretion was shown in CCK_B receptor transfected epithelial cells *in vitro* (Miyazaki *et al.*, 1999). Increased expression of HB-EGF and TGF-α in gastric tissue was also shown in transgenic mice with chronic hypergastrinaemia (Wang *et*

al., 2000b). Beales (2004) demonstrated that gastrin stimulated the secretion of HB-EGF and amphiregulin (AR), but not TGF-α, from parietal cells *in vitro*.

Kirton *et al.* (2002) reported that gastrin also stimulates cell migration and determines the position of parietal cells along the gland axis, although it has no effect on their life span. Other studies have shown that parietal cell maturation is influenced by gastrin (Koh *et al.*, 1997; Friis-Hansen *et al.*, 1998; Chen *et al.*, 2000). In addition, Nagata *et al.* (1996) and Koh *et al.*, (1997) demonstrated that gastrin is essential for the normal expression of the H^+/K^+-ATPase in parietal cells.

1.2.4.3.2 Regenerating Protein (Reg)

Reg, the product of the regenerating gene (*reg*), is expressed by rat (Asahara *et al.*, 1996) and human (Higham *et al.*, 1999) ECL cells as well as human chief cells (Higham *et al.*, 1999). Fukui *et al.* (1998) demonstrated that the expression of Reg in ECL cells was stimulated by gastrin and had mitogenic effects on gastric epithelilal cells *in vitro*. *In vivo*, using transgenic mice, Reg overexpression had a growth-promoting effect on gastric progenitor cells, chief and parietal cell populations, but not surface mucous, ECL or G cells (Miyaoka *et al.*, 2004). In a previous study, the Reg receptor was detected predominantly in chief and parietal cells and only at a low level in surface mucous and progenitor cells (Kazumori *et al.*, 2002).

1.2.4.3.3 EGF-Family Peptides

The EGF receptor ligands TGF-α (Beauchamp *et al.*, 1989; Abe *et al.*, 1997), HB-EGF (Murayama *et al.*, 1995) and AR (Abe *et al.*, 1997) are expressed by parietal cells, some of which are also expressed by chief (Beauchamp *et al.*, 1989) and surface mucous cells (Abe *et al.*, 1997). EGF is produced by submandibular glands among others (Poulsen *et al.*, 1986; Milani and Calabrò, 2001), but its expression was not detected in gastric mucosal cells (Mori *et al.*, 1987; Beauchamp *et al.*, 1989).

The action of EGF peptides is mediated via binding to the EGF receptor (Derynck, 1988), which has tyrosine kinase activity, triggering a signalling pathway that finally leads to the regulation of gene transcription (Milani and Calabrò, 2001). The EGF receptor is widely expressed in the gastric mucosa, including in progenitor cells (Abe *et al.*, 1997), surface mucous cells (Ichikawa *et al.*, 2000), chief cells (Beauchamp *et al.*, 1989; Fiorucci *et al.*, 1996) and parietal cells (Mori *et al.*, 1987; Beauchamp *et al.*, 1989; Abe *et al.*, 1997).

TGF-α and EGF also play important roles after mucosal injury by promoting cell migration, stimulating proliferation and mucus production and suppressing acid production (see also 1.2.2.3.3.5) (Beauchamp *et al.*, 1989; Jones, M. K. *et al.*, 1999; Milani and Calabrò, 2001). TGF-α acts mainly under normal conditions and after acute injury, while EGF mainly acts during chronic ulcer healing (Jones, M. K. *et al.*, 1999). Other growth factors, including HGF, insulin-like growth factor (IGF), keratinocyte growth factor (KGF), TGF-β and TFFs are also involved in gastrointestinal regeneration following injury (Jones, M. K. *et al.*, 1999; Milani and Calabrò, 2001). Furthermore, TGF-α also inhibits apoptosis of pit cells *in vitro* (Kanai *et al.*, 2001) as does EGF in breast adenocarcinoma and embryonic kidney epithelial cells (Gibson *et al.*, 1999). Kanai *et al.* (2001) suggested that this might be important during cell migration, especially of pit cells with their short life span and fast migration, preventing apoptosis due to possible loss of cell contacts (anoikis). On the other hand, inhibition of apoptosis could also play a role in pathology.

1.2.4.3.4 Musashi-1

In rat gastric mucosa, parietal cells located close to the isthmus express Musashi-1 (Nagata *et al.*, 2006), which was first identified by Nakamura *et al.* (1994) in Drosophila as a neural RNA-binding protein. Nagata *et al.* (2006) suggested that these mature parietal cells are the source of Musashi-1, which is probably required for maintenance of neighbouring stem cells and involved in proliferation and differentiation of isthmus-lineage precursors. Musashi-1 expression in the neck of the gland is also enhanced in the initial stages of epithelial regeneration (Nagata *et al.*, 2006). The experiments of Nagata *et al.* (2006) also revealed that some of the Musashi-1 positive cells coexpressed HES5 (mammalian hairy and Enhancer-of-split homologue; basic helix-loop-helix protein), supporting their role in

stem cell maintenance. Among other functions, HES5 is essential during mammalian neural differentiation for activity of the transmembrane receptor Notch, which is activated by Musashi-1 by repressing the translation of m-Numb, the Notch inhibitor (Okano *et al.*, 2002).

1.3 The Parasitised Abomasum

1.3.1 Pathophysiology

During infection with abomasal nematodes, serum gastrin and pepsinogen and abomasal pH generally all increase abruptly either around the time the parasites emerge into the abomasal lumen after a single larval infection (Lawton *et al.*, 1996; Simpson *et al.*, 1997; Scott *et al.*, 2000) or more rapidly after transplantation of adult *H. contortus* (Simpson *et al.*, 1997), *T. circumcincta* (Anderson *et al.*, 1985; Lawton *et al.*, 1996; Scott *et al.*, 2000) or *Ostertagia ostertagi* (McKellar *et al.*, 1987).

Pepsinogen levels usually increase before the increase in abomasal pH and serum gastrin (Jennings *et al.*, 1966; Anderson *et al.*, 1985; McKellar *et al.*, 1986; 1987; Hertzberg *et al.*, 1995; 1999b; Lawton *et al.*, 1996). Low pepsinogen responders may also be observed, with only minimal increase in pepsinogen, but typical increases in gastrin and abomasal pH (Lawton *et al.*, 1996; Simpson *et al.*, 1997). The increase in serum pepsinogen is suggested to be due to leakage through a more permeable epithelium (Holmes and MacLean, 1971; McLeay *et al.*, 1973; McKellar, 1993), perhaps due to damage to tight junctional integrity.

Likely causes of increased circulating gastrin levels are the removal of the inhibitory effects of acid feedback on the G cell (Becker *et al.*, 1973; Fox *et al.*, 1988; 1993; Nicholls *et al.*, 1988; Lawton *et al.*, 1996) caused by inhibition and loss of parietal cells (Scott *et al.*, 2000), at least initially, before other factors may become responsible for maintaining the hypergastrinaemia, such as stimulation by inflammatory mediators, such as histamine (Bado *et al.*, 1984), TNF-α (Lehmann *et al.*, 1996; Weigert *et al.*, 1996) and interleukin (IL)-1β

(Weigert *et al.*, 1996), which are known to increase gastrin release. The involvement of other gastrin stimulants, like inflammation or excretory/secretory (ES) products of the parasites (reviewed in 1.3.3), were suggested because serum gastrin levels may remain elevated in sheep after abomasal pH had already decreased later in an infection (Lawton *et al.*, 1996; Simpson *et al.*, 1997) or when abomasal pH did not rise (Scott *et al.*, 2000). The hypothesis that ES products are responsible for the stimulation of gastrin secretion and elevation of serum gastrin could not be confirmed in *in vitro* experiments with ES products of *T. circumcincta* (Lawton *et al.*, 2002) or *H. contortus* (Haag *et al.,* 2005). The gastrin inhibitor detected in occasional ES preparations was suspected to be due to bacterial contamination. Simcock *et al.,* (2006b) demonstrated that these bacteria are probably rumen bacteria, which survive in the parasitised abomasum due to increases in pH, and release chemicals inhibitory to gastrin secretion. Further experiments with abomasal fluid from parasitised sheep with elevated abomasal pH confirmed the presence of an inhibitor of gastrin release *in vitro*, however, it did not seem to affect gastrin secretion *in vivo* (Simcock *et al.*, 2006a).

A rise in abomasal pH was proposed to be beneficial for the survival of the worms as acid sensitivity experiments *in vitro* (Eiler *et al.*, 1981; Haag *et al.*, 2005) and *in vivo* (Simpson *et al.*, 1999) demonstrated that only L_3 were insensitive to acid conditions. In contrast, the studies of McKellar *et al.* (1987) and Scott *et al.* (2000) revealed that there were also worms present in calves or sheep, respectively, in which abomasal pH did not change or was only moderately increased. This suggested that the parasites may associate with the more neutral environment of secreted mucus or they are able to abolish or neutralise acid secretion only in their direct environment and not in the whole abomasum. The latter could be important if the worm burdens are low.

Increased abomasal pH is associated with parietal cell loss, as well as inhibition of remaining parietal cells (Scott *et al.*, 2000). After parasite removal by drenching, the pH decreased rapidly to normal levels or sometimes even to below pre-infection levels, suggesting that a parasite-derived factor inhibited the parietal cell function temporarily and, once removed, the secretory function recovered quickly (Armour *et al.*, 1967; Simpson *et al.*, 1997; Scott *et al.*, 2000). This period of recovery can be too short to be dependent on substantial reparation of the mucosa and is most likely due to a reactivation or re-differentiation of a resting cell population (Hertzberg *et al.*, 2000). It may also be due to

generation of new parietal cells, which mature within two days (Karam, 1993) and then become very active (Coulton and Firth, 1983; Karam *et al.*, 1997). Successful stimulation of acid secretion with histamine or carbachol in sheep infected with *Ostertagia leptospicularis* (Hertzberg *et al.*, 2000) or during feeding in sheep infected with *T. circumcincta* (Lawton *et al.*, 1996) indicated that there must still be a population of functional parietal cells in the abomasum. Hertzberg *et al.* (2000) found a population of parietal cells in infected sheep which were not identified using immunohistochemistry with a H^+/K^+-ATPase antibody. They suggested that failure to label parietal cells might be due to the proton pump being in an inactive form in the tubulovesicles of resting parietal cells. However, the H^+/K^+-ATPase antibody would be expected to bind even to an inactive form of the proton pump. Inactive parietal cells have been identified ultrastructurally in parasitised tissue (McLeay *et al.*, 1973; Hertzberg *et al.*, 2000; Scott *et al.*, 2000).

Temporary increases in pH observed in sheep, which were exposed to adult worms confined in porous bags, supported the suggestion of parietal cell inhibition by a parasite-derived factor (Simpson *et al.*, 1999). Although, this mainly occurred in the sheep receiving a high worm dose (18,000 versus 9,000 adult *T. circumcincta*) and was transient, it occurred without direct contact between the parasites and the abomasal mucosa suggesting an ES product could be responsible for the parietal cell inhibition. The secreted chemicals may act either directly on the parietal cell or act indirectly via other cells such as the histamine-secreting ECL cell (Hertzberg *et al.*, 2000). Merkelbach *et al.* (2002) have shown that ES products of *H. contortus* are capable of directly inhibiting parietal cell function *in vitro* (see also 1.3.3.7.1). In addition to transient increases in abomasal pH, Simpson *et al.* (1999) reported that adult worms placed into porous bags and out of contact with the abomasal mucosa were dead within 16 hours of transplant. It is possible that the increased pH in response to these worms was due to dead and dying worms, which could induce an inflammatory response which affects abomasal function.

The host may contribute to the inhibition of acid secretion through the inflammatory response. Large numbers of eosinophils and neutrophils are seen infiltrating the mucosa during ostertagiosis (Scott *et al.*, 1998a; 2000). Chemicals released by inflammatory cells, which might damage the host tissue as well as the pathogens, include cationic proteins and reactive oxygen metabolites (Harlan, 1985; Levy and Kita, 1996; Meeusen, 1999). In

general, granulocytes produce several cytokines, including IL-1β and TNF-α, which are able to inhibit acid secretion (Lord *et al.*, 1991; Robert *et al.*, 1991). IL-1β also inhibits the ECL cell (Prinz *et al.*, 1997). Similarly, in *Helicobacter pylori* induced enlarged fold gastritis, IL-1β levels correlated with the degree of inhibition of acid production (Yasunaga *et al.*, 1997). In *T. circumcincta* infected sheep, the infiltration of inflammatory cells coincides with alterations in gut morphology and function (Scott *et al.*, 2000). The experiments of Przemeck (2003) also indicated that the inflammatory response might play a role in the development of hypoacidity and could be involved in mucosal thickening. Hypoacidity was associated with numbers of tissue eosinophils and reduction in parietal cells in both larval infection and after adult transplant.

1.3.2 Histopathology

During infection, the cellular composition of the glands is altered, initially in the regions where larvae are developing, but more generally after the parasites emerge. Nodules can be observed macroscopically around developing larvae within the glands. Parietal and chief cells in and around infected glands are lost and replaced by mucous cells or minimally differentiated cells, although there are usually no changes in abomasal pH during this time (Armour *et al.*, 1966; Durham and Elliott, 1976; Scott *et al.*, 1998a). In addition, parietal cells may become vacuolated (Przemeck, 2003). After the parasites emerge, these cellular changes can be seen throughout the fundus, notably reduced parietal cell numbers, which correlate with increased abomasal pH (Scott *et al.*, 1998a; 2000). Parietal cell loss and vacuolation appear also after adult worm transfer. Only one day after adult *T. circumcincta* transfer into the sheep abomasum, parietal cell numbers are reduced and eight days after adult transfer, there is mucous cell hyperplasia, marked accumulation of inflammatory cells (eosinophils, neutrophils and lymphocytes), fundic mucosal thickening (Scott *et al.*, 2000), and the number of recognisable parietal cells was approximately halved (Scott *et al.*, 1998a).

In sheep infected with larval *T. circumcincta*, parietal cells were also larger than normal, especially close to the gland base (Scott *et al.*, 1998a). Scott *et al.* (1998a) suggested that possibly the length of time the cells were exposed to high concentrations of circulating

gastrin increased their size or they may have a different function from acid secretion, such as maintenance of gland growth.

Gastrin is a known growth stimulating agent (reviewed in 1.2.4.3.1). Konda *et al.* (1999) and Wang *et al.* (2000b) demonstrated foveolar hyperplasia in response to hypergastrinaemia. However, hypergastrinaemia resulting from increased pH after inhibition of the H^+/K^+-ATPase by omeprazole (Karam and Forte, 1994) or inhibition of the H_2 receptors by ranitidine (Karam and Alexander, 2001) increased only the production of parietal cell progenitors. Chronic hypergastrinaemia can also have a different effect from an acute increase in gastrin, resulting in decreased parietal cells numbers (Wang *et al.*, 2000b; Cui *et al.*, 2006). This was suggested to be due to apoptosis mediated via gastrin/CCK_B and H_2 receptors (Cui *et al.*, 2006) or up-regulation of the growth factors HB-EGF and TGF-α (Wang *et al.*, 2000b).

In a wide spectrum of gastric diseases, such as infection of diverse host species with nematodes including *Teladorsagia* spp. (Barker *et al.*, 1993), Ménétrier's disease (Dempsey *et al.*, 1992), the response of the stomach to chronic exposure to noxious chemicals (Lacy *et al.*, 1996) and infection of mice with *Helicobacter felis* (Fox *et al.*, 1996), the pathology is almost identical, including mucous cell hyperplasia and parietal cell loss. Therefore, Scott *et al.* (1998a) suggested that these cellular changes may not be parasite specific, but due to the host response with an altered production of growth factors.

The role of EGF peptides in the normal maintenance of the gastric epithelium has been summarised in 1.2.4.3.3, but they may also act *in vivo* during infection. Overexpression of TGF-α in transgenic mice was shown to result in loss of parietal and chief cells but also foveolar hyperplasia, a phenotype similar to that in Ménétrier's disease in humans (Dempsey *et al.*, 1992; Takagi *et al.*, 1992; Sharp *et al.*, 1995). In addition to the upregulated expression of peptides from the EGF-family, which was demonstrated in surface mucous cells of *T. circumcincta* infected sheep (Scott *et al.*, 1995), another source of TGF-α could be eosinophils (Elovic *et al.*, 1990; Wong *et al.*, 1990), neutrophils or monocytes (Calafat *et al.*, 1997).

The loss of parietal cells and concomitant loss of trophic agents released by parietal cells is possibly an important factor in the pathology observed in abomasal parasitism and may play a role in mucous cell hyperplasia or the loss of chief cells, which was similarly seen by Li *et al.* (1996) in a transgenic mouse model. In addition, hypergastrinaemia as a result of increased pH due to inhibition and loss of parietal cells could affect gland morphology as described above.

Scott *et al.* (1998a) suggested that the decrease in parietal cell numbers may be due to both the loss of mature parietal cells and the failure to produce new cells. Parietal cells from sheep infected with either larvae or adult worms often appear vacuolated, a response possibly caused by parasite ES products. This effect may be similar to *H. pylori* vacA-induced vacuolation to which the vacuolation was previously compared (Przemeck, 2003; Huber *et al.*, 2005; Przemeck *et al.*, 2005), although the mechanism of parietal cell loss and vacuolation remains unknown.

1.3.3 Parasite Excretory/Secretory Products

ES products are molecules released during *in vitro* culture of parasites including abomasal nematodes, which are known or presumed to be released also *in vivo*. ES products may originate from the secretory glands, products of the parasite metabolism or the parasite surface and include metabolic endproducts, chemotaxins, enzymes and immunomodulators.

The biological functions of ES products are believed to be diverse and few are well characterised, but likely aid in tissue penetration, feeding and immune evasion (Knox, 2000). Direct interaction with the host has been shown for several ES proteins from their recognition by the host immune system, although the variation in immunogenicity was high (Yatsuda *et al.*, 2003). Antigenic ES products have been used for vaccination studies, such as total adult *H. contortus* ES products and low molecular weight antigens (Schallig and Leeuwen, 1997), thiol-binding ES proteins of *H. contortus* (Bakker *et al.*, 2004) and 15kDa and 24kDa ES antigens of *H. contortus* (Schallig *et al.*, 1997). These also include the

H. contortus galactose-containing glycoprotein complex (H-gal-GP) from the parasites intestine, which are so-called hidden antigens, containing various antigens some of which are also present in ES products, like the metallopeptidases (Smith, W. D. *et al.*, 1994) and H11 (Munn *et al.*, 1977; Andrews *et al.*, 1995). The hidden antigens are considered of particular interest as they are not normally seen by the host.

Stage specific differences in ES products have been shown for some parasites. Gamble and Mansfield (1996) demonstrated that the amount of ES products released by *H. contortus in vitro* increased after larvae had moulted to the fourth stage, when feeding also started, suggesting a possible role in nutrient digestion by the parasite. The composition and antigenic behaviour were also different: L_4 ES products contained several enzymes which were not present in L_3 ES products and antigenic reactivity was greater against L_4 ES products. Similarly, there were differences between ES products from *T. circumcincta* post-infective L_3 and L_4 (Smith *et al.*, 2009) and L_4 and adult parasites (Craig *et al.*, 2006).

1.3.3.1 Proteases

Much attention has focussed on the proteases in ES products because of their potential importance in parasite invasion and nutrition. Proteomic analyis by Yatsuda *et al.* (2003) detected 224 and identified 107 proteins in adult *H. contortus* ES products. Among those were several proteases, including zinc metallopeptidases, serine proteases and aspartic proteases. Cysteine proteases have also been detected (Oliver *et al.*, 2006; Yatsuda *et al.*, 2006). This group includes cathepsin B-like proteases (CBLs) and asparaginyl proteinase (legumain). A putative cysteine protease was also identified in *T. circumcincta* L_4 ES products (Craig *et al.*, 2006), as well as cathespsin F and an *O. ostertagi* homologous astacin-like metalloprotease in post-infective L_3 and L_4 ES products (Smith *et al.*, 2009).

Yatsuda *et al.* (2003) identified four different metallopeptidases, including H11/concortin, in *H. contortus* ES products; these enzymes were also identified from the intestinal brush border of *H. contortus* (Munn, 1977; Newlands *et al.*, 2006; Geldorf and Knox, 2008). H11 is usually classified as a hidden antigen which is not presented to the host immune system, but was found in all their ES preparations examined (Yatsuda *et al.*, 2003). H11 degraded

Facing page 33

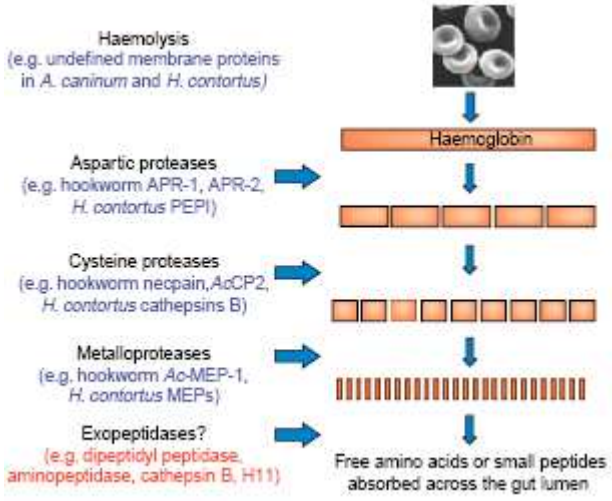

Figure 1.25: Putative proteolytic cascade for hemoglobin degradation by blood-feeding nematodes. Host hemoglobin (Hb) is initially attacked by aspartic proteases, degraded to smaller peptides by cysteine proteases, then by metalloproteases and finally to free amino acids or small peptides by exopeptidases. APR: aspartic protease; PEPI: parasite pepsinogen-like aspartic protease; Ac: *A. canium*; CP: cysteine protease; MEP metalloprotease. (Williamson *et al.*, 2003)

fibrinogen and was suggested to function as an anti-coagulant during blood feeding (Geldorf and Knox, 2008). Serine proteases were also proposed to be anticoagulants. Furthermore, serine proteases in ES of *Schistosoma mansoni* degraded IgE (McKerrow *et al.*, 2006). Serine and metalloproteases of *Trichostrongylus vitrinus* ES products were shown to degrade fibrinogen, plasminogen and fibronectin (Maclennan *et al.*, 1997) and aspartic proteases of shistosomes and *H. contortus* degraded hemoglobin (Longbottom *et al.*, 1997; Brindley *et al.*, 2001). *S. mansoni* asparaginyl proteinases activated cathepsin B, which is also believed to be the case for *H. contortus* asparaginyl proteinase (Sajid *et al.*, 2003; Oliver *et al.*, 2006).

Cysteine proteases, including CBLs, are the most widely reported protease class from parasitic nematodes. CBLs of *H. contortus* are encoded by 22 genes (Jasmer *et al.*, 2001) and at least seven CBLs have been identified in ES products (Yatsuda *et al.*, 2006). *H. contortus* cysteine proteases present in adult ES products, as well as in live L_4 and adult parasites, were able to degrade a model extracellular matrix consisting of glycoproteins, elastin and collagen (Rhoads and Fetterer, 1996). In addition, cysteine proteases in extracts of *H. contortus* digested hemoglobin, fibrinogen, collagen and IgG (Williamson *et al.*, 2003). A putative proteolytic cascade for hemoglobin digestion, shown in Figure 1.25, was proposed to include all protease classes (Williamson *et al.*, 2003; 2004).

1.3.3.2 Protease Inhibitors

In addition to proteases, different classes of protease inhibitors have also been identified in a variety of parasites, including *Schistosoma* spp., *Ascaris* spp., *Brugia malayi*, *Onchocerca volvulus*, *Trichuris suis*, *T. vitrinus*, *O. ostertagi* and *H. contortus*. Functions assigned to the inhibition range from regulating parasite proteases, protection against degradation of proteins by host proteases, modulation of the host immune response and/or a role during feeding as anticoagulants (McKerrow *et al.*, 2006; Knox, 2007). A serine proteinase inhibitor (serpin) was identified in ES products of L_4 and adult *T. vitrinus* (MacLennan *et al.*, 2005). Serpins were also detected in *H. contortus* adult ES products, but were thought to be of host origin (Yatsuda *et al.*, 2003). Homologues of *Ancylostoma caninum* anticoagulant proteins of the serine protease inhibitor family have also been detected in *H. contortus* (Knox, 2007).

1.3.3.3 Antioxidant Enzymes

The antioxidant enzymes superoxide dismutase (SOD) and glutathione S-transferase have been identified in ES products of adult *H. contortus* (Yatsuda *et al.*, 2003) and thioredoxin peroxidase in ES of *T. circumcincta* L_4 (Craig *et al.*, 2006). These enzymes are used by the parasites to protect against oxidative stress generated by their own cellular metabolism or by the host, including potentially damaging reactive oxygen and nitrogen intermediates produced by immune cells. SOD and thioredoxin peroxidase were also found in other parasitic nematodes, including *O. volvulus* and *B. malayi* (Henkle-Dührsen and Kampkötter, 2001; Hewitson *et al.*, 2008). In *O. volvulus*, SOD was located in the intestine, where it could minimise oxidative damage after ingestion of host erythrocytes.

1.3.3.4 Other Enzymes

Fetterer and Rhoads (2000) detected acid phosphatase and phosphorylcholine hydrolase in adult *H. contortus* ES products. Acid phosphatase was suggested to play a role in intestinal digestion, as the highest tissue concentrations were detected in the worm intestine. This is consistent with the suggestion that acid phosphatase secretion by fourth stage larvae coincides with the onset of feeding (Gamble and Mansfield, 1996). The proposed role for the secreted acid phosphatase was to act in combination with cysteine proteases in extracorporeal digestion and tissue penetration (Fetterer and Rhoads, 2000).

Nucleoside diphosphate kinase has been identified in ES products from adult *H. contortus* (Yatsuda *et al.*, 2003), adult *T. circumcincta* (Craig *et al.*, 2006) and *Trichinella spiralis* (Gounaris *et al.*, 2001). Proposed functions range from regulation of host cell proliferation and differentiation, ATP-dependent cytotoxity for macrophages and mast cells and prevention of apoptosis (Zaborina *et al.*, 1999; Punj *et al.*, 2000; Gounaris *et al.*, 2001).

Acetylcholinesterase has been detected in a range of nematode ES products, primarily from adult parasites, including *Nippostrongylus brasiliensis*, *T. vitrinus*, *Nematodirus battus*, *Trichostrongylus colubriformis*, as well as *T. circumcincta* and *H. contortus* (Knox and Jones, 1990; Mallet *et al.*, 1997; Joshi and Singh, 2000). A role for acetylcholinesterase has been

suggested in the prevention of peristalsis and parasite expulsion (Opperman and Chang, 1992), inhibition of mucus secretion (Philipp, 1984) and alteration of the immune response (Rhoads, 1984). *In vitro*, *T. colubriformis* acetylcholinesterase stimulated cell growth at low concentrations and had an inhibitory effect at high concentrations, suggesting a role in intestinal crypt cell repair and renewal during parasitism (Huby *et al.*, 1999).

In their adult *H. contortus* ES products, Yatsuda *et al.* (2003) detected the cytosolic enzymes glutamate dehydrogenase (GDH) and glycolytic enzymes including enolase, but no other intracellular proteins such as ribosomal or cytoskeletal proteins, which might have indicated some cell damage. However, several metabolic enzymes are secreted into ES or are present on the helminth surface and do not necessarily indicate cell damage. Skuce *et al.* (1999) demonstrated that GDH is located in the gut of *H. contortus* and may be shed into ES products. Similarly, a range of homologous metabolic enzymes, including enolase, have been detected in *T. circumcinta* L_4 and adult ES products (Craig *et al.*, 2006). Several structural proteins including actin, tropomyosin and paramyosin have been detected in ES products of both these stages and may or may not be derived from degrading parasites in culture.

Enolase has been detected in ES products from *Fasciola hepatica*, *Echinostoma caproni*, adult *Schistosoma bovis*, *T. spiralis* as well as in most tissues of adult *O. volvulus* and infective larvae (Jolodar *et al.*, 2003; Bernal *et al.*, 2004; Pérez-Sánchez *et al.*, 2006; Marcilla *et al.*, 2007). Even though enolase lacks a signal peptide for secretion in most cases, a conserved region at the amino-terminus has been suggested as a signal peptide for *T. spiralis* and *E. caproni*. Enolase of *F. hepatica*, *E. caproni* and *O. volvulus* bound human plasminogen *in vitro*. Host activators convert plasminogen to plasmin, which has proteolytic activities. It was suggested that this might have a role in host tissue invasion by promoting attachment to the mucosa and, through plasmin-mediated proteolysis, might cause degradation of the extracellular matrix (Jolodar *et al.*, 2003; Marcilla *et al.*, 2007).

1.3.3.5 Calreticulin

Suchita and Joshi (2005) found that adult *H. contortus* ES products contain calreticulin, which prolonged the plasma coagulation time, suggesting a function in the prevention of

blood clotting by binding Ca^{2+}, clotting factors and C-reactive protein (CRP), presumably aiding blood feeding of the parasite. Another proposed function is the modulation of the host immune response by binding to CRP and complement C1q. Binding to secreted calreticulin may limit the concentration of free CRP, blocking its procoagulant function as well as the activation of the classical complement pathway. This pathway can be activated by CRP-C1q interaction and inhibition may take place by calreticulin binding to CRP or directly to C1q (Suchita and Joshi, 2005; Suchita *et al.*, 2008). Secretion of calreticulin and its interaction with C1q was also shown for *Necator americanus* and *Trypanosoma cruzi* (Kasper *et al.*, 2001; Ferreira *et al.*, 2004).

1.3.3.6 Non-Protein Compounds

Generally, studies have investigated the proteins present in ES products, although a few studies have also reported the release of other components by *H. contortus* and *T. circumcincta*. These include the metabolic endproducts propan-1-ol, acetate and propionate, as well as small amounts of ethanol, lactate and succinate (Ward and Huskisson, 1978; Ward *et al.*, 1981).

Hadás *et al.* (1998) detected the prostaglandins PGA_2 and PGB_2 in *T. colubriformis* and *H. contortus* larval ES products, as well as PGA_2, PGB_2, PGD_2 and $PGF_{2\alpha}$ in extracts from larvae and adults of both species. The release of prostaglandins was also reported for *Trypanosoma brucei* and *T. cruzi*, *Schistosoma* spp., *N. americanus* and *O. volvulus* (Daugschies and Joachim, 2000; Kubata *et al.*, 2007). It has been suggested that prostaglandins are released by the parasites to modulate host physiology and/or immune reaction in their vicinity, which might include the induction of inflammation, downregulation of cytokines or decreased gastric secretion.

1.3.3.7 *In vitro* Functions - Further Possibilities for *in vivo* Actions

1.3.3.7.1 Effects on Secretion

ES products of abomasal nematodes have been shown to stimulate pepsinogen secretion, inhibit the ECL cell and acid secretion, but not secretion of gastrin. Merkelbach *et al.* (2002) found that adult *H. contortus* ES products were able to inhibit acid secretion by rabbit gastric glands *in vitro*. The active ES component(s) for this effect was found to be smaller than 5kDa. Ammonia was suggested as a possible active component as parallel testing with ammonium chloride in equivalent concentrations to those in the ES preparations showed a similar response. Hertzberg *et al.* (1999a) demonstrated that adult *H. contortus* ES products were able to inhibit the secretory activity of ECL cells *in vitro*. They suggested that parietal cell stimulation, and therefore acid secretion, was suppressed by the inhibition of the ECL cells by parasite ES products. *In vitro*, pepsinogen release from abomasal tissue was demonstrated after exposure to ES products from *T. circumcincta*, but only in tissues from animals that had been previously exposed to parasites (Scott and McKellar, 1998). It was suggested that hypersensitivity reactions to antigens present in ES products were responsible. Neither Lawton *et al.* (2002) nor Haag *et al.* (2005) were able to find evidence for a gastrin stimulant in ES products of several life cycle stages of *T. circumcincta* or *H. contortus*, respectively (see also 1.3.1).

1.3.3.7.2 Immunomodulatory Effects

A variety of molecules with immunomodulatory effects have been identified in extracts and ES products of numerous helminths (Johnston *et al.*, 2009). These immunomodulatory effects include induction of eosinophil and neutrophil chemotaxis, inhibition of eosinophils or monocytes, reduction or increase in cytokine levels and induction of growth factor release.

An inhibitor of monocytes has been found in adult *H. contortus* ES products (Rathore *et al.*, 2006). The 66kDa ES antigen was able to reduce the production of hydrogen peroxide and nitric oxide from monocytes *in vitro* by as yet undefined mechanisms. This may be another

possible antioxidative strategy in addition to the antioxidant enzymes described above (1.3.3.3).

An eosinophil chemoattractant is produced by both *H. contortus* and *T. circumcincta* (Reinhardt, 2004; Wildblood *et al.*, 2005). Extracts from L_3, L_4 and adult parasites had a dose-dependent stimulatory effect on the migration of eosinophils. Similar effects were obtained with ES products from L_3 as well as live L_3 (Wildblood *et al.*, 2005). A lectin in ES products from *O. ostertagi* was responsible for eosinophil chemotaxis (Klesius, 1993) whereas in *H. contortus* it was likely due to a galectin or galectin mixture (Turner *et al.*, 2008). Galectins were also found in ES products of *T. circumcincta* L_4 and different stages of *B. malayi* (Craig *et al.*, 2006; Hewitson *et al.*, 2008; Moreno and Geary, 2008). In addition, using cDNA cloning, Greenhalgh *et al.* (2000) detected three novel galectins, which were stage specifically expressed at different concentrations in *H. contortus*. Turner *et al.* (2005) suggested that it is possible that parasite galectins mimic the action of host galectins, which have been shown to have diverse functions, including eosinophil chemoattractant activity (galectin-9 (Hirashima, 2000)), modulation of cell adhesion and apoptosis (galectin-8 (Hadari *et al.*, 2000; Zick *et al.*, 2004)). Neutrophil chemotaxins have been detected in a range of parasites including *H. contortus* (Reinhardt, 2004), *T. circumcincta* (Reinhardt, 2004), *Ascaris* (Tanaka *et al.*, 1979) and *O. volvulus*, where the activity has been shown to be dependent on *Wolbachia* endobacteria (Brattig *et al.*, 2001). It was suggested that the recruitment of inflammatory cells might be beneficial for the parasites by damaging parietal cells thus reducing acid secretion and pepsinogen activation (Simpson, 2000) and/or tissue damage being beneficial for parasitic invasion (Wildblood *et al.*, 2005). Alternatively, they could just evoke an inflammatory response.

1.3.3.7.3 Effects on Cell Proliferation

A few studies examined the effects of ES products on cell proliferation (Hoste *et al.*, 1995; Huby *et al.*, 1995; 1999). *T. colubriformis* ES products increased cell proliferation in a dose-dependent manner in most cell lines tested, including epithelial cells of digestive (RIC, IEC-6, IRD-98 and HT29-D4) and non-digestive origin (MDCK) and inhibition only in epithelial cells of non-digestive origin (CHO and 3T3) (Hoste *et al.*, 1995; Huby *et al.*, 1999).

T. circumcinta ES products also had a stimulatory effect on HT29-D4 cells, but no significant effect was observed for *H. contortus* (Huby *et al.*, 1995). In contrast, Abner *et al.* (2002) found a dose-dependent cytotoxic response of *T. suis* ES products on intestinal epithelial cells, particularly IPEC-1 and INT407. Furthermore, Przemeck *et al.* (2005) and Huber *et al.* (2005) noted an increased rate of cell detachment after exposure of ES products from L_3 and adult *H. contortus* and *T. circumcincta* to HeLa cells (epithelial, human cervix adenocarcinoma cells), but this was not quantitated.

1.3.3.7.4 Cell Vacuolation

ES products from L_3 and adult *H. contortus* and *T. circumcincta* have been shown to cause vacuolation in HeLa cells in a stage- and parasite-density dependent manner (Huber *et al.*, 2005; Przemeck *et al.*, 2005). The effect of vacuolation was enhanced by adding 8mM ammonium chloride to the medium (Przemeck *et al.*, 2005). The ammonia in ES products was therefore considered as a possible contributor of the vacuolation activity in the ES products of abomasal nematodes, similar to *H. pylori*-induced vacuoles. VacA, the vacuolating cytotoxin from *H. pylori*, forms anion-selective channels, which are internalised and insert into late endosomes. This changes the permeability of late endosomes and enhances the vacuolar ATPase proton pumping activity to compensate for the increased anion concentration. Ammonia generated by *H. pylori* urease enters the acidic organelles and is protonated to ammonium and trapped. Osmotic influx of water leads to vesicle swelling, forming a vacuole (Montecucco and de Bernard, 2003; Cover and Blanke, 2005). However, observations by Huber *et al.* (2005) indicated that ES component(s) other than ammonia might be involved. Larval and adult ES preparations contained the same concentrations of ammonia, but larval ES preparations induced less severe vacuolation. Additionally, incorporated Neutral red (NR), which is a lipophilic free base and commonly used for quantitative analysis of VacA induced vacuolation by *H. pylori* (Cover *et al.*, 1991; Garner and Cover, 1996), was observed to be localised in the cytosol and peri-nuclear regions and not inside the numerous small vacuoles. In contrast, in vacuoles induced by *H. pylori* VacA, NR accumulates almost exclusively within the vacuoles, which were fewer in number and significantly larger in size than those induced by ES products.

1.4 Conclusions

Despite the extensive knowledge which has been gained of the pathophysiological and histopathological effects in response to abomasal parasitism, the underlying host-parasite interactions and mechanisms resulting in the observed pathology are mainly unknown. The number of reports about the contents of ES products has grown immensely over recent years, but the functionality of ES products remained in many cases speculative and was often gained from comparisons with analogous components of other pathogenic species or eukaryotic components in general.

Experiments described in the following chapters were aimed at further investigating host-parasite interactions, especially the early stages of infection. The particular focus was on the fate of the parietal cell and possible roles for ES products, which might initiate the characteristic pathology. Experiments were aimed to develop techniques to study the early events of parasitism by *H. contortus* and *T. circumcincta in vivo* (chapter 2). ES was examined *in vitro* using several model systems. The main focus was on potential roles of ES products during abomasal parasitism, with the model systems mimicking some of the pathological effects of parietal cells *in vivo*, including induction of cellular vacuolation (chapter 3) and the detachment and loss of cells (chapter 4). In addition, effects of ES products on the epithelial barrier function were investigated (chapter 5).

Chapter 2

EFFECTS OF PARASITISM ON THE ABOMASAL MUCOSA

2.1 Introduction

Despite numerous extensive descriptions of the histopathology associated with abomasal parasitism, the specific initiating factors and the contributions of host and parasite to the pathology remain speculative. These histological changes during infection with abomasal parasites include mucous cell hyperplasia and decreased numbers of chief and parietal cells (Scott *et al.*, 1998a, c; 1999; 2000; Przemeck, 2003). Vacuolation of parietal cells has been observed after infection with *T. circumcincta* larvae and after adult worm transfer (Scott *et al.*, 1998a; 2000; Przemeck, 2003). Inhibition and loss of parietal cells could be a key factor in the cellular changes in the fundic glands, as parietal cells play an important role in maintenance and differentiation of gastric gland cells (1.2.4.2). Many other models of similar pathologies involve depletion or functional abnormalities in the parietal cells. One example is the loss of mature parietal cells evoked by diphtheria toxin, which causes

mucosal hyperplasia and affects the differentiation of the chief cell lineage and causes loss of chief cells (Li *et al.*, 1996).

ES products are likely to be involved at least in the early initial contact between the parasite and the host tissues and to play a part in initiating the pathophysiology and inflammatory response. This is supported by the rapid effects on gastric function by transplantation of adult worms, which do not invade the tissues in the same way as larvae do. Widespread inhibition of gastric acid secretion coincides with emergence of parasites from the glands (Lawton *et al.*, 1996; Simpson *et al.*, 1997; Scott *et al.*, 2000) and can be mimicked by transplantation of adult worms (Anderson *et al.*, 1985; Lawton *et al.*, 1996; Scott *et al.*, 2000). Evidence of nematode ES products being involved in targeting parietal cell function *in vivo* has been reported (Simpson *et al.*, 1999; Hertzberg *et al.*, 2000). I*n vitro*, ES products were demonstrated to inhibit acid secretion (Merkelbach *et al.*, 2002) and also, in preliminary findings, to inhibit the secretory activity of the ECL cell (Hertzberg *et al.*, 1999a).

It has been suggested that parasites may target parietal cell function as a deliberate strategy to increase the abomasal pH and promote their survival in the abomasum (Simpson, 2000). The experiments of Lawton *et al.* (2002) and Haag *et al.* (2005) demonstrated that parasitic stages (day 15 to week 8 p.i.) of *T. circumcinta* and *H. contortus* did not survive long at pH 2.5 or 3.5, but tolerated incubations at pH 4.5 and above. In contrast, exsheathed L_3 survived even at pH 2.5 for at least a few days. Additionally, the optimal pH for egg laying by adult *H. contortus* was found to be between 4 and 4.5 (Honde and Bueno, 1982).

Alternatively, the observed histopathological and pathophysiological changes could be accounted for by the response of the host to the presence of the parasites (Scott *et al.*, 1998a; 2000; Simpson, 2000). Parasitised tissues usually contain large numbers of eosinophils and neutrophils (Scott *et al.*, 1998a; 2000), which are capable of damaging host tissue by the release of cationic proteins and reactive oxygen metabolites (Harlan, 1985; Levy and Kita, 1996; Meeusen, 1999). In addition, inflammatory cytokines and growth factors could affect gastric secretion and cellular composition of the glands. IL-1β, TNF-α, TGF-α, EGF and HGF have been shown in different studies to inhibit acid secretion (Beales, 2000). Overexpression of TGF-α led to foveolar hyperplasia (Beales, 2000). In *H. pylori* induced enlarged fold gastritis, IL-1β release was shown to correlate with

hypoacidity (Yasunaga *et al.*, 1997). This could also be a possibility in nematode infections. Among other factors, IL-1β and TNF-α were up-regulated after *T. circumcincta* infection (Craig *et al.*, 2006).

Experiments reported in this chapter were aimed at investigating parasite interactions with the host tissue soon after larval infection and the early effects of adult parasites on host tissue. For the former approach, different fluorescent dyes were used to label larvae before infection in order to facilitate the identification of larvae inside the tissue. Collection of abomasal tissue containing parasitised glands has previously proved difficult because of minimal visible effects on the abomasal mucosa for a period after larval infection (Przemeck, 2003). The early effects of adult parasites on host tissue were studied using tissue of infected sheep after transplantation of adult *T. circumcincta* at different time points post infection, with a particular focus on the function of parietal cells. Parietal cells were labelled with TGF-α antibody, which identifies those cells expressing that growth factor, which is known to be involved in the pathology associated with parietal cell loss (Dempsey *et al.*, 1992; Takagi *et al.*, 1992; Sharp *et al.*, 1995; Li *et al.*,1996). In addition, parietal cells were labelled with H^+/K^+-ATPase-antibodies to identify cells expressing the proton pump. Different lectins were also assessed as markers for sheep parietal cells. Kessiman *et al.* (1986) identified four lectins that stained parietal cells intensely: *Bandieraea simplicifolia* lectin (BSL), *Dolichos biflorus* agglutinin (DBA), peanut agglutinin (PNA) and Soybean agglutinin (SBA). *Ulex europaeus* agglutinin (UEA) was reported to have a weak binding intensity. The use of different markers of parietal cell function aimed to identify subpopulations of parietal cells showing different labelling characteristics.

2.2 Early Changes within the Abomasal Mucosa after Infection with Labelled *H. contortus* L_3

2.2.1 Materials and Methods

2.2.1.1 Experimental Overview

First, a non-toxic method of fluorescent labelling of *H. contortus* L_3 was developed with the aim of facilitating identification of infected glands. Sheep were infected with a 1:1 mixture of labelled and unlabelled *H. contortus* L_3 and euthanased at times between 18h and 48h p.i. for collection of tissues for examination by confocal microscopy with the aim of investigating early larva interactions with the host tissue.

2.2.1.2 Parasites

A laboratory strain of *H. contortus* was maintained by regular passage through sheep for *in vitro* studies and infection of sheep for tissue collection (Appendix I). Before infection of sheep, the viability of the L_3 was checked and confirmed to be greater than 95%. For *in vitro* labelling, *H. contortus* L_3 from the larval culture stock were centrifuged for 5min at 3000rpm (centrifuge 5810R, Eppendorf) and the supernatant removed.

2.2.1.3 Labelling of *H. contortus* L_3

Three different fluorescent dyes were assessed as labels for *H. contortus* larvae. The dyes tested were: (1) the DNA dye Hoechst 33258 (UV (ultraviolet) laser/405nm excitation with emission maximum at ~460nm/blue fluorescence) at a concentration of 15µg/ml for 1h or 15h; (2) the DNA dye Syto®17 (green laser/546nm excitation with emission maximum at ~650nm/red fluorescence) at concentrations of 20µM and 50µM for 1h and 4h or (3) the lipophilic dye Nile Red (green laser/546nm excitation with emission maximum at

~630nm/red fluorescence) at 5μg/ml for 1h (Appendix I; suppliers of all chemicals used for the thesis are listed in Appendix VI). After incubation of the larvae with the different dyes for the specified time, they were washed with water to remove excess dye and examined in an inverted confocal microscope (TE-2000 U Eclipse, Nikon) with 20x and 40x objectives with UV and green laser excitation. Images were processed with Adobe Photoshop (version CS).

2.2.1.4 Infection of Sheep with Labelled *H. contortus*

Sheep used were male Romney or Romney cross ranging from four to seven months of age. They were drenched when brought indoors and confirmed negative for nematode parasites before infection (Appendix I).

Five sheep were infected with a 1:1 mixture of unlabelled *H. contortus* L_3 and labelled *H. contortus* L_3 with Hoechst 33258 for 1h. The total infective doses were 25,000, 30,000 or 50,000 L_3. The sheep were euthanased by captive bolt and exsanguination 18h (two sheep), 30h, 36h or 48h after infection for collection of abomasal tissue. An additional sheep was infected with 200,000 L_3 labelled for 15h with Hoechst 33258 to assess the infectivity of labelled L_3. This sheep was euthanased 24h p.i. for counting the number of larvae in the abomasal contents and tissue.

2.2.1.5 Preparation of Abomasal Tissue for Microscopy

Tissue folds were removed as soon as possible after death (~30min) and washed with phosphate buffered saline (PBS) warmed to 37°C (Appendix I). The mucosa was teased apart on each side of the fold by carefully cutting and ripping the connective tissue, laid flat in the lid of a petri dish and covered with fixative. Whole folds were similarly fixed. For confocal microscopy, 4% paraformaldehyde was used as fixative (Appendix II). The bottom of the dish was laid on top to hold the tissue flat during fixation for 30min at room temperature. The tissue was washed twice with PBS for 10min each and stored in PBS at 4°C.

In addition, tissue was fixed for paraffin embedded sections in a similar procedure. The tissue was initially fixed with Carnoy's fluid for 24h in glass petri dishes, followed by fixation in 2% calcium acetate : 4% paraformaldehyde (1:1 v/v) for 3h. The fixed tissue was stored in 70% ethanol at 4°C. Solutions used are listed in Appendix V. Fixed tissue was trimmed to ~1cm^2 and routinely processed and embedded in paraffin wax by the IVABS histology laboratory.

To cover a larger portion of the fundic fold, sections were cut 50-60µm thick from tissue collected from one sheep euthanased 18h after infection with labelled *H. contortus* L_3. These thick sections were dewaxed in xylene (twice for 5min), rehydrated in a series of absolute ethanol, 90%, 70% and 40% ethanol and MilliQ water for 2min each, then dehydrated by dipping 5 to 20 times in each of 40%, 70%, 90% and absolute ethanol, followed by 2min in xylene. Unstained sections were then mounted with mounting solution Entellan.

Both live and fixed tissue was also cut into slices 1-2 mm thick with a razor blade.

2.2.1.6 Microscopy

Whole or dissected folds of live or paraformaldehyde-fixed tissues were examined with an inverted confocal microscope from the luminal side, under bright field or UV excitation (405nm) with 20x, 40x or 60x/water immersion objectives. Razor blade-cut sections and thick sections were also examined under the same conditions. Images were processed with Adobe Photoshop.

2.2.1.7 Recovery of Labelled *H. contortus* from the Abomasum

The number of larvae in abomasal contents and tissue 24h after infection with 200,000 L_3 was determined by a modification of the method of Balic *et al.* (2003). After death, the abdomen was opened, the abomasum was ligated and removed with its contents. The abomasum was opened along the greater curvature and the contents were collected. The

abomasum was washed with 0.9% saline, warmed to 37°C and the washings added to the abomasal contents amounting to 1l.

The number of L_3 in the abomasal contents was determined by a modified Baermann technique (Baermann, 1917). Briefly, the contents and washings were placed in sieves lined with tissue paper and the sieve placed in a tray filled with water for 4h at 37°C. The water, which contained L_3 that had migrated through the tissue paper, was centrifuged at 3000rpm for 5min, the supernatant discarded and the remaining solution containing the larvae was stored at 10°C for counting. The whole procedure was repeated for another 20h. The numbers of L_3 in ten 100µl aliquots of each of the solutions were counted and the total number of larvae calculated.

For the determination of L_3 inside the tissue, the abomasum was cut into two lengthwise. A small fold was removed first from each half and fixed in 4% paraformaldehyde to examine larvae directly inside the tissue (2.2.1.5 and 2.2.1.6). One half of the abomasum was divided into fundus and antrum (fundus 1 and antrum 1) and the whole mucosa was scraped off. The number of L_3 in each part was determined using the Baermann technique as described above, with the modification that the sieves were placed in funnels with short tubing and not in trays. After 4h at 37°C, the water containing the larvae was drained from the tubing and stored at 10°C for counting. A further Baermannisation of the fundic and antral tissue was carried out for 20h at 37°C. Numbers of L_3 in ten 100µl aliquots of each of the solutions were counted and the total number of larvae calculated.

The other half of the abomasum was placed in a tray of PBS for 4h at 37°C and larvae, which migrated into the PBS, were recovered by Baermannisation for 20h at 37°C. From this second half of abomasal tissue, the fundus and antrum (fundus 2 and antrum 2) were separated after the 4h incubation in PBS, the mucosa scraped from each and baermannised for 20h at 37°C in water, followed by collection of the water in the tubing. The water containing the larvae was stored at 10°C for counting. The numbers of L_3 in ten 100µl aliquots of each of the solutions form both whole fold and abomasal tissue scrapings were counted and the total number of larvae calculated for antral mucosa, fundic mucosa and whole abomasal tissue in PBS.

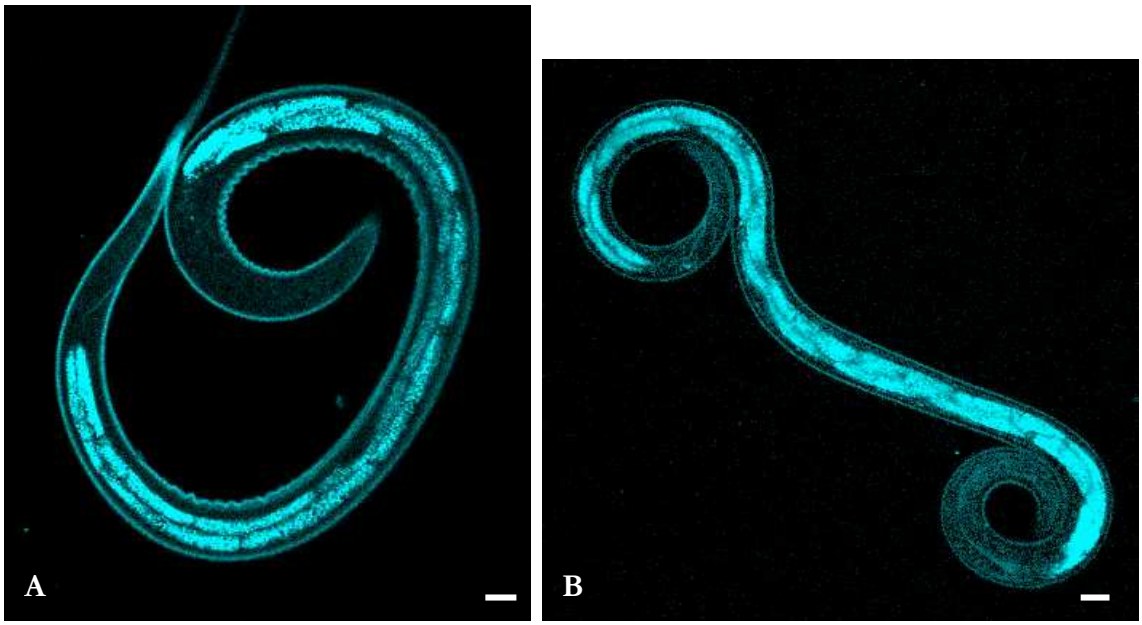

Figure 2.1: Characteristic autofluorescence in the gut region of sheathed (A) and exsheathed (B) *H. contortus* L_3. UV excitation, original magnification 400x, bars 10µm.

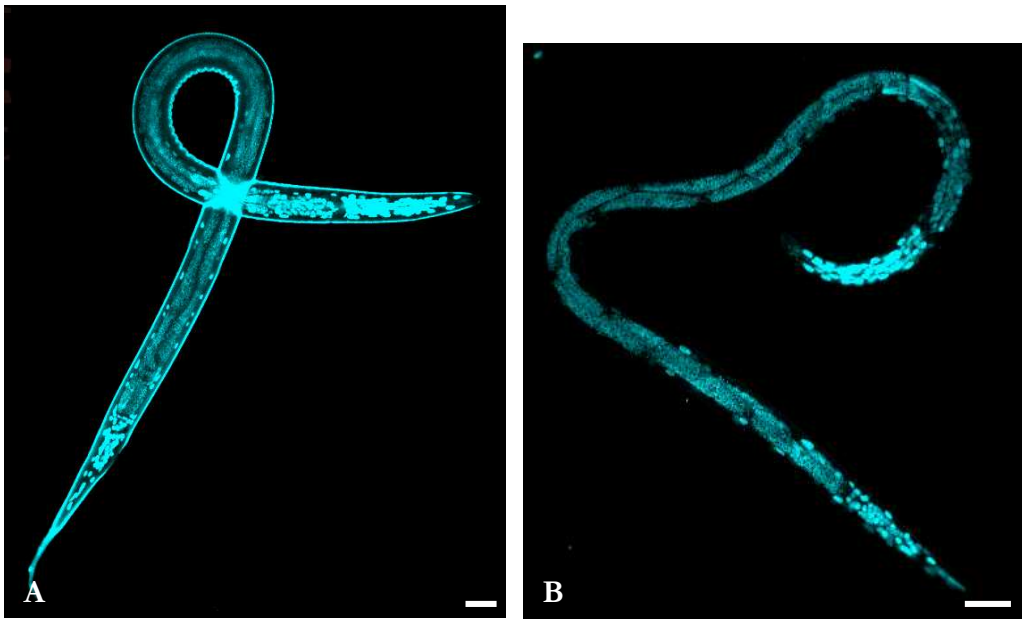

Figure 2.2: Hoechst 33258 labelled sheathed (A) and exsheathed (B) *H. contortus* L_3. Note the staining of nuclei mainly in the head and tail region after Hoechst 33258 labelling in addition to the autofluorescence. UV excitation, original magnification 400x, bars 20µm.

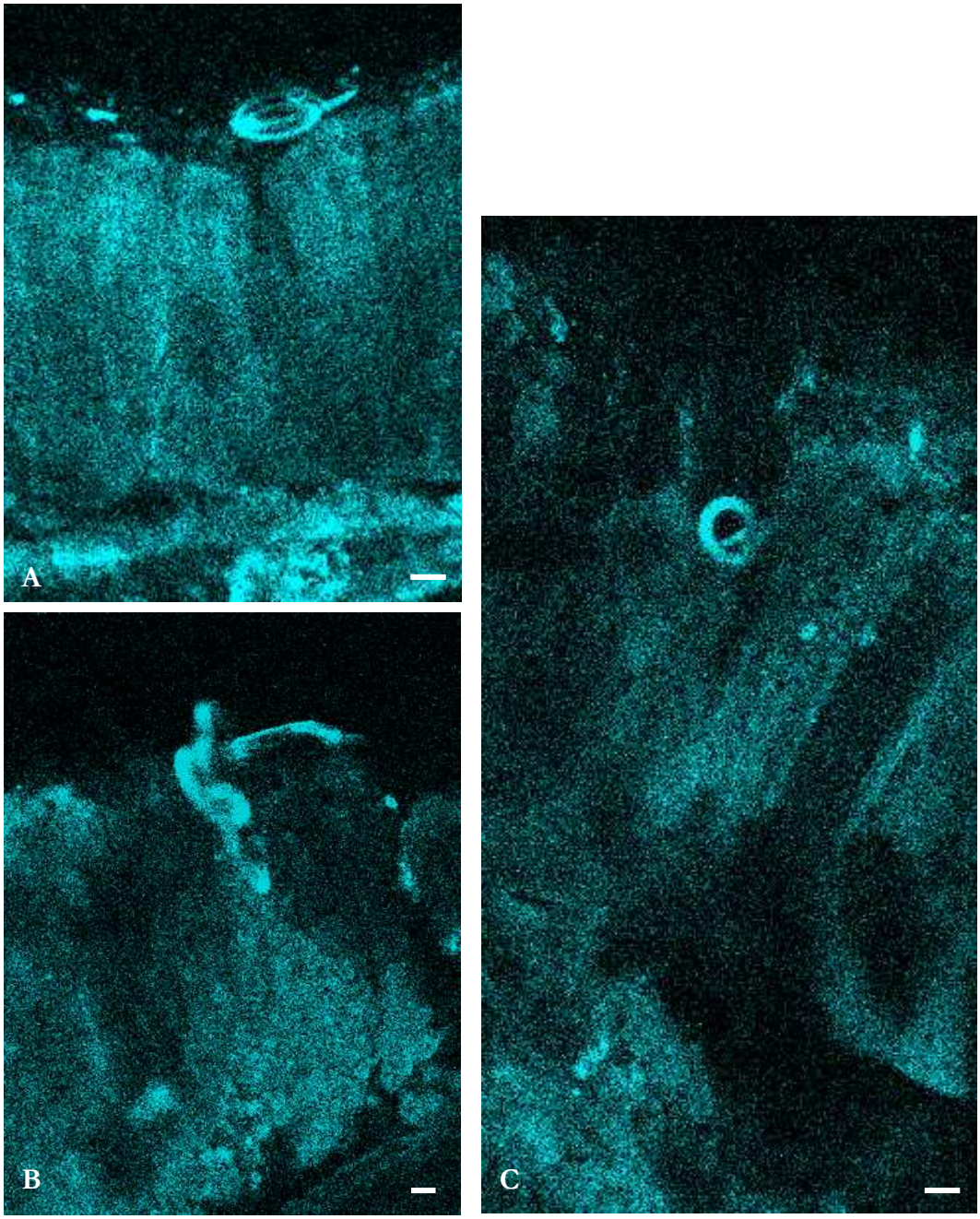

Figure 2.3: Razor blade-cut sections of fundic mucosa collected 24h p.i. (A. and B.) and 30h p.i. (C.) from sheep infected with *H. contortus* L_3. The sheep in A. and B was infected with 200,000 labelled L_3 and in C. with 30,000 labelled and unlabelled (1:1) *H. contortus* L_3. A. Larva on the surface of the gastric mucosa, B. larva penetrated a gastric pit and C. larva penetrated a relatively damaged gastric pit. All paraformaldehyde fixed tissue, UV excitation, original magnification 100x (A. and C.), bars 30µm; 200x (B.), bar 20µm.

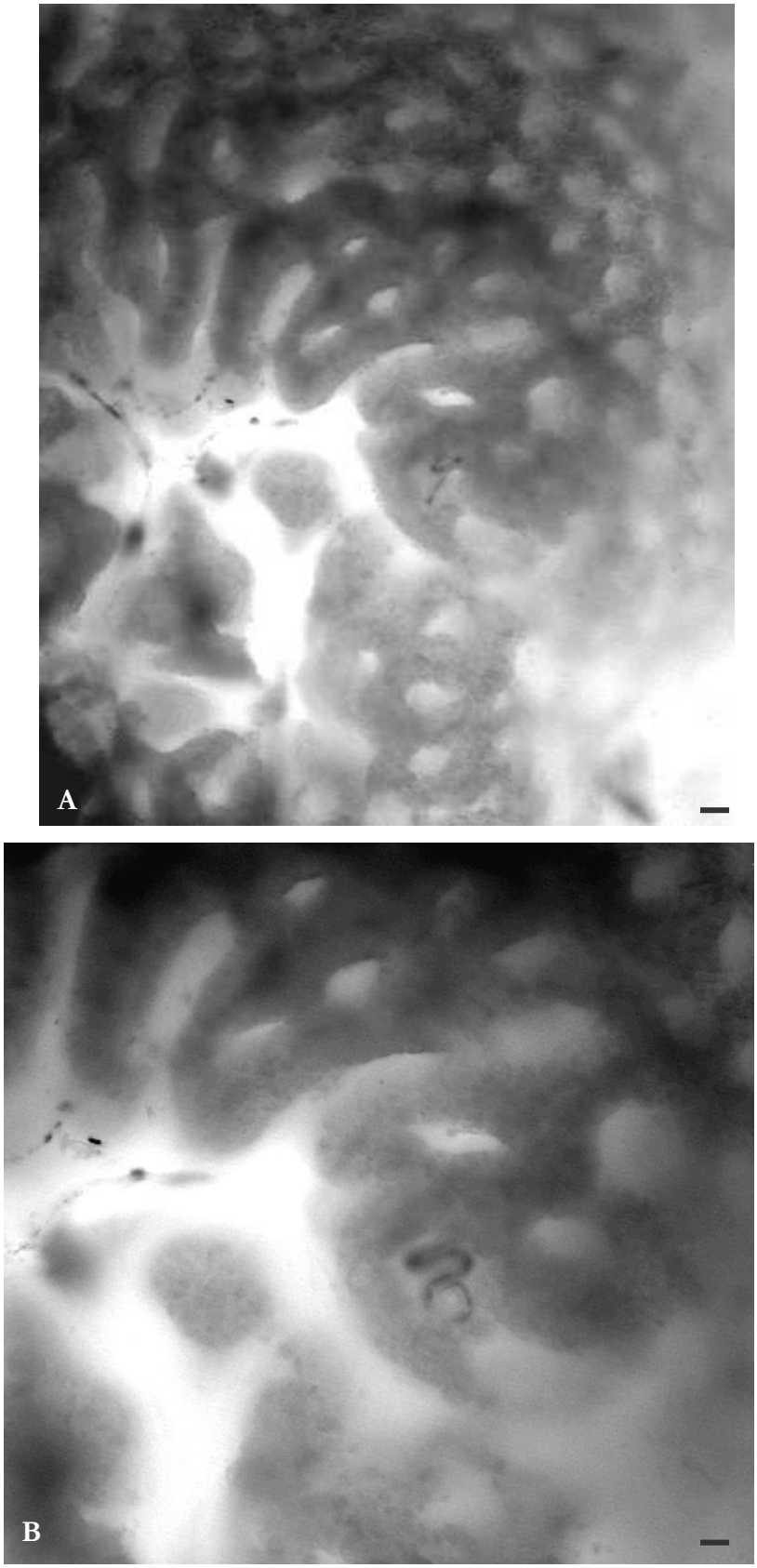

Figure 2.4: Luminal surface of a nodular area of fundic mucosa from a sheep 18h after infection with 30,000 labelled and unlabelled (1:1) *H. contortus* L_3. Note the larva in the gland lumen. Unfixed tissue, (A) original magnification 10x, bar 20μm (B) original magnification 20x, bar 10μm.

2.2.2 Results

2.2.2.1 Fluorescent Labelling of *H. contortus* L_3

H. contortus L_3 had a characteristic autofluorescence under UV light (Figure 2.1). This was at a similar wavelength to that of the sheep tissue. L_3 stained with 15μg/ml Hoechst 33258, in addition to the autofluorescence, exhibited fluorescence from binding of the dye to DNA in the nuclei in the head and tail regions (Figure 2.2). No binding of the DNA dye Syto®17 was apparent after incubations for 1h or 4h with 20μM or 50μM dye. Staining with the lipophilic dye Nile Red in a concentration of 5μg/ml produced unsatisfactory results, as the larvae were only partly labelled and the staining disappeared after 1 day. Hoechst 33258 was chosen for all subsequent experiments with labelled *H. contortus* L_3.

2.2.2.2 Identification of Glands Parasitised by *H. contortus* Larvae

Tissues were visually inspected for nodules to locate parasitised glands. Only a few small nodules and a small number of larger ones were apparent in one of the two sheep euthanased 18h p.i. and none in the other. After 30h of infection, large numbers of big nodules were detected, at 36h p.i. only a few nodules were seen and there were almost no nodules in the sheep euthanased 48h p.i.

Live tissue, fixed tissue and thick sections of fixed tissue, either cut with a razor blade or as 50-60μm sections using a microtome, were examined using an inverted confocal microscope. Examination of all of these tissues from five sheep infected for 18h (two sheep), 30h, 36h or 48h, resulted in a total of six larvae being found inside the tissue and approximately 30-50 on top of the tissue (Figures 2.3 and 2.4). All larvae detected were seen because of autofluorescence, rather than labelling with Hoechst 33258. Tissue was also collected and fixed very quickly from one sheep, probably taking about 5min in total, but resulted in similar results and no additional larvae being seen. A 5ml sample of the abomasal contents of each sheep was also examined, but only two larvae were seen in one sample.

Table 2.1: Number of larvae (mean ± SEM, n=10) recovered from abomasal contents, fundus and antrum from a sheep 24h p.i. with 200,000 labelled *H. contortus* L_3.

Source	Incubation time	No. of larvae
Abomasal contents	**total**	**7056 ± 474**
	0-4h	2961 ± 242
	4-24h	4095 ± 233
Half abomasum (as whole)	**total**	**293 ± 17**
	0-4h	293 ± 17
Fundus	**total**	**2685 ± 303**
Fundus 1[a]	0-4h	78 ± 12
	4-24h	1054 ± 102
Fundus 2[b]	4-24h	1553 ± 188
Antrum	**total**	**1292 ± 142**
Antrum 1[a]	0-4h	205 ± 34
	4-24h	284 ± 29
Antrum 2[b]	4-24h	803 ± 79
Total		**11325 ± 936**

[a] mucosal tissue scrapings incubated and baermannised immediately after the collection of the tissue for 0-4h and a second incubation for 4-24h, [b] mucosal tissue scrapings from the half abomasum, which was first incubated 0-4h as a whole half, incubated and baermannised for 4-24h

Parasitised glands could not be confidently recognised unless they contained a larva, which was rarely the case even in areas of nodules cut into thin slices with a razor blade. Using the confocal microscope, the full depth of the gland could not be visualised and larvae deep in the gland may not have been seen. Tissues proved too thick for the whole gland depth to be visualised in the confocal microscope.

An interesting observation in the course of the experiments involved the larva shown in Figure 2.4. While this live tissue was being studied, the larva clearly left the gland and appeared on the surface of the tissue.

2.2.2.3 Counts of Labelled *H. contortus* in Abomasal Contents and Tissues

Visual inspection of the tissue collected 24h p.i. after an infective dose of 200,000 labelled *H. contortus* detected almost no nodules and the tissue appeared normal macroscopically. The total number of larvae counted was 11,325, representing 5.7% of the infective dose. The full results are summarised in Table 2.1. The majority of larvae (7056) were present in the abomasal contents with more being recovered from 4-24h than in the first 4h of Baermannisation. One half of the abomasum was used immediately to provide mucosal scrapings (fundus 1 and antrum 1), from which 1132 larvae were recovered from the fundus, almost all during 4-24h of Baermannisation, whereas 489 were recovered from the antrum, equally spread from 0-4 and 4-24h. When the whole tissue was incubated in PBS, 293 larvae were recovered in 4h. A further 1553 larvae were recovered from the fundus (fundus 2) and 803 from the antrum (antrum 2) after the next 20h incubation of mucosal scrapings from the separated fundus and antrum.

2.3 Early Changes within the Abomasal Mucosa after Infection with Adult *T. circumcincta*

2.3.1 Materials and Methods

2.3.1.1 Experimental Overview

The early effects of luminal stages of abomasal parasites were studied using fixed fundic tissues from a previous experiment involving adult transplantation of *T. circumcincta* into parasite-naive sheep. These tissues were kindly provided by I. Scott and H. V. Simpson. A particular focus was the counting of parietal cells stained with two different markers, using an antibody to the proton pump and a TGF-α antibody. Lectin staining was also investigated as a third marker for parietal cells.

2.3.1.2 Infection with *T. circumcincta*

Parasite-naive lambs, at about four months of age, each received approximately 10,000 adult *T. circumcincta* through an abomasal cannula and were euthanased 6h, 12h, 24h and 72h after the transplant. Adult worms, obtained from donor sheep 21d after infection with 100,000 *T. circumcincta* L_3, were given to the recipient animals within 1-2h of collection. Uninfected control lambs were euthanased at the start of the experiment.

Abomasal tissue was fixed in Bouin's fluid and routinely processed and embedded. Sections from the tissue blocks were cut at 5μm.

2.3.1.3 Histochemistry

Fundic tissues from two sheep in three experimental groups (control and euthanased at 12h or 72h p.i.) were stained with an antibody to the proton pump and a TGF-α antibody. For

each sheep, parietal cells labelled with each of the two stains were counted in three 300µm wide columns of fundic mucosa. Lectin staining was carried out on tissues from one animal per group (control and euthanased at 6h, 12h or 24h p.i.) and from fundic tissue from a parasite-naive lamb which was infected at three months of age with 35,000 *T. circumcincta* L_3 intraruminally and euthanased on 30d p.i.

For all staining procedures, the sections were dewaxed in xylene twice for 5min and rehydrated for 2min each through a series of ethanol concentrations (absolute ethanol, 90%, 70%, 40%) and finally MilliQ water. After permeabilising with 1% Triton-X-100 in PBS for 30min at room temperature, the sections were again washed with PBS three times each for 1min. This was followed by specific staining steps for lectin staining (2.3.1.2.1) or proton pump and TGF-α antibody staining (2.3.1.2.2). Subsequent counterstaining, dehydration and mounting was the same after all stains. Following the last wash with PBS, sections were rinsed with tap water, incubated with hematoxylin for 20-60s and then rinsed again with tap water until cleared. Counterstaining was followed by dehydration and mounting: the sections were dipped 5 to 20 times in each of 40%, 70%, 90% and absolute alcohol and finally in xylene for 2min before they were mounted immediately with mounting solution Entellan. All solutions used for histochemistry are listed in Appendix V. Tissue sections were examined using a fluorescent microscope (Eclipse E600, Nikon, equipped with a DS-Fi 1 Nikon camera, using a 20x or 40x objective) if not stated otherwise. All images were processed with Adobe Photoshop.

2.3.1.3.1 Lectin Staining

After dewaxing, rehydration and permeabilising, the sections were incubated for 1h at room temperature with the biotinylated lectins DBA, SBA, PNA or UEA in PBS at a concentration of 7.5 or 10µg/ml. For the negative control, the same incubation was carried out with omission of the lectin. The lectin incubation was either together with a streptavidin-Alexa Fluor® 546 conjugate or the lectin incubation was followed by the strepavidin incubation in the dark (streptavidin at concentrations of 1.5, 2 or 5µg/ml). Following three 1min washes with PBS, the sections were counterstained, dehydrated, mounted and then examined. The Streptavidin-Alexa Fluor® 546 conjugate has an

excitation maximum of ~556nm (green laser) and emission maximum of 573nm (red fluorescence).

2.3.1.3.2 Proton Pump and TGF-α

Successive sections were used for proton pump and TGF-α antibody staining. After the permeabilising step, sections were incubated with sodium borohydride (1mg/ml; three times for 10min) to minimise the autofluorescence of the tissue and then rinsed several times with PBS. This was followed by an incubation with blocking buffer for 30 to 45min at room temperature. For the negative control, the blocking buffer was not drained off. The liquid from the samples was removed and the sections were incubated for 1h at room temperature with antibody. Sections were stained with either (1) H^+/K^+-ATPase (β-subunit) mouse monoclonal IgG (1:2000 in blocking buffer), which was directly labelled with Zenon® Mouse IgG label Kit-Alexa Fluor® 488 following the suppliers protocol or (2) TGF-α mouse monoclonal IgG diluted 1:100 in blocking buffer. For TGF-α staining, the incubation of sections with the first antibody was followed by washing with PBS (three times for 1min) before they were incubated with the second biotinylated goat anti-mouse antibody (1µg/ml). Following another wash with PBS (three times for 1min), the sections were incubated with streptavidin-Alexa Fluor® 546 conjugate (1µg/ml). For both staining protocols (using directly labelled H^+/K^+-ATPase or TGF-α with a second biotinylated antibody followed by streptavidin), this was followed by another wash with PBS (three times for 1min) and then counterstaining, dehydration, mounting and examination. The Streptavidin-Alexa Fluor® 546 conjugate has an excitation maximum of ~556nm (green laser) and emission maximum of 573nm (red fluorescence). The Zenon® Alexa Fluor® 488 label kit has an excitation maximum of 495nm (blue laser) and emission maximum of 519nm (green fluorescence).

Additionally, a double-stain using both H^+/K^+-ATPase and TGF-α antibody was tested: the same protocol as described above for TGF-α antibody staining was followed and after the last wash with PBS following the streptavidin incubation for the TGF-α antibody, the Alexa Fluor® 488 directly labelled H^+/K^+-ATPase antibody was applied to the same section for 1h. The rest of the procedure followed the general staining protocol.

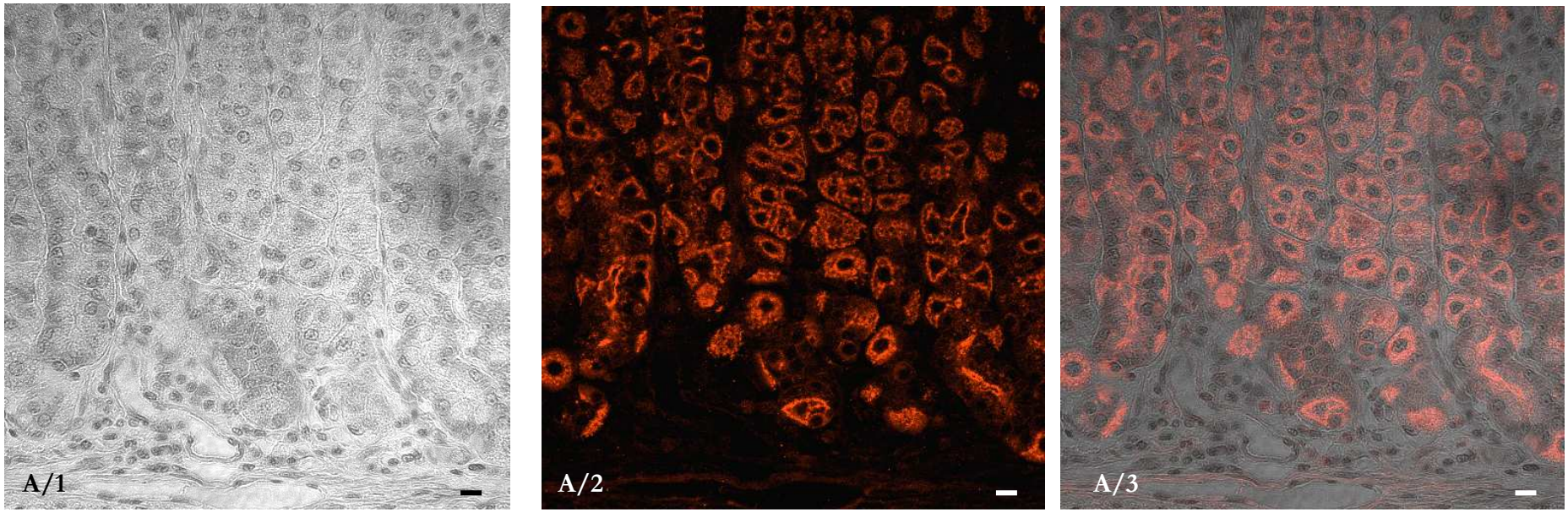

Figure 2.5: Lectin stained (DBA) fundic tissue 30d p.i. from a sheep infected with 35,000 *T. circumcincta* L_3. Tissue was stained with DBA 7.5µg, streptavidin 1.5µg and counterstained with hematoxylin. A/1 Hematoxylin counterstain, bright field image, A/2 Lectin staining, fluorescence image, A/3 Merge A/1 and A/2. Paraffin embedded 5µm section, original magnification 600x (confocal microscope), bars 10µm.

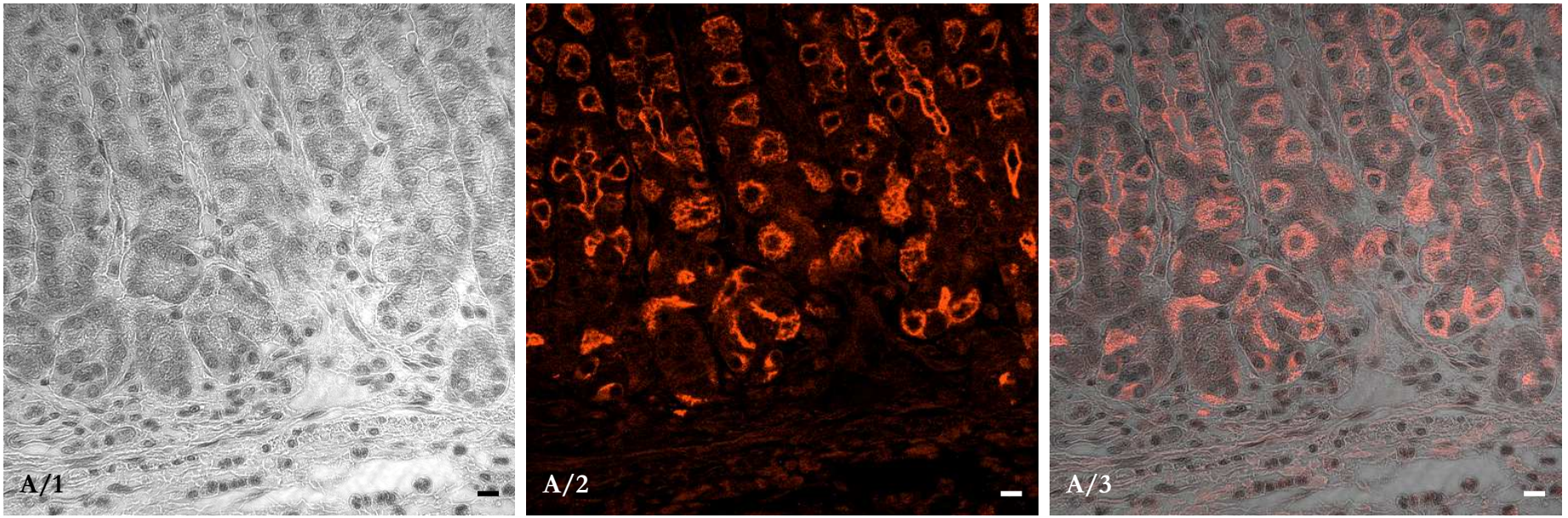

Figure 2.6: Lectin stained (SBA) fundic tissue 30d p.i. form a sheep infected with 35,000 *T. circumcincta* L_3. Tissue was stained with SBA 7.5µg, streptavidin 1.5µg and counterstained with hematoxylin. A/1 Hematoxylin counterstain, bright field image, A/2 Lectin staining, fluorescence image, A/3 Merge A/1 and A/2. Paraffin embedded 5µm section, original magnification 600x (confocal microscope), bars 10µm.

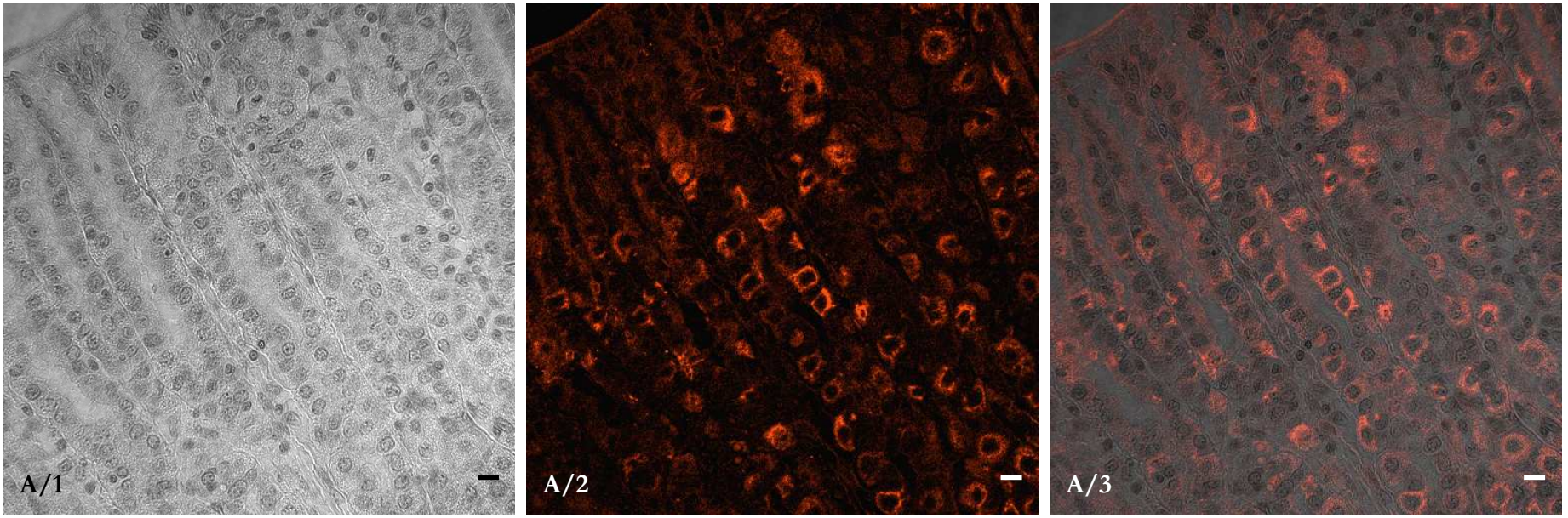

Figure 2.7: Lectin stained (PNA) fundic tissue 30d p.i. from a sheep infected with 35,000 *T. circumcincta* L_3. Tissue was stained with PNA 7.5µg, streptavidin 1.5µg and counterstained with hematoxylin. A/1. Hematoxylin counterstain, bright field image, A/2. Lectin staining, fluorescence image, A/3. Merge A/1 and A/2. Paraffin embedded 5µm section, original magnification 600x (confocal microscope), bars 10µm.

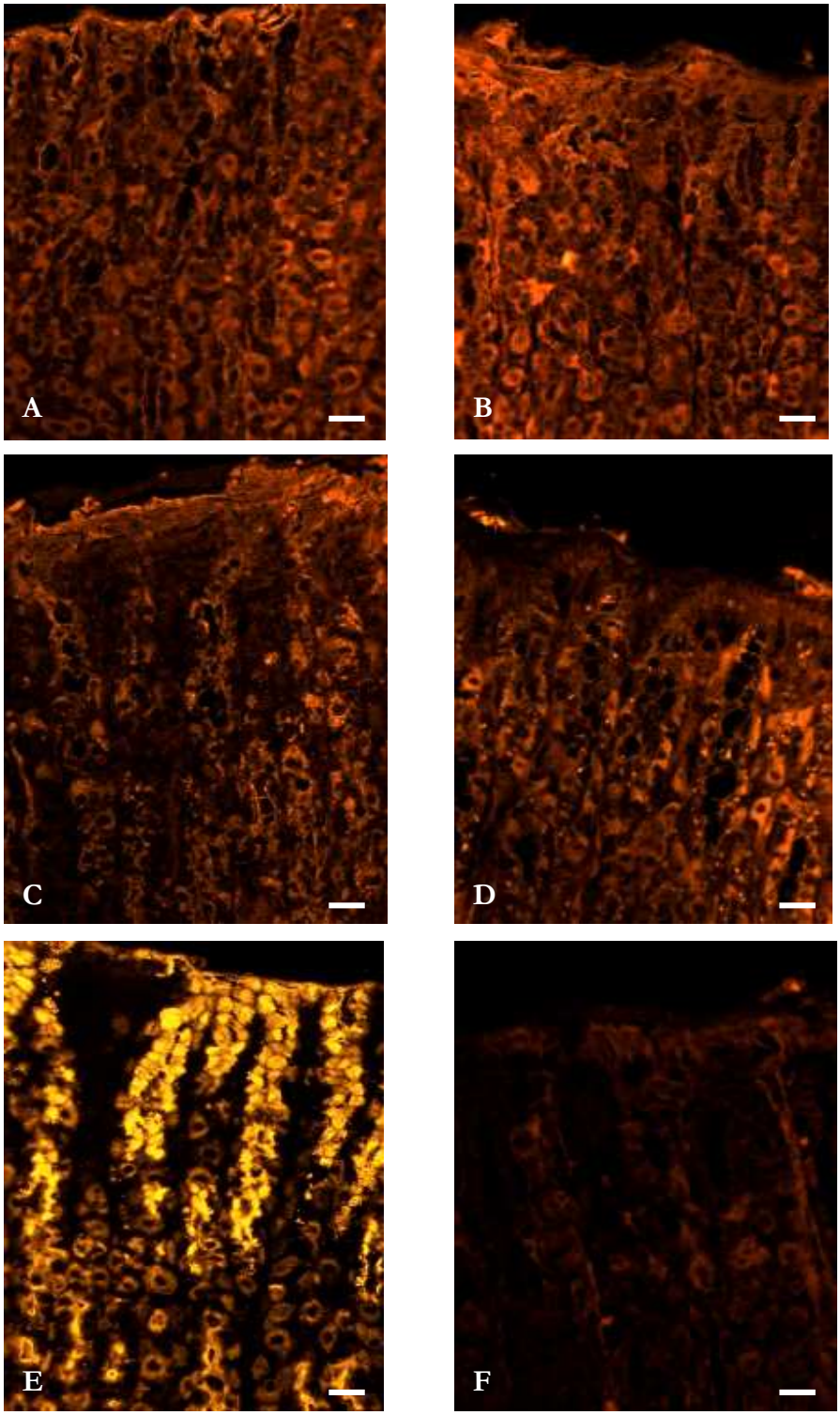

Figure 2.8: Lectin stained (DBA) ovine fundic tissue before (control) and 12 and 72h after transplantation of 10,000 adult *T. circumcincta*. Fluorescent images after excitation with 546nm. A. 6h p.i., 7.5µg DBA, 1.5µg streptavidin, B. uninfected control, 7.5µg DBA, 1.5µg streptavidin, C. 24h p.i., 10µg DBA, 2µg streptavidin, D. 12h p.i., 10µg DBA, 5µg streptavidin, E. uninfected control, 7.5µg DBA, 1.5µg streptavidin, F. uninfected control, negative control (omission of DBA). Paraffin embedded 5µm sections, original magnification 400x, bars 10µm.

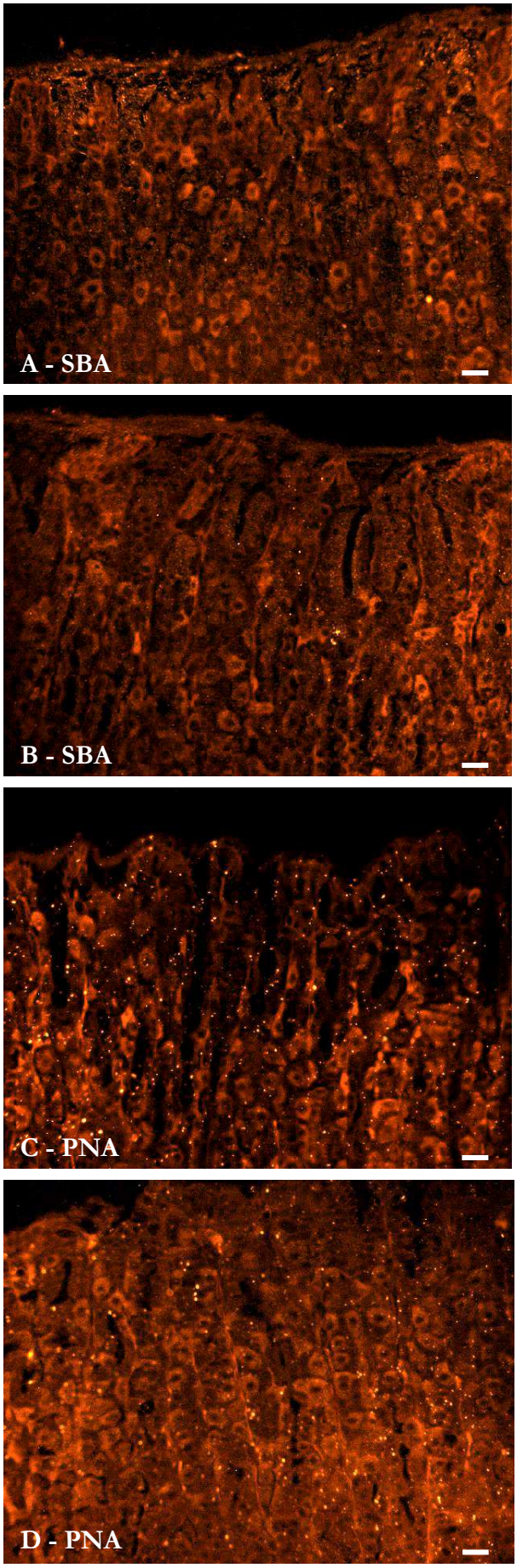

Figure 2.9: Lectin stained ovine fundic tissue before (control) or 6h after transplantation of 10,000 adult *T. circumcincta*. Fluorescent images after excitation with 546nm. A. 6h p.i., 7.5µg SBA, 1.5µg streptavidin, B. uninfected control, 7.5µg SBA, 1.5µg streptavidin, C. 6h p.i., 7.5µg PNA, 1.5µg streptavidin, D. uninfected control, 7.5µg PNA, 1.5µg streptavidin. Paraffin embedded 5µm sections, original magnification 400x, bars 10µm.

2.3.1.4 Statistical Analysis

Data are presented as mean ± SEM. One-way ANOVA with Tukey's *post hoc* test (Prism version 4.03) was used to compare parietal cell counts, abomasal pH and mucosal thickness in infected and uninfected tissues.

2.3.2 Results

2.3.2.1 Lectin Staining

In the preliminary experiment using tissue from a sheep infected with *T. circumcincta* L_3, binding of DBA and SBA to parietal cells was strong, it was slightly weaker with PNA and there was no staining with UEA (Figures 2.5 to 2.7). For tissue from an uninfected sheep and one euthanased 6h p.i., there was moderate staining with DBA, PNA and SBA using the same concentrations of lectins (7.5µg/ml) and streptavidin (1.5µg/ml) as before and staining was not exclusively to parietal cells (Figures 2.8 A. and B. and 2.9). Tissues collected 12 and 24h after adult *T. circumcincta* transplantation were stained with DBA (10µg/ml) and streptavidin (2 or 5µg/ml) together and again produced moderate but uneven staining (Figure 2.8 C. and D.). Separate incubations with DBA (7.5µg/ml) and streptavidin (1.5µg/ml) for uninfected control tissues resulted in strong staining of the gastric pit region and weaker, uneven staining in the gland region (Figure 2.8 E.). The negative control in each experiment (omission of lectin) did not show any staining apart from weak background staining (Figure 2.8 F.). In general, lectin staining was not specific for parietal cells, uneven in tissues and not consistent between animals.

2.3.2.2 Proton Pump and TGF-α Labelled Parietal Cells

Using double staining with directly labelled H^+/K^+-ATPase antibody and TGF-α antibody on the same slide, H^+/K^+-ATPase staining was inconsistent and weak compared with single staining with labelled H^+/K^+-ATPase antibody. In an effort to compare H^+/K^+-

Facing page 54

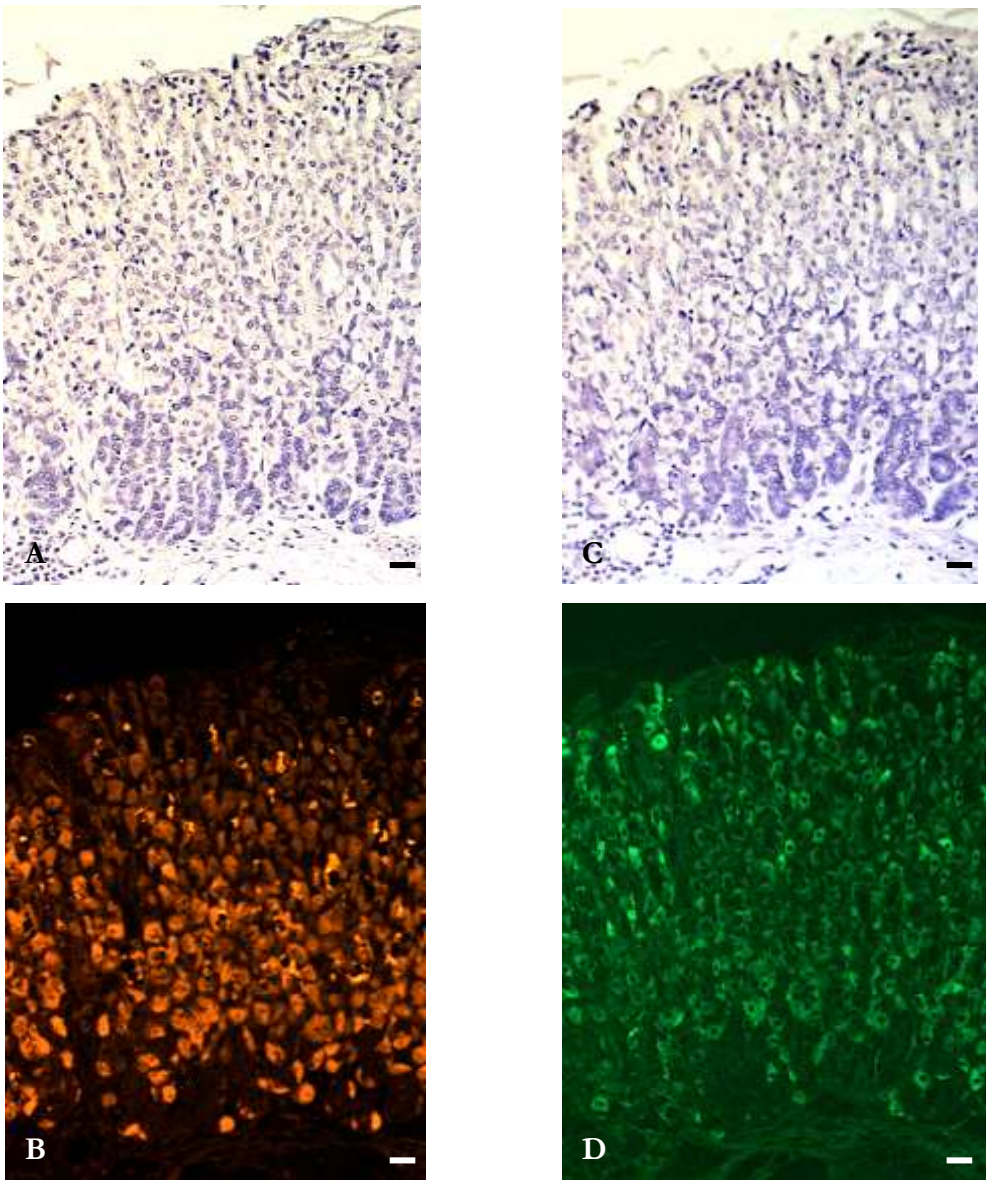

Figure 2.10: TGF-α and H^+/K^+-ATPase positive parietal cell staining of successive ovine fundic sections (12h after transplantation of 10,000 adult *T. circumcincta*). A. Hematoxylin counterstaining of TGF-α stained section, B. Fluorescent image of TGF-α stained section (after excitation with 546nm), C. Hematoxylin counterstaining of H^+/K^+-ATPase stained section, D. Fluorescent image of H^+/K^+-ATPase stained section (after excitation with 488nm), E. Merge B. and D. showing that TGF-α and H^+/K^+-ATPase positive parietal cells did not align even though the cut sections are only 5 μm apart. Paraffin embedded 5μm sections, Mayer's Hematoxylin counterstain and fluorescent TGF-α and H^+/K^+-ATPase staining, original magnification 200x, bars 10μm.

Table 2.2: Numbers of TGF-α and H^+/K^+-ATPase positive parietal cells (mean ± SEM, n=2) in fundic tissue of sheep before (uninfected control, Ct) or 12 and 72h after the transplantation of 10,000 adult *T. circumcincta*. Cell numbers are expressed as total cell numbers per 300µm wide column of fundic mucosa. Means with the same superscript are significantly different ($p<0.05$).

Parameter	Group		
	Ct	12h	72h
TGF-α positive PC	262.00 ± 14.74[a]	238.67 ± 15.53	222.33 ± 5.25[a]
H^+/K^+-ATPase positive PC	263.33 ± 12.43[b, c]	224.33 ± 8.80[b]	162.00 ± 10.41[c]

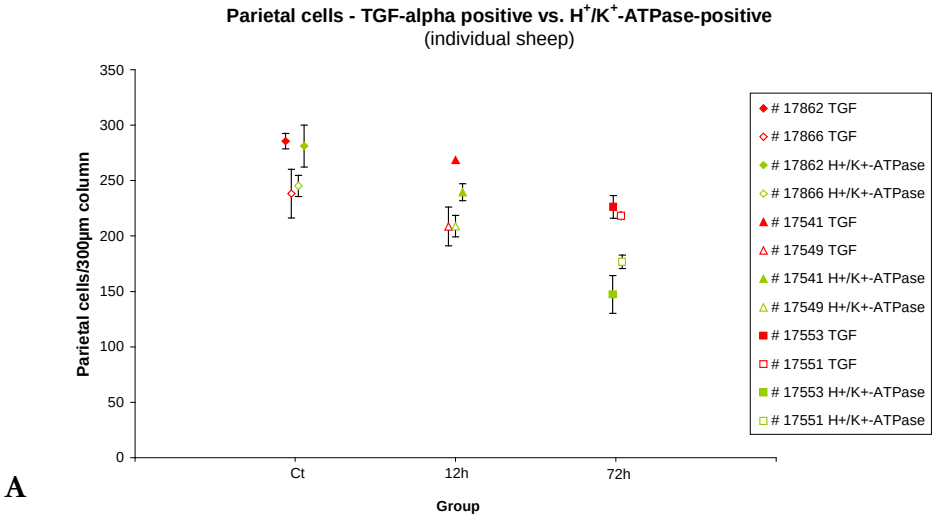

A

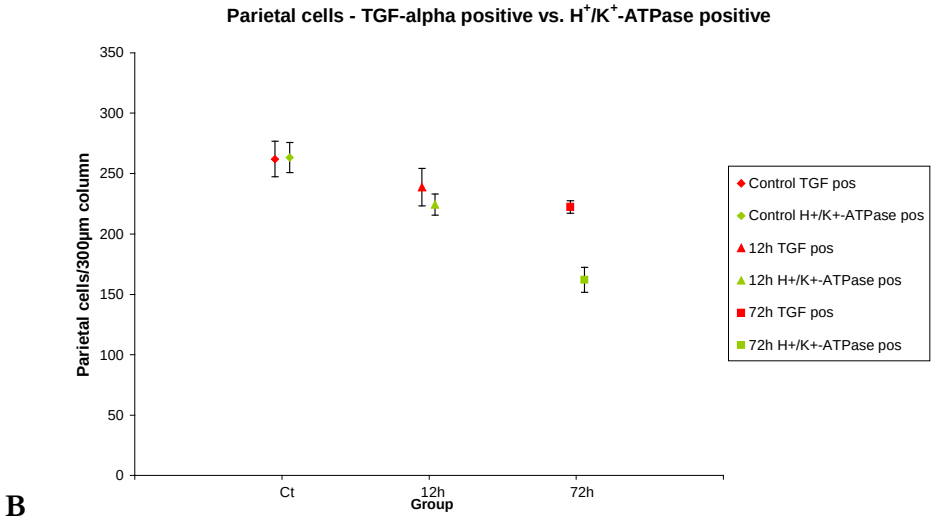

B

Figure 2.11: Numbers of parietal cells - TGF-α positive vs. H^+/K^+-ATPase positive of individual sheep (A) and group mean (B) before (control) and 12 and 72h after transplantation of 10,000 adult *T. circumcincta*. Cell numbers are expressed as total cell numbers per 300µm wide column of ovine fundic mucosa.

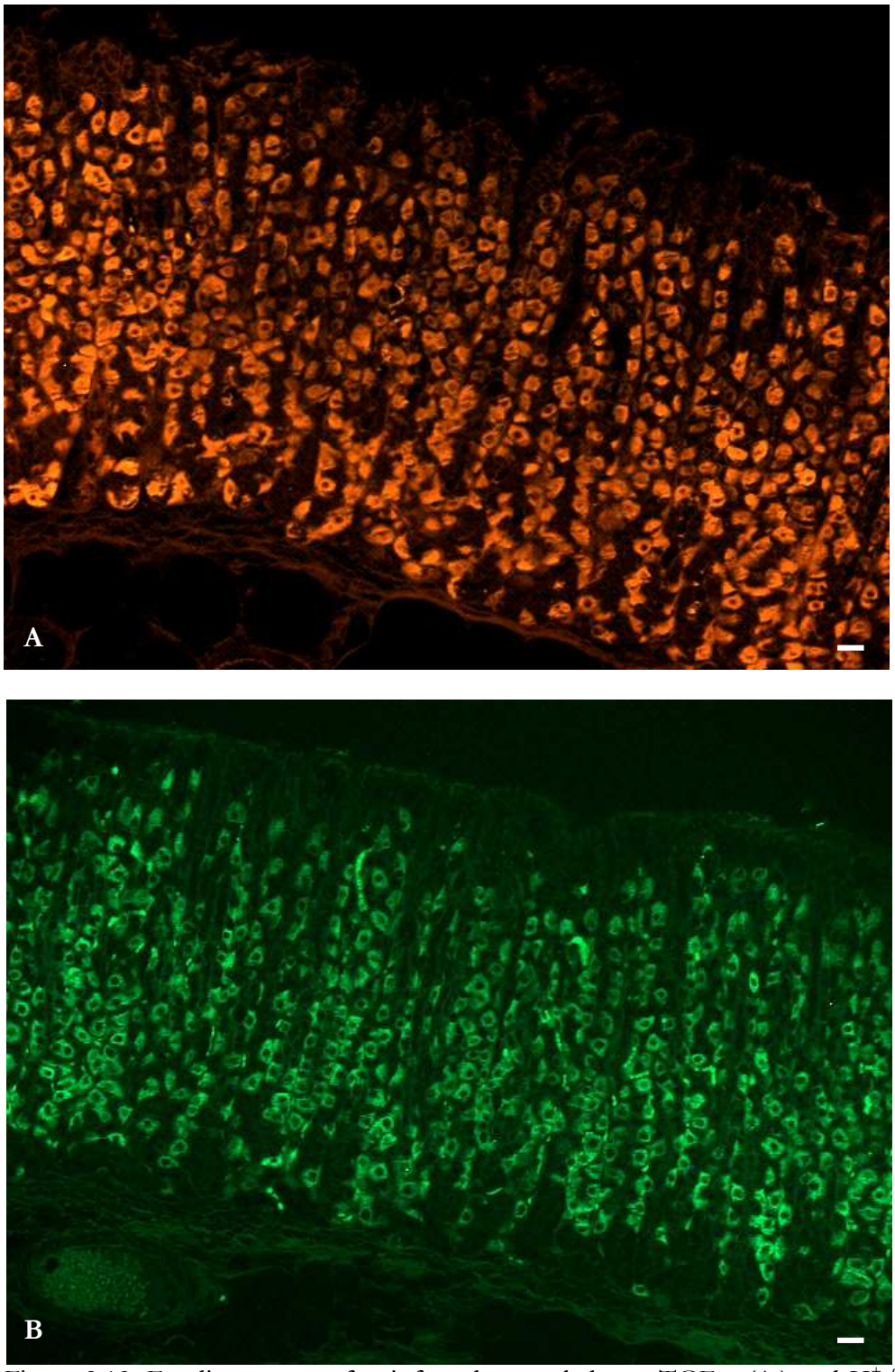

Figure 2.12: Fundic mucosa of uninfected control sheep. TGF-α (A.) and H^+/K^+-ATPase positive (B.) parietal cells are distributed within the pits and glands with the majority in the middle part of the glands. Fluorescent images after (A.) 546nm and (B.) 488nm excitation. Paraffin embedded 5µm sections, original magnification 200x, bars 10µm.

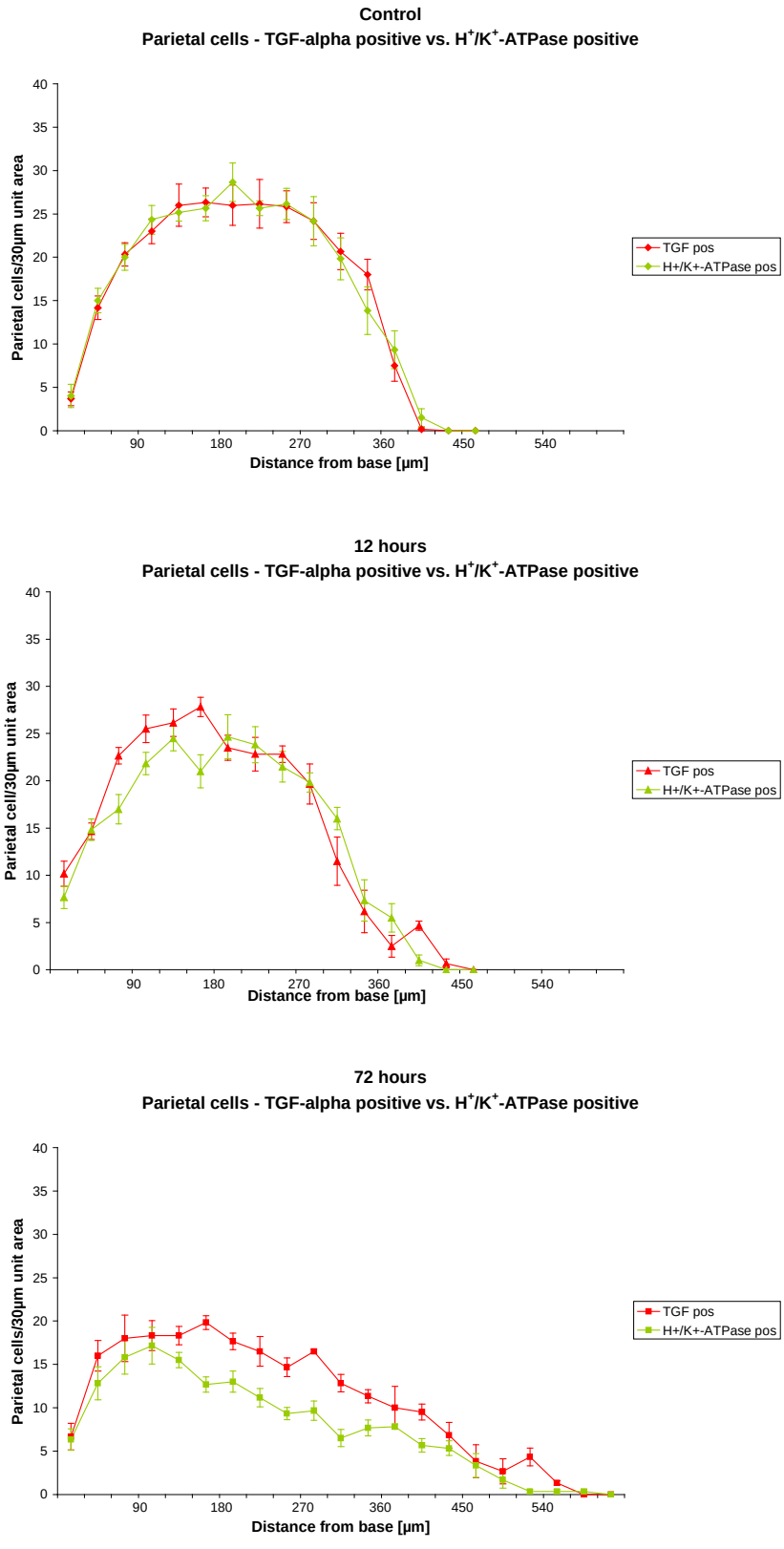

Figure 2.13: Numbers of TGF-α positive vs. H^+/K^+-ATPase positive parietal cells per 30µm unit area in a 300µm wide column of ovine fundic mucosa for each group (control and 12 and 72h after transplantation of 10,000 adult *T. circumcincta*).

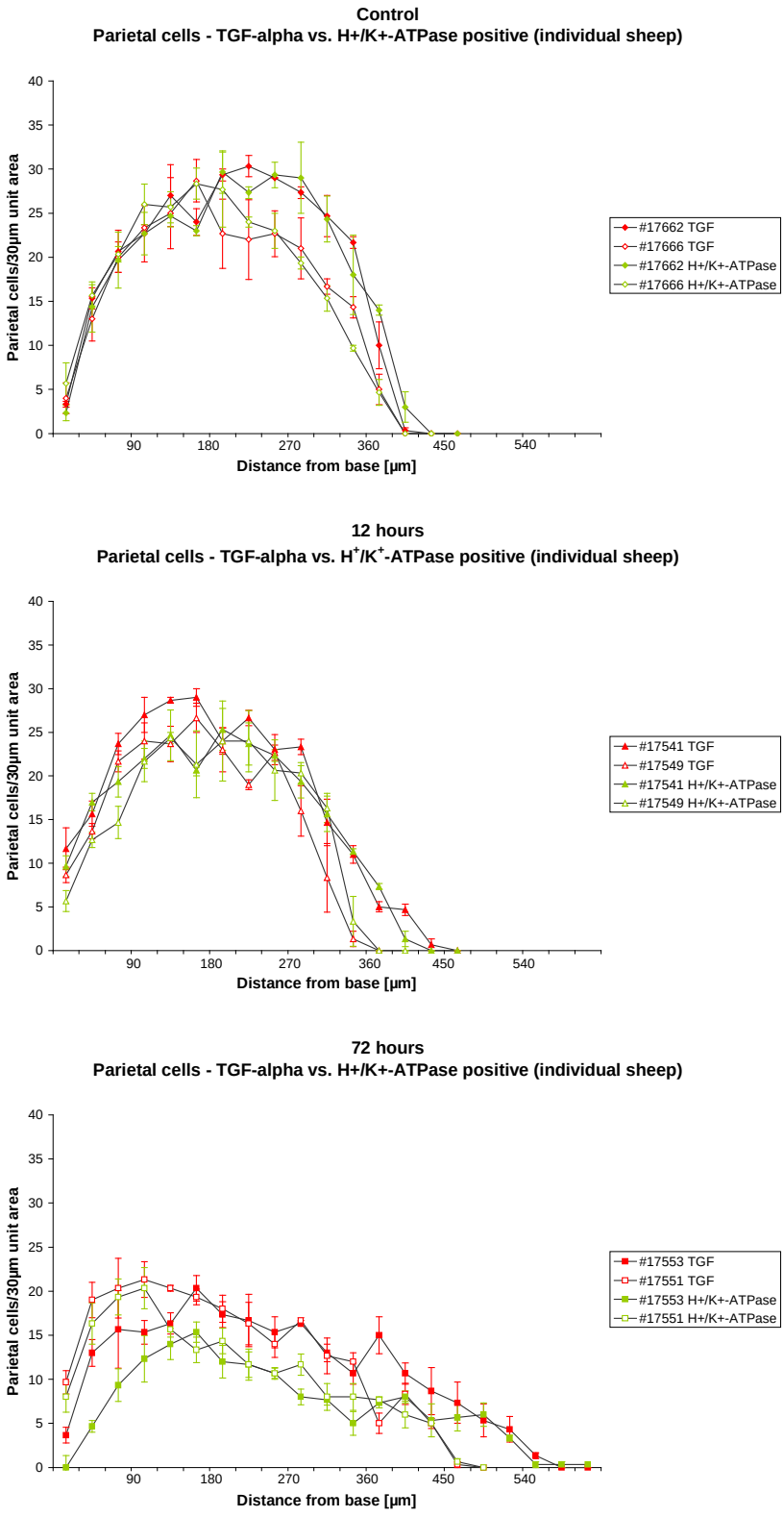

Figure 2.14: Numbers of TGF-α positive vs. H^+/K^+-ATPase positive parietal cells per 30µm unit area in a 300µm wide column of fundic mucosa of individual sheep for each group (control and 12 and 72h after transplantation of 10,000 adult *T. circumcincta*).

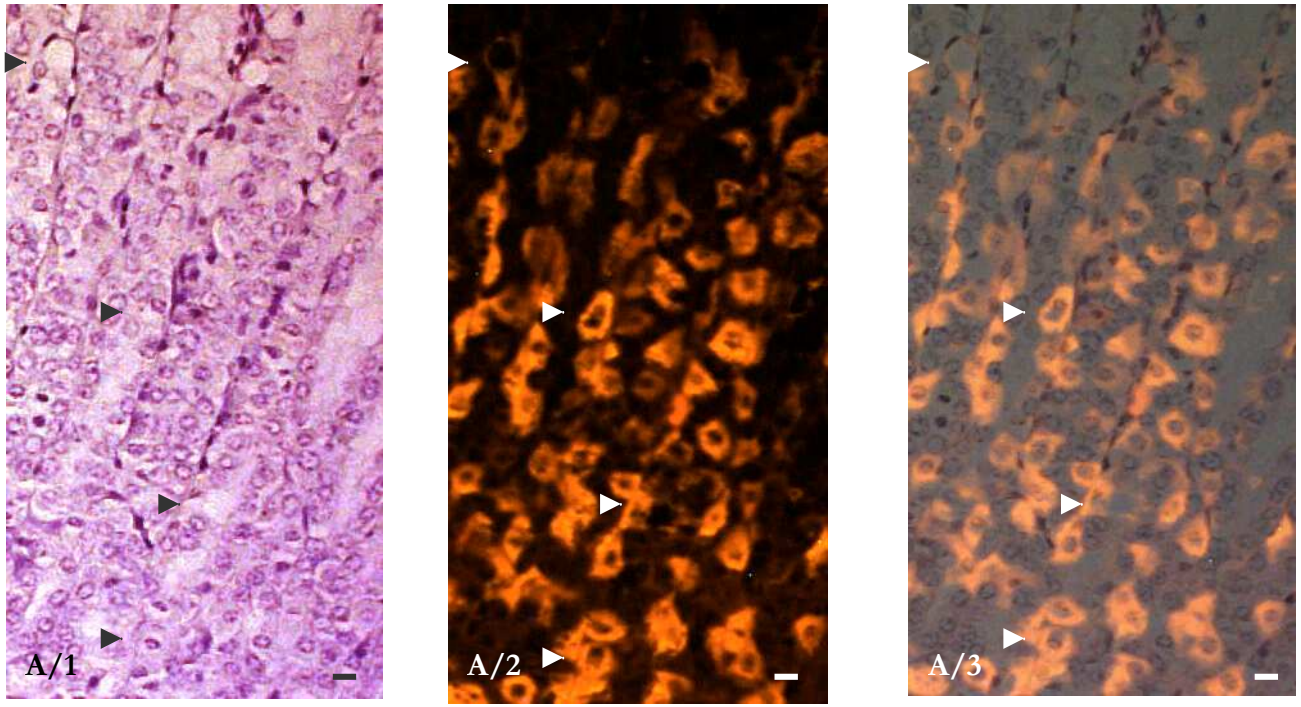

Figure 2.15: Fundic mucosa of uninfected control sheep - Parietal cell vacuolation. A. A few TGF-α positive parietal cells are vacuolated (arrowheads). The number of vacuolated parietal cells is less than in tissues taken 12 and 72h after transplantation though. A/1 Hematoxylin counterstain, A/2 fluorescent TGF-α immunohistochemistry (excitation 546nm), A/3 merge A/1 and A/2. Shown are the middle part (A) of glands. Paraffin embedded 5µm sections, original magnification 200x, bars 10µm.

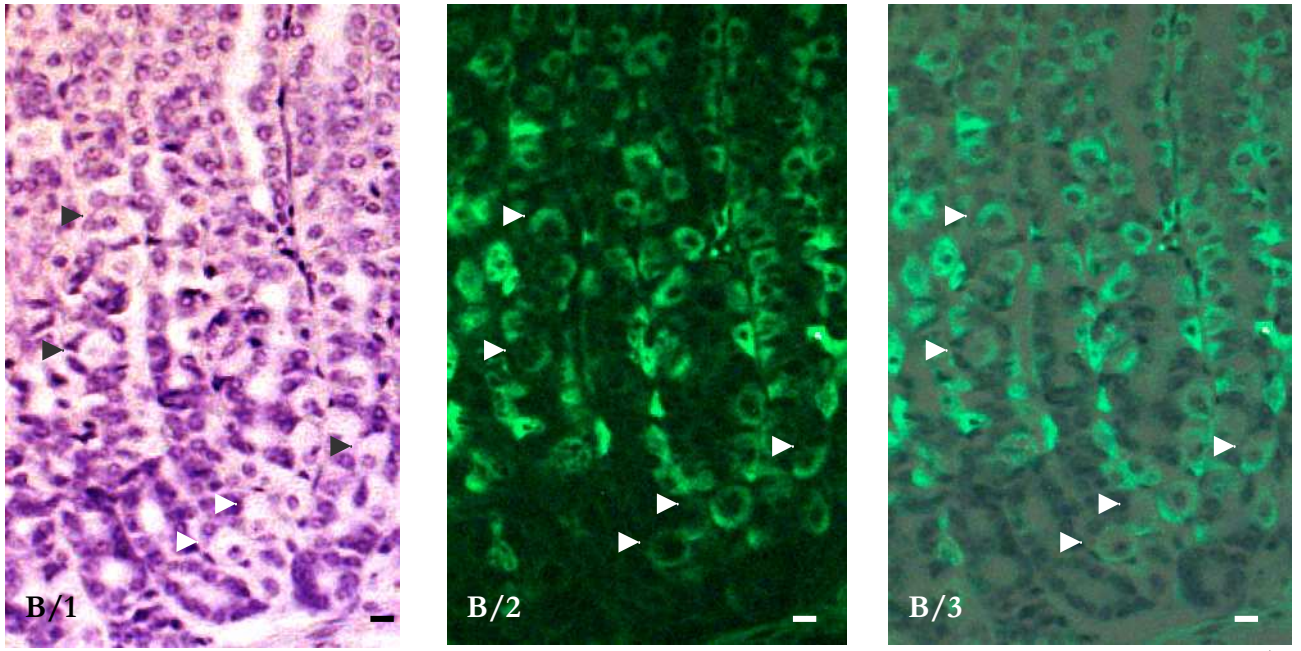

Figure 2.15 continued: Fundic mucosa of uninfected control sheep - Parietal cell vacuolation. B. A few H^+/K^+-ATPase positive parietal cells are vacuolated (arrowheads). The number of vacuolated parietal cells is less than in tissue taken 12 and 72h after transplantation though. B/1 Hematoxylin counterstain, B/2 fluorescent H^+/K^+-ATPase immunohistochemistry (excitation 488nm), B/3 merge B/1 and B/2. Shown are the bottom part (B) of glands. Paraffin embedded 5µm sections, original magnification 200x, bars 10µm.

ATPase and TGF-α positive staining, successive sections were stained with single stains. Unfortunately, even though the sections were only 5μm apart it was impossible to align the cells and then compare directly H^+/K^+-ATPase and TGF-α positive staining of the same cells (Figure 2.10).

Cell counts of H^+/K^+-ATPase and TGF-α positive parietal cells of individual sheep and group means are shown in Table 2.2 and Figure 2.11. Compared with the control counts, the number of TGF-α positive and H^+/K^+-ATPase positive parietal cells decreased, but only significantly for H^+/K^+-ATPase positive parietal cells 72h after the transplant ($p<0.05$).

2.3.2.2.1 Abomasal Tissue from Uninfected Control Sheep

H^+/K^+-ATPase and TGF-α positive parietal cells were distributed along the pits and glands (Figure 2.12). The highest numbers of parietal cells were counted between ~100 to ~330μm of the mucosal length, representing the upper base and neck in this group. For comparison, the length of the different gland regions (base-neck-pit) are shown in Figure 2.27 (2.3.2.3). Group means of H^+/K^+-ATPase and TGF-α positive parietal cells are shown in Figure 2.13 and counts of individual sheep in Figure 2.14. The profiles of H^+/K^+-ATPase and TGF-α stained parietal cells along the pits and glands were almost identical (Figure 2.13). In general, the variation in H^+/K^+-ATPase or TGF-α positive parietal cells between control animals was low; slight variations between the animals occurred mainly in the neck region (Figure 2.14). H^+/K^+-ATPase staining appeared in most cases evenly intense along the pits and glands compared with TGF-α staining, however, some variation in intensity between cells of the same section and between sections occurred. In contrast, in some cases, TGF-α staining appeared to be less intense in the pit regions, in addition to some overall variation in staining intensity. There was a small number of parietal cells which showed signs of vacuolation (Figure 2.15), but the number was comparatively low compared with the occurrence in the 12h and 72h p.i. groups. The vacuoles present were mainly similar to the size of the nucleus or smaller, although some larger ones also occurred. Inside the cell, vacuoles were located close to the nucleus. Vacuoles did not take

Facing page 55

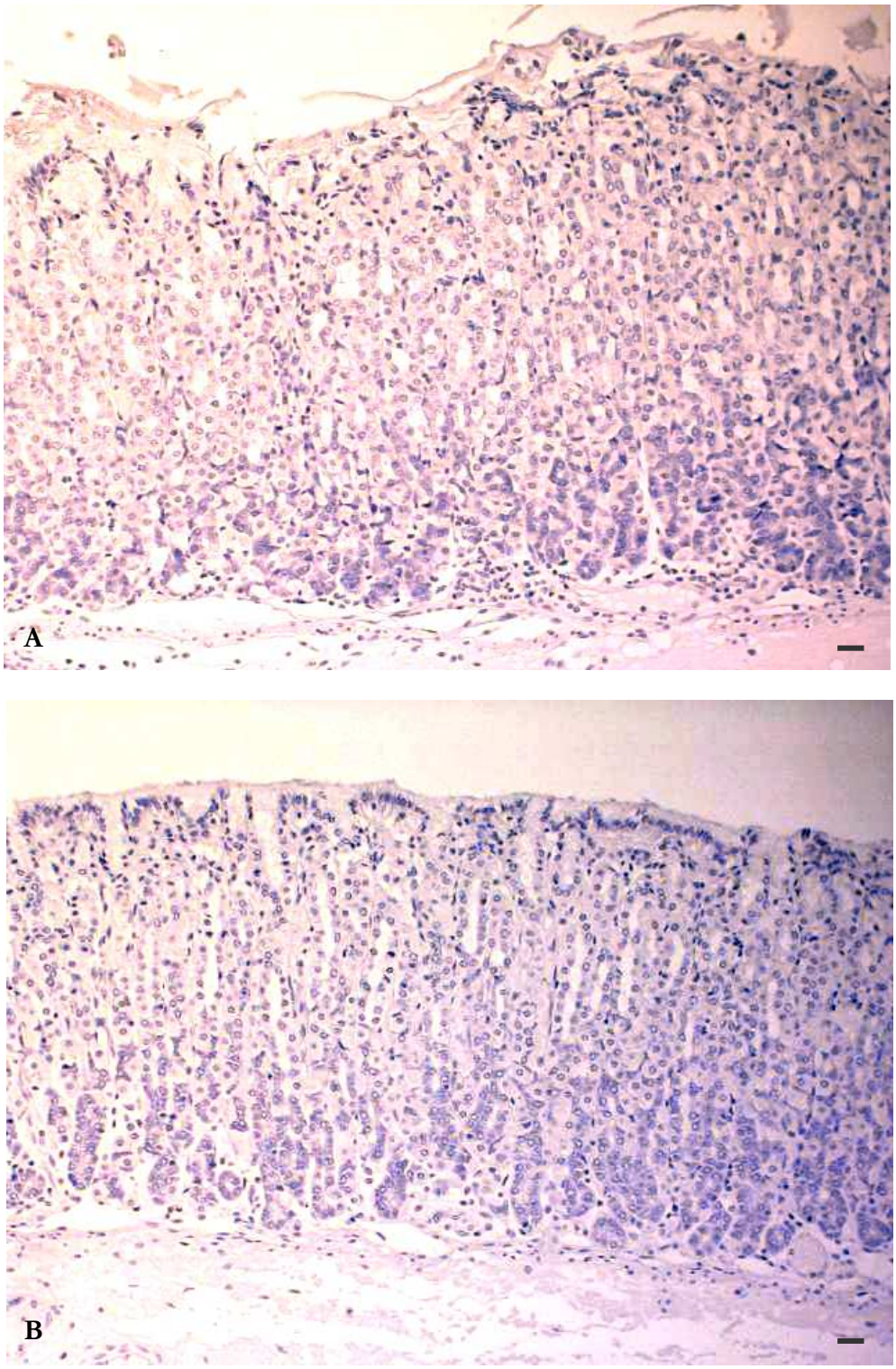

Figure 2.20: Fundic mucosa of sheep 12h after transplantation of 10,000 adult *T. circumcincta*. A. # 17541, B. # 17549. Some eosinophils can be seen entering the lamina propria. Paraffin embedded 5µm sections, Mayer's Hematoxylin counterstain, original magnification 200x, bars 10µm.

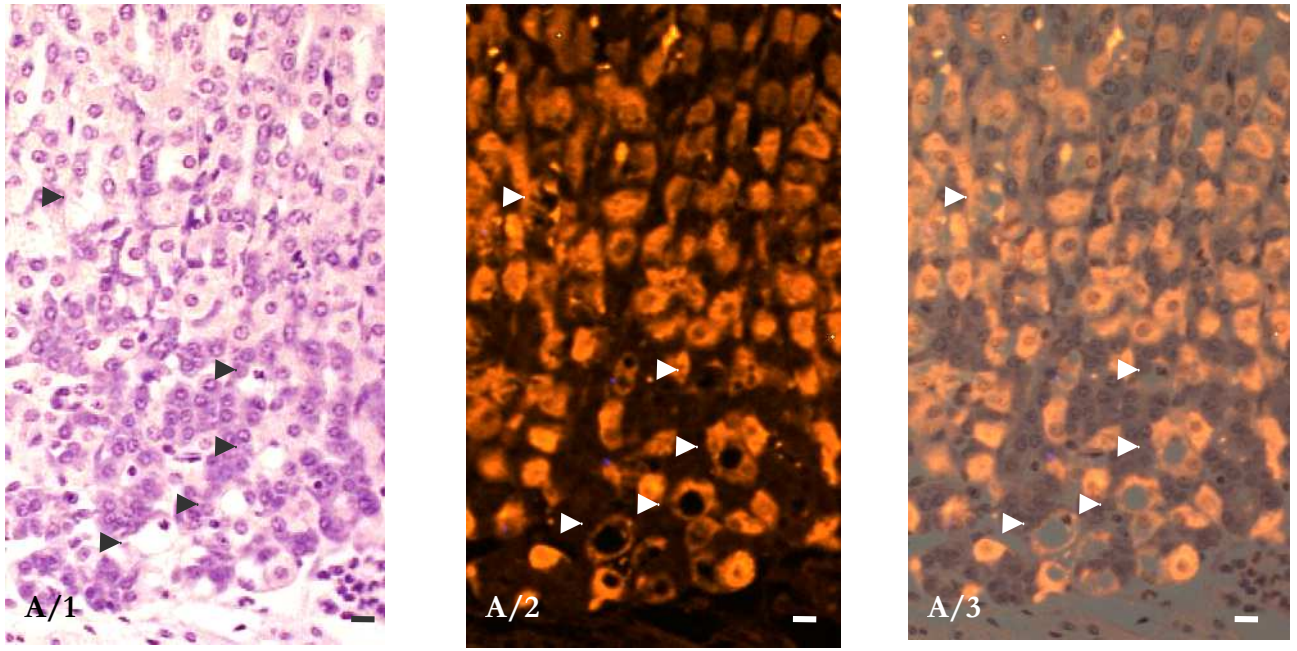

Figure 2.19: Fundic mucosa of sheep 12h after transplantation of 10,000 adult *T. circumcincta* - Parietal cell vacuolation. A. Vacuolated TGF-α positive parietal cells are marked by arrowheads. A/1 Hematoxylin counterstain, A/2 fluorescent TGF-α immunohistochemistry (excitation 546nm), A/3 merge A/1 and A/2. Shown are only the bottom parts of glands. Paraffin embedded 5µm sections, original magnification 200x, bars 10µm.

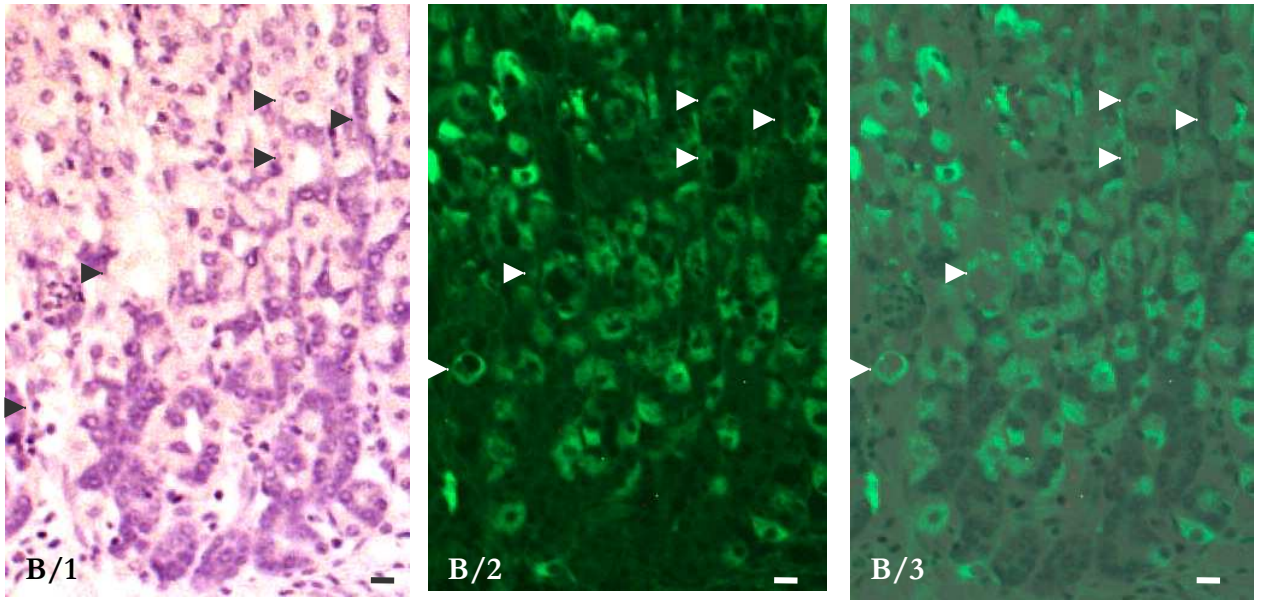

Figure 2.19 continued: Fundic mucosa of sheep 12h after transplantation of 10,000 adult *T. circumcincta* - Parietal cell vacuolation. Vacuolated H^+/K^+-ATPase positive parietal cells are marked by arrowheads. B/1 Hematoxylin counterstain, B/2 fluorescent H^+/K^+-ATPase immunohistochemistry (excitation 488nm), B/3 merge B/1 and B/2. Shown are only the bottom parts of glands. Paraffin embedded 5µm sections, original magnification 200x, bars 10µm.

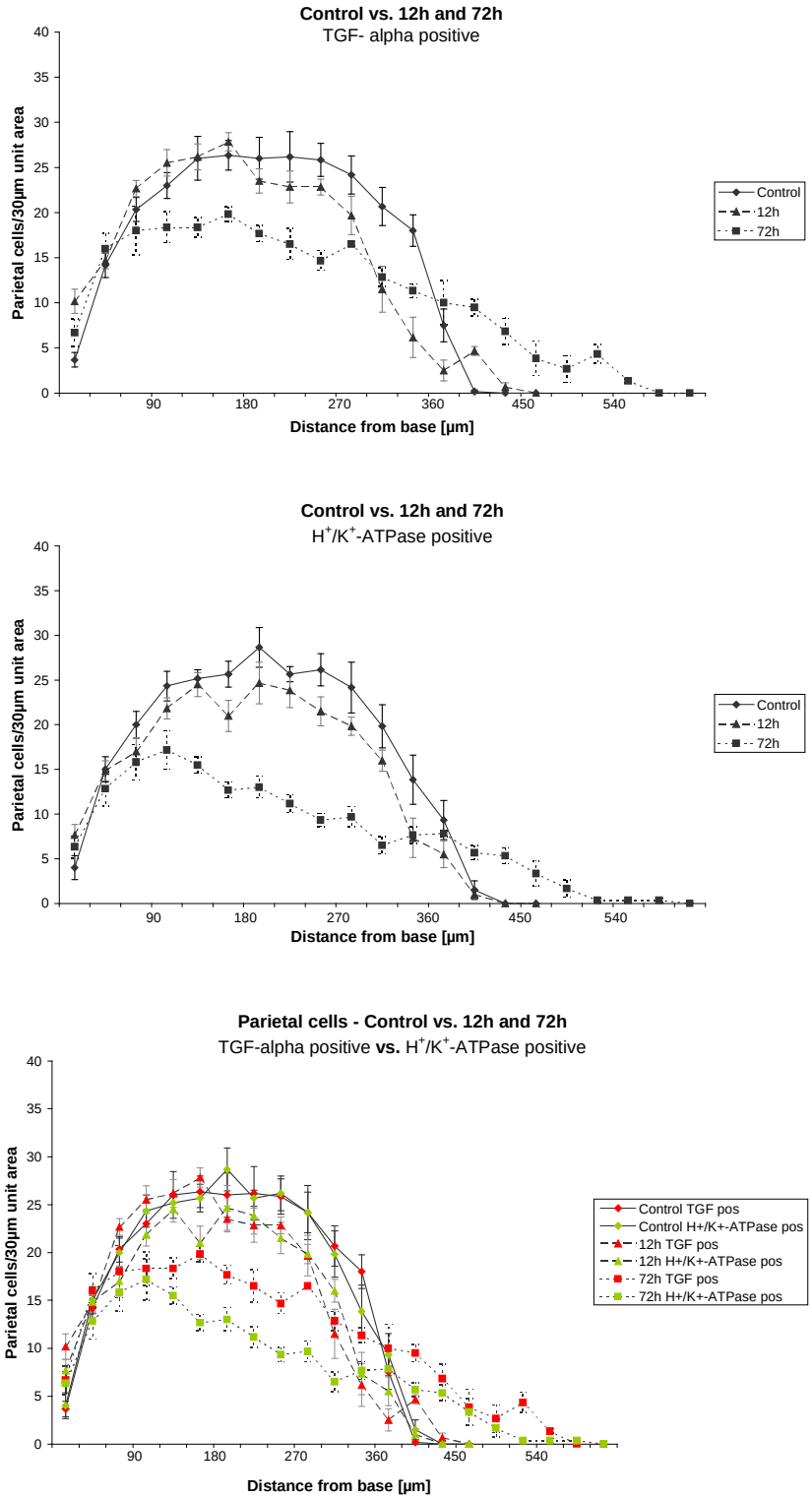

Figure 2.18: Numbers of TGF-α positive, H^+/K^+-ATPase positive, and TGF-α positive vs. H^+/K^+-ATPase positive parietal cells per 30µm unit area in a 300µm wide column of ovine fundic mucosa before (control) and 12 and 72h after transplantation of 10,000 adult *T. circumcincta*.

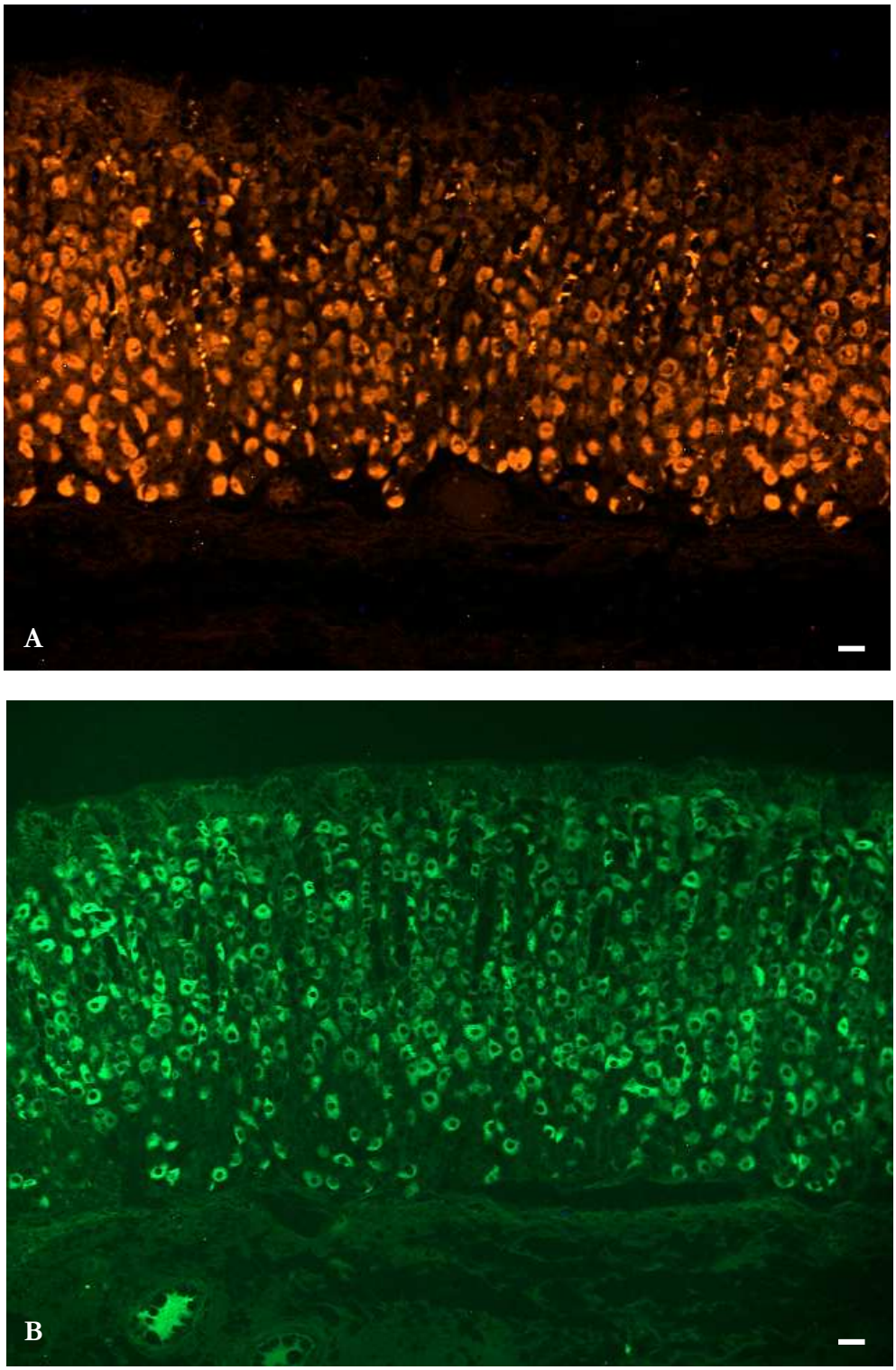

Figure 2.17: Fundic mucosa of sheep 12h after transplantation of 10,000 adult *T. circumcincta*. TGF-α (A.) and H^+/K^+-ATPase positive (B.) parietal cells are distributed within the pits and glands with the majority located in the middle part of the glands. Their distribution is similar. Some of the TGF-α positive parietal cells are more weakly stained in the pit regions. Fluorescent images after (A.) 546nm and (B.) 488nm excitation. Paraffin embedded 5μm sections, original magnification 200x, bars 10μm.

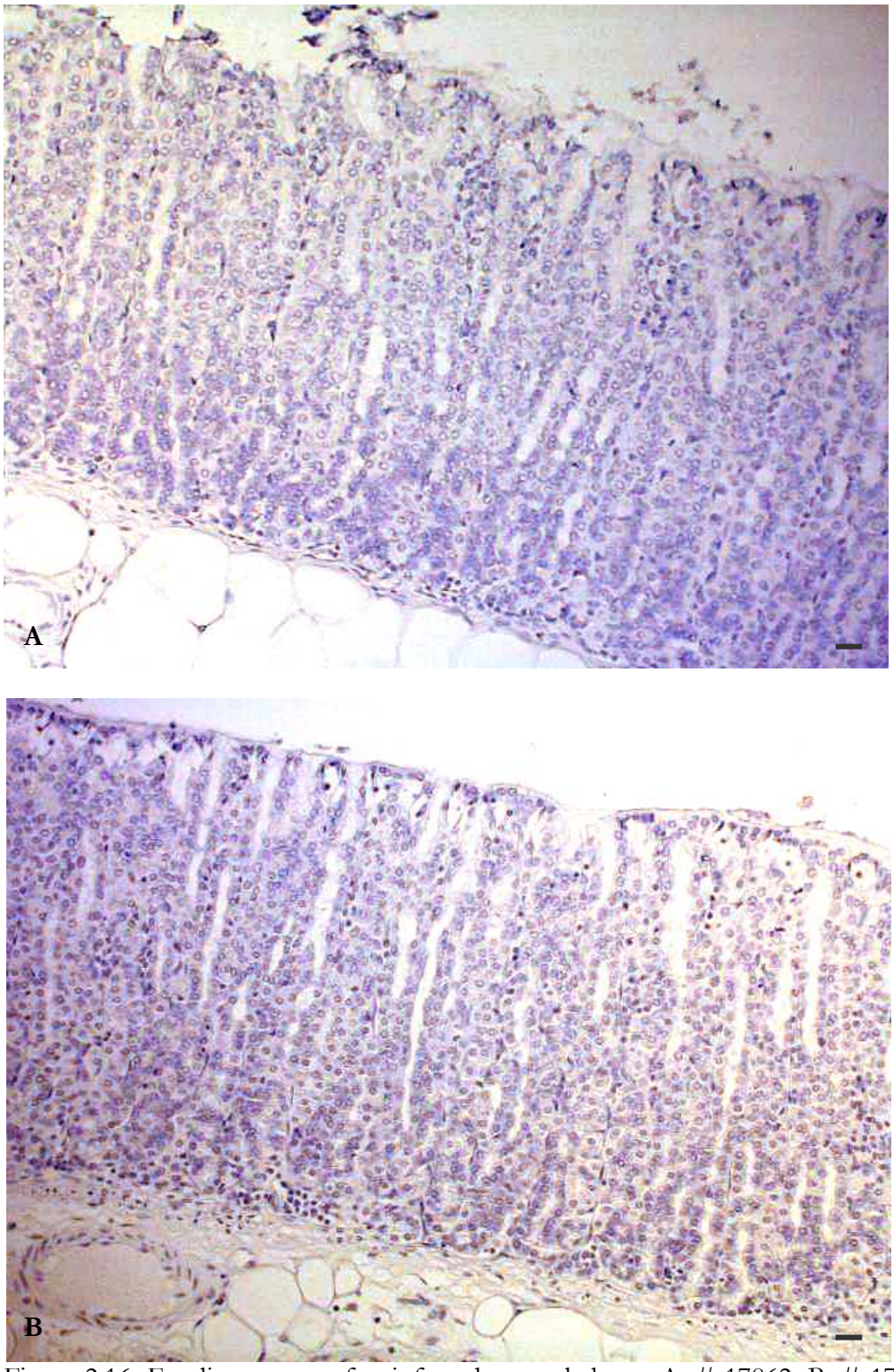

Figure 2.16: Fundic mucosa of uninfected control sheep. A. # 17862, B. # 17866. A few eosinophils can be seen, mainly at the bottom of the glands. Paraffin embedded 5μm sections, Mayer's Hematoxylin counterstain, original magnification 200x, bars 10μm.

any stain. In addition, a few eosinophils were detected in some sections at the bottom of the glands (Figure 2.16).

2.3.2.2.2 Abomasal Tissue 12h after Adult Transplant

The distributions of H^+/K^+-ATPase and TGF-α positive parietal cells along the pits and glands were similar to those in the controls, but parietal cell numbers were lower (Figures 2.17 and 2.18). Group means of H^+/K^+-ATPase and TGF-α positive parietal cells are shown in Figure 2.13 and counts of individual sheep in Figure 2.14. There were slight variations between numbers of H^+/K^+-ATPase and TGF-α positive parietal cells per animal, mainly in the upper base and lower neck for sheep #17541 and in the upper base and neck for #17549 (Figure 2.14). Overall, the H^+/K^+-ATPase positive parietal cells appeared to be fewer in number in this region (Figure 2.13). TGF-α positive parietal cell counts varied between animals in the 12h group in the neck and pit regions and for H^+/K^+-ATPase positive parietal cells mainly in the pit regions. However, for this comparison between animals it has to be noted that the mucosal thickness was greater in #17541 compared with #17549 (see also 2.3.2.3). Staining intensity with both H^+/K^+-ATPase and TGF-α varied slightly along the length of the gland, particularly being less intense with TGF-α antibody in the pit region. Vacuolated parietal cells appeared more numerous than in control sheep (Figure 2.19) and were located mainly in the base and neck. The size of the vacuoles were generally larger compared with those observed in the control sections. In some cases, the vacuole occupied almost the whole cell and it appeared as if the nucleus was pushed to the side. A few eosinophils could be observed at the bottom of the glands, as well as entering the lamina propria (Figure 2.20). In general, these numbers appeared to be higher than in the controls.

2.3.2.2.3 Abomasal Tissue 72h after Adult Transplant

Overall, mucosal changes in sections from the 72h group were extensive. H^+/K^+-ATPase and TGF-α positive parietal cells were distributed along the pits and glands, but the

Table 2.3: Mucosal thickness (fundus) and abomasal pH (mean ± SEM, n=2) in sheep before (uninfected control, Ct) or 12 and 72h after the transplantation of 10,000 adult *T. circumcincta*. Means with the same superscript are significantly different ($p<0.05$).

Parameter	Group		
	Ct	12h	72h
Mucosal thickness [µm]	$439.50 \pm 1.93^{a, b}$	398.44 ± 3.42^{a}	533.50 ± 5.46^{b}
Abomsal pH	2.65 ± 0.06	2.93 ± 0.14	4.71 ± 0.69

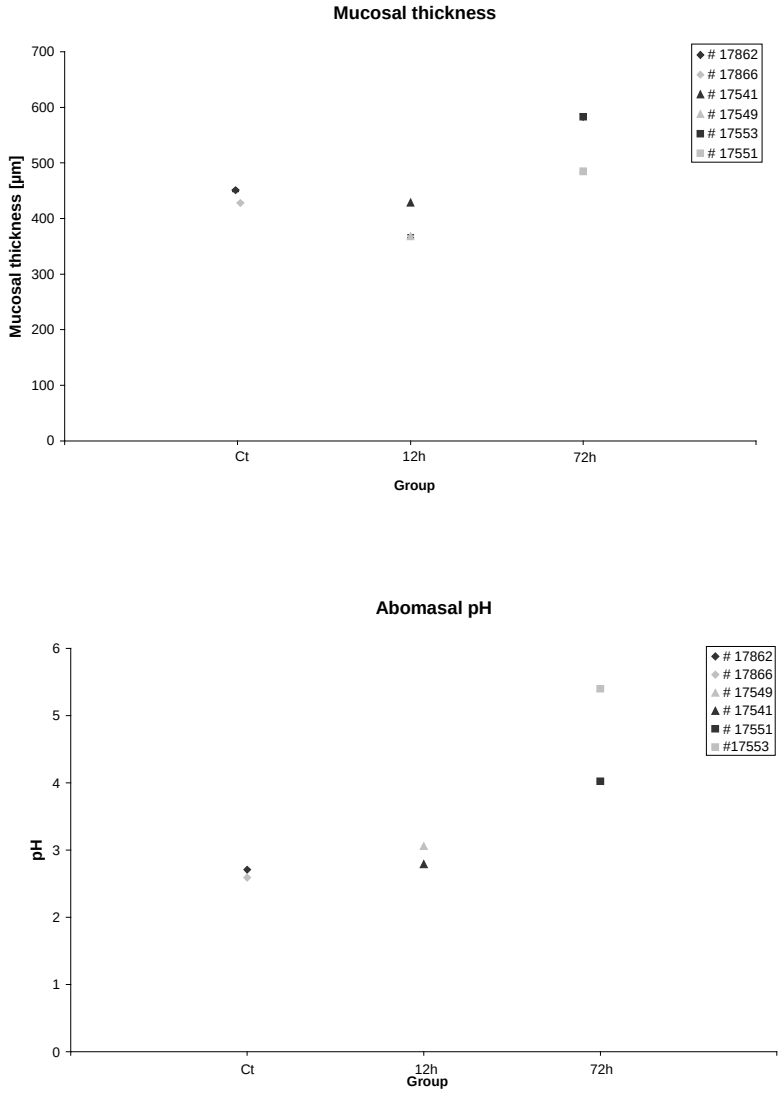

Figure 2.26: Mucosal thickness (µm) and abomasal pH of individual sheep before (control) and 12 and 72 hours after transplantation of 10,000 adult *T. circumcincta*.

Facing page 56

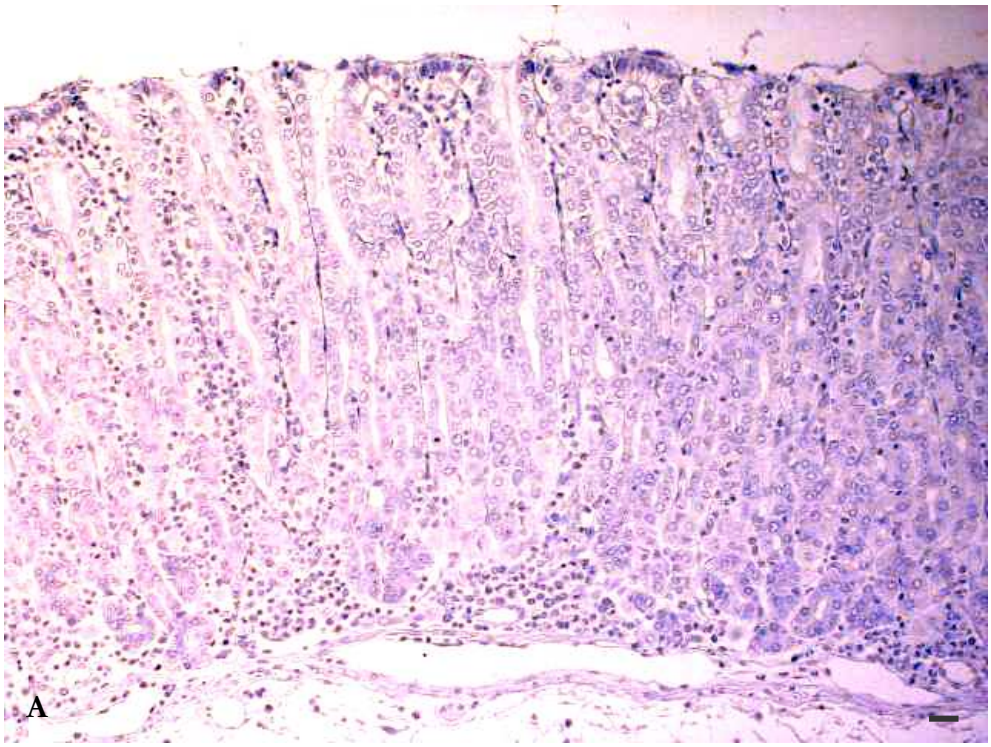

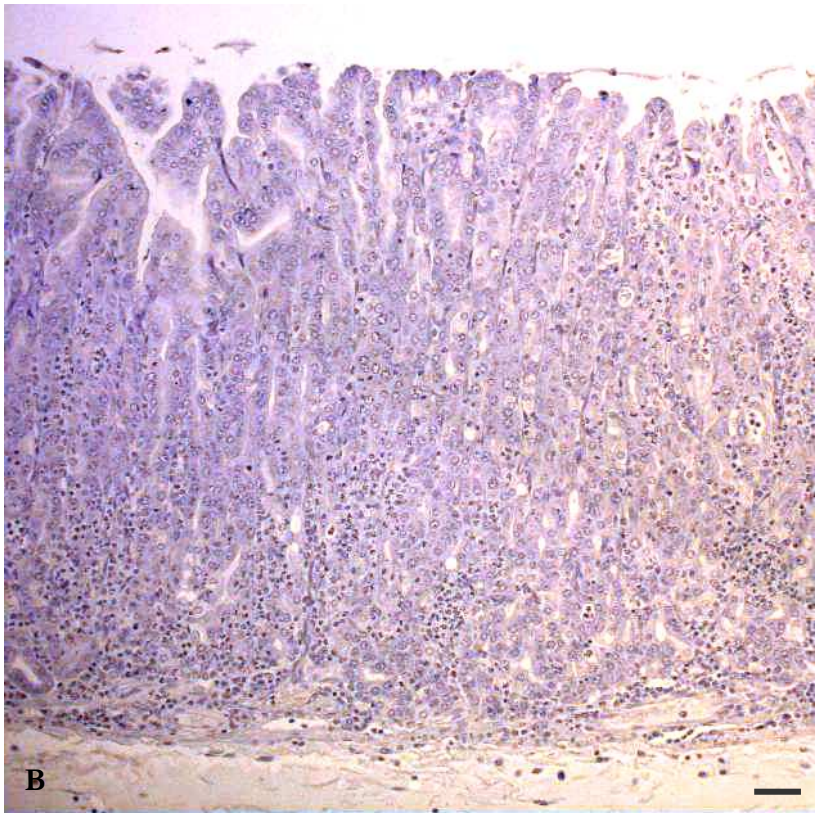

Figure 2.25: Fundic mucosa of sheep 72h after transplantation of 10,000 adult *T. circumcincta*. A. # 17551, B. # 17553. Large numbers of eosinophils can be seen entering the lamina propria. Paraffin embedded 5µm sections, Mayer's Hematoxylin counterstain, original magnification 200x, bars A. 10µm, B. 20µm.

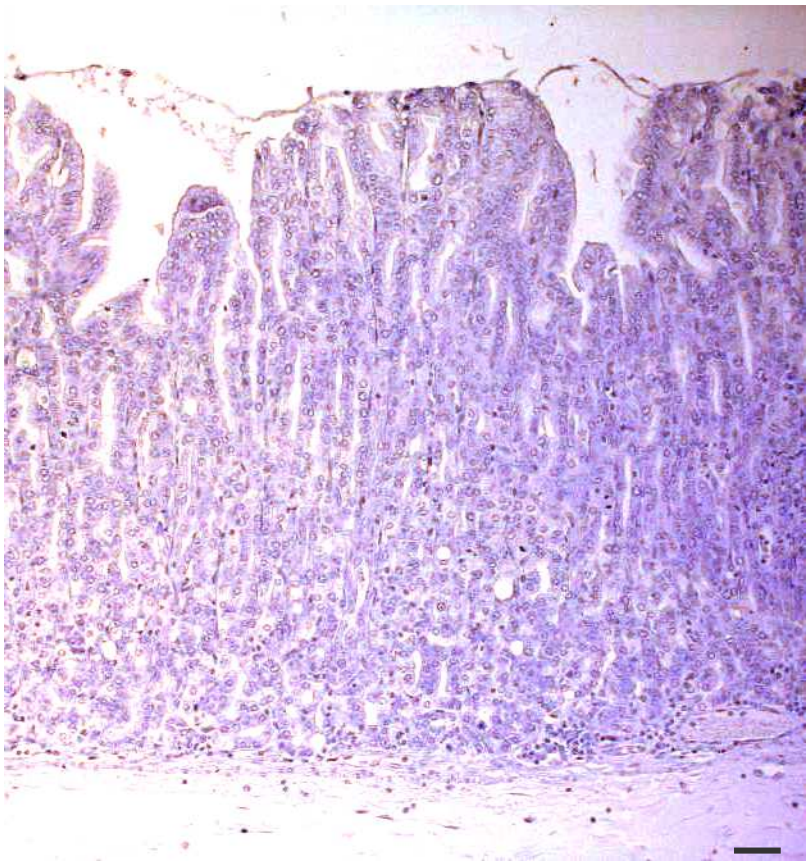

Figure 2.24: Fundic mucosa of sheep 72h after transplantation of 10,000 adult *T. circumcincta*. Extensive damage to the gastric pits can be seen. Paraffin embedded 5µm section, Mayer's Hematoxylin counterstain, original magnification 200x, bar 20µm.

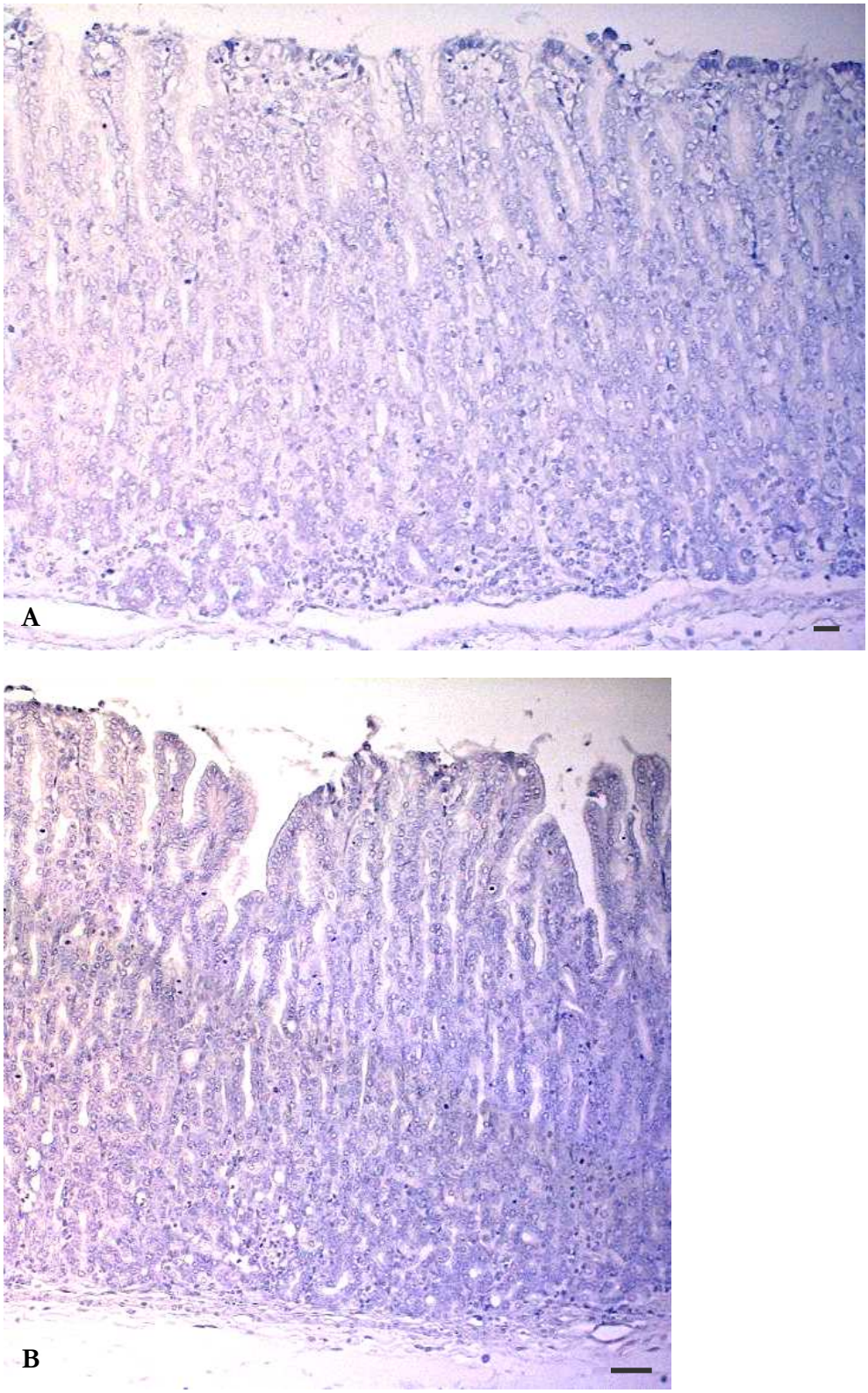

Figure 2.23: Fundic mucosa of sheep 72h after transplantation of 10,000 adult *T. circumcincta*. A. # 17551, B. # 17553. Mucosal thickness increased, which appeared to be associated with elongated pits. Cell differentiation seems poor with indistinctive division between pits and glands, but also neck and base. Paraffin embedded 5µm sections, Mayer's Hematoxylin counterstain, original magnification 200x, bars A. 10µm, B. 20µm.

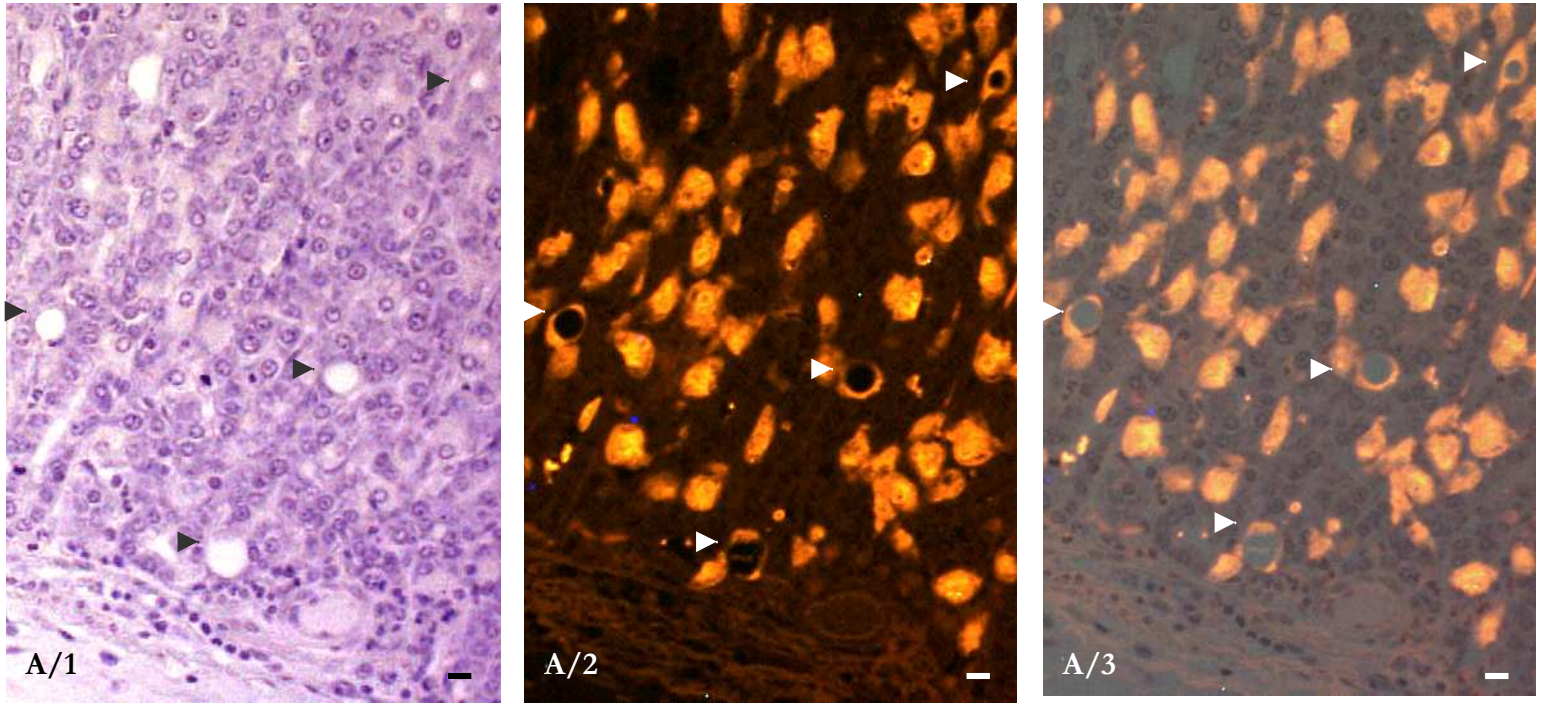

Figure 2.22: Fundic mucosa of sheep 72h after transplantation of 10,000 adult *T. circumcincta* - Parietal cell vacuolation. A. Vacuolated TGF-α positive parietal cells are marked by arrowheads. A/1 Hematoxylin counterstain, A/2 fluorescent TGF-α immunohistochemistry (excitation 546nm), A/3 merge A/1 and A/2. Shown are only the bottom parts of glands. Paraffin embedded 5µm section, original magnification 200x, bars 10µm.

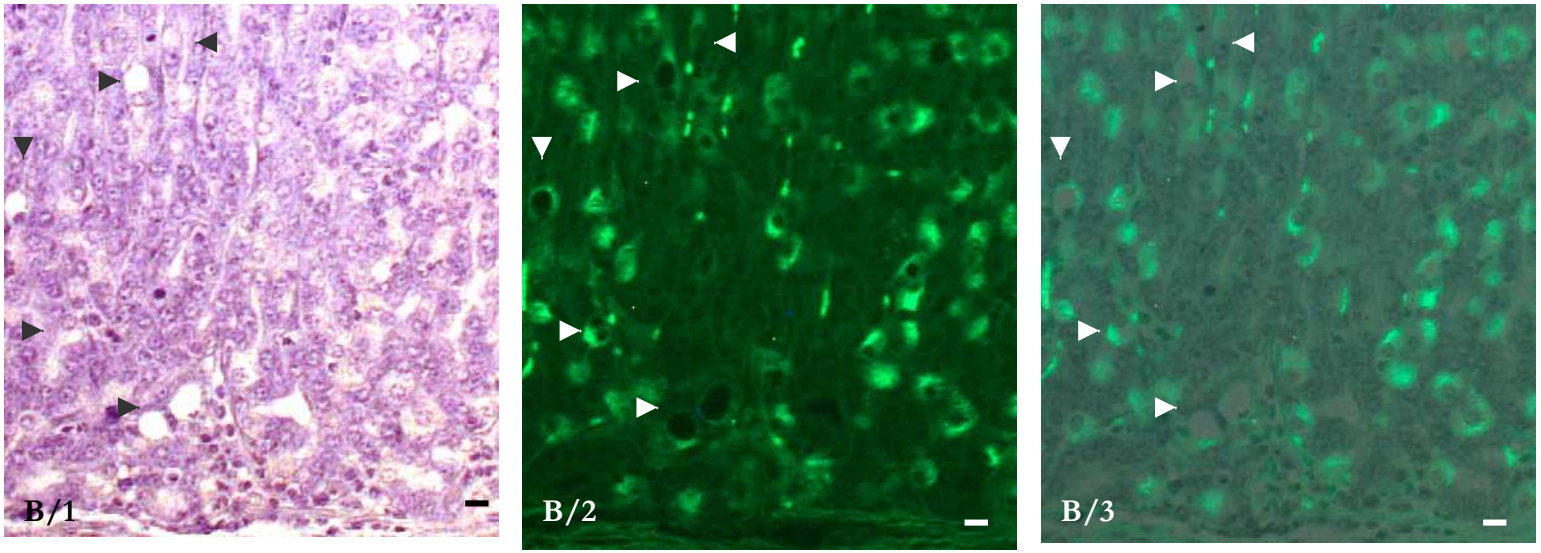

Figure 2.22 continued: Fundic mucosa of sheep 72h after transplantation of 10,000 adult *T. circumcincta* - Parietal cell vacuolation. B. Vacuolated H^+/K^+-ATPase positive parietal cells are marked by arrowheads. B/1 Hematoxylin counterstain, B/2 fluorescent H^+/K^+-ATPase immunohistochemisty (excitation 488nm), B/3 merge B/1 and B/2. Shown are only the bottom parts of glands. Paraffin embedded 5µm section, original magnification 200x, bars 10µm.

Facing page 56

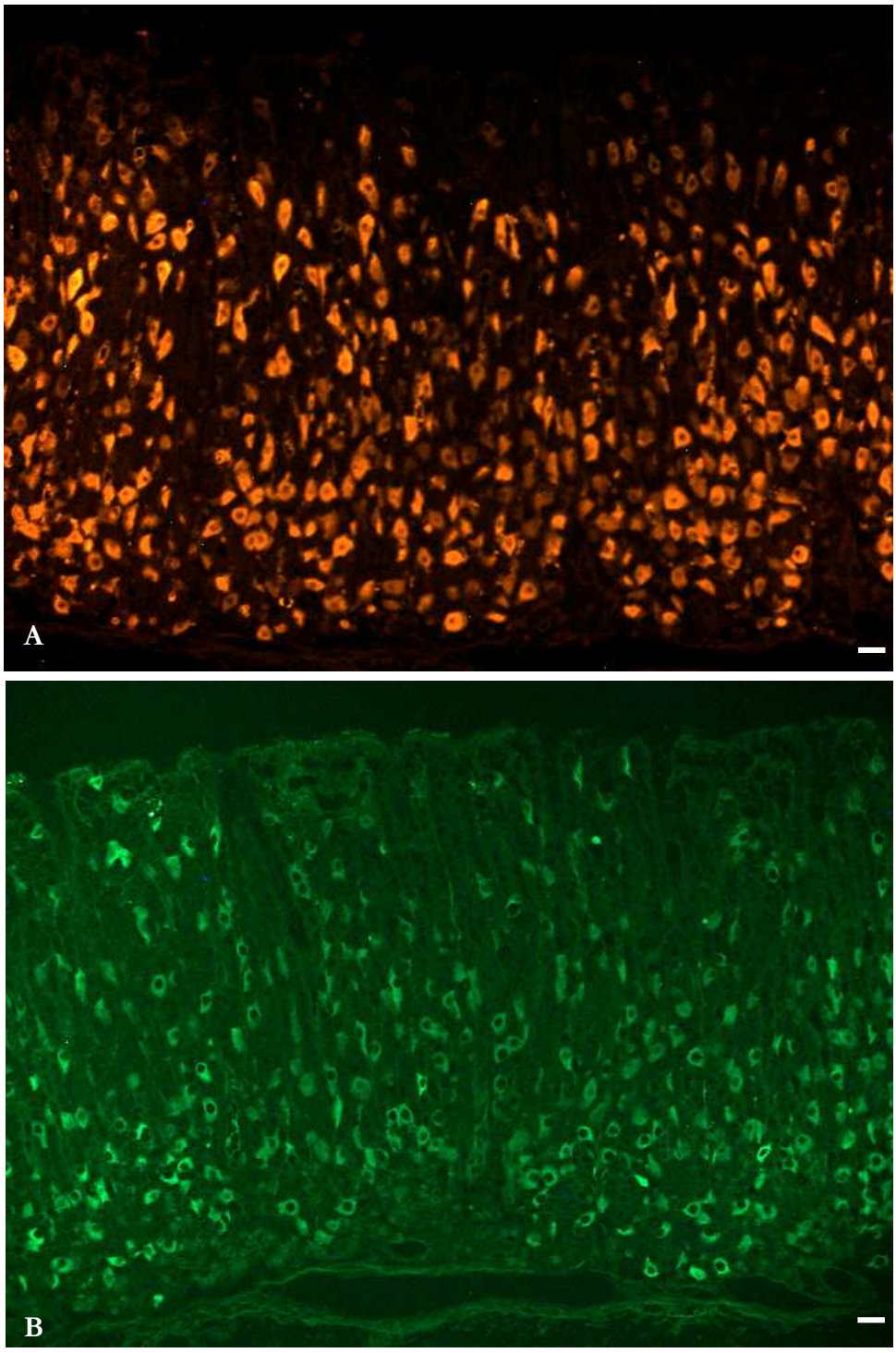

Figure 2.21: Fundic mucosa of sheep 72h after transplantation of 10,000 adult *T. circumcincta*. TGF-α (A.) and H^+/K^+-ATPase positive (B.) parietal cells are distributed within the pits and glands with the majority located in the lower middle part of the glands. The number of both TGF-α and H^+/K^+-ATPase positive parietal cells is markedly decreased compared with control tissue. Some of the TGF-α positive parietal cells are more weakly stained, especially in the pit regions. Fluorescent images after (A.) 546nm and (B.) 488nm excitation. Paraffin embedded 5μm sections, original magnification 200x, bars 10μm.

numbers were significantly reduced for H^+/K^+-ATPase positive parietal cells ($p<0.05$), mainly in the upper base and neck (Figures 2.21 and 2.18). Group means of H^+/K^+-ATPase and TGF-α positive parietal cells are shown in Figure 2.13 and counts of individual sheep in Figure 2.14. Variation between H^+/K^+-ATPase and TGF-α positive parietal cell staining occurred most prominently from the upper base to the lower pit (Figure 2.13), with overall H^+/K^+-ATPase positive cells being fewer compared with TGF-α positive cells. The variation in H^+/K^+-ATPase or TGF-α positive parietal cells between sheep in the 72h group was most prominent in the base and then again in the upper pit regions (Figure 2.14). However, the same restriction as for the 12h group applies for this comparison between animals in that the mucosal thickness was greater in #17553 compared with #17551 (see also 2.3.2.3). The staining intensity of both stains was comparable to that in the control and 12h groups, with some overall variation in intensity and less intense TGF-α staining in the pit regions. The 72h group contained the greatest number of parietal cells which were vacuolated (Figure 2.22). The majority of these were located in the base and lower neck. The vacuoles were similar to those observed in the 12h group. Generally there was one large vacuole per cell and, in some cases, it occupied almost the whole of the cell. As in all other cases, the vacuoles failed to stain. Sections from the 72h group showed a generalised hyperplasia, which seemed to be associated with an increase in the pit length (Figure 2.23; see also 2.3.2.3). Overall, cells were poorly differentiated and the division between pits and glands was less precise. Extensive damage to the pit regions was also observed in some areas (Figure 2.24). Large numbers of eosinophils could be observed infiltrating the lamina propria (Figure 2.25).

2.3.2.3 Abomasal pH and Mucosal Thickness

Abomasal pH in individual sheep and group means after the transplantation of adult *T. circumcincta* are shown in Table 2.3 and Figure 2.26. The difference in abomasal pH values across the groups was approaching significance ($p=0.0676$).

Mucosal thickness in individual sheep and group means after the transplantation of adult *T. circumcincta* are shown in Table 2.3 and Figure 2.26. In comparison with the control

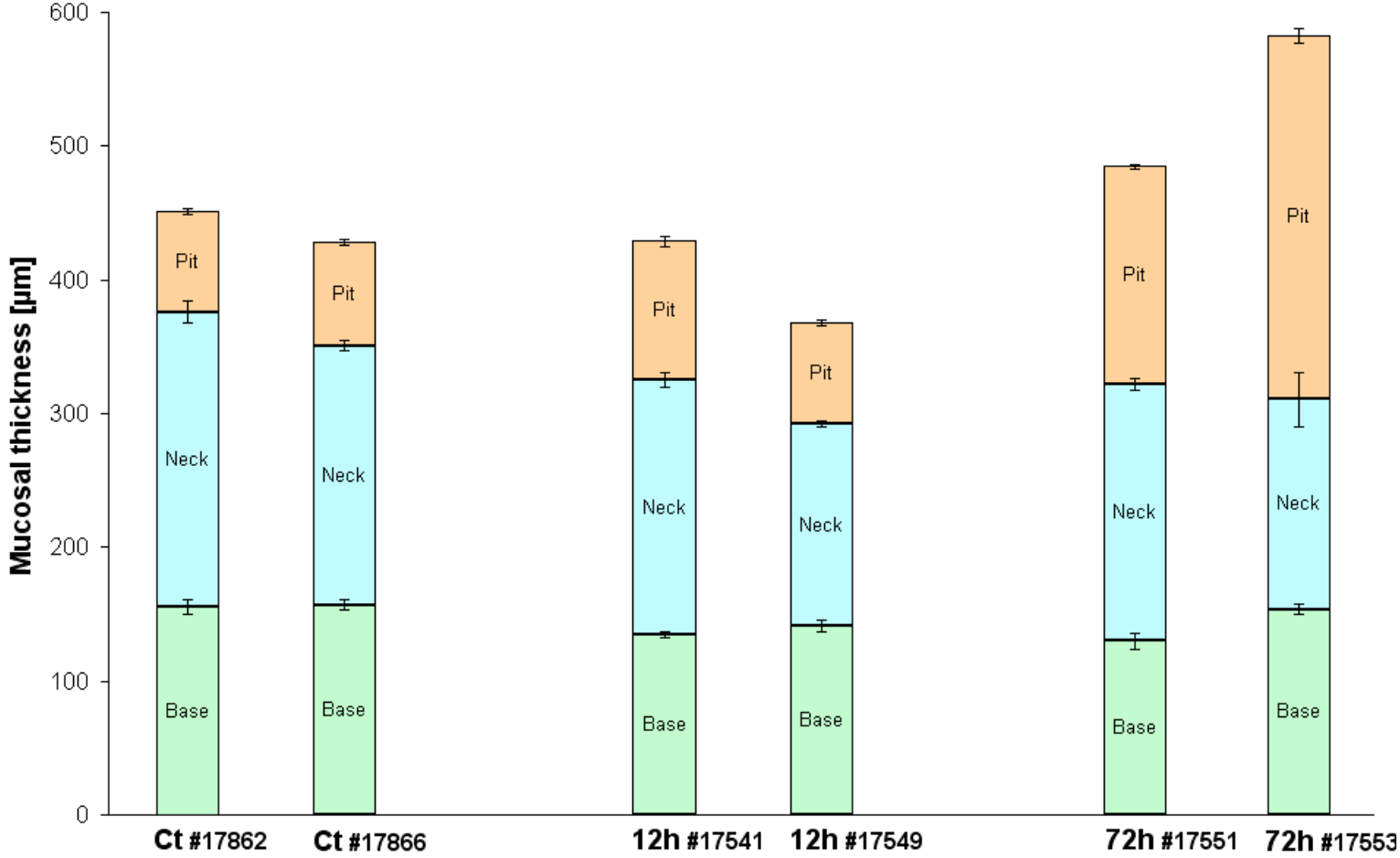

Figure 2.27: Thickness of the different regions (base-neck-pit) of fundic glands of individual sheep before (control), 12 and 72h after transplantation of 10,000 adult *T. circumcincta*.

sheep, there was a decrease in mucosal thickness in tissue sections from the 12h group (by ~40μm, mean) and an increase in the 72h group (by almost 100μm, mean), but differences were not significant. In the 72h group, it appeared that the pit regions were elongated, most prominently in sheep #17553 (Figure 2.27; see also 2.3.2.2.3).

2.4 Discussion

2.4.1 Early Changes within the Abomasal Mucosa after Infection with Labelled *H. contortus* L_3

During infection with *H. contortus*, the larvae invade the gastric glands and pits for 2-4 days (Christie, 1970; Nicholls *et al.*, 1987; 1988; Simpson *et al.*, 1997). During this time, particularly in the first few hours when changes in the host cells are initiated, identification of areas of interest is difficult. To facilitate the location of larvae in the glands, higher infective doses were chosen to maximise numbers entering the glands and larvae were fluorescently labelled.

Three dyes to label larvae were tested for suitable intensity of staining without compromising viability. Autofluorecence was marked in both the parasites and host tissue. *H. contortus* L_3 had a characteristic autofluorescence under UV light (Figure 2.1), which was at a similar wavelength to that of the sheep tissue. In addition to the autofluorescence, the DNA dye Hoechst 33258 also bound to DNA in the nuclei in the head and tail regions (Figure 2.2). However, both emit at a similar wavelength around 460nm using UV excitation (405nm). The additional labelling did not contribute significantly to detection of larvae inside the tissue. A better option would be a dye that emits at a different wavelength from the autofluorescence, such as Syto®17 and Nile Red, however, both proved unsuccessful. The lack of larval staining with Syto®17 was surprising since this dye has been used successfully in fluorescent sperm tracking in *Caenorhabditis elegans*, labelling mitochondria in nematode sperm without affecting sperm function (Hill and L'Hernault, 2001). Hoechst 33258 was then used for the experiments, which has been used for labelling

larvae for other *in vitro* experiments in this laboratory. The larvae retained the dye for days or even weeks without any obvious damage (unpublished observations), despite binding to DNA. The lack of effect on larval infectivity was confirmed by an infection with 200,000 L_3 (Table 2.1). After 24h, the total number of larvae recovered was 11,325, representing 5.7% of the infective dose, although the majority (7056) were recovered from contents. Overall, parasite recovery was less than would be expected with a routine pepsin-HCl tissue digest, but this was not carried out, as the experiment had a dual purpose. In addition to confirmation of viable larvae, the migration of larvae out of tissue *in vitro* was also of interest to explain observations on tissue in the confocal microscope (see below).

Both live and fixed tissues were examined to try to capture the early changes in parasitised tissues. Different infection periods were chosen (18 to 48h) to cover this phase of the infection before larvae normally emerge, which for *H. contortus* is usually after 2-4 days of development in the glands (Christie, 1970; Nicholls *et al.*, 1987; 1988; Simpson *et al.*, 1997). Tissue was mainly fixed in 4% paraformaldehyde, which penetrates tissue rapidly with minimal shrinkage, which can occur with fixing in Bouin's solution (Martins *et al.*, 2000; Ma *et al.*, 2002). It was hoped that the use of inverted confocal microscopy would allow easy scanning through the whole depth of the tissue with no need for long-term preservation in tissue blocks, so abomasal folds were fixed in paraformaldehyde for rapid short-term processing. However, the thickness of the tissue made it difficult to examine the tissue folds as whole. To be able to easily scan through larger areas of the tissue compared with 5µm sections, sections were also cut with a razor blade. A large number of tissues were examined, but failed to provide any useful tissues for studying cellular changes in the glands. Tissues proved too thick for the whole gland depth to be visualised using confocal microscopy, which was the main objective of this technique. This was due to the loss of excitation and emitted light due to absorption by the 0.5 to 1mm thick tissue.

Detection of parasitised glands was not possible unless they contained a larva. However, this was rarely the case even in areas of nodules cut into thin slices. As the full depth of the gland could not be visualised with the confocal microscope, larvae deep in the gland may not have been detected. Another possible reason for few larvae being seen inside the tissue may be that larvae leave the tissue after the sheep has been euthanased or later during the tissue preparation. Although larvae would not be expected to leave the gland as early as 24h

p.i. *in vivo*, it is possible that larvae leave the tissue rapidly *post mortem* due to changes in blood flow and O_2/CO_2 levels. One larva was seen leaving unfixed tissue while being studied using the confocal microscope. This larva was photographed (Figure 2.4) after it left the gland and appeared on the surface of the tissue. Usually, the time from euthanasia of the sheep to fixing the tissue pieces was about 30min, however, when this was reduced to about 5min for one sheep, there were no noticeable benefits. The time taken for paraformaldehyde fixation could also permit larval migration, as fixing L_3 *in vitro* takes about 1 to 2min before larvae stopped moving.

During the Baermannisation of the abomasal tissue collected for studying larval viability, 293 larvae left the unprocessed half of the abomasum during a 4h incubation in PBS at 37°C. Subsequently, more larvae migrated out of the tissue during incubation of mucosal scrapings from the same abomasal half over a 24h period (Table 2.1), totalling 1553 larvae from the fundus and 803 from the antrum. In an experiment in which larvae applied to the exteriorised abomasum of a sheep anaesthetised with barbiturate, larvae were later seen leaving the tissue when the sheep was euthanased with an overdose of barbiturate (H. V. Simpson, personal communication). It seems that larvae are capable of rapidly leaving glands before completing their normal development which further complicates studies of early stages of larval infection.

Almost certainly, another reason for failure to identify parasitised glands is that the number of larvae in relation to the number of glands is quite low (in humans ~135 glands/mm^2 (Kurbel *et al.*, 2001)) and only a small tissue sample of the whole abomasum was examined. Even in a heavy infection, the percentage of glands invaded by larvae would still be low. This would be further reduced if some larvae leave the tissue after the sheep has been euthanased.

2.4.2 Early Changes within the Abomasal Mucosa after Infection with Adult *T. circumcincta*

2.4.2.1 Identification of Functionally Different Parietal Cells

Parietal cells have different functions depending on their position in the fundic gland (1.2.2.3): those in the isthmus and neck are more metabolically active, secrete more acid and migrate at a faster rate than those in the base of the gland (Coulton and Firth, 1983; Karam *et al.,* 1997). A different function has been suggested for parietal cells in the base, which may be in controlling cell differentiation and regeneration through secretion of growth factors (1.2.4). In hematoxylin and eosin (H&E) stained tissues from uninfected sheep, there were parietal cells which were not labelled by TGF-α antibodies and this number appeared greater in parasitised sheep (Przemeck, 2003). In order to identify these subpopulations of parietal cells, both antibodies to TGF-α and the H^+/K^+-ATPase β-subunit were used as parietal cell markers. Lectin staining was investigated as a third marker, but did not provide unequivocal identification of parietal cells.

Lectin staining of parietal cells has been used in a number of studies in different species (Malchiodi Albedi *et al*., 1985; Kessiman *et al*., 1986; Callaghan *et al*., 1990; 1992). Callaghan *et al.* (1990) tested a variety of lectins on tissues from different species, including dog, rat and pig and reported some variation in their results from those of others. An example is for human parietal cells: whereas they observed intense staining only with *Lycopersicon esculentum* (tomato) agglutinin (LEA) and *Solanum tuberosum* (potato) agglutinin (STA), weak staining with PNA and no staining with SBA, Kessiman *et al.* (1986) reported intense staining of human parietal cells with DBA, PNA and SBA. Over a number of studies, parietal cells have been labelled with BSL, DBA, LEA, PNA, *Ricinus communis* (castor oil plant) agglutinin (RCA), SBA and STA.

In the present experiments, staining of sheep fundic tissue with DBA, PNA, SBA and UEA resulted in inconsistent staining between animals and was not reliably repeatable. As lectins bind specifically to terminal or subterminal carbohydrate residues and linkages (Rhodes and Milton, 1998), binding can be affected by the presence of divalent cations in

the medium or changes in sulphation or attachment of sialic acids to the carbohydrates. PBS, without the addition of divalent cations, was used as a buffer for the staining protocol, as reported by Malchiodi Albedi *et al.* (1985) and Callaghan *et al.* (1990), who successfully labelled parietal cells of other species. However, lectin binding to sheep gastrointestinal tissues could be altered by infection. There are changes in the glycosylation profile of mucins (V. C. Hoang, personal communication) with both age and abomasal parasitism. Antibodies to TGF-α and the H^+/K^+-ATPase β-subunit were used as the parietal cell markers, as lectin staining of parietal cells was not specific for parietal cells, uneven in tissues and not consistent between animals.

Different populations of parietal cells were apparent using TGF-α and H^+/K^+-ATPase antibodies together with hematoxylin counterstaining (Figures 2.13 and 2.14). Parietal cells that did not stain for H^+/K^+-ATPase were not readily detected by only hematoxylin counterstaining, in contrast to the study of *O. leptospicularis* infection in sheep by Hertzberg *et al.* (2000), who reported parietal cells which did not stain with the H^+/K^+-ATPase antibody, but only in infected animals. Some parietal cells, which did not label for TGF-α were detected, but showed no specific location in the glands. Overall, parietal cells strongly stained for TGF-α compared with occasional weak staining of surface mucous cells in the pits (Thomas *et al.,*1992; Przemeck, 2003). The number of parietal cells which did not stain with TGF-α was lower (0.8% for the control group, 2.1% after 12h and 2.7% after 72h) than up to 35% and on average about 11.5%, which was reported by Przemeck (2003). This may be partly caused by being unable to include eosin for visualising the parietal cells, which is not possible together with the fluorescent labelling. Staining of successive sections with TGF-α and H&E or H^+/K^+-ATPase and H&E may help identify non-staining parietal cells, which were difficult to detect, especially in the 72h group where many cells appeared de-differentiated. However, even though parietal cells are the largest cells in the fundic mucosa (height 18μm and width 25μm in humans, Karam *et al.*, 2003), staining of successive sections (5μm thick) with TGF-α and H^+/K^+-ATPase showed that large numbers of parietal cells did not align.

2.4.2.2 The Fate of the Parietal Cell and H^+/K^+-ATPase

Overall, compared to the control group, the number of parietal cells decreased at both 12h and 72h after adult *T. circumcincta* transplant. Though, this was statistically significant only for H^+/K^+-ATPase positive parietal cells numbers 72h after the transplant. Decreased parietal cell numbers were associated with higher abomasal pH values of 4.02 and 5.4, although the group means were not significantly different with only two sheep in each group. Other studies with larger numbers of animals clearly showed an increased pH soon after transplantation of adult parasites (Lawton *et al.*, 1996; Simpson *et al.*, 1997; Scott *et al.*, 2000).

Parietal cell numbers were not only decreased, but different parietal cell populations were apparent 72h after infection from comparison of the profiles of TGF-α positive and H^+/K^+-ATPase positive parietal cells (Figure 2.13). Whereas the profiles of TGF-α positive and H^+/K^+-ATPase positive parietal cells were almost identical in the control animals and similar 12h p.i., the profile for H^+/K^+-ATPase positive parietal cells was consistently lower at all positions in the gland 72h after infection. This could indicate that a sequence of events may be leading to the observed pathology and pathophysiology during abomasal parasitism. It is possible that the H^+/K^+-ATPase is lost first, which may be a result of inhibition by an ES product or inflammatory cytokine. Loss of the H^+/K^+-ATPase might be sufficient to increase the abomasal pH, without a major change in the number of parietal cells, before parietal cells are then lost later in infection.

Hertzberg *et al.* (2000) reported parietal cells in infected sheep which did not stain with the H^+/K^+-ATPase antibody and equated these with inhibited parietal cells with an inactive form of the proton pump, although antibody binding would be expected even to an inactive form of the proton pump. However, these inactive parietal cells were also identified ultrastructurally. Furthermore, Karam and Forte (1994) have shown that continuous inhibition of the H^+/K^+-ATPase by omeprazole induced degeneration of parietal cells including dilated canaliculi and vacuoles and cell death by necrosis and apoptosis. Similar results were observed with inhibition of the parietal cell H_2 receptors by ranitidine (Karam and Alexander, 2001). In addition, Crothers *et al.* (1993) showed that the amount of H^+/K^+-ATPase decreased after omeprazole treatment, which was found to

result from an increased breakdown rather than decreased synthesis. In contrast, Tari *et al.* (1991) demonstrated an increase in H^+/K^+-ATPase expression after omeprazole treatment.

The expression of H^+/K^+-ATPase is also affected by *H. pylori* infection, which is often compared to abomasal parasitism as it shares similarities in pathology like hypoacidity, mucosal hyperplasia and induction of vacuoles (Murayama *et al.*, 1999; Przemeck, 2003; Cover and Blanke, 2005; Huber *et al.*, 2005; Przemeck *et al.*, 2005). Furuta *et al.* (1999) showed that H^+/K^+-ATPase mRNA levels in chronic gastritis patients positive for *H. pylori* were lower than in the uninfected control group and increased after *H. pylori* eradication (one month) to almost the same as the control group. Moreover, another study demonstrated that 12 weeks after *H. pylori* eradication H^+/K^+-ATPase mRNA levels increased 250-fold without alteration of parietal cell numbers (Osawa *et al.*, 2006).

Upregulation of the H^+/K^+-ATPase expression could also be a possibility for the fast recovery of acid secretion after sheep have been drenched, which was reported to start within two hours of drenching (Simpson *et al.*, 1997; Scott *et al.*, 2000). It was suggested that a parasite-derived factor inhibited the parietal cell function temporarily and, once removed, the secretory function recovered quickly. Alternatively, Simpson (2000) suggested that production of new parietal cells could be responsible for recovery from acid inhibition. Young parietal cells, which mature within two days (Karam, 1993) and then become very active (Coulton and Firth, 1983; Karam *et al.*, 1997), could also be responsible for the drop in abomasal pH to below pre-infection levels after drenching of infected sheep. Inhibition of the H^+/K^+-ATPase by omeprazole (Karam and Forte, 1994) or inhibition of the H_2 receptors by ranitidine (Karam and Alexander, 2001) also increased the production of pre-parietal cells accounting for fast recovery of parietal cell numbers in these studies. However, Scott *et al.* (2000) did not find evidence for the recovery of parietal cell numbers within seven days after drenching in sheep that had received an adult transplant of 20,000 *T. circumcincta*. This suggests that the recovery of acid secretion after drenching could be due to an increased expression of the proton pump in the remaining parietal cells.

Further experiments are needed to clarify whether the proton pump is lost before parietal cell loss during abomasal parasitism, whether increased proton pump expression is indeed responsible for the fast recovery of acid secretion after drenching and whether the parietal

cell population is recovering at some stage after drenching. This could include experiments to double stain parietal cells for H^+/K^+-ATPase and TGF-α or another reliable parietal cell marker, staining pre-parietal cells and their precursors and examining H^+/K^+-ATPase mRNA levels before and during infection as well as after drenching. In addition, *in vitro* experiments using a stable transfected cell line that is expressing the proton pump (Kimura *et al.*, 2002) could clarify whether ES products are able to directly affect the proton pump (inhibition or breakdown). Experiments with transfected cells could also clarify whether the expression of the H^+/K^+-ATPase is repressed during infection as it was shown for *H. pylori* (Saha *et al.*, 2008). *In vitro*, *H. pylori* infection of transfected AGS cells (epithelial human gastric adenocarcinoma cells) was demonstrated to repress the activity of the transfected promotor of the H^+/K^+-ATPase α-subunit by increased NFκB binding.

Increased numbers of vacuolated parietal cells compared to the control group were observed 12h and 72h after adult transplant. This has been described previously in sheep infected with *T. circumcincta* (Scott *et al.*, 1998a; 2000; Przemeck, 2003). Vacuolation could occur as one of the steps of parietal cell degeneration. Karam *et al.* (2003) reported that occasionally parietal cells in the neck and base degenerate, a process which is characterised by extensive dissolution of canaliculi and intermitochondrial cytoplasm with formation of vacuoles. This could explain the small number of vacuolated parietal cells in the control group. Furthermore, as already mentioned above, continuous inhibition of the H^+/K^+-ATPase by omeprazole (Karam and Forte, 1994) or inhibition of the H_2 receptors by ranitidine (Karam and Alexander, 2001) induced increased degeneration of parietal cells including vacuolation. Alternatively, vacuolation could be a result of a direct effect of ES products, which were shown to induce vacuolation *in vitro* in HeLa cells (Przemeck, 2003; Huber *et al.*, 2005; Przemeck *et al.*, 2005).

The host inflammatory response may also contribute to parietal cell inhibition and the development of hypoacidity during parasitism (Scott *et al.*, 1998a; 2000; Przemeck, 2003). The results presented here showed a slightly increased number of eosinophils after 12h and large numbers 72h after the adult transplant, which coincides with a raised abomasal pH and loss of parietal cells. However, Przemeck (2003) also observed vacuolated parietal cells 5d p.i. with *T. circumcincta* when abomasal pH was unchanged and inflammation was minimal, suggesting that both direct effects of parasites and an inflammatory response,

might be involved. The recruitment of inflammatory cells could also be mediated by the parasites indirectly as eosinophil and neutrophil chemoattractants have been detected in *H. contortus* and *T. circumcincta* ES products (Reinhardt, 2004; Wildblood *et al.*, 2005; reviewed in 1.3.3.7.2). Simpson (2000) and Wildblood *et al.* (2005) suggested that the recruitment of inflammatory cells might be beneficial for the parasites by damaging parietal cells and/or tissue improving their environment by reducing acid secretion or tissue invasion.

Various inflammatory cytokines and growth factors interfere with acid secretion, including IL-1β, TNF-α, TGF-α, EGF and HGF (Beales, 2000). IL-1β release correlated with hypoacidity in *H. pylori* induced enlarged fold gastritis (Yasunaga *et al.*, 1997) and moreover, IL-1β mRNA levels decreased by 40% after *H. pylori* eradication possibly also contributing to the restoration of acid secretion (Osawa *et al.*, 2006). In addition, IL-1β inhibited histamine secretion by ECL cells *in vitro* (Prinz *et al.*, 1997). Overexpression of TGF-α in transgenenic mice induced a loss of parietal and chief cells without an associated loss of their precursors (Sharp *et al.*, 1995). TNF-α also caused apoptosis of parietal cells in isolated perfused rat stomachs (Neu *et al.*, 2003). The elevated rate of apoptosis during chronic *Trichuris muris* infection is independent of the infection dose, but associated with increased TNF-α and IFN-γ levels (Cliffe *et al.*, 2007). It was suggested that this is a mechanism to counteract epithelial hyperplasia during infection.

The inflammatory response could also be involved in mucosal thickening. An increase in mucosal thickness occurred in the 72h group compared to the control, which was also associated with the infiltration of large numbers of eosinophils. It appeared that the pits were elongated, however the margins between the different gland areas were not as distinct in tissue from infected sheep, especially in the 72h group, as in uninfected animals. Scott *et al.* (1998c) have previously shown that increasing mucosal thickness in *H. contortus* infected sheep was due to mucous cell hyperplasia, which were identified as having a similar phenotype as mucous neck cells. However, Przemeck (2003) reported elongation of the pits in *T. circumcincta* infected sheep.

The similarity of the cellular changes, including mucosal hyperplasia, elongated pits, mucous neck cell hyperplasia and reduced numbers of parietal cells, to other conditions

involving loss of parietal cells is reviewed in 1.3.2. The loss of trophic agents released by parietal cells, including TGF-α, has been implicated in the effects on other cell lineages and accumulation of de-differentiated cells (Canfield *et al.*, 1996). Hypergastrinaemia, as a result of increased pH due to inhibition and loss of parietal cells, and the inflammatory response could also be involved in mucosal thickening.

Another approach to assessing the contribution of ES products in isolation from indirect effects caused by the reaction of the host to the presence of the parasites is to use model cell systems *in vitro*. Further studies extending the work of Przemeck (2003), Huber *et al.* (2005) and Przemeck *et al.* (2005) on the induction of vacuolation in HeLa cells by ES products are reported in chapter 3. The ability of ES products to induce cell detachment and loss and changes in tight junction permeability of epithelial cell monolayers are reported in chapters 4 and 5 respectively.

Chapter 3

EFFECTS OF *H. CONTORTUS* ES PRODUCTS *IN VITRO*: CELL VACUOLATION

3.1 Introduction

In addition to parietal cell loss, vacuolation of parietal cells was observed in abomasal tissue sections of sheep infected with *T. circumcincta* larvae and after adult worm transfer (Scott *et al.*, 1998a; 2000; Przemeck, 2003). It was suggested that cellular changes might be mediated indirectly by ES products released by the parasites (Scott *et al.*, 1998a; Simpson, 2000; Przemeck, 2003).

A rapid decrease in acid secretion was shown after adult worm transplant of *H. contortus* (Simpson *et al.*, 1997) and *T. circumcincta* (Scott *et al.*, 2000) and an equally rapid recovery after parasite removal by anthelmintic treatment for both parasites. An effect on acid secretion was also obtained in sheep where adult *T. circumcincta* were confined to porous bags (Simpson *et al.*, 1999) and in rats given *O. ostertagi* extracts intraperitoneally (Eiler *et al.*, 1981). It was also shown that adult *H. contortus* ES products could inhibit acid secretion *in*

vitro, with the possibility that ammonia was involved (Merkelbach *et al.*, 2002). These studies all suggested that a parasite-derived factor was involved in the decreased parietal function.

ES products (reviewed in 1.3.3) contain a variety of components that could have detrimental effects on abomasal tissue and cells, including causing parietal cell vacuolation (other aspects are discussed in chapters 4 and 5). These could include the proteases released as well as prostaglandins.

Serine proteases in products of microorganisms appear to be involved in vacuolation of epithelial cells. The vacuolating activity of *H. pylori* VacA was previously compared with that of ES products (Przemeck, 2003; Huber *et al.*, 2005; Przemeck *et al.*, 2005) and shares some similarities with *Neisseria gonorrhoeae* IgA1 protease, an autotransporter protein as classified by translocation through the outer membrane without the need of any separately encoded factors. Vacuolating activity of IgA1 protease was reduced by serine protease inhibitors, although serine protease activity has not been directly demonstrated, nor its target been identified (Cover, 1996; Rosetto *et al.*, 2000; Nguyen *et al.*, 2001). Secreted autotransporter toxin (Sat) from uropathogenic *Escherichia coli*, belonging to the subclass of serine protease autotransporters of *Enterobacteriaceae* (SPATE), also induced vacuolation in human bladder and kidney epithelial cells *in vitro*, as well as in mouse kidney cells *in vivo* (Guyer *et al.*, 2002). In addition, dengue virus serine proteases induced vacuolation and apoptosis in Vero cells (Shafee and AbuBakar, 2003).

Prostaglandins play a role in phagocytosis in *Amoeba proteus*, eliciting vacuole formation (Prusch *et al.*, 1989). Furthermore, PGD_2 and PGD_2 metabolites of the J-series induced apoptosis in *T. brucei*, with an increase in vacuolation in the cytoplasm (Figarella *et al.*, 2005; 2006). It was proposed that this occurs as part of the population density regulation of *T. brucei*. In addition, PGA_1 and PGE_1 caused degeneration of neuroblastoma cells, shown by cytosolic vacuolation and fragmentation of soma, nuclei and neurites (Prasad *et al.*, 1998).

Przemeck (2003), Huber *et al.* (2005) and Przemeck *et al.* (2005) demonstrated vacuolation and increased NR uptake in HeLa cells exposed to larval and adult ES preparations from *T. circumcincta* and *H. contortus*. In all experiments, larval ES preparations induced less

vacuolation than did adult ES preparations. In addition, adult *H. contortus* ES preparations caused a greater increase in NR uptake compared with adult *T. circumcincta* ES preparations (Przemeck, 2003). Addition of 8mM ammonium chloride to the medium enhanced vacuolation, but did not cause vacuolation in control cells at the same concentration (Huber *et al.*, 2005; Przemeck *et al.*, 2005). Similarly, *H. pylori* vacuolation is enhanced by ammonium ions (see 1.3.3.7.4). However, measurements of ammonia concentrations in ES products have reported a maximum of 30μM and this seemed for this component too low to be the primary vacuolating factor. In addition, the ammonia concentrations were similar in larval and adult preparations despite the differences in their vacuolating ability, further suggesting another factor was responsible for vacuolation.

Taking account of the previous studies, experiments were designed to characterise the vacuolating factor(s), as well as the resulting vacuoles. For the characterisation of the vacuoles, this included the use of different cell lines, the investigation of the time course of vacuolation and reversibility of vacuolation. Ammonia was also examined as a possible enhancer of vacuolation (Huber *et al.*, 2005; Przemeck *et al.*, 2005). Different approaches were used for the characterisation of the vacuolating factor(s), including the investigation of successive *in vitro* incubations of the same worm batch and the fractionation of ES products, which was hoped would identify the size range of the active ES component(s). Experiments also examined the lipid content, including prostaglandins, of ES products and their possible involvement in vacuolation. Other experiments investigated whether the vacuolating factor(s) was a protein.

Table 3.1: Scheme of incubation periods for successive ES samples with the same worm batch per experiment for three experiments.

<table>
<tr><th>Experiment I</th><th>Experiment II</th><th>Experiment III</th></tr>
<tr><td rowspan="2">0-6h</td><td>0-1h</td><td>0-1h</td></tr>
<tr><td>1-6h</td><td>1-6h</td></tr>
<tr><td>6-12h</td><td>6-12h</td><td>6-12h</td></tr>
<tr><td rowspan="4">12-36h</td><td rowspan="2">12-24h</td><td>12-18h</td></tr>
<tr><td>18-24h</td></tr>
<tr><td rowspan="3">24-48h</td><td>24-30h</td></tr>
<tr><td>30-36h</td></tr>
<tr><td>-</td><td>36-48h</td></tr>
</table>

3.2 Materials and Methods

3.2.1 ES Preparations of Adult *H. contortus*

Adult worms of *H. contortus* were obtained 21d after the infection of sheep, as described in Appendix I. Worms were incubated for 12h in PBS or cell culture media CEM or F12-Hams in 15ml and 50ml tubes or T75 cell culture flasks (compositions of CEM and F12-Hams are listed in Appendix II). Incubations were in an incubator in an atmosphere containing 5% CO_2 and 95% humidified air at 37°C. Cell culture media (CEM or F12-Hams) and PBS were also incubated under the same conditions to serve as negative controls. The supernatants of the ES preparations and the negative controls were sterile filtered through 0.2μm filters (Minisart, Sartorius) into new tubes. The pH of each preparation was readjusted to 7.4 if necessary. The preparations were stored at 4°C if being used immediately or frozen at -20°C in small aliquots, which were used only once.

ES products were also harvested at different incubation time points after the initial collection of adult worms from the abomasum, using a modified method of the protocol of Craig *et al.* (2006). Worms were incubated either in CEM or CEM without fetal bovine serum (FBS) if concentrated afterwards and the supernatant was then collected after 1h. Aliquots were filtered and frozen and the remainder immediately concentrated by centrifugation at 4°C at 3000g, using a Vivaspin concentrator 20 (Sartorius) with a pore size of 3kDa. The worms were then re-incubated with fresh CEM, or CEM without FBS, for the next incubation period (5 to 24h, depending on the experiment and time point) and the procedure described above repeated to generate ES preparations and ES concentrates of successive incubation periods. The worm viability was also monitored. The last sample collected contained only degrading dead worms to examine whether these degrading products could also induce vacuolation. The different successive ES preparations are summarised in Table 3.1. ES preparations and ES concentrates were stored at 4°C if being used immediately or frozen in small aliquots, which were used only once.

3.2.2 Further Modifications or Treatments of ES Preparations

3.2.2.1 Different Storage Conditions

Frozen ES preparations were stored at -20°C in small aliquots, which were used only once, for a maximum of four months if they were used on cells. Other storage conditions included 7d at 4°C, 3d at room temperature and 3d at 37°C (warm room). Storage for 3d at room temperature of ES preparations and control samples also functioned as a control for vacuolating ability after the elution of lipid spots from the thin-layer chromatography (TLC), which involved evaporation of methanol from the extracted spots for 3d at room temperature (see 3.2.2.5).

3.2.2.2 Dilutions of ES Preparations

To determine the maximum dilution of ES products possible while retaining the ability to induce vacuolation in cells, dilutions of ES preparations with cell culture medium were used: 2-fold (50%), 4-fold (25%) and 10-fold (10%) dilutions.

3.2.2.3 Ammonia

Ammonia was added to ES preparations and control media to make a final concentration of 1mM and 8mM (stock solution: Appendix II).

3.2.2.4 Fractionation of ES Products

ES products were fractionated using a series of molecular weight cut-off membranes. ES preparations generated in PBS were pooled for fractionation: (I) 115ml from two different batches, which were frozen; (II) 140ml from three different batches, which were frozen and (III) 100ml from two different batches, which were used on the day of worm collection (fresh). Pooled ES preparations were first concentrated by centrifugation at

Table 3.2: Molecular weight ranges of ES fractions generated with Vivaspin centrifugal concentrators.

Molecular weight ranges	
>100kDa	>50kDa
50-100kDa	
30-50kDa	10-50kDa
10-30kDa	
5-10kDa	0-10kDa
3-5kDa	
0-3kDa	

3000g using Vivaspin 20 (polyethersulfone membrane; all concentrators were rinsed once with 10ml MilliQ water before use), pore size 100kDa, to ~4ml (fractionation I and II). The eluate of this concentration (0-100kDa) was then concentrated with the next smallest filter, Vivaspin 20, pore size 50kDa, to ~4ml (I and II) and the eluate (0-50kDa) again used with the next smallest filter (Vivaspin 20, 30kDa). This series was continued using Vivaspin 20, pore sizes 10, 5 and 3kDa until the eluate from the smallest filter (0-3kDa) was obtained. This 0-3kDa fraction was used either as collected (for gels and as a dilution with CEM on cells) or freeze-dried and then reconstituted with 4ml PBS. Table 3.2 gives an overview of the different molecular weight sizes of the fractions generated.

In addition, fractions were generated only using Vivaspin 20, pore sizes 50kDa and 10kDa, resulting in fractions >50kDa, 10-50kDa and 0-10kDa (fractionation III). These fractions were concentrated to ~1ml each.

All fractions generated were washed three times with 15 to 20ml MilliQ water (except the final eluates from 0-3kDa and 0-10kDa). Five ml samples of each eluate were also retained as a sample. All fractions were used either as collected (for gels) or re-diluted to the original concentration (on cells).

Fractionation was also carried out with addition of Triton-X-100 (1%) and β-mercaptoethanol (0.1%) (I and II: 20ml ES preparation, frozen; concentrated to ~0.5ml each) or only 0.2% Triton-X-100 (III: 10ml ES preparation, frozen; concentrated to ~0.15ml each) to the ES perparation (generated in PBS) using the Vivaspin concentrator 20 with pore sizes 50kDa and 10kDa.

Fractions of protein standards were also generated as a control fractionation for the Vivaspin concentrators. A solution (5ml) of the protein standards β-galactosidase (116kDa), bovine serum albumin (BSA; 66kDa), trypsin inhibitor (20kDa) and aprotonin (6.5kDa) were used with Vivaspin 20, pore sizes 100kDa and 30kDa. Fractions were concentrated to ~0.2ml each.

3.2.2.5 TLC (Thin-Layer Chromatography)

TLC was used for the detection of lipids and prostaglandins. The empty TLC plate (Silica gel 60 ADAMANT on glass plates) was pre-developed to reduce background staining using the ethylacetate : acetic acid solvent system (98:2). The plate was dried and then activated for 10min at 110°C. Prostaglandin standards (Appendix II) and different ES preparations were then applied. The plate with the applied samples was developed using the same solvent system. The plate was first checked under UV light for possible spots and then stained using ready-to-use phosphomolybdic acid spray reagent. The sprayed plate was dried and the staining developed by incubation for 10min at 120°C (Hadás *et al.*, 1998). Stained plates were photographed with a Canon Power Shot G1 digital camera.

Lipids detected were also eluted from the TLC plate for further testing on HeLa cells. One TLC plate was run as described above and a second plate was run under the same conditions but without staining. From the unstained plate, the silica gel was scraped off at areas that related to stained spots from the first plate. The scrapings were placed in tubes and lipids were eluted by adding 1ml methanol. The samples were well shaken before they were transferred to a clean tube without the silica gel debris. Methanol was evaporated for 3d at room temperature and the sample re-diluted in CEM and sterile filtered (0.2µm).

3.2.2.6 Protease and Phosphatase Inhibition

For the inhibition of proteases and phosphatases in ES products, protease inhibitor cocktail and phosphatase inhibitor cocktail 2 were added to the cell culture media (CEM or F12-Hams) before the cells (HeLa or AGS) were incubated in a preliminary experiment to determine the sensitivity of the cells to the inhibitors. Protease inhibitor cocktail was used at concentrations of 1:800 and 1:1000 and phosphatase inhibitor cocktail 2 at 10µl/ml and 7.5µl/ml.

ES preparations and control media were also generated with added protease inhibitors. Protease inhibitor cocktail was added at a concentration of 1:800 during the 12h incubation period of *H. contortus* adults in F12-Hams medium for the generation of ES preparations.

3.2.2.7 Proteinase K Digestion

Proteinase K (Appendix II) was used to digest the protein content of the ES preparations. ES preparations were incubated with 100 and 200µg/ml proteinase K, with 0.1mg/µl $CaCl_2$ added to support activation of the enzyme (supplier data sheet), at times varying between 48h and 7d at 37°C.

3.2.2.8 Heat-Treatment

ES preparations, generated in CEM or PBS, were heat-treated for 30min at either 60°C, 75°C or 100°C in a water bath and then used as a 50% dilution with cell culture medium on HeLa cells.

3.2.2.9 Acid-Treatment

For the acid-treatment of ES preparations generated in PBS, the pH was lowered with 6M HCl to pH 2 using a pH meter (PHM 220, Radiometer Copenhagen). A maximum of 2.5µl 6M HCl was added. After 30min at pH2, it was raised again with 5M NaOH to pH 7.2 to 7.4, with a maximum of 3.4µl 5M NaOH added. The acid-treated ES preparation was used as a 50% dilution in cell culture medium on HeLa cells.

3.2.3 Protein Concentration of ES Preparations

The concentration of protein in ES preparations and control samples was measured by the Bradford assay (Bradford, 1976). Binding of Coomassie Brilliant Blue G-250 to proteins causes a shift in the absorption maximum of the dye from 470nm to 595nm. The method is described in Appendix IV.

3.2.4 Ammonia Determination in ES

The ammonia concentration in ES preparations was determined using a modified method of Bolleter *et al.* (1961), which is based on the reaction of ammonia with hypochlorite and phenol to produce indophenol. The method is described in Appendix IV.

3.2.5 Cell Culture

HeLa cells were used for most experiments. They had been passaged between 7 and 33 times (p7-p33). Additionally, AGS cells were used (p45 and 46). For experiments, cells were grown on coverslips (22x22mm/No 1 ½, BDH or ESCO). Cell culture techniques for both cell lines are described in detail in Appendix II.

3.2.6 Incubation of Cells with ES Preparations

For experiments testing ES preparations on cells (HeLa or AGS), the culture media of the cells were discarded and replaced by either ES preparations or control media and incubated routinely for 24h in an incubator in an atmosphere containing 5% CO_2 and 95% humidified air at 37°C.

Other incubation periods included 1h, 2h and 48h. HeLa cells were also incubated for 24h with ES preparations, which was then replaced by cell culture medium and the cells incubated for a further 24h or 48h.

ES product lipids, extracted by TLC (3.2.2.5), were also applied to HeLa cells. Additionally, single solutions of 0.5µg/ml of each prostaglandin standard were applied to HeLa cells and AGS cells.

3.2.7 Neutral Red Uptake

The method used followed the protocol of Przemeck *et al.* (2005), which was a modification of the method of Cover *et al.* (1991). The NR stock solution of 0.5% in 0.9% NaCl (stored at 4°C) was diluted for each experiment to 0.05% with PBS. After incubation with the test solution (ES preparation or control), excess medium in the petri dish (2ml) was discarded and the cells were washed once with PBS (1ml). One ml of the freshly prepared 0.05% NR-PBS solution was added to the petri dish and incubated for 4min in an incubator in an atmosphere containing 5% CO_2 and 95% humidified air at 37°C. The NR-PBS solution was then withdrawn and the cells were washed several times with PBS before they were examined with an inverted confocal microscope. This sequence was repeated for each petri dish separately to avoid further uptake of NR or changes in the uptake of NR if they were processed all at once.

3.2.8 Microscopic Examination of Cells

The state of vacuolation in each experiment after NR uptake was examined with an inverted confocal microscope (40x or 60x/water immersion objective). Samples were examined under bright field and in addition an UV laser (405nm) was used for NR excitation (blue fluorescent emission). Examination and photographing of the cells was limited to 15min after the withdrawal of NR. All images were processed with Adobe Photoshop. The estimated percentage of vacuolated cells was determined by examination of the whole coverslip followed by estimation of the vacuolated cells compared with the total number of cells on the coverslip.

3.2.9 Electrophoresis

3.2.9.1 Sodium Dodecylsulfate-Polyacrylamide Gel Electrophoresis (SDS-PAGE)

Gradient gels (5 to 20%) and single percentage gels (20%) were cast (gel compositions are described in detail in Appendix III). After polymerisation, the gel was loaded with the

different ES preparations and controls, which were mixed with gel loading buffer. The protein concentration of the samples was determined by the Bradford assay (3.2.3) and up to 89µg protein was loaded on the gel. All samples were also heated at 100°C for 3min (Mastercycler, Eppendorf) before applying to the gel. A protein marker (either unstained or pre-stained) was also loaded on the gel. The gel was run at 80V for 30 to 45min until the proteins reached the border between the stacking and resolving gel. The voltage was then increased to 100V for the resolving gel. The total running time was approximately 3.5h.

Gels were stained for proteins with Coomassie Brilliant Blue G250 or with silver for more sensitive staining. Additionally, a modified silver stain for proteins and carbohydrates (Kittelberger and Hilbink, 1993; Harrison *et al.*, 2003) was used. Lipids were detected with Sudan Black staining, either staining the gel after running it (following the suppliers protocol) or by pre-staining of the samples (Yepiz-Plascencia *et al.*, 2002). All gel staining techniques are described in detail in Appendix III. Gels were stored in MilliQ water until photographed with a Canon Power Shot G1 digital camera on a light box (Coldlight Illuminator Series 2, Kodak).

3.2.9.2 Blue Native-Polyacrylamide Gel Electrophoresis (BN-PAGE)

The protocol used followed the method described by Shi and Jackowski (1998). Five to 20% gradient gels were cast (gel compositions are described in detail in Appendix III). After polymerisation, the gel was loaded with the different ES preparations and controls, which were mixed with gel loading buffer. The protein concentration of the samples was determined by the Bradford assay (3.2.3) and up to 20µg protein was loaded on the gel. A pre-stained protein marker was also applied to the gel. The buffer chambers were filled with the two different buffers, one of which contained Coomassie Brilliant Blue G250 staining the gel while it runs (Appendix III). The gel was run at 80V for 30 to 45min until the proteins reached the border between the stacking gel and resolving gel. The voltage was then enhanced to 100V for the resolving gel. The total running time was approximately 3-4h.

Table 3.3: Summary of the different ES applications on HeLa and AGS cells.

Experiment	Cell line	No. of Repeats	No. of ES & Ct batches used
Cell vacuolation due to ES products			
24h	HeLa	5	3
48h	HeLa	3	2
24h	AGS	3	1
Stability of the vacuolating factor			
-20°C (short-term, <4 months)	HeLa	7	3
-20°C (short-term, <4 months)	AGS	3	1
-20°C (long-term, >6 months)	HeLa	2	1
-20°C (long-term, >6 months)	AGS	2	1
4°C, 7d	HeLa	2	2
RT, 3d	HeLa	2	2
37°C, 3d	HeLa	2	2
Potency of ES products			
Undiluted, 100%	HeLa	3	2
2x diluted, 50%	HeLa	3	2
4x diluted, 25%	HeLa	3	2
10x diluted, 10%	HeLa	3	2
Time course of vacuolation			
1h	HeLa	2	2
2h	HeLa	2	2
Reversibility of vacuolation			
24h	HeLa	2	1
48h	HeLa	2	1
Potency of ES at different time points of ES harvest			
Experiment I			
0-6h	HeLa	2	1
6-12h	HeLa	2	1
12-36h	HeLa	2	1
Experiment II			
0-1h	HeLa	3	2
1-6h	HeLa	3	2
6-12h	HeLa	3	2
12-24h	HeLa	3	2
24-48h	HeLa	3	2

Ammonia and ES			
1mM in CEM	HeLa	4	
8mM in CEM	HeLa	4	
1mM in ES	HeLa	2	1
8mM in ES	HeLa	2	1
Vacuolating activity of			
prostaglandin standards (5)	HeLa	1	
	AGS	2	
extracted lipids (5 spots)	HeLa	1	1
Protease and phosphatase inhibiton			
Protease inhibitors 1:800	HeLa	1	
	AGS	1	
Protease inhibitors 1:800 (during ES generation)	AGS	3	1
Protease inhibitors 1:1000	HeLa	1	
Phosphatase inhibitors 10µl/ml	HeLa	2	
Phosphatase inhibitors 7.5µl/ml	HeLa	2	
	AGS	1	
Proteinase K digestion			
50µg/ml	HeLa	1	
37.5µg/ml	HeLa	1	
25µg/ml	HeLa	1	
after preincubation with proteinase K, 48h or 72h			
50µg/m, 48h	HeLa	2	
50µg/ml, 72h	HeLa	2	
37.5µg/ml, 48h	HeLa	2	
37.5µg/ml, 72h	HeLa	2	
25µg/ml, 48h	HeLa	4	
25µg/ml, 72h	HeLa	4	
Heat treatment			
Sample in CEM			
75°C, 30min	HeLa	4	1
Sample in PBS			
100°C, 30min	HeLa	4	2
75°C, 30min	HeLa	4	2
60°C, 30min	HeLa	2	1
Acid treatment			
pH2, 30min	HeLa	2	1

The gels were destained with several solution changes of destaining solution until a clear staining pattern of the protein bands was obtained. Gels were stored in MilliQ water until photographed.

3.2.9.3 Two-Dimensional (2D) BN/SDS-PAGE

The method followed was that of Nijtmans *et al.* (2002) and Eubel *et al.* (2005). The first dimension BN-PAGE was performed as described above (3.2.9.2). After destaining, the relevant lane was excised and placed in a solution of 1% Triton-X-100 and 1% β-mercaptoethanol for 1h on a platform rocker. The gel strip was rotated by 90° to the first dimension and placed between the glass plates of the gel casting stand. Excess solution was drained with a filter paper. After the second dimension SDS resolving gel was cast, the first dimension gel strip was embedded into the stacking gel of the second dimension gel. The second dimension SDS-PAGE was performed and the gel stained with silver as described above (3.2.9.1). Gels were stored in MilliQ water until photographed.

3.3 Results

3.3.1 Cell Vacuolation Due to ES Products

H. contortus ES products induced vacuolation in HeLa and AGS cells after routine 24h incubations. In addition, incubation of HeLa cells for a longer incubation time of 48h with ES preparations did not cause noticeably more severe vacuolation.

24h incubations of ES preparations and control samples on HeLa cells were performed five times with three different ES and control batches (a summary of the different applications on cells described in this chapter and the number of repeats is shown in Table 3.3). All control cells appeared normal, with no vacuolation or vacuoles occurring in only a few cells, which could be up to 5 to 10% of the total number of cells on the coverslip.

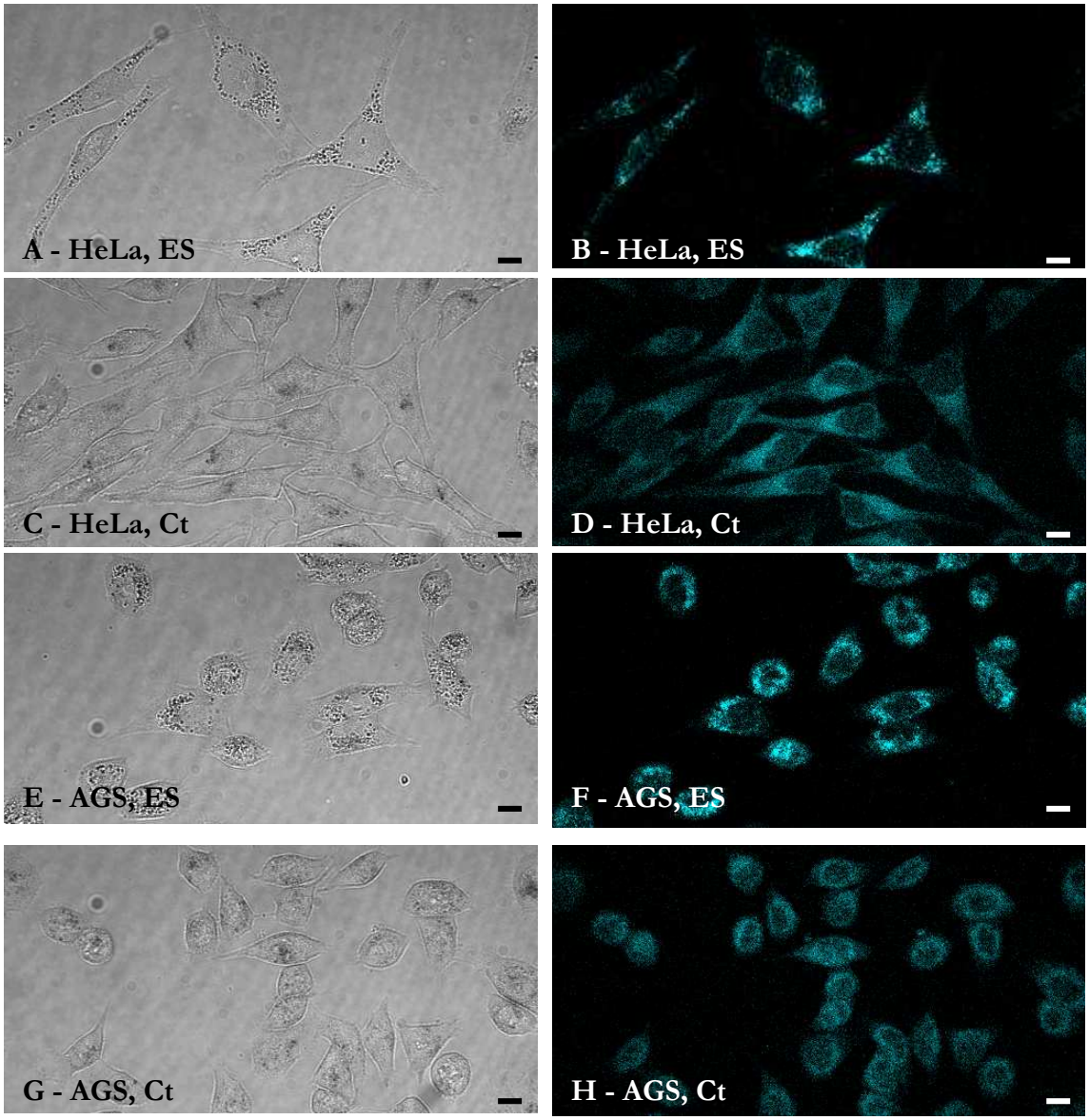

Figure 3.4: Vacuolation in HeLa and AGS cells induced by *H. contortus* ES products (after short-term freezing). 24h incubation. Neutral red staining. Left, bright field images; right, fluorescent imaging (UV/405nm excitation). A. and B. HeLa cells, Control (CEM), C. and D. HeLa cells, ES (in CEM), E. and F. AGS cells, Control (F12-Hams), G. and H. AGS cells, ES (in F12-Hams). Original magnification 600x, bars 10μm.

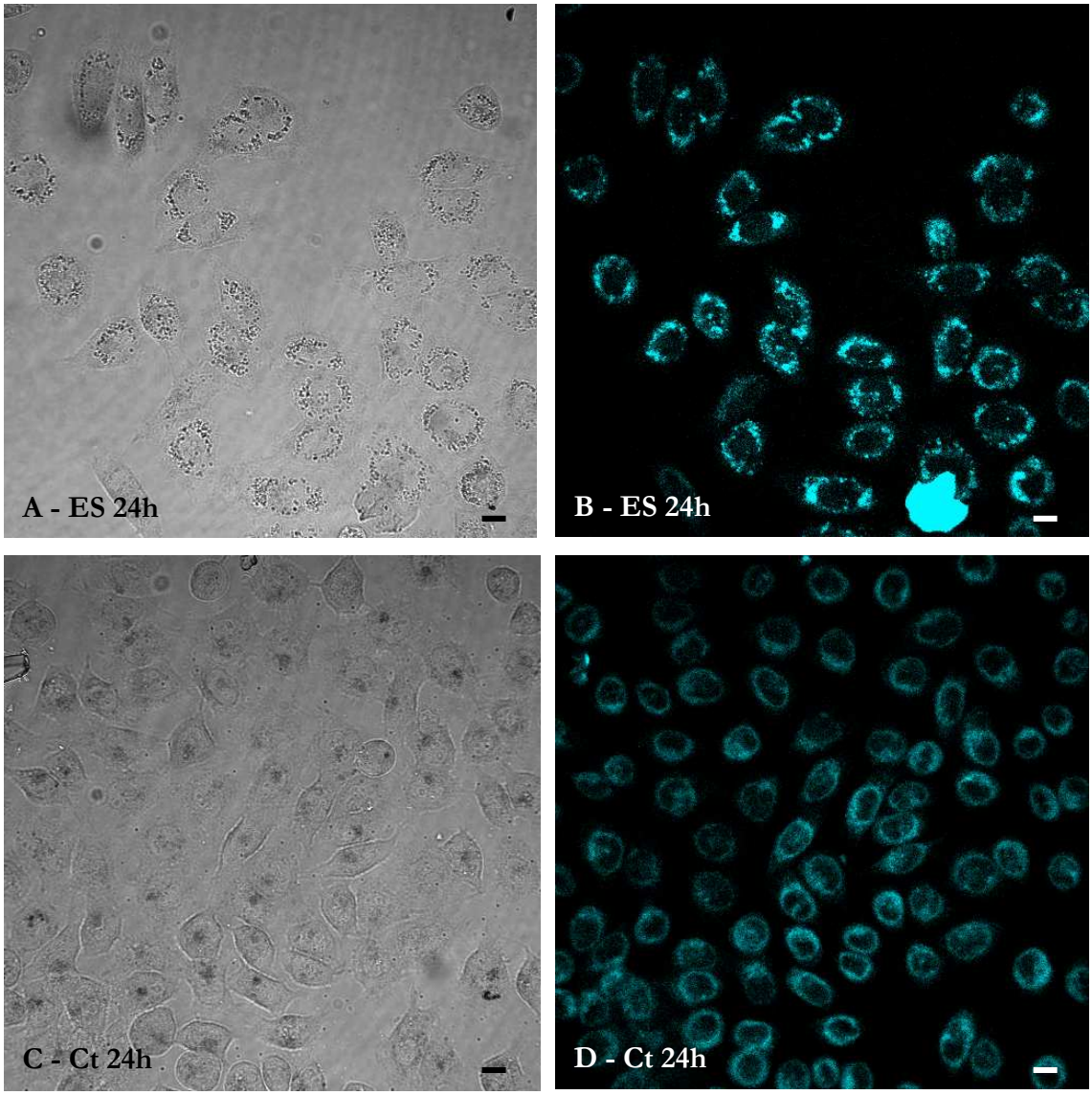

Figure 3.3: Vacuolation in AGS cells induced by *H. contortus* ES products (fresh). 24h incubation. Neutral red staining. Left, bright field images; right, fluorescent imaging (UV/405nm excitation). A. and B. ES (in F12-Hams), C. and D. Control (F12-Hams). Original magnification 600x, bars 10μm.

Facing page 79

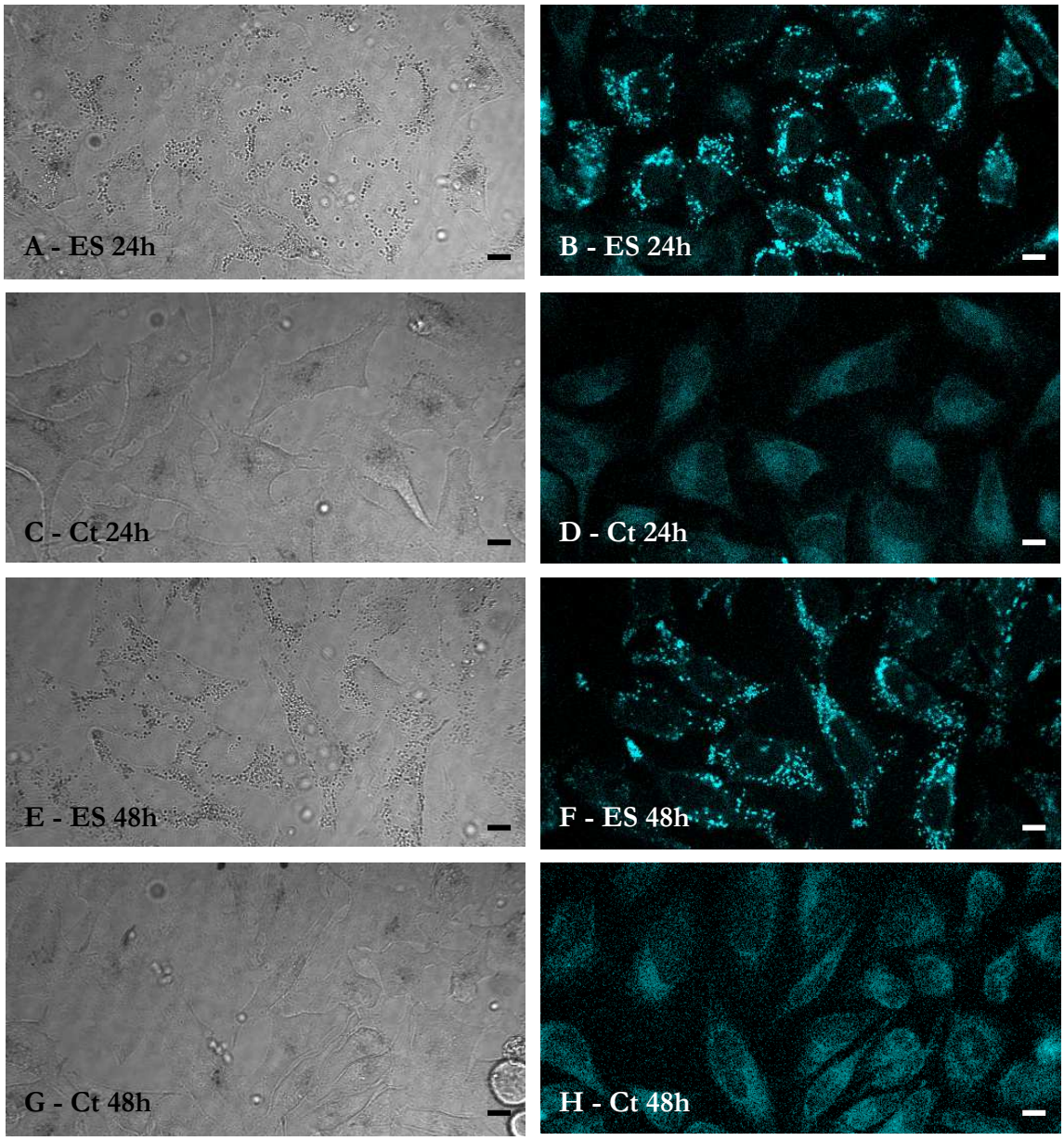

Figure 3.2: Vacuolation in HeLa cells induced by *H. contortus* ES products (fresh). 24h and 48h incubation. Neutral red staining. Left, bright field images; right, fluorescent imaging (UV/405nm excitation). A. and B. ES (in CEM), 24h incubation, C. and D. Control (CEM), 24h incubation, E. and F. ES (in CEM), 48h incubation, G. and H. Control (CEM), 48h incubation. Original magnification 600x, bars 10µm.

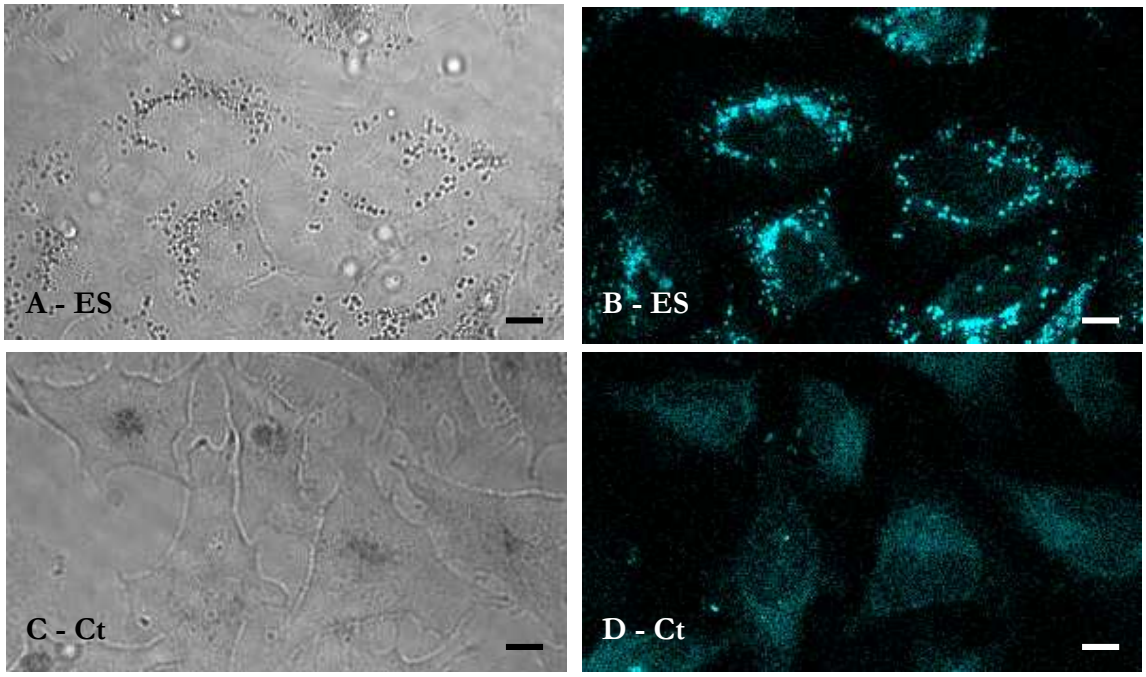

Figure 3.1: Vacuolation in HeLa cells induced by *H. contortus* ES products (fresh). 24h incubation. Neutral red staining. High-definition images; left, bright field images; right, fluorescent imaging (UV/405nm excitation). A. and B. ES (in CEM), C. and D. Control (CEM), 24h incubation. Original magnification 600x, bars 10µm.

However, any vacuolation in control cells usually resulted in fewer vacuoles per cell compared with the ES-exposed cells. After the same incubation period with ES products, HeLa cells were severely affected: vacuolation occurred in 80 to 100% of the cells with many vacuoles per cell. Vacuoles stained very dark red with Neutral red and usually appeared more black than red. Exposure of HeLa cells to ES preparations and control samples for 48h was performed three times with two different ES and control batches. The extended incubation period of 48h led to almost the same result: the control cells appeared normal and those exposed to ES preparations were heavily vacuolated. For some cells, the number of vacuoles per cell appeared to be slightly increased compared with a routine 24h incubation. High-definition images of the 24h incubation show the typical vacuolation induced by ES products (Figure 3.1). Further images demonstrating ES-induced vacuolation presented in this chapter are of lower definition, but show a larger area of cells. Results of the 24h and 48h incubations are shown in Figure 3.2. Additionally, AGS cells were incubated with ES preparations and control samples for 24h (three times with the same ES and control batch), which resulted in the same vacuolation as in HeLa cells (Figure 3.3).

3.3.2 Stability of the Vacuolating Factor

The stability of the vacuolating factor was determined under different storage conditions. ES preparations could be stored at -20°C for periods less than 4 months without loss of the vacuolating activity of the ES products. In addition, incubations of ES preparations stored for 3d at 37°C, 3d at room temperature and 7d at 4°C also showed no loss of the vacuolating activity.

ES preparations and control samples that had been stored frozen at -20°C after the ES generation (<4 months) induced vacuolation of the same intensity in both cell lines for the ES preparations and none or almost none for the control media (Figure 3.4). Incubation of HeLa cells was performed seven times with three different batches of ES and control media and three times with the same batch on AGS cells. After long-term storage at -20°C (>6 months), the vacuolating activity of ES products was markedly decreased or lost. This was examined on HeLa and AGS cells (twice each) with one batch of ES preparation an

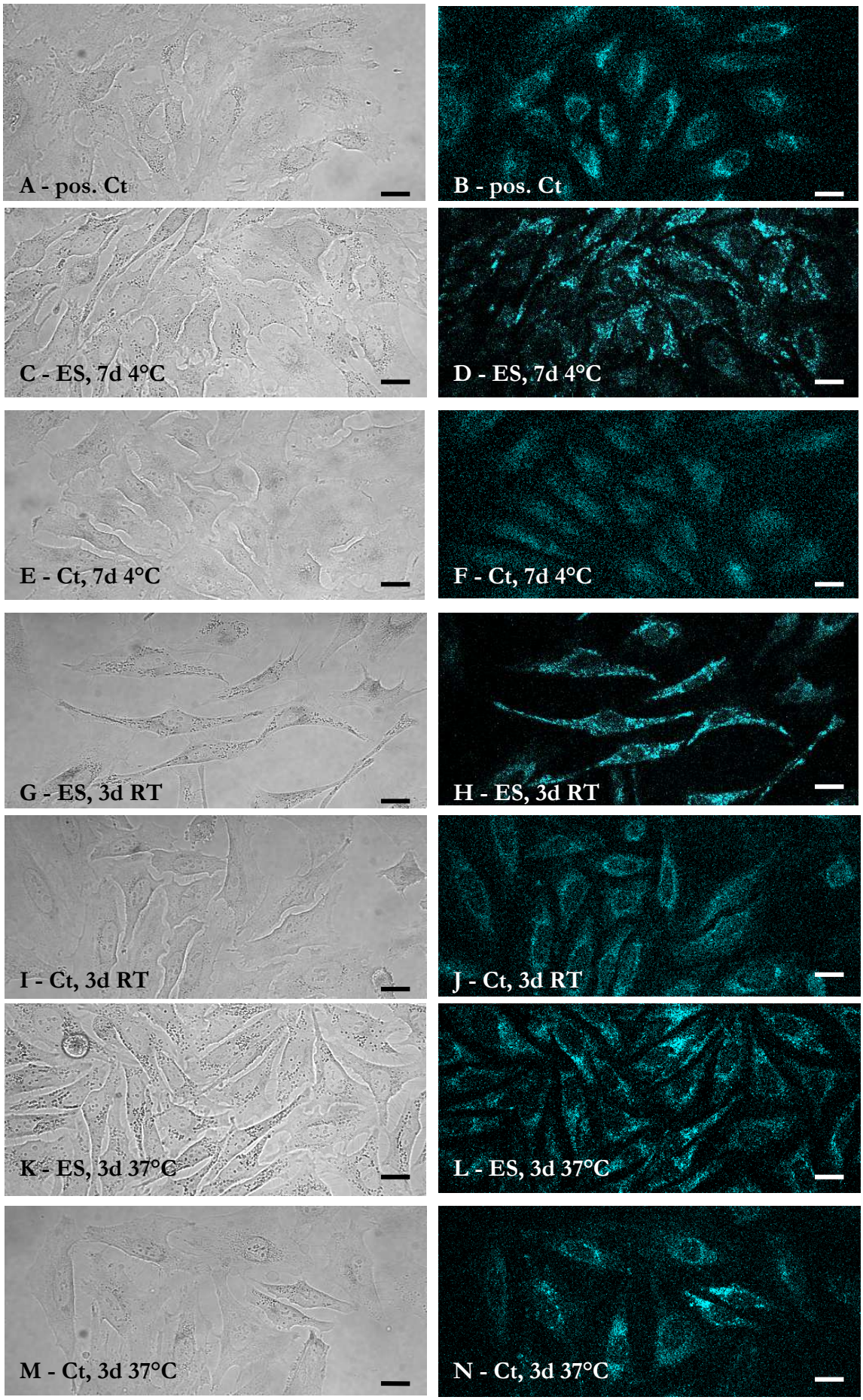

(Figure description see facing page 81)

control. Short-term frozen aliquots of ES preparations and control samples (in small aliquots, which were used only once, stored at -20°C for less than 4 months) were subsequently used for most experiments, if not stated otherwise, because no loss in vacuolating ability of the ES preparations could be observed after short-term freezing.

Storage at 4°C for 7d did not decrease the ability of ES products to induce vacuolation in HeLa cells. Approximately 90% of the cells were heavily vacuolated (Figure 3.5 C. and D.). HeLa cells that were exposed to control media after the same storage conditions appeared normal (Figure 3.5 E. and F.). Three day storage at room temperature resulted in similar vacuolation. ES-exposed HeLa cells were heavily vacuolated (Figure 3.5 G. and H.) and vacuolation in control cells was only slightly increased compared with typical control applications (15% of the cells, Figure 3.5 I. and J.). Exposure of HeLa cells to ES preparations stored at 37°C for 3d also resulted in heavily vacuolated cells (90 to 100%, Figure 3.5 K. and L.). The control samples after the same storage conditions also produced an increase in vacuolation compared with typical control applications (40% of the cells, Figure 3.5 M. and N.), but most of them with markedly fewer vacuoles per cell and markedly fewer vacuolated cells in total than did the ES preparations. Incubations were performed twice for each storage condition with two different batches. The positive control (50% dilution in CEM) induced typical vacuolation, but the number of vacuolated cells was slightly decreased (80% of the cells, Figure 3.5 A. and B.).

3.3.3 Vacuolating Ability of ES Preparations

The vacuolating ability of individual batches of ES products varied slightly, but nonetheless the vacuolating ability of ES preparations in general was determined using different dilutions of these. After application to HeLa cells for 24h (three times with two different ES and control batches), vacuolation was similar to an undiluted ES preparation only at 2-fold (50%) dilution.

HeLa cells exposed to undiluted ES preparations (100%, positive control) showed the typical vacuolation (almost all cells were vacuolated with many vacuoles per cell). The 2-fold (50%) dilution of ES preparations had a very similar effect to that with undiluted ES

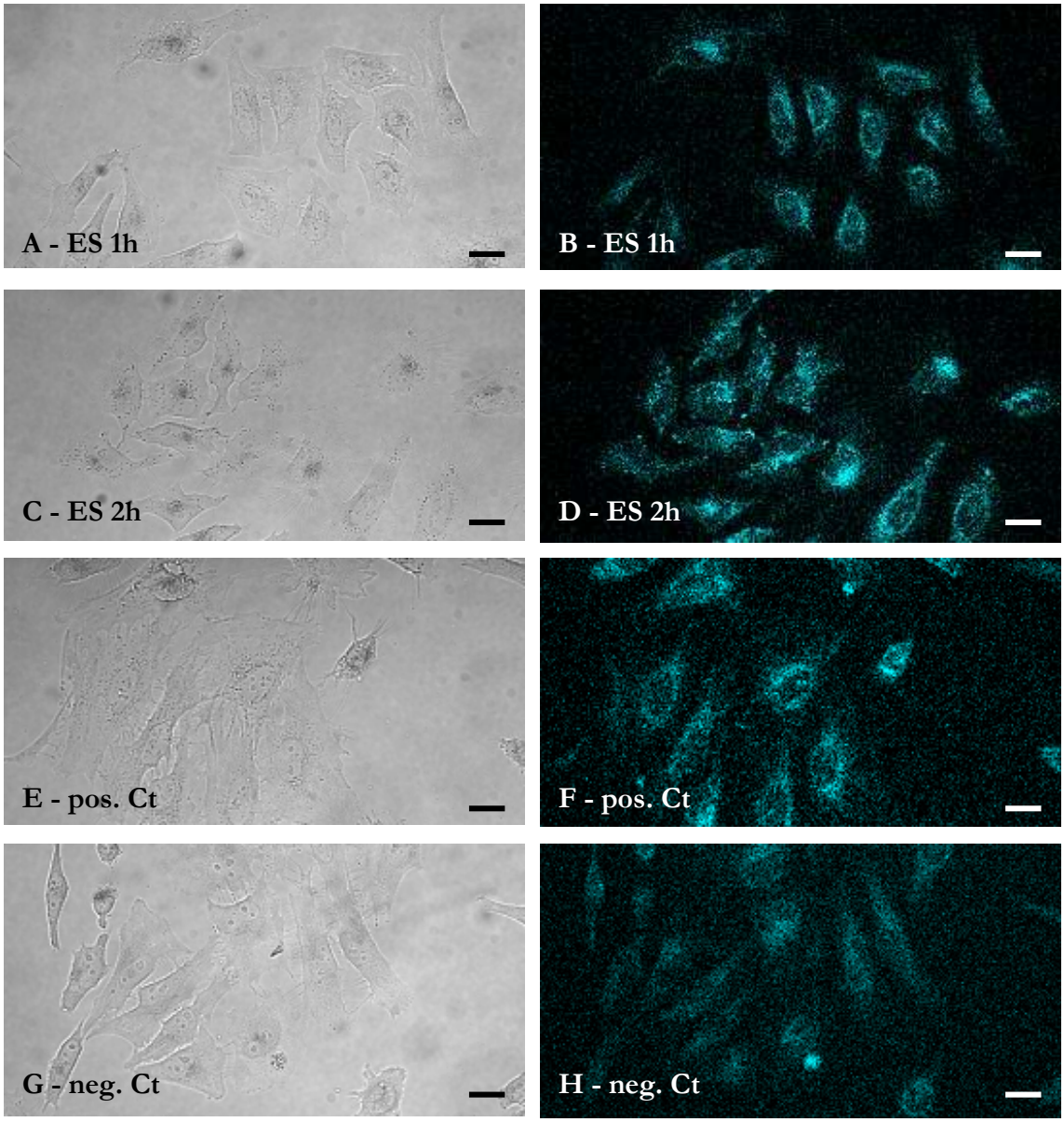

Figure 3.7: Time Course of vacuolation after exposure to *H. contortus* ES products to HeLa cells. 24h incubation. Neutral red staining. Left, bright field images; right, fluorescent imaging (UV/405nm excitation). A. and B. ES incubation for 1h, C. and D. ES incubation for 2h, E. and F. Pos. Control (ES 50% in CEM), G. and H. Neg. Control (CEM). Original magnification 400x, bars 20µm.

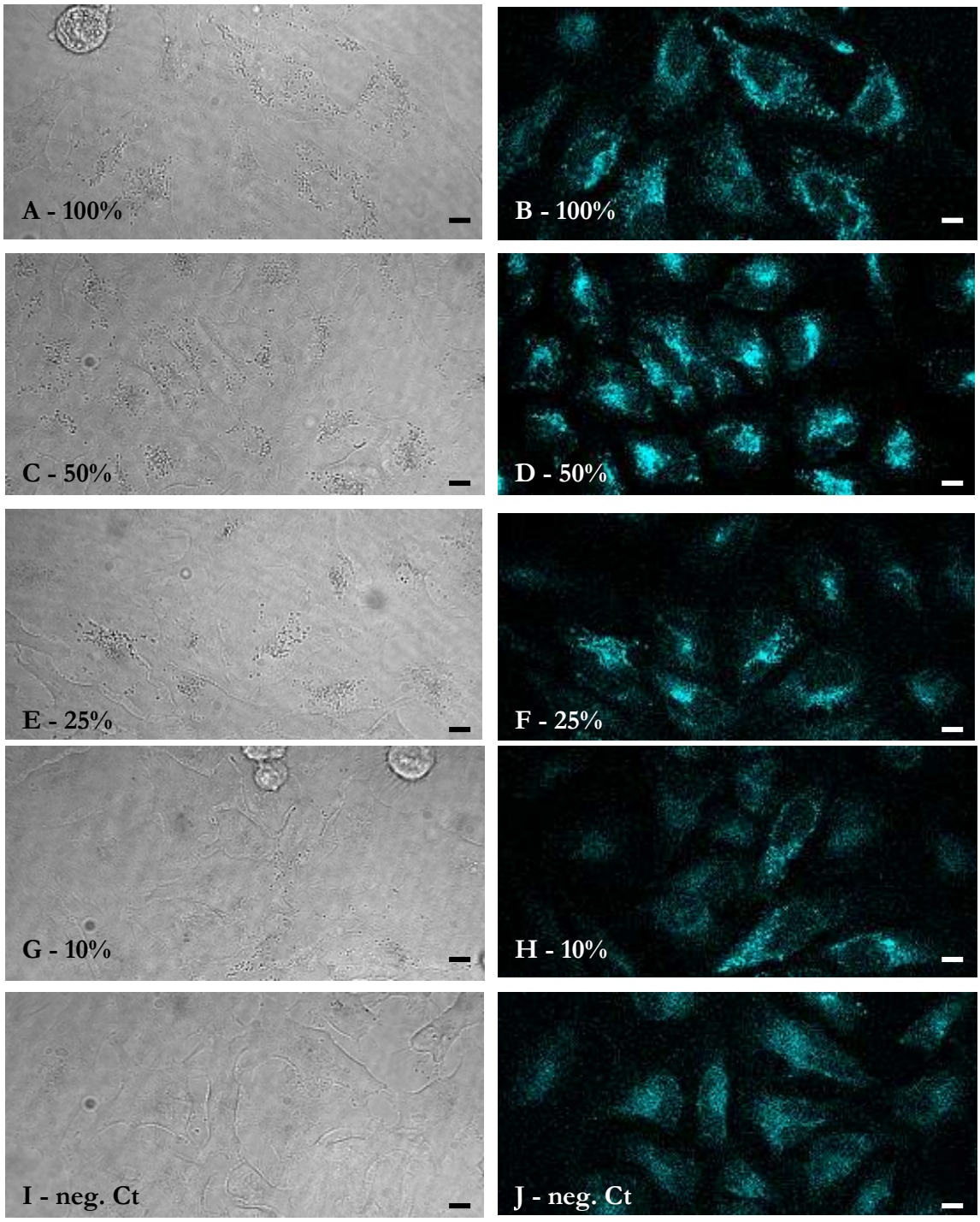

Figure 3.6: Vacuolating ability of dilutions of *H. contortus* ES products on HeLa cells. 24h incubation. Neutral red staining. Left, bright field images; right, fluorescent imaging (UV/405nm excitation). A. and B. Positive control (undiluted ES, 100%), C. and D. 2-fold dilution of ES (50%), E. and F. 4-fold dilution of ES (25%), G. and H. 10-fold dilution of ES (10%), I. and J. Negative control (CEM). Original magnification 600x, bars 10μm.

Facing page 81

Figure 3.5: Effect of different storage conditions of *H. contortus* ES on its ability to induce vacuolation in HeLa cells. 24h incubation. Neutral red staining. Left, bright field images; right, fluorescent imaging (UV/405nm excitation). A. and B. Pos. Control (ES 50% in CEM), C. and D. ES (in CEM) stored at 4°C for 7d, E. and F. Control (CEM) stored at 4°C for 7d, G. and H. ES (in CEM) stored at room temperature for 3d, I. and J. Control (CEM) stored at room temperature for 3d, K. and L. ES (in CEM) stored at 37°C for 3d, M. and N. Control (CEM) stored at 37°C for 3d. Original magnification 400x, bars 20μm.

preparations with batch I and vacuolation was slightly decreased with batch II. Almost all cells exposed to batch II were affected, but the number of vacuoles per cell and the size of the vacuoles was decreased compared with typical ES applications in ~20 to 30% of the cells. There were also a few cells without vacuolation. Vacuolation induced by the 4-fold (25%) dilution of ES preparations of batch I was seen in ~70 to 80% of the cells and ~40 to 50% with batch II. The number of vacuoles induced by batch II was also decreased in some cells. The 10-fold dilution of ES preparations (10%) induced vacuolation in only ~10 to 20% of the cells and in general with fewer vacuoles per cell for both batches. These results are shown in Figure 3.6.

3.3.4 Time Course of Vacuolation

HeLa cells exposed to ES products for different incubation periods, in order to determine the approximate time that was needed for the onset of ES-induced vacuolation, showed that vacuolation occurred as early as 1h after ES exposure.

One and two hour incubations with ES products were performed twice with two different batches. Exposure of HeLa cells to ES products for 1h resulted in vacuolation in ~75% of the cells and most of them had fewer vacuoles per cell compared with typical ES applications (Figure 3.7 A. and B.). Incubation with ES preparations for 2h induced vacuolation in ~90% of the cells, which was similar to a routine 24h incubation with ES products. Only some of the cells had fewer vacuoles per cell (Figure 3.7 C. and D.). HeLa cells exposed to ES products (50% in CEM) for 24h (positive control) showed the usual vacuolation, but the number of vacuolated cells was slightly decreased (80% of the cells, Figure 3.7 E. and F.). Control cells, which were exposed to a negative control sample (CEM) appeared normal (Figure 3.7 G. and H.).

3.3.5 Reversibility of Vacuolation

HeLa cells exposed to ES products for 24h and examined at different time points after replacement of ES preparations with cell culture media to examine possible recovery and

Table 3.4: Time scheme of viability of worms in successive ES samples from experiment I and II.

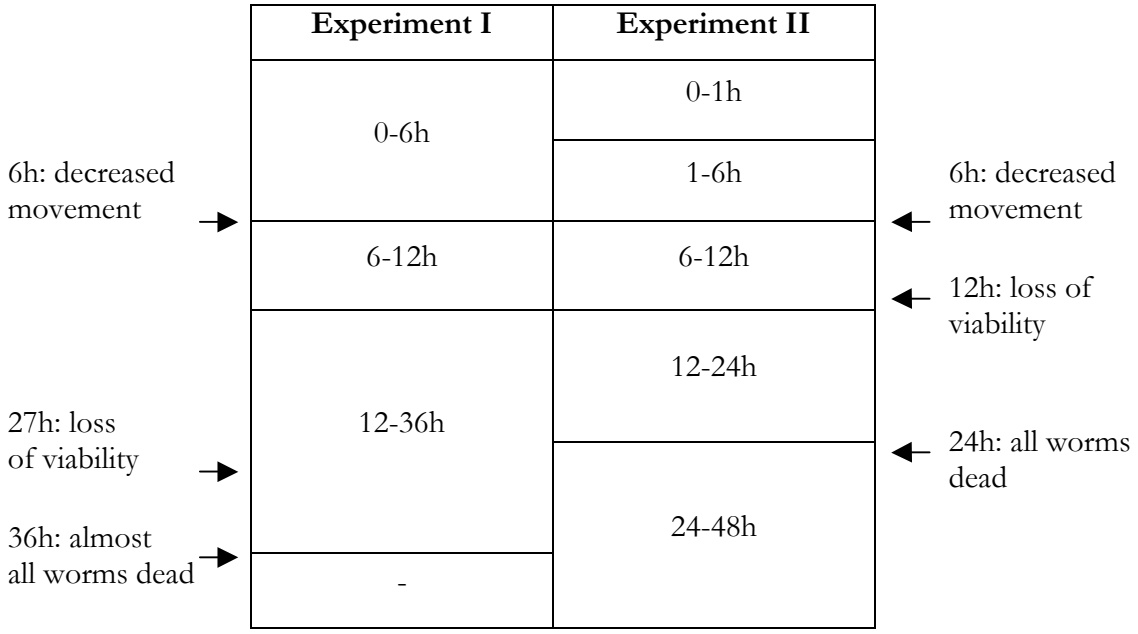

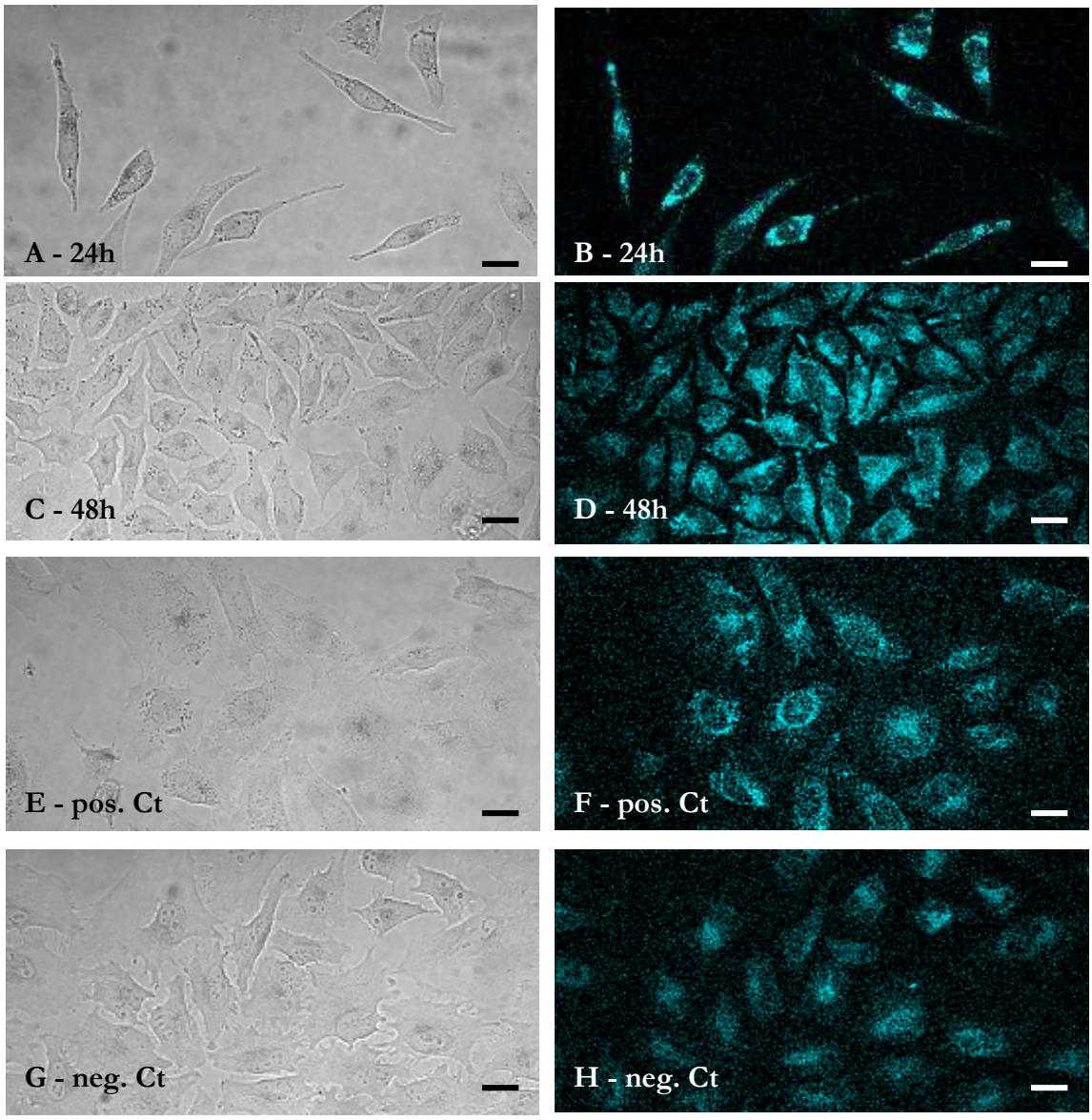

Figure 3.8: Reversibility of *H. contortus* ES-induced vacuolation in HeLa cells. 24h ES incubation. Neutral red staining. Left, bright field images; right, fluorescent imaging (UV/405nm excitation). A. and B. 24h after ES replaced by CEM, C. and D. 48h after ES replaced by CEM, E. and F. Pos. Control (50% ES in CEM), G. and H. Neg. Control (CEM). Original magnification 400x, bars 20µm.

reversibility of the vacuolation showed that vacuolation was partly reversible.

Incubations for 24h and 48h after the replacement of ES preparations with cell culture media were performed twice with two different ES and control batches. Twenty four hours after the replacement of ES, 60 to 70% of the cell were still vacuolated, but most of them with fewer vacuoles per cell. The rate of cell division appeared normal with approximately twice the number of cells present on the coverslip (the normal doubling time of HeLa cells is ~24h). The same applied to the second sample, but only ~30% of the cells were still affected. Vacuolation of ~30% of the cells occurred in both samples incubated for 48h after the ES replacement. The number of vacuoles in most of the vacuolated cells was decreased compared with typical ES applications. The number of cells present on the coverslip was approximately three times that following the initial 24h incubation with ES products. The positive control (50% dilution in CEM) induced vacuolation in ~80% of the cells and cells exposed to the negative control (CEM) appeared normal. Results of this experiment are shown in Figure 3.8.

3.3.6 Vacuolating Ability of ES at Different Time Points of ES Harvest

ES products from successive incubations with the same worm batch (3.2.1) applied to HeLa cells demonstrated differences in their ability to induce vacuolation: vacuolating ability decreased over incubation time of the worms, but was greatest in preparations generated after the worms had died. Some differences in their protein patterns were also detected by gel electrophoresis.

In experiment I, successive ES preparations were collected from incubations 0-6h, 6-12h and 12-36h and a control sample (0-6h). Movement of the worms decreased after 6h. Worms were then in an aggregate (similar to Figure 1.4 B), but still alive and moving. After 27h, a marked loss in viability could be observed with only a few worms still alive after 36h (worm viability summarised in Table 3.4). Incubations with ES preparations and control samples (originating from one worm batch) on HeLa cells were performed twice. Vacuolation in HeLa cells occurred in 90 to 100% of the cells which were exposed to the

Table 3.5: Protein concentrations of ES samples from successive incubation periods. All sample concentrations were re-calculated to their original unconcentrated volumes.

ES sample	**Experiment I** Protein conc. [µg/ml]	**Experiment III** Protein conc. [µg/ml]
0-1h	15.99	3.05
1-6h		10.95
6-12h	10.01	1.88
12-18h	23.66	7.72
18-24h		2.92
24-30h		9.83
30-36h		4.76
36-48h	-	9.45

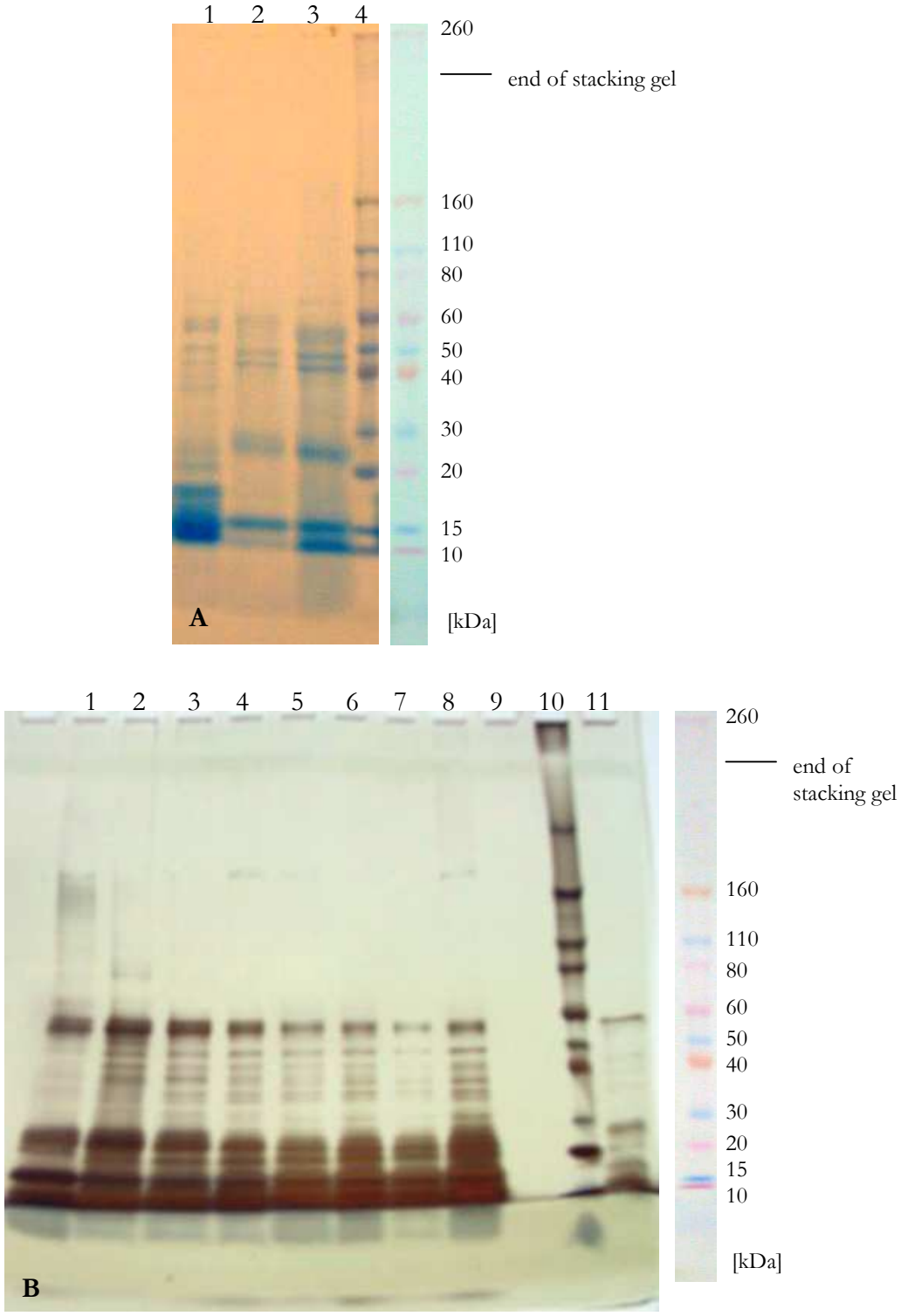

Figure 3.10: SDS-PAGE 5-20% of ES harvested at different time points (successive incubation periods). A. Experiment I, coomassie stain, (1) 0-6h, 60µg, (2) 6-12h, 38µg, (3) 12-36h, 89µg, (4) pre-stained marker; pre-stained marker before gel staining on the right, B. Experiment III, silver stain, (1) 0-1h, 7µg, (2) 1-6h, 20µg, (3) 6-12h, 3.5µg, (4) 12-18h, 20µg, (5) 18-24h, 8µg, (6) 24-30h, 20µg, (7) 30-36h, 12µg, (8) 36-48h, 20µg, (9) control (PBS), 50µl, (10) pre-stained marker, (11) ES in PBS (unconcentrated; positive control), 50µl; pre-stained marker before gel staining on the right.

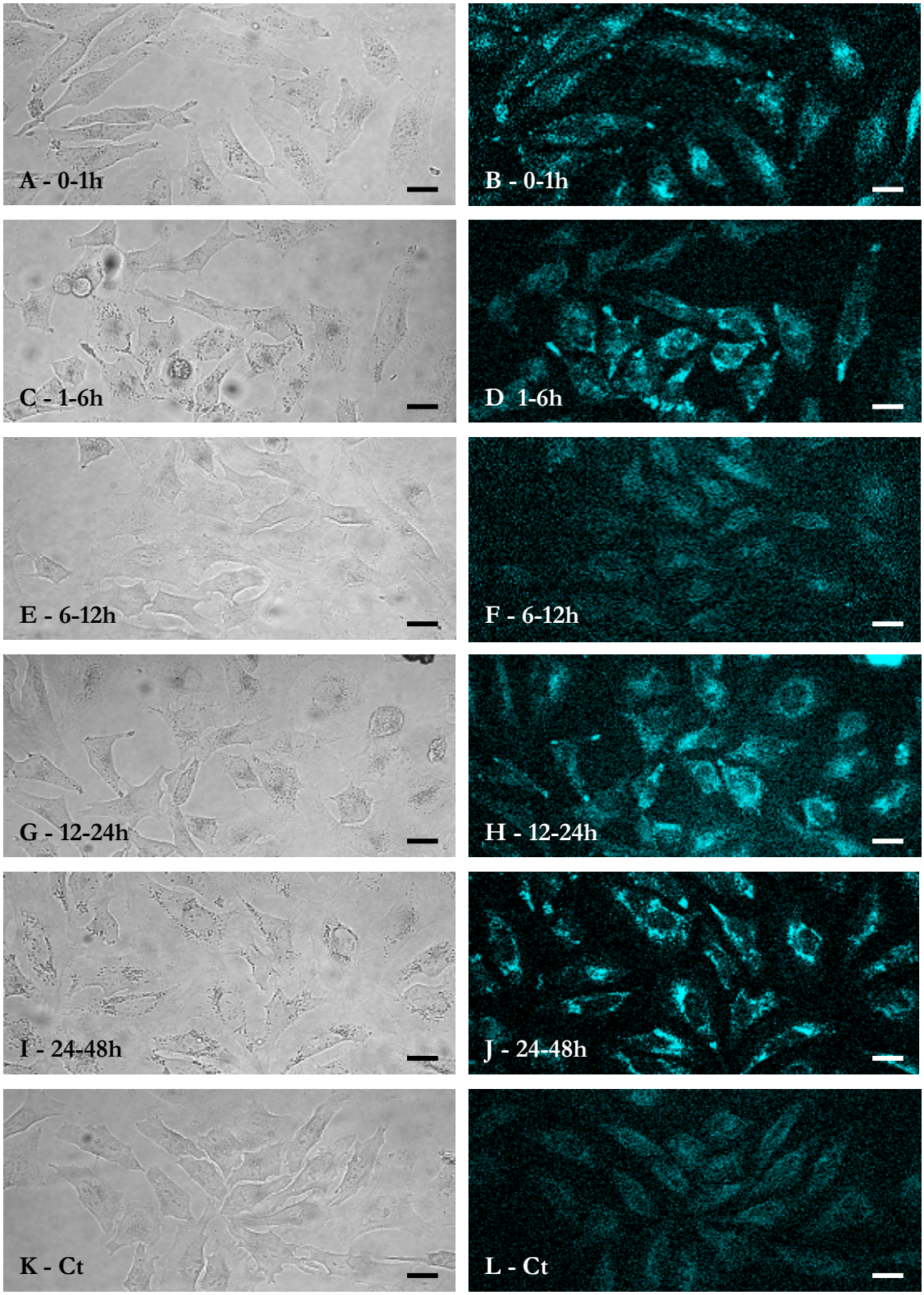

Figure 3.9: Vacuolation in Hela cells induced by *H. contortus* ES which was harvested at different time points (successive incubation periods). 24h incubation. Neutral red staining. Left, bright field images; right, fluorescent imaging (UV/405nm excitation). A. and B. ES 0-1h, C. and D. ES 1-6h, E. and F. ES 6-12h, G. and H. ES 12-24h, I. and J. ES 24-48h, K. and L. Control (CEM, 0-6h). Original magnification 400x, bars 20μm.

0-6h ES preparation. ES products generated during the second incubation period (6-12h) lost most of their vacuolating ability with only a few vacuolated cells (<10%) appearing. Exposure to the 12-36h ES preparation resulted in vacuolation in ~70% of the cells. The number of vacuoles per cell was reduced in some cells compared with typical ES applications. HeLa cells exposed to the control sample appeared normal.

In experiment II, successive ES preparations were collected from incubations 0-1h, 1-6h, 6-12h, 12-24h and 24-48h. The control sample was collected after 6h (0-6h incubation). The experiment was performed twice with two different worm batches. In both of these incubations, worms formed an aggregate after 1h and their movement decreased after 6h. Marked loss in viability occurred after 12h with none of the worms alive after 24h (worm viability summarised in Table 3.4). Incubations of ES preparations and control samples on HeLa cells were performed three times with two different ES and control batches. ES products generated during the first incubation hour (0-1h) induced vacuolation in ~80 to 90% of the cells. The vacuolating ability of the second ES preparation (1-6h) was slightly decreased, with ~70% of the cells affected and the number of vacuoles per cell also reduced in some cells compared with typical ES applications. Vacuolation of HeLa cells exposed to the 6-12h ES preparation was markedly reduced, with only ~20% of the cells vacuolated and the number of vacuoles per cell also reduced. Exposure to the 12-24h ES preparation resulted in 80 to 85% of vacuolated cells. The greatest response for all samples was seen in HeLa cells exposed to the 24-48h ES preparations. Vacuolation occurred in 95 to 100% of the cells. The control sample did not induce any vacuolation. These results are shown in Figure 3.9.

The protein concentration of ES products from each time period was also measured with the Bradford assay and the protein patterns monitored by SDS-PAGE. This was carried out for experiments I and III, where the samples had been concentrated. All protein concentrations are shown in Table 3.5. Protein concentrations decreased after 6h, quite dramatically in experiment III, before they increased again. Partly, this coincided with the ability of the different ES preparations to induce vacuolation in HeLa cells.

The different protein patterns from ES products at each time period resolved by SDS-PAGE are shown in Figure 3.10. For experiment I, the pattern of the 0-6h sample differed

Facing page 84

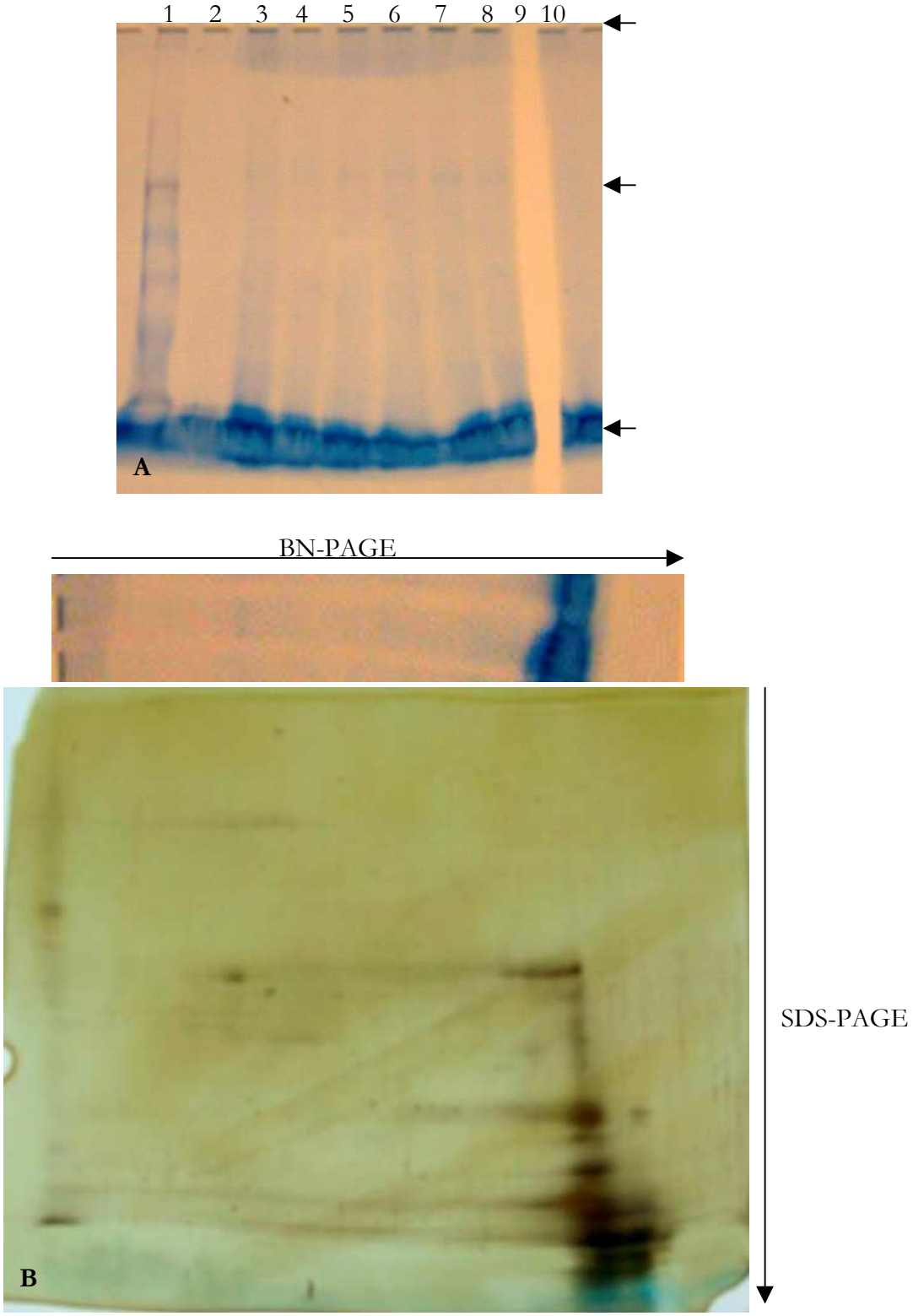

Figure 3.11: 2D BN/SDS-PAGE of ES harvested at different time points (successive incubation periods). A. BN-PAGE 5-20%, coomassie stain (1) pre-stained marker, (2) control (CEM without FBS), (3) 36-48h, 20µg, (4) 30-36h, 12µg, (5) 24-30h, 20µg, (6) 18-24h, 8µg, (7) 12-18h, 20µg, (8) 6-12h, 3.5µg, (9) 1-6h, 20µg (lane cut for 2D in B.), (10) 0-1h, 7µg, B. SDS-PAGE 5-20% of lane (9) 1-6h from the BN-PAGE, silver stain; the excised band was rotated 90° and run in a second dimension under denaturing conditions.

from the other two (6-12h and 12-36h). Two weak bands could be detected between 35 and 40kDa, a stronger band at ~20kDa and a very strong band at ~17kDa. In contrast, only one strong band at ~10kDa was detected compared with two strong bands at 10 and 15kDa in the 6-12h and 12-36h samples. The latter two samples also had a strong band at ~25kDa, that was barely detectable in the 0-6h sample.

The differences in the protein patterns were less noticeable in experiment III. The 0-1h sample differed most from the other samples: there was some diffuse staining between 140 and 160kDa, a few really weak bands between 65 and 140kDa and a weak band at ~65kDa, that was strongest in this sample compared with the other samples. Additionally, fewer bands could be detected between 25 and 55kDa and no band at ~18kDa, which was present in all the other samples. The other samples were more similar to each other. A weak band at ~75kDa could be detected in the 1-6h sample, that was also only detectable in the 0-1h sample. Another weak band, at ~175kDa, was strongest in the 0-1h, 12-18h and 36-48h samples and was not present in the 1-6h, 24-30h and 30-36h samples. The intensity of the strong band at ~25kDa decreased from 0-1h to 30-36h and was highest at 36-48h, together with the band at ~20kDa.

Additionally, the protein pattern of the ES products in their native state was examined using BN-PAGE and their protein-protein interactions using 2D BN/SDS-PAGE. These results are shown in Figure 3.11. In contrast to the SDS-PAGE, no difference in the staining pattern occurred with the BN-PAGE: there was one high molecular weight band and some diffuse staining at the bottom of the gel stained for each ES preparation. Also, a small amount of protein did not enter the gel properly and stained inside their gel pockets.

Following the second dimension (SDS-PAGE), the protein complex inside the gel pocket related to two major spots and a few really weak ones between. The sharp high molecular band from the BN-PAGE related to a single spot and the diffuse staining at the bottom to numerous bands and spots, which had a similar pattern to an ES preparation only run on a 1D SDS-PAGE.

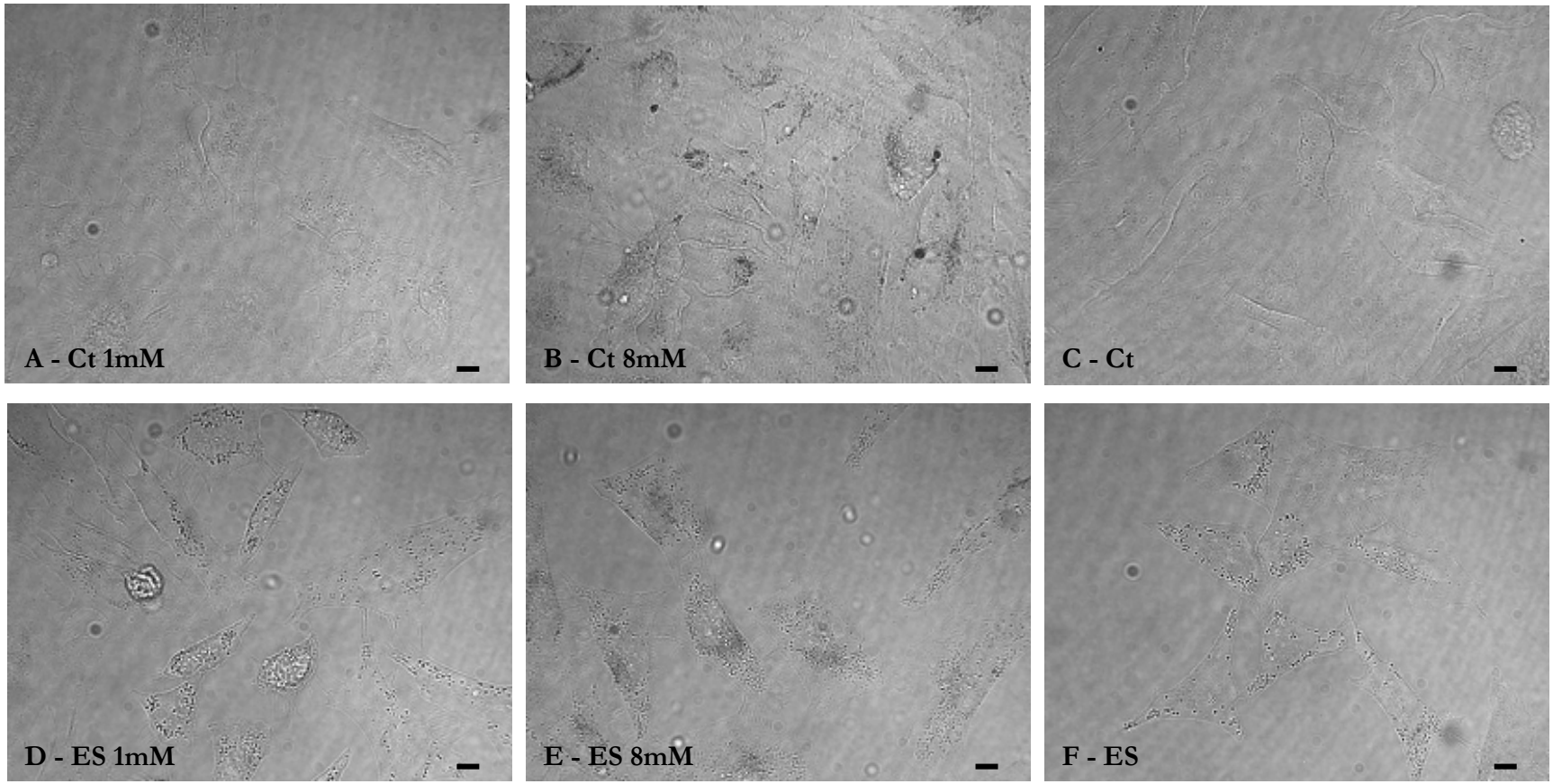

Figure 3.12: Effect of 1mM and 8mM ammonia in CEM and in ES on HeLa cells. A. Control (CEM) + 1mM ammonia, B. Control (CEM) + 8mM ammonia, C. Control (CEM), D. ES + 1mM ammonia, E. ES + 8mM ammonia, F. Control/ES (in CEM). Original magnification 600x, bars 10μm.

3.3.7 Ammonia and ES

Exposure to control samples with added ammonium chloride to HeLa cells resulted in small reddish vacuoles. These were induced in addition to the typical ES vacuolation when ammonia was added to ES preparations.

Incubations with 1mM and 8mM ammonium chloride in CEM were performed four times and in two cases ammonium chloride was also added to an ES preparation (one batch). The pH of all samples was adjusted to 7.4-7.5 after adding ammonium chloride. Adding 1mM or 8mM ammonium chloride to CEM raised the pH by less than 0.25. The pH of the ES preparations did not change with either concentration of ammonia. As shown in Figure 3.12 (B.), 8mM ammonium chloride in CEM had a detrimental effect on the cells. The HeLa cells contained numerous reddish vacuoles, which were in general smaller than ES-induced vacuolation and a few that were much larger. Vacuolation in HeLa cells was also increased by 1mM ammonium chloride in CEM, compared with control cells without ammonium chloride, but the effect was less severe than with 8mM ammonium chloride (Figure 3.12 A.). Most of these vacuoles were also reddish and small.

ES-induced vacuolation did not change with ammonium chloride: neither 1mM nor 8mM enhanced vacuolation. Particularly, after addition of 8mM ammonium chloride to the ES preparation, the reddish vacuoles that were observed in the control cells with 8mM ammonium chloride appeared in addition to the ES-induced vacuoles (Figure 3.12 D. and E.).

The ammonia concentrations of ES preparations and control media was also measured. Two different batches of ES and control generated in CEM were measured and two batches generated in PBS. For both PBS batches, ES and control, the measurements were inconclusive and no values could be obtained. Control samples of CEM had concentrations of ammonia of 20.26 and 22.37μM and ES preparations of 3.68 and 4.7μM.

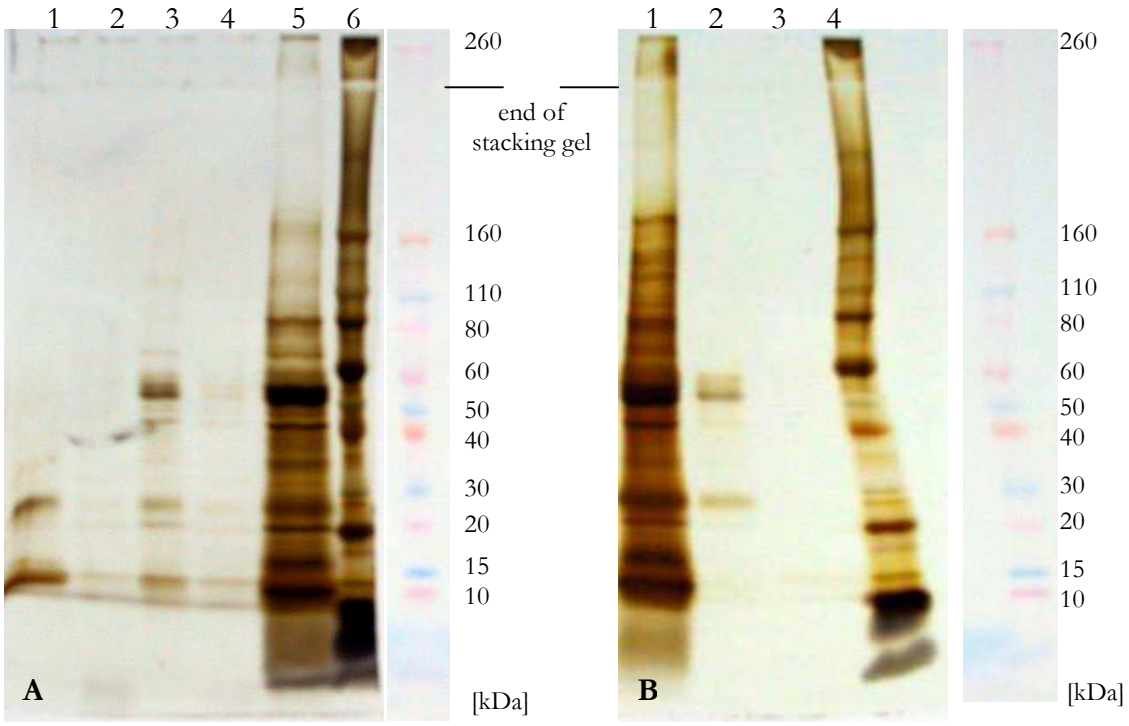

Figure 3.13: SDS-PAGE 5-20% of ES fractions. A. Fractionation I, modified silver stain (0-3 to >100kDa; omitting fractions 0-3kDa and 3-5kDa on the gel) (1) 5-10kDa, 15µg, (2) 10-30kDa, 15µg, (3) 30-50kDa, 15µg, (4) 50-100kDa, 15µg, (5) >100kDa, 15µg, (6) pre-stained marker; pre-stained marker before gel staining on the right, B. Fractionation III, modified silver stain (0-10 to >50kDa) (1) >50kDa, 45µl, (2) 10-50kDa, 45µl, (3) 0-10kDa, 45µl, (4) pre-stained marker; pre-stained marker before gel staining on the right.

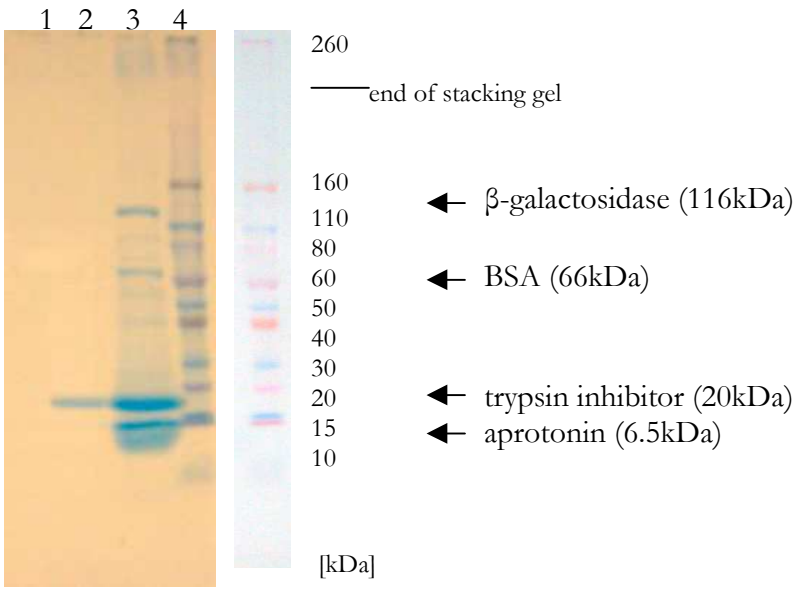

Figure 3.14: SDS-PAGE 5-20% of fractions of protein standards. Coomassie staining. (1) 0-30kDa, 40µl, (2) 30-100kDa, 40µl, (3) >100kDa, 40µl, (4) pre-stained marker; pre-stained marker before gel staining on the right.

3.3.8 Fractionation of ES Products

H. contortus ES products (in PBS) were processed through different size cut-off filters in order to produce ES fractions that were separated by size and can be use in experiments to identify the approximate size of the active ES component(s). The fractionation was unsuccessful and attempts to improve the separation involved chemicals that were shown not to be compatible with the cell test system.

ES products were first fractionated using 100kDa, 50kDa, 30kDa, 10kDa, 5kDa and 3kDa cut-off filters (fractionations I&II, 3.2.2.4) or by only 50kDa and 10kDa cut-off filters (fractionation III, 3.2.2.4). The success of the fractionation process was monitored by SDS-PAGE. Both separation processes (fractionations I&II or III) resulted in fractions with the majority of ES components remaining in the high molecular weight fraction (>100kDa or >50kDa, respectively) and only low concentrations in the smaller fractions. There did not appear to be effective separation: none of the filters separated ES preparations into clear molecular weight ranges and the detected components covered the whole molecular weight range of ES products in each fraction (Figure 3.13). Interestingly, comparing the different fractions below 100kDa in the first fractionation process (I&II) (Figure 3.13 A.) only the 30-50kDa and 5-10kDa fractions contained a few stronger bands: for the 30-50kDa fraction bands appeared at around 55-60kDa, 30kDa, 20kDa and 15kDa and for the 5-10kDa fraction at around 30kDa and 15kDa. For the other fractionation process (III), the strongest bands in the fractions below 50kDa were in the 10-50kDa fraction at around 55-60kDa and 30kDa (Figure 3.13 B.).

The unsuccessful attempt to fractionate ES products was followed by a general control for the method using protein standards (β-galactosidase 116kDa, BSA 66kDa, trypsin inhibitor 20kDa and aprotonin 6.5kDa) with 100kDa and 30kDa cut-off filters. The result was similar to the ES fractionation: all four standards were detected in the high molecular weight fraction (>100kDa) and only parts of trypsin inhibitor (20kDa) in the 30-100kDa fraction, and no protein was detected in the smallest fraction of 0-30kDa (Figure 3.14).

Table 3.6: Effects of fractions generated in the presence of Triton-X-100 (1%)/ β-Mercaptoethanol (0.1%) (in CEM; single applications) and Triton-X-100 and β-Mercaptoethanol itself at different concentrations (in CEM; double applications) on HeLa cells.

Solution	Time [min] after application	Cell state after application
>50kDa [a]	1	all cells are dead
10-50kDa [b]	1	all cells are alive
	20	~50% of the cells are dead
	60	still ~50% of the cells are dead
	120	all cells are dead
0-10kDa [c]	1	all cells are alive
	20	~50% of the cells are dead
	60	almost all cells are dead
1% Triton-X-100	1	all cells are dead
0.2% Triton-X-100	1	all cells are dead
0.1% Triton-X-100	2	cells start to die
	5	all cells are dead
0.01% Triton-X-100	2	a few cells are dead
	30	~50% of the cells are dead
	60	still ~50% of the cells are dead
	120	50-70% of the cells are dead
0.1% β-Mercaptoethanol	5	all cells are alive
	20	~50% of the cells are dead
	60	still ~50% of the cells are dead
	120	50-70% of the cells are dead
0.01% β-Mercaptoethanol	5	all cells are alive
	20	30-50% of the cells are dead
	60	~50% of the cells are dead
	120	still ~50% of the cells are dead
0.1% Triton-X-100, 0.1% β-Mercaptoethanol	2	all cells are dead
Control (CEM)	1-120	all cells are alive

[a] (40µl in 2ml CEM ≙ 1:1.3 dilution of re-expanded original volume ≙ ~0.8% Triton-X-100 and 0.08% β-Mercaptoethanol (if it stayed in that fraction)), [b] (40µl in 2ml CEM ≙ approx. original volume ≙ 1%Triton (if it went through the filter) and 0.1% β-Mercaptoethanol (if it stayed in that fraction)), [c] (1ml+2ml CEM ≙ 1:3 dilution of original volume ≙ 0.3% Triton (if it went through the filter) and ~0.03% β-Mercaptoethanol)

Facing page 87

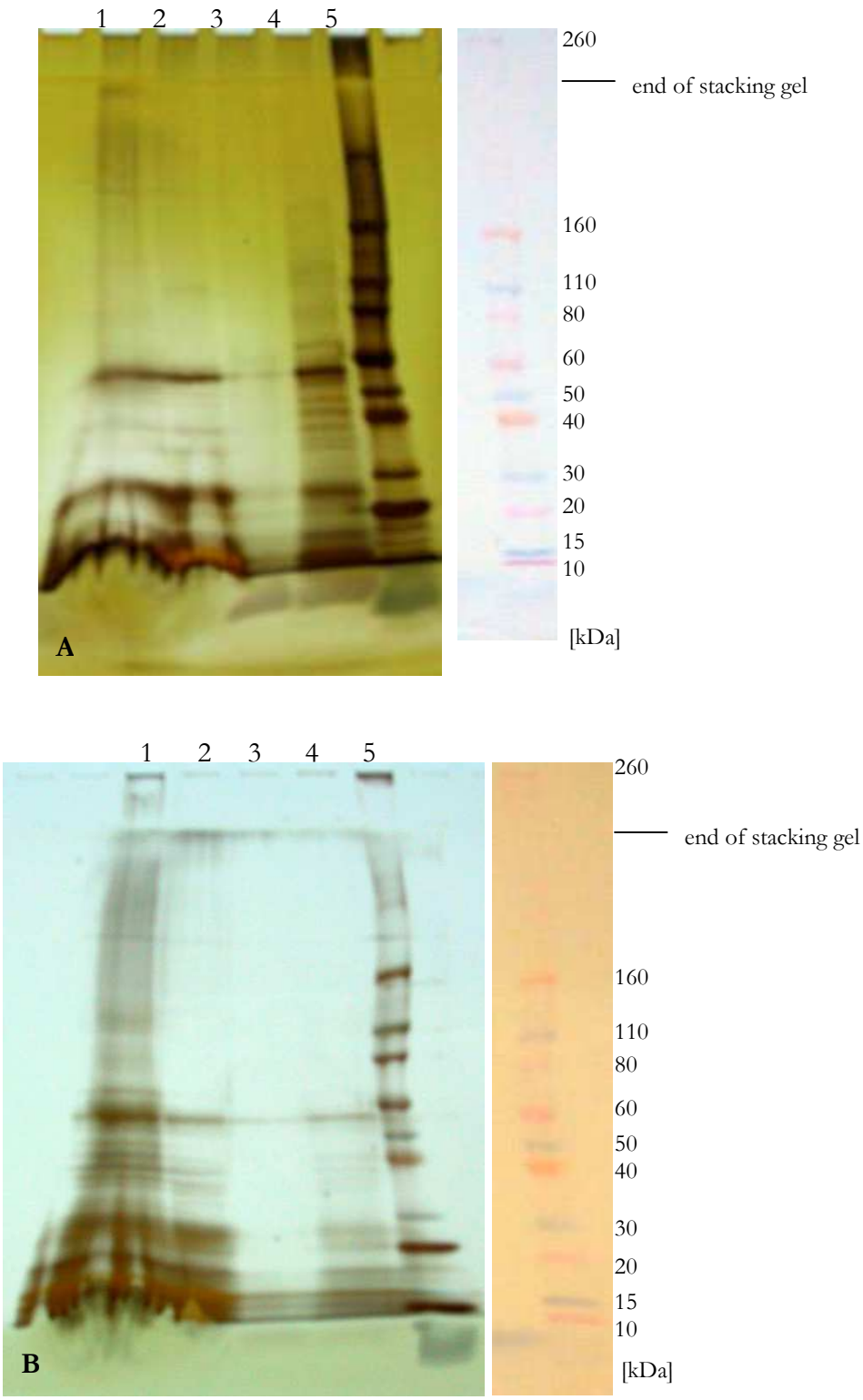

Figure 3.15: SDS-PAGE 5-20% of ES fractions (Triton-X-100- and β-Mercaptoethanol-treated). A. ES fractions 1% Triton, 0.1% β-Mercaptoethanol, silverstain (1) >50kDa, 50µl, (2) 10-50kDa, 50µl, (3) 0-10kDa, 50µl, (4) ES/PBS 50µl (5) pre-stained marker; pre-stained marker before gel staining on the right, B. ES fractions 0.2% Triton, silverstain (1) >50kDa, 40µl, (2) 10-50kDa, 40µl, (3) 0-10kDa, 40µl, (4) ES/PBS 40µl (5) pre-stained marker; pre-stained marker before gel staining on the right.

Triton-X-100 (1%) and β-mercaptoethanol (0.1%) were added in an attempt to improve the separation. Adding the detergent Triton-X-100 promotes the solubilisation of proteins without denaturation: the low critical micelle concentration (CMC) limits the monomeric concentration sufficient for the cooperative binding and denaturation. The reducing agent β-mercaptoethanol cleaves the disulphide bonds, both preventing aggregation. Fractionation in the presence of Triton-X-100 or Triton-X-100 and β-mercaptoethanol (0.1%) was performed twice, both times leading to the same result (Figure 3.15 A.). Addition of Triton-X-100 and β-mercaptoethanol did not appear to enhance fractionation. The >50kDa fraction contained around half of the ES components, which were spread across the whole molecular weight range of ES products. In addition, it appeared that this fraction also contained the majority of the added Triton-X-100. With the low CMC of 0.24mM (Helenius and Simons, 1975; ≙ ~0.015%) many Triton-X-100 micelles are probably formed which have an average weight of 90kDa (Helenius and Simons, 1975). The high Triton-X-100 concentration in this fraction led to a poor separation on the gel and also interfered with the Bradford assay (false positive increased values; >0.5% Triton-X-100 interferes with this method, Lottspeich and Zorbas, 1998). The 10-50kDa fraction contained about the other half of the ES components and the smallest fraction (0-10kDa) only ES products at a quite low concentration. This could also be due to the fact that this fraction was the last eluate and was not concentrated. Components of both fractions, 10-50kDa and 0-10kDa, also were spread over the whole molecular weight range of ES products. Additionally, judged by the sulphuric odour, the smallest fractions contained the majority of the added β-mercaptoethanol. Fractionation with added 0.2% Triton-X-100 led to a similar result (Figure 3.15 B.). The >50kDa fraction contained around three quarter of the ES components and probably the majority of the added Triton-X-100, the 10-50kDa fraction more or less the remaining third and only a low concentration in the 0-10kDa fraction. ES components of each fraction also spread over the whole molecular weight range.

The tolerance of cells to the added detergent and reducing agent was determined by applying different concentrations on HeLa cells as well as the different fractions of the fractionation with Triton-X-100 (1%) and β-mercaptoethanol (0.1%). These results are shown in Table 3.6. To summarise these results, HeLa cells did not tolerate concentrations of Triton-X-100 as low as 0.1%. The survival rate improved slightly with 0.01% Triton-X-

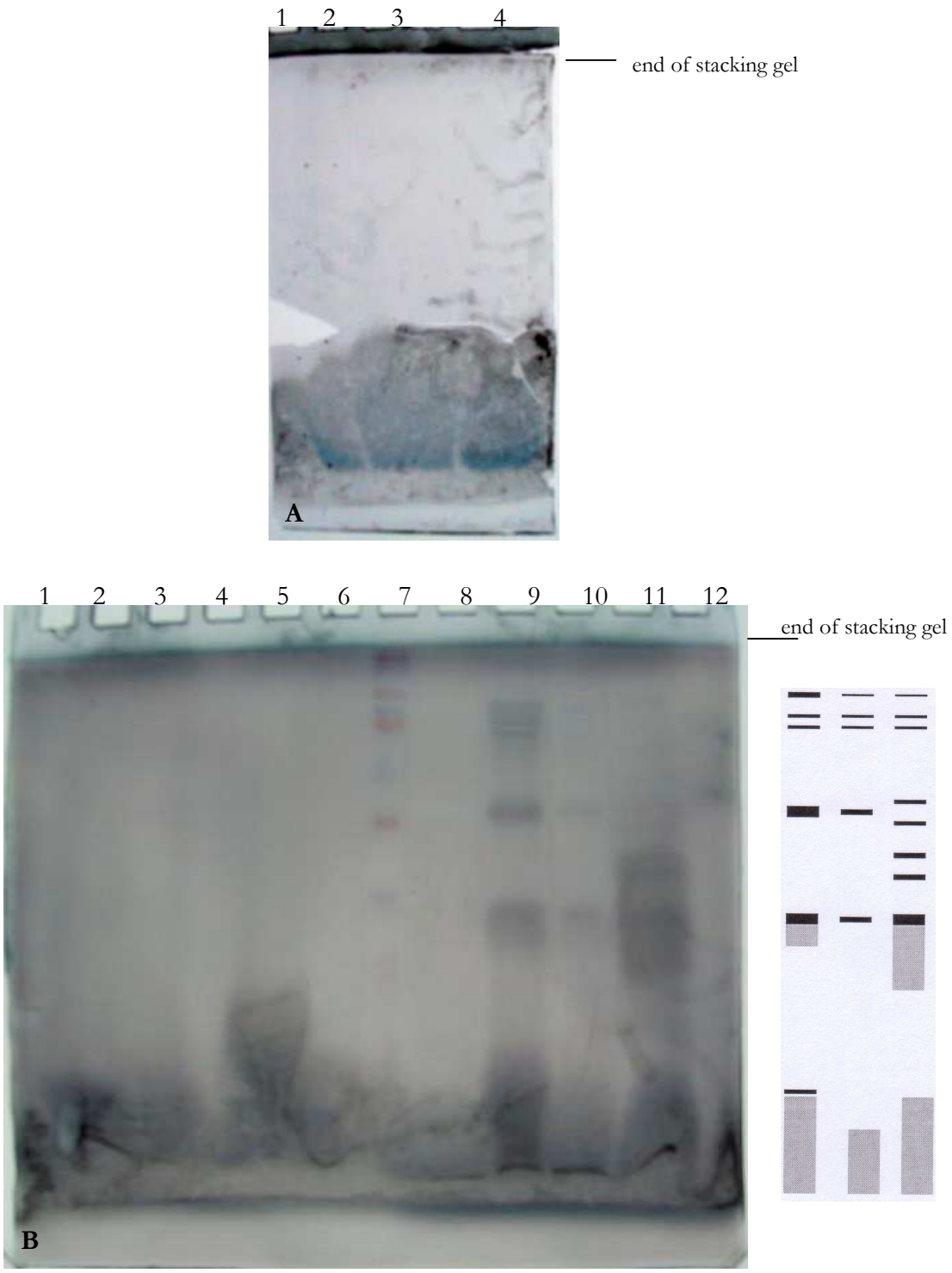

Figure 3.16: Detection of prostaglandins and lipids in *H. contortus* ES products via SDS-PAGE 20%. A. and B. Sudan Black staining. A. (1) 3-5kDa 59µl ≙ 15µg, (2) 0-3kDa 42µl ≙ 3µg, (3) 0-3kDa 167µl ≙ 12µg, (4) 0-3kDa 104µl ≙ 7.5µg, B. (1) -, (2) PGA_2, 30µg (3) PGB_2, 30µg, (4) PGD_2, 30µg, (5) PGE_2, 30µg, (6) $PGF_{2\alpha}$, 30µg, (7) Pre-stained protein marker 15µl, (8) PBS/ES, unconcentrated, 45µl, (9) Time Trial 0-6h (~100x conc.), 40µl, (10) Time Trial 6-12h (~100x conc.), 40µl, (11) Time Trial 12-36h (~100x conc.), 40µl, (12) - ; band pattern as seen in the gel on the right.

100, although half of the cells were dead after only 30min. The tolerance to β-mercaptoethanol was slightly higher, but also after 20min (0.1%) or 60min (0.01%) half of the cell population had died.

3.3.9 Lipids and Prostaglandins - A Possible Role in Vacuolation?

Prostaglandins and ES product lipids were detected via TLC and SDS-PAGE. No vacuolating activity could be detected for either lipids eluted from the TLC plate or prostaglandin standards.

3.3.9.1 Lipid and Prostsglandin Detection via SDS-PAGE

Prostaglandin standards [30µg] were applied as a reference for the different ES preparations: ES generated in PBS, fractions 0-3kDa (freeze-dried), 3-5kDa and 0-10kDa (3.2.2.4) and ES harvested at different incubation time points (in CEM without FBS, time periods 0-6h, 6-12h and 12-36h, all concentrated ~100-fold; 3.2.1). Either gels were stained with Sudan Black or the samples were pre-stained with Sudan Black.

The pre-staining method resulted in no staining, but the Sudan Black gel staining method gave positive results. Lipid were detected both in the 0-3kDa fraction and in the samples from three successive incubations (0-6h, 6-12h, 12-36h). One band was seen at the bottom of the gel for the three applications of the 0-3kDa fraction, independent of the three different amounts applied (3 to 12µg) (Figure 3.16 A.). The band pattern for the three time trial preparations was slightly different. The first two, 0-6h and 6-12h, had similar bands, only with a different staining intensity: bands of the 6-12h preparation were much weaker and there was no clear band at the bottom, but diffuse staining, compared with the 0-6h sample. The 12-36h preparation had the same three bands at the top with an intensity comparable to the 6-12h sample and the two bands/diffuse staining at the bottom, but had four different bands compared with the other two preparations in the middle section of the gel (Figure 3.16 B.). The detection of the prostaglandin standards was not clear, with

Figure 3.17: Detection of prostaglandins and lipids in *H. contortus* ES products via TLC. (1) Time trial 0-6h, 20µl, (2) Time trial 6-12h, 20µl, (3) Time trial 12-36h, 20µl, (4) PGA_2, 1µg, (5) PGB_2, 1µg, (6) PGD_2, 1µg, (7) $PGF_{2\alpha}$, 1µg, (8) PGE_2, 1µg.

Table 3.7: Rf-values of prostaglandin standards and lipids present in *H. contortus* ES (solvent system ethylacetate : acetic acid 98:2).

Sample	Rf value
PGA_2 [a]	0.600
PGB_2 [a]	0.572
PGD_2 [a]	0.489
PGE_2 [a]	0.310
$PGF_{2\alpha}$ [a]	0.189
6h bottom [b]	0.241
6h top [b]	0.732
12h bottom [b]	0.183
36h bottom [b]	0.183
36h top [b]	0.751

[a] average of 4 experiments, [b] average of 3 experiments (different concentrations)

possible bands/diffuse staining of PGA_2, PGB_2, PGE_2 and $PGF_{2\alpha}$ at the bottom of the gel (Figure 3.16 B.).

3.3.9.2 Lipid and Prostaglandin Detection via TLC

The detection limit of the TLC for each prostaglandin standard (PGA_2, PGB_2, PGD_2, PGE_2, $PGF_{2\alpha}$) was 1µg.

TLC was then performed on different ES preparations: ES generated in CEM (routine 12h incubation), ES generated in PBS (routine 12h incubation), both 5µl and 10µl sample, and ES harvested at different incubation time points (in CEM without FBS, time periods 0-6h, 6-12h and 12-36h, all ~100-fold concentrated), each time period 5µl, 15µl and 20µl sample. All prostaglandin standards, applied as a reference, were detected at a concentration of 1µg. In the two unconcentrated ES preparations, none of the prostaglandins could be detected. Phosphomolybdic acid stains for lipids, steroids, lactones, keto acids, hydroxy acids, unsaturated fatty acids and phenolic compounds, but none of these compounds could be detected. ES preparations collected from the different time periods (6h, 12h and 36h) each had a really weak dot at around a quarter of the running length that was at approximately the same height as PGE_2 and samples 6h and 36h each a dot above all standards. These results are shown in Figure 3.17 and the Rf-values (retention factor) in Table 3.7.

3.3.9.3 Vacuolating Activity of Prostaglandins and Extracted Lipids

The vacuolating activity of prostaglandin standards and extracted lipid spots from the TLC was examined using HeLa and AGS cells, resulting in no vacuolation or no vavuolation above background respectively.

Prostaglandin standards [0.5µg/ml] were applied to either HeLa or AGS cells in single applications of each standard for 24h and their ability to induce vacuolation examined. Experiments with Hela cells were performed once and with AGS cells twice. None of the

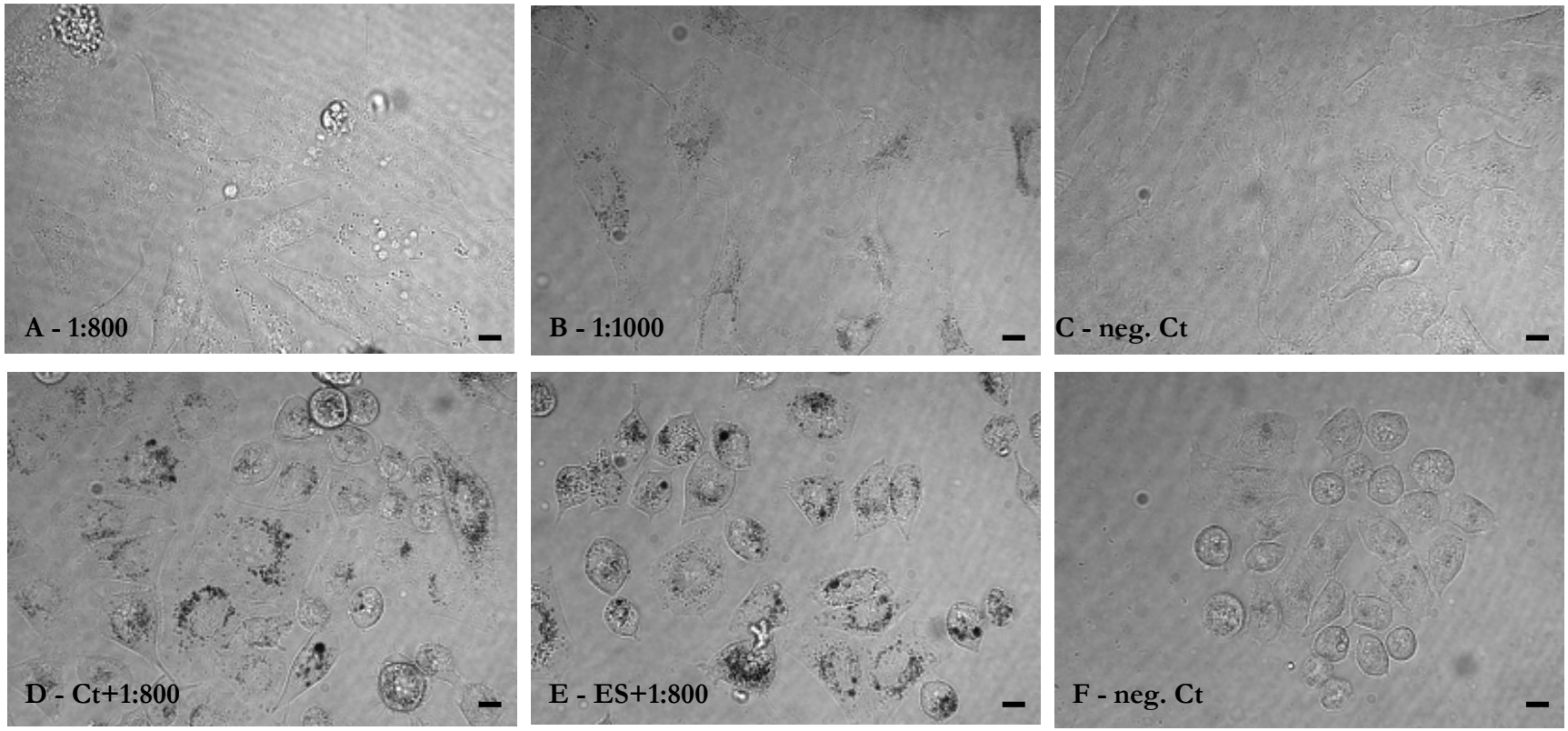

Figure 3.21: Effect of protease and phosphatase inhibitors on HeLa and AGS cells. Neutral red staining. A. HeLa cells, CEM mixed with protease inhibitor cocktail 1:800, B. HeLa cells, CEM mixed with protease inhibitor cocktail 1:1000, C. HeLa cells, normal control cells (CEM), D. and E. AGS cells, control (F12-Hams) (D.) and ES (E.) mixed with protease inhibitor cocktail 1:800 during ES generation, F. AGS cells, normal control cells (F12-Hams). Original magnification 600x, bars 10μm.

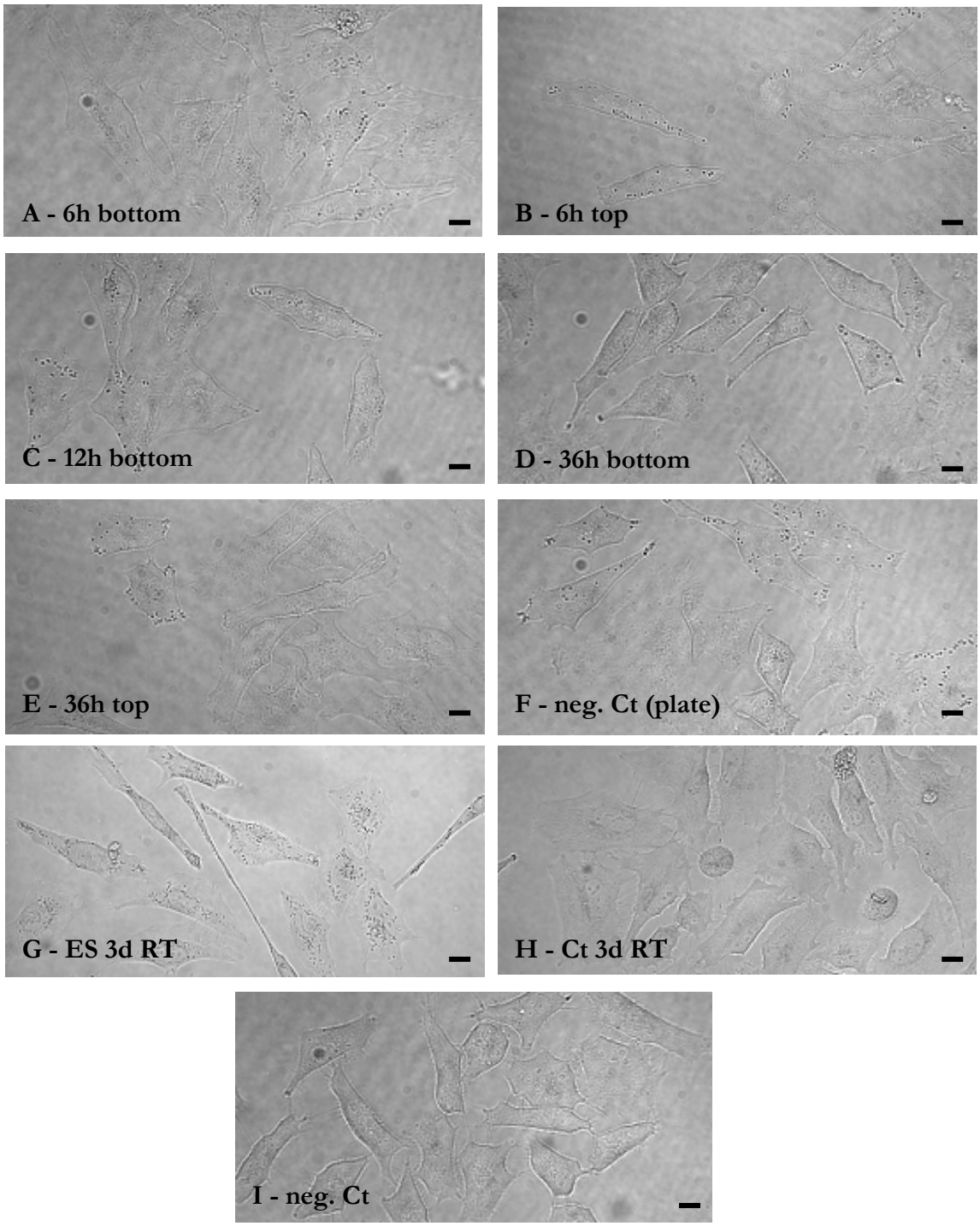

Figure 3.20: Vacuolating ability of extracted lipid spots from TLC in HeLa cells. A. 6h bottom, B. 6h top, C. 12h bottom, D. 36h bottom, E. 36h top, F. Negative control (plate), G. ES (in CEM) stored at room temperature for 3d, H. Control (CEM) stored at room temperature for 3d, I. Control (CEM). Original magnification 600x, bars 10μm (A. to F. and I.); original magnification 400x, bars 2μm (G. and H.)

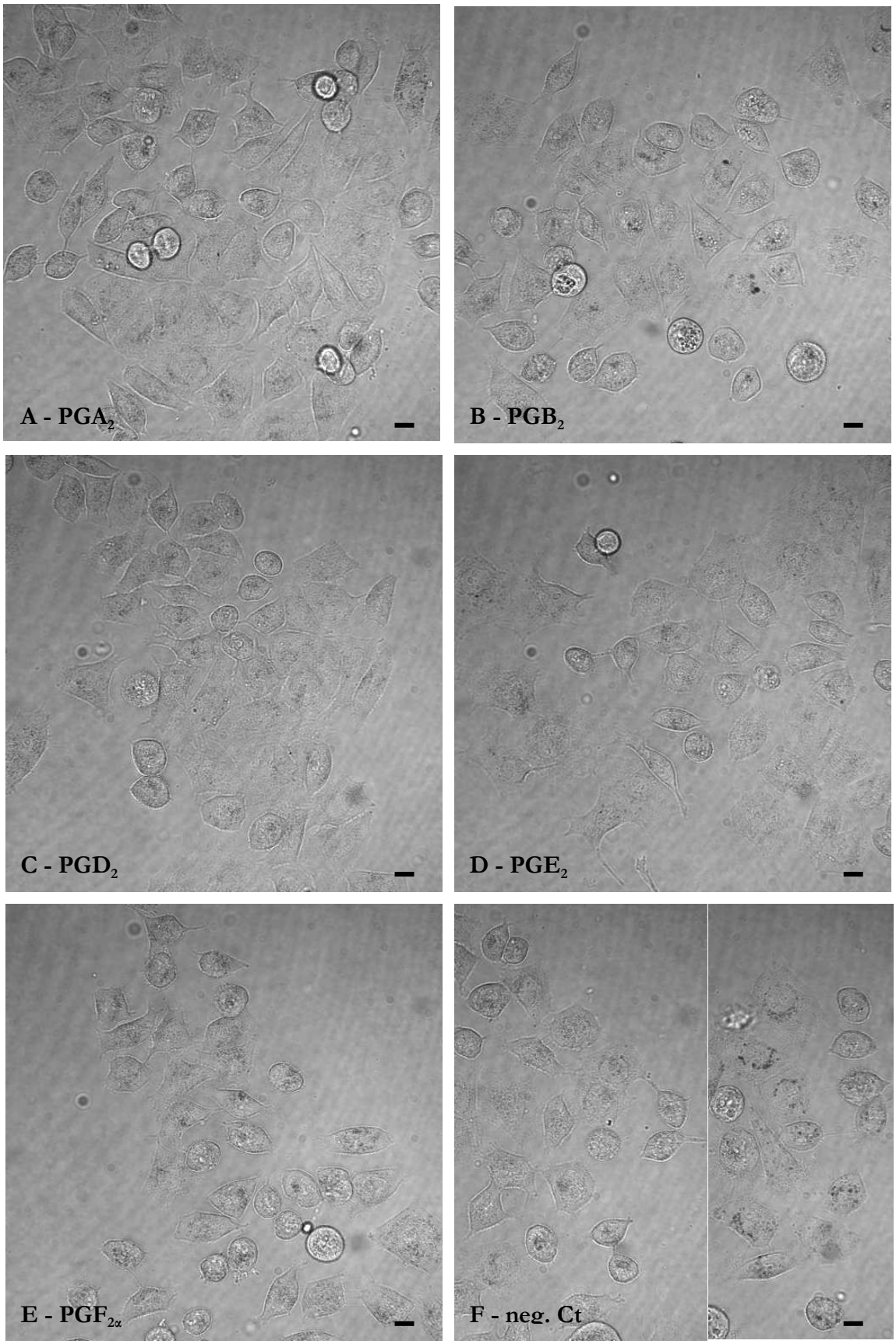

Figure 3.19: Vacuolating ability of prostaglandin standards [0.5mg/ml] in AGS cells. A. PGA_2 in F12-Hams, B. PGB_2 in F12-Hams, C. PGD_2 in F12-Hams, D. PGE_2 in F12-Hams, E. $PGF_{2\alpha}$ in F12-Hams, F. Control cells/F12-Hams. Original magnification 600x, bars 10µm.

Facing page 90

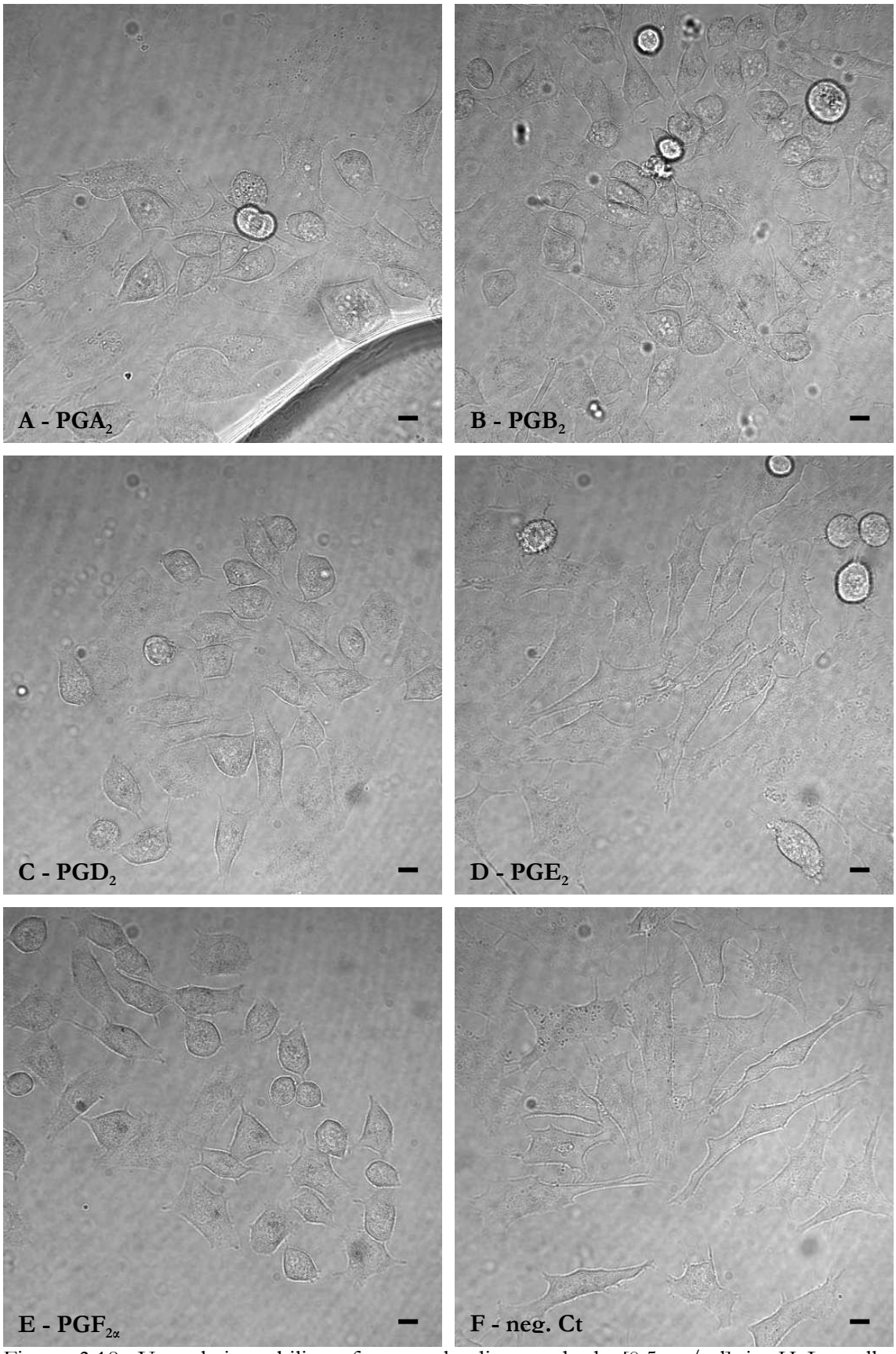

Figure 3.18: Vacuolating ability of prostaglandin standards [0.5mg/ml] in HeLa cells. A. PGA_2 in CEM, B. PGB_2 in CEM, C. PGD_2 in CEM, D. PGE_2 in CEM, E. $PGF_{2\alpha}$ in CEM, F. Control cells/CEM. Original magnification 600x, bars 10μm.

standards was able to induce vacuoles similar to those caused by ES or any vacuoles in HeLa cells and AGS cells. These results are shown in Figure 3.18 and 3.19.

The five lipid spots, that were detected on the TLC plate in the ES preparations of the successive ES incubations (see above), were eluted from the plate and also tested on HeLa cells. Exposure to the negative control from the TLC plate (elution from the silica gel without any sample) resulted already in many vacuolated cells even though vacuoles were fewer per cell than after application of an ES preparation (Figure 3.20 F.). Vacuoles were formed probably due to chemical residues in the sample (solvent system ethylacetate : acetic acid 98:2, scrapings of silica gel, elution in methanol). The five lipid samples eluted from the TLC plate (Figure 3.20 A. to E.) had a similar to slightly less number of cells with vacuoles with fewer vacuoles per cell like the negative control from the TLC plate, compared with normal control cells. Controls from the 3d storage at room temperature of ES preparation and control sample showed normal vacuolation for the ES preparation (~95% of the cells vacuolated) and a slightly increase in vacuolation (~15%) for the control cells but with fewer vacuoles per cell (Figure 3.20 G. and H.).

3.3.10 Protease and Phosphatase Inhibition

Protease and phosphatase inhibitors added to the cell culture medium in preliminary experiments and during ES generation with the objective of investigating proteases and/or phosphatases as the cause of the ES-induced vacuolation were unsuccessful as cells did not tolerate the inhibitors used.

Incubation of HeLa cells for 24h with protease inhibitor cocktail at concentrations of 1:800 and 1:1000 (in CEM) (recommended dosage by the supplier: 1:800 for HeLa cells) resulted in heavily vacuolated cells, while the control cells appeared normal (Figure 3.21 A. to C.). These preliminary experiments were performed once for each concentration.

AGS cells treated with protease inhibitor cocktail (1:800 in F12-Hams) appeared normal during the preliminary experiment, however after incubation of the cells with ES

Facing page 91

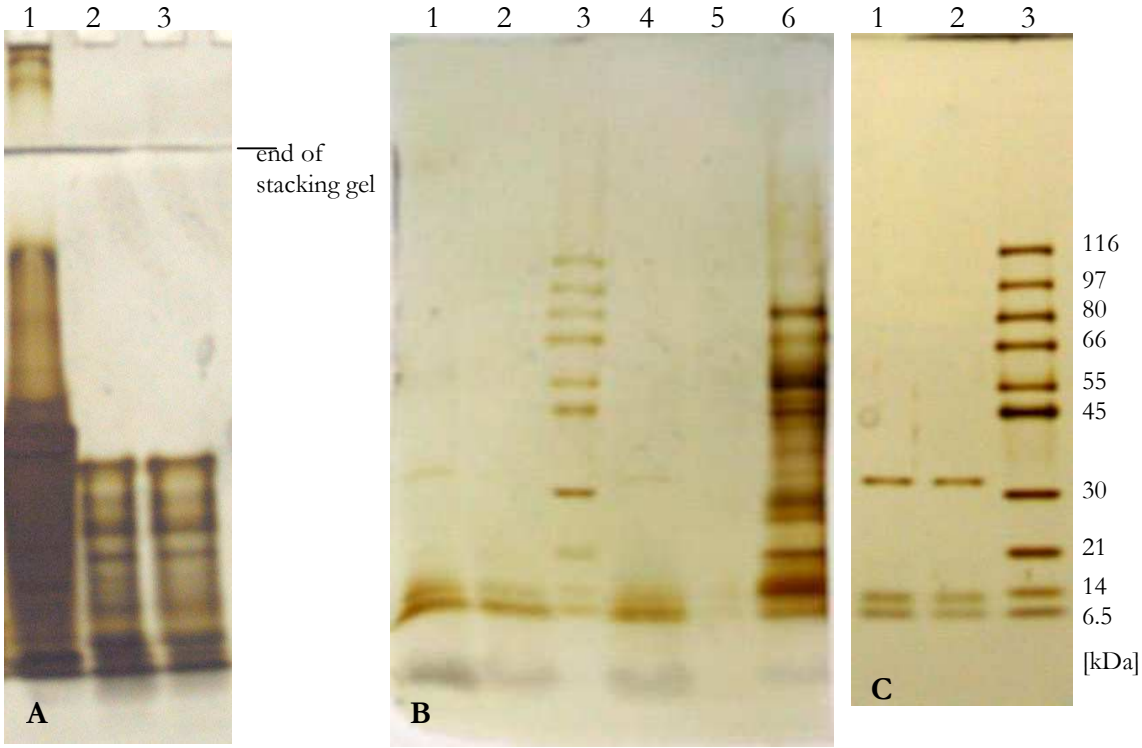

Figure 3.22: SDS-PAGE 5-20% of proteinase K digested control (CEM) and ES products. A. to C. Modified silverstain. A. Digestion of CEM 30µg protein, (1) CEM, (2) 100µg proteinase K, 48h, (3) 100µg proteinase K, 72h, B. and C. Digestion of 30µg ES concentrate (in PBS), B. (1) 100µg proteianse K, 49h digestion, (2) 100µg proteinase K, 78h digestion, (3) Marker, (4) 200µg proteinase K, 49h digestion, (5) 100µg proteinase K (in PBS), 78h digestion, (6) ES concentrate (in PBS) 30µg, C. (1) 100µg proteinase K, 5d digestion, (2) 100µg proteinase K, 7d digestion, (3) Marker. B. and C. are shown without stacking gel.

preparation and control mixed with inhibitors during the ES generation (1:800), all cells were also heavily vacuolated. This occurred in three incubations with the same batch for each ES preparation and control sample. The vacuoles looked different from ES-induced vacuolation and appeared more reddish with generally smaller vacuoles, but also some much larger ones than ES-induced vacuolation. Cells incubated with control samples (F12-Hams) appeared normal (Figure 3.21 D. to F.).

During incubation with phosphatase inhibitor cocktail [10 and 7.5µl/ml] (recommended dosage by the supplier: 10µl/ml), HeLa and AGS cells were mostly killed. These preliminary experiments were performed twice with 10µl/ml for HeLa cells and once each cell line with 7.5µl/ml.

3.3.11 Proteinase K Digestion

Experiments to digest the protein content of ES products with proteinase K to examine ES proteins as the cause of vacuolation in HeLa cells were only partly successful: ES proteins could be digested, but cells did not tolerate proteinase K at different concentrations tested.

In preliminary experiments, proteinase K was added to HeLa cells at concentrations of 50µg/ml, 37.5µg/ml and 25µg/ml (recommended dosage by the supplier: typically used at 50-200µg/ml in nucleic acid preparations) in CEM, once each concentration. Additionally, CEM with the same concentrations of proteinase K added was pre-incubated for 48 and 72h at 37°C before applying to HeLa cells (twice 50µg and 37.5µg and four times 25µg). Pre-incubations with proteinase K were tested to investigate whether autodigestion of the enzyme during pre-incubation aid the survival of the cells. All cells died within a period of a few minutes to one hour after exposure to the samples, independent of proteinase K concentration and pre-digestion time.

The state of digestion was monitored via SDS-PAGE (Figure 3.22). Most of the cell culture medium proteins were digested after 48 and 72h with 100µg proteinase K. Proteins in ES products (30µg in PBS) were almost completely digested by 100 or 200µg proteinase K for 49 or 78h at 37°C. The two bands that appeared at the bottom of the gels in Figure 3.22 B.

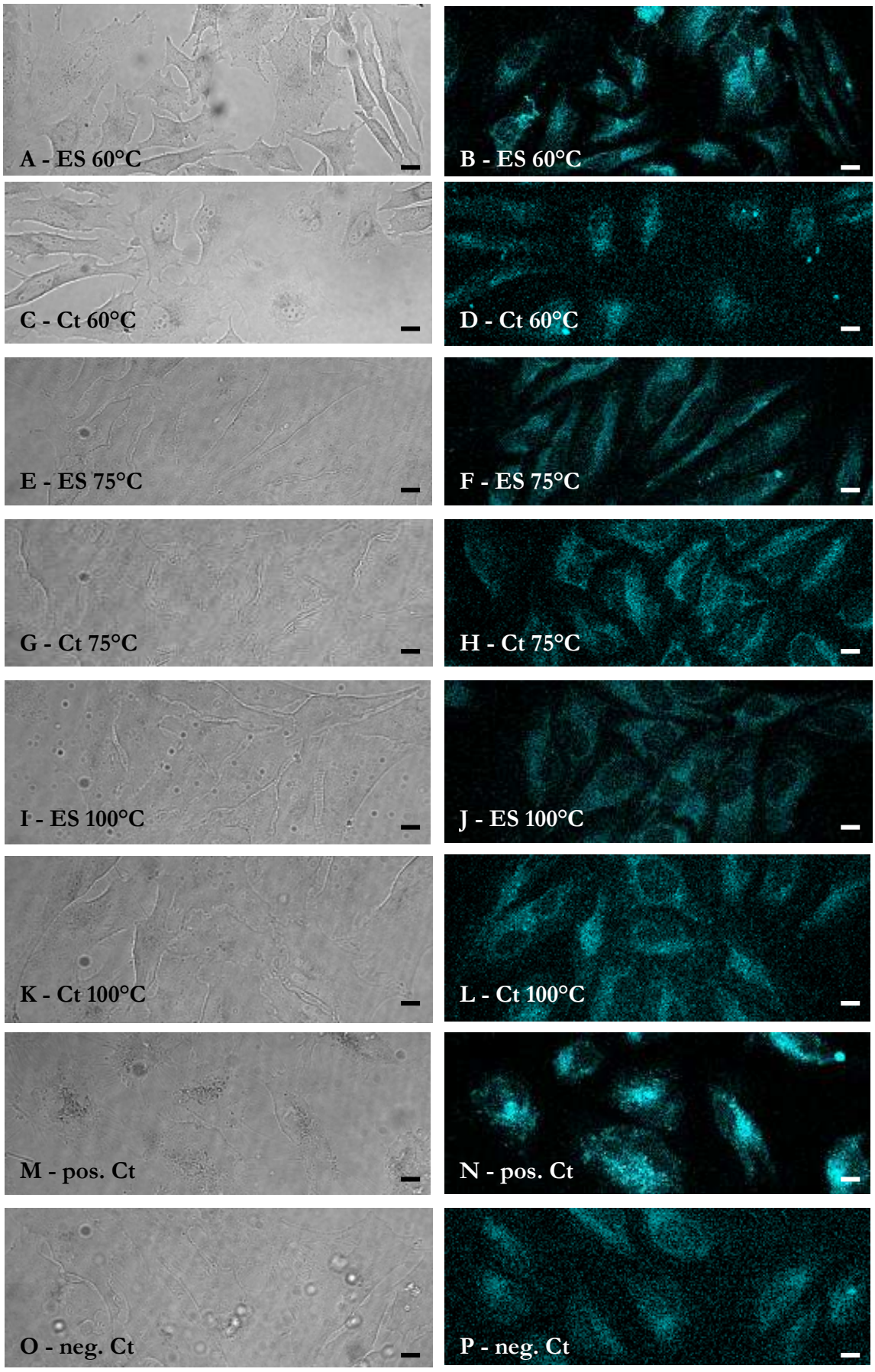
A - ES 60°C
B - ES 60°C
C - Ct 60°C
D - Ct 60°C
E - ES 75°C
F - ES 75°C
G - Ct 75°C
H - Ct 75°C
I - ES 100°C
J - ES 100°C
K - Ct 100°C
L - Ct 100°C
M - pos. Ct
N - pos. Ct
O - neg. Ct
P - neg. Ct

and C. at around 6.5 and 14kDa were probably a mixture of small digestion endproducts and autodigestion products of proteinase K, as weak bands of the same size also appeared in Figure 3.22 B. lane 5, which showed digestion products only of proteinase K (78h autodigestion of proteinase K in PBS). One band appeared at ~32kDa in all digested ES preparations (Figure 3.22 B. and C.).

3.3.12 Heat-Treatment

ES products heat-treated at different temperatures in order to investigate the protein content of ES products as the cause of vacuolation in HeLa cells resulted in reduced ES-induced vacuolation with increasing temperatures.

ES products generated in CEM that were heat-treated for 30min at 75°C induced vacuolation in ~60% of the cells, with the exception of one application of four where there were only ~15% vacuolated cells. All four applications of heat-treated control samples (30min at 75°C) showed a slight increase in vacuolated cells compared with typical control applications (15 to 20%).

Incubations with ES products that were generated in PBS and control samples (PBS) were performed four times with two different batches heat-treated at 100°C and 75°C (each 30min) and twice with the same batch treated at 60°C (30min). Heat-treated ES products at 60°C showed a decreased ability to induce vacuolation in HeLa cells with only 30 to 40% of the cells affected (Figure 3.23 A. and B.). The number of vacuoles per cell was reduced

---

Figure 3.23: Vacuolation in Hela cells induced by heat-treated *H. contortus* ES. 24h incubation. Neutral red staining. Left, bright field images; right, fluorescent imaging (UV/405nm excitation). A. and B. ES/PBS (50% in CEM) heat-treated 60°C, C. and D. Control (PBS 50% in CEM) heat-treated 60°C, E. and F. ES/PBS (50% in CEM) heat-treated 75°C, G. and H. Control (PBS 50% in CEM) heat-treated 75°C, I. and J. ES/PBS (50% in CEM) heat-treated 100°C, K. and L. Control (PBS 50% in CEM) heat-treated 100°C, M. and N. Positive control (ES/PBS 50% in CEM), O. and P. Negative control (PBS 50% in CEM). Original magnification 600x, bars 10µm.

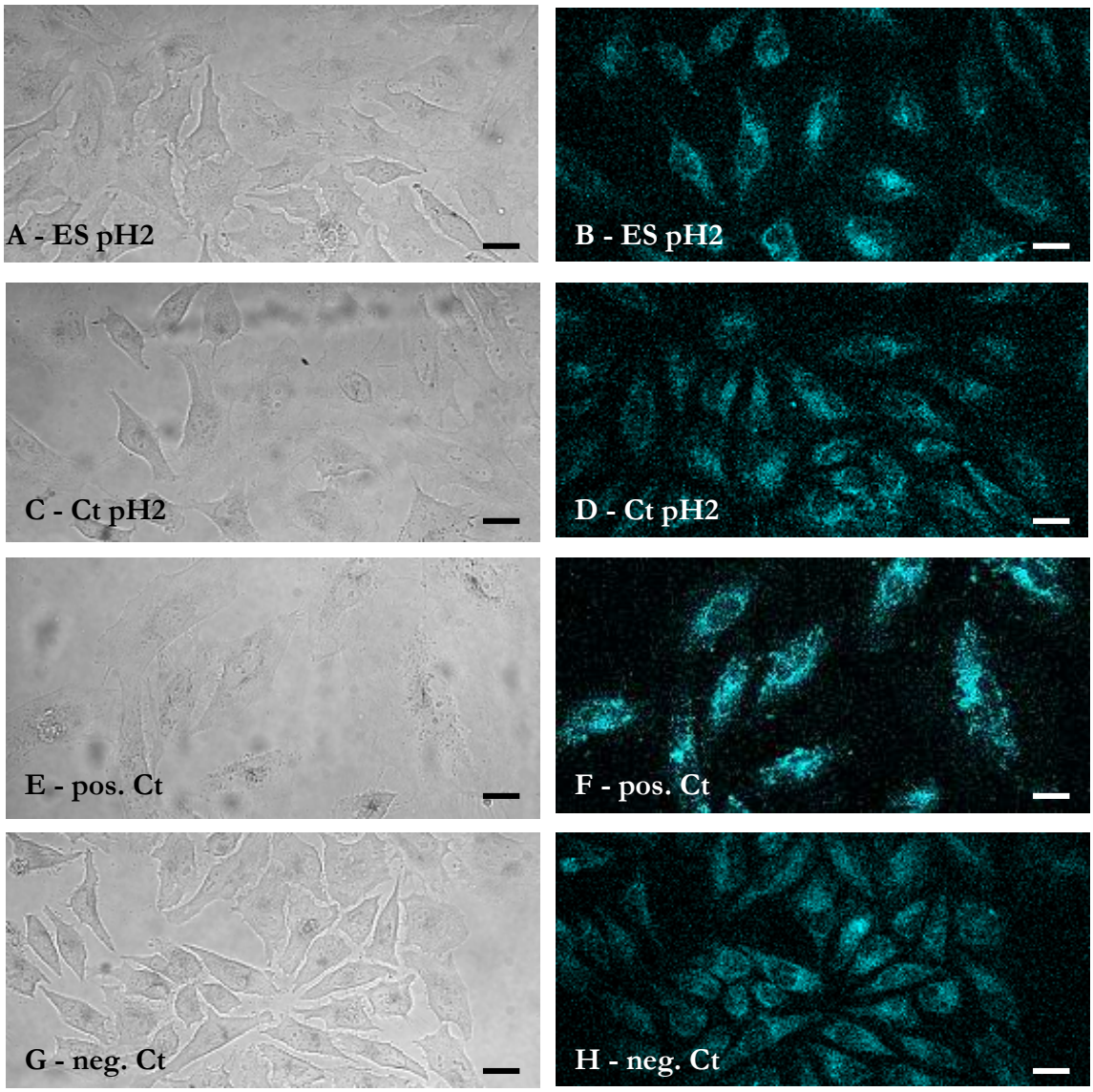

Figure 3.24: Vacuolation in Hela cells induced by acid-treated *H. contortus* ES. 24h incubation. Neutral red staining. Left, bright field images; right, fluorescent imaging (UV/405nm excitation). A. and B. ES/PBS (50% in CEM) acid-treated at pH2, C. and D. Control (PBS 50% in CEM) acid-treated at pH2, E. and F. Positive control (ES/PBS 50% in CEM), G. and H. Negative control (PBS 50% in CEM). Original magnification 400x, bars 20µm.

compared with a typical ES application. HeLa cells exposed to control samples heat-treated at 60°C appeared normal with no vacuolation (Figure 3.23 C. and D.). Heat-treated ES products at 75°C induced vacuolation in ~15% of the cells. The number of vacuoles per cell was reduced and the vacuoles appeared reddish rather than dark red, unlike those seen after a typical ES application (Figure 3.23 E. and F.). The corresponding controls induced no vacuolation (Figure 3.23 G. and H.). Heat-treatment of ES products at 100°C almost eliminated the vacuolating ability with only a few cells showing some reddish vacuoles (Figure 3.23 I. and J.). Heat-treated control samples at 100°C appeared normal (Figure 3.23 K. and L.). The positive control of 50% ES/PBS in CEM induced vacuolation in 70 to 80% of the cells. The number of vacuoles per cell was reduced in some cells compared with a typical ES application (Figure 3.23 M. and N.). HeLa cells exposed to the negative control (50% PBS in CEM) showed no vacuolation (Figure 3.23 O. and P.).

3.3.13 Acid-Treatment

In addition to the heat-treatment, acid-treatment of ES products, also carried out to investigate whether the protein content of ES products was a cause of vacuolation resulted in a reduced vacuolating ability of ES preparations.

Incubations with acid-treated (30min at pH 2) samples were performed twice with the same ES and control batch. HeLa cells exposed to acid-treated ES products showed a reduced number of vacuolated cells with ~30% of the cells affected compared with a typical ES application of 80 to 100% affected cells. The number of vacuoles per cell was also reduced in some cells (Figure 3.24 A. and B.). The number of vacuolated cells was slightly increased to ~20 to 30% by acid-treated control samples compared with a typical control application, but with only a few vacuoles per cell appearing (Figure 3.24 C. and D.). The positive control (50% ES/PBS in CEM) induced vacuolation in ~70 to 80% of the cells, some of these with a reduction in vacuoles per cell compared with a typical ES application (Figure 3.24 E. and F.). Negative control cells (50% PBS in CEM) appeared normal (Figure 3.24 G. and H.).

3.4 Discussion

The experiments described in this chapter were conducted to investigate different aspects of ES-induced vacuolation and to characterise the vacuolating factor of ES products.

3.4.1 Characteristics of the Vacuolation

The application of adult *H. contortus* ES products caused vacuolation in an epithelial cell line (HeLa, human cervix adenocarcinoma cells), which was revealed by NR uptake, as previously reported (Huber *et al.*, 2005; Przemeck *et al.*, 2005). HeLa cells are commonly used for a wide range of cytotoxity tests, as they are easy to prepare and maintain. In addition, the present study has shown that the same effect can also be induced in AGS cells, which are epithelial human gastric adenocarcinoma cells. As they originate from the stomach, AGS cells represent cells from the corresponding human organ to the sheep abomasum. Furthermore, similar vacuolation due to ES products could also be induced in undifferentiated CaCo-2 (human epithelial colonic adenocarcinoma) cells (K. C. Pedley, unpublished data). Together, these results demonstrated that ES products are able to induce vacuolation in different epithelial cell lines.

However, it remains speculative whether ES products could be responsible for the vacuolation of parietal cells *in vivo*. In addition, vacuolation observed *in vitro* appears to be different, with numerous small vacuoles compared with much larger vacuoles observed in parietal cells, sometimes occupying almost the whole cell, (see also Chaper 2). The use of isolated parietal cells in culture could clarify whether ES products are capable of directly inducing vacuolation in parietal cells as in the other epithelial cell lines and are a possible cause of the observed *in vivo* vacuolation. Furthermore, it would be interesting to determine whether vacuoles show similarities to either the *in vitro* or *in vivo* vacuolation, which could be indicative that host factors may be involved or vacuoles are generated during cell degeneration. Vacuoles observed in parasitised tissues were suggested to be due to necrosis (Scott *et al.*, 2000), however this appears not to be the case for the observed *in vitro* vacuolation. Although the morphology of parietal cells in culture changes and the apical

intracellular canaliculi appear to close off, cultured parietal cells are widely used to analyse intracellular signalling and cell function (Chew, 1994). In addition, it may be useful to further test the vacuolating ability of ES products on other isolated fundic abomasal cells as vacuolation *in vivo* was exclusively observed in parietal cells (see also chapter 2). Furthermore, the use of different vacuole markers (e.g. early endosome markers Rab5 and EEA1 (early endosome antigen), recycling endosome markers Rab4 and Rab11, lysosome marker LAMP1 (lysosome-associated membrane protein)) could determine the origin of the vacuoles. Comparing this for different cell lines could clarify whether these vacuoles have the same origin.

The time for the onset of vacuolation in HeLa cells due to *H. contortus* adult ES products was determined to take place in the first two hours after exposure to ES products (full manifestation was reached after 2h exposure and 75% after only 1h). These experiments showed that the cell damage due to ES products can occur very quickly. When related to pathophysiological and pathological abomasal responses, these results are consistent with previous observations of rapid changes in abomasal function and morphology due to adult parasites, either after the emergence from the glands (2-4 days after infection with *H. contortus* (Simpson *et al.*, 1997); 5-6 days with *T. circumcincta* (Lawton *et al.*, 1996; Scott *et al.*, 2000)), direct transfer of adult *H. contortus* (Simpson *et al.*, 1997) or *T. circumcincta* (Lawton *et al.*, 1996; Scott *et al.*, 2000) into the abomasum, or exposure of adult *T. circumcincta* prevented from physical contact with the gastric mucosa (Simpson *et al.*, 1999).

Rapid reversibility of acid inhibition after anthelmintic treatment, as seen in experiments of Simpson *et al.* (1997) and Scott *et al.* (2000), is most likely to follow different mechanisms from vacuolation in HeLa cells, as recovery of HeLa cells took a very long time (numerous vacuolated cells were still observed 48h after the removal of ES products) compared with parietal cell/acid-secreting recovery beginning within 2h of drenching (Simpson *et al.*, 1997). Possible mechanisms for the rapid recovery of acid secretion are also discussed in chapter 2. For the HeLa cell recovery experiment, it is also not certain whether the cells recovered from vacuolation, as cell division appeared normal and the slightly reduced numbers of vacuolated cells could also be due to the increasing number of cells through normal cell proliferation.

3.4.2 Characteristics of the Vacuolating Factor of *H. contortus* ES Products

Adult *H. contortus* ES preparations were used for all experiments, because Huber *et al.* (2005) and Przemeck *et al.* (2005) had previously shown that adult ES preparations induce more severe vacuolation than larval ES preparations. The vacuolating ability of adult ES preparations was so high that it could be diluted 2-fold (50%) without losing much of this ability, allowing dilution of ES preparations to allow more experiments. Two-fold dilutions were subsequently used for positive control incubations in some experiments described here. However, vacuolating ability was also dependent on the worm batch as slight differences in the vacuolating ability of different batches were noted

The stability of the vacuolating factor was also investigated after different storage conditions. Only long-term (>6 months) storage at -20°C caused notable decreases or loss in activity, whereas storage for less than 4 months at -20°C did not cause any loss in vacuolating ability. Short-term freezing was used for almost all samples and provided a significant facilitation of the experimental procedure. The use of frozen samples allowed replication of experiments and a greater range of experiments to be performed on preparations from the same batch. Short-term (3 and 7d) storage at different temperatures also showed no signs of loss in vacuolating ability. Of particular interest is that storage for 3d at 37°C still showed full vacuolating activity, which suggests that ES products could be effective *in vivo* (normal body temperature of sheep is ~39°C, Noffsinger *et al.*, 1961; daSilva and Minomo, 1995) for a few days.

3.4.2.1 Ammonia and Vacuolation

Ammonia was previously suggested as an active component of ES products, which were able to inhibit acid secretion *in vitro*, as did ammonia itself in parallel testing (Merkelbach *et al.*, 2002). In general, 1mM ammonium chloride significantly reduced acid secretion. Ammonia concentrations in ES preparations ranged from 0.2 to 1mM with final concentrations in the incubation medium of 5 to 100µM. In addition, the ability of

ammonia to induce vacuolation was shown in HeLa cells, by NR uptake assay, in concentration as low as ≥1.56mM (ammonium chloride and ammonium sulfate) (Cover *et al.*, 1991) and in HEp2 cells at 8mM (ammonium chloride) (Mégraud *et al.*, 1992). Therefore, ammonia is a candidate as the vacuolating factor in ES products.

However, the experiments presented here confirm suggestions of Huber *et al.* (2005) and Przemeck *et al.* (2005) that it is very unlikely that ammonia is the origin of the observed vacuolation. A maximum concentration of 4.7µM was measured for ES preparations, even lower than the max. 30µM measured by Huber *et al.* (2005) and Przemeck *et al.* (2005). Furthermore, vacuolation was not enhanced by addition of either 1 or 8mM ammonium chloride to ES preparations in contrast to observations of Przemeck *et al.* (2005), who observed vacuolation enhancing effects for 8mM. Additionally, ammonia itself induced vacuolation in HeLa cells at both concentrations used, but more prominently with 8mM which also resulted in a few larger vacuoles. This is consistent with the results of Cover *et al.* (1991). In contrast, Huber *et al.* (2005) and Przemeck *et al.* (2005) both used 8mM ammonium chloride in control applications on HeLa cells without any vacuolation. The vacuole pattern, comparing ES with VacA induced vacuolation, was also notably different. VacA vacuoles are generated by ammonia which enters endosomal compartments, is protonated to ammonium and then trapped, causing osmotic swelling (see also 1.3.3.7.4). The vacuoles induced by VacA were fewer in number, but mainly significant larger in size than ES-induced vacuoles (Huber *et al.*, 2005), which were similar to the observed ES-induced vacuolation presented here. Additionally, longer incubation periods of 48h with ES products also did not increase the size of the vacuoles.

3.4.2.2 Differences in ES Products from Successive *in vitro* Incubations

The ES products from successive incubations showed a difference in their vacuolating activity. ES products released in the first six hours of the incubation had a high vacuolating ability (70 to 100% of the cells were vacuolated), which was comparable to that of the routine 12h incubations for the generation of ES products. The vacuolating activity dropped markedly for the 6-12h incubation (10 to 20% vacuolated cells). This could be possibly due to some changes in the release of ES products. Incubation conditions and

media are very different from the natural environment of the parasites, which could have changed the amount or composition of the ES products released. This was partly shown by different protein concentrations and different band patterns in the SDS-PAGE of individual incubations, although under native conditions there was no obvious difference between the individual incubations. However, this could also be due to the fact that the separation was not complete. There was diffuse staining at the bottom of the gel in all samples which separated to a similar band pattern in the second dimension as it did in 1D SDS-PAGEs. However, the protein concentration and differences in the band pattern do not necessarily mirror the vacuolating activity. For example, this was demonstrated by comparing the 0-6h with the 12-36h incubate in experiment I. The protein concentration in the 0-6h sample was ~8µg/ml lower, yet the vacuolating activity was higher.

The vacuolating activity then increased again once the worms started to die and degrade. This was in particular demonstrated by the 24-48h incubation in experiment II representing products released exclusively from dead worms, which showed the highest vacuolating ability. It has been shown that cytoskeletal components, which are likely to originate from dying and degrading parasites, induce host responses. These were often subject of vaccine studies and include tropomyosin of *T. colubriformis* (O'Donnell *et al.*, 1989) and *O. volvulus* (Jenkins *et al.*, 1998) and paramyosin of *A. canium* (Hüsken, 2007), *F. hepatica* (Cancela *et al.*, 2004) and *Schistosoma* spp. (Gobert and McManus, 2005). In the latter two species, paramyosin is also expressed on the surface. For the results shown here, it is possible that increased amounts of ES products or other worm constituents, which were also able to induce vacuolation in HeLa cells, were released from dying and degrading worms. Overall, minor differences in the band pattern between incubates with live worms and after they started to die would argue more for the release of ES products that are released after death. However, exact differences can only be determined using more advanced proteomic analysis. In addition, there was no obvious difference in the observed vacuoles. Similarly, it was shown *in vivo* that *T. circumcincta*, which were confined to porous bags, were able to mediate an increase in abomasal pH although worms died within 16h (Simpson *et al.*, 1999). It was argued that the short survival time decreased the amount of ES released and in turn resulted in reduced effects on abomasal secretion. However, it could also be that the abomasal response was reduced because the components from live and dead worms were not released as close to the mucosa as they normally would be.

Another factor that needs to be considered for all *in vitro* experiments involving ES products is the possibility that the cell culture medium was altered due to the incubation with worms during ES preparation. Such alteration could contribute to any affects of ES on cells in subsequent incubations and might be particularly significant in the longer, 24-48h worm incubations. These longer incubations were associated with an increased presence of dead worms. In addition to possible medium degradation, the osmolarity of ES might have been affected by the release of electrolytes from dying tissue. Measurement of electrolyte concentrations and osmolarity of ES preparations and control media could determine whether these changes were significant. In addition, an additional control medium could be used containing ES from other nematode species, like T. *colubriformis* or C. *elegans*. These species do not release a vacuolating agent when prepared under the same conditions and this could clarify whether worm-induced degradation of the medium has an effect on cells.

3.4.2.3 Fractionation of *H. contortus* ES Products

Experiments to fractionate ES products by passing through size exclusion membranes were conducted in an attempt to identify the approximate molecular weight range of active component(s) as a step to facilitate its identification. This fractionation process using Vivaspin ultracentrifugation devices with polyethersulfone membrane was unsuccessful nor could a correct separation be achieved of protein standards. One explanation could be that the major part of the ES products is either sticking together and preventing it from passing though the first filter (>100 or >50kDa) or some ES products block the pores of the filter. ES products spread also over the whole size range in every fraction. This could have been explained by the filter membrane being damaged, but that definitely does not fit with the major part of the ES products found each time in the biggest size fraction. Neither detergent nor reducing agent did improve the separation, a correct separation could not be obtained. Additionally, these chemicals were toxic (as low as 0.01%) to the final cell culture test system.

Alternatively, other methods such as gelfiltration columns could be used, but the dilution of the sample might be a problem for further testing of the sample on cells, possibly losing

vacuolating ability. Another possibility could be the elution of bands from ES preparations, which was run under native conditions, with testing on cells afterwards. Although, for this option the gel conditions have to be optimised first as it is likely that the samples did not separate completely (see also 3.4.2.2). In addition, it could be possible that the eluted sample would contain chemical residues which are not compatible with cell viability.

3.4.2.4 Do Lipids Play a Role in Vacuolation?

Prostaglandins play a role in many biological processes, including host-parasite interactions and are synthesised by both host and a number of parasites, including nematodes (Hadás *et al.*, 1998; Daugschies and Joachim, 2000; Kubata *et al.*, 2007). Prostaglandins have been reported to play a role in vacuole formation in protozoa (Prusch *et al.*, 1989; Figarella *et al.*, 2005; 2006) and neuroblastoma cells as part of the cell degeneration process induced by prostaglandins (Prasad *et al.*, 1998). However, it is not certain whether prostaglandins are potential vacuolating factors for parietal cells observed in abomasal parasitism. Therefore, the existence of lipid components in adult *H. contortus* ES products was investigated and their ability to induce vacuolation in HeLa cells.

Lipids, but not prostaglandins, were detected by SDS-PAGE and TLC. The concentrations in ES products appear to be very low as lipid detection was possible only in concentrated samples (~100x concentration or freeze dried sample). Prostaglandin standards [0.5µg/ml] did not induce any vacuolation in HeLa or AGS cells, nor did the extracted lipids separated by TLC (above background vacuolation). The background vacuolation was probably due to chemical residues in the samples, shown by the control scrapings from regions of the TLC plate devoid of sample. Taken together, these results demonstrate that it is very unlikely that the lipid compounds in *H. contortus* ES products are responsible for vacuole formation in HeLa cells. Furthermore, as prostaglandin standards were not able to induce vacuolation in HeLa or AGS cells, it is also very unlikely that host prostaglandins, as part of the inflammatory response, play a role in parietal cell vacuolation during abomasal parasitism.

3.4.2.5 Is the Vacuolating Factor of *H. contortus* ES Products a Protein?

Experiments were conducted to further characterise the vacuolating factor(s). These included the examination of the sensitivity of ES products to heat and acid. Experiments involving heating for 30min at 60°C, 75°C and 100°C documented the heat sensitivity of the vacuolating factor(s). As a slight increase in vacuolation, compared with a typical control application, was observed in control cells after the incubation with samples generated in CEM, additional experiments were undertaken with samples generated in PBS to exclude any factor that may have arisen from heating the medium. These experiments demonstrated a decrease in vacuolating activity of ES preparations with increasing temperature with a complete loss of vacuolating ability after heating to 100°C.

Incubations of ES preparations at pH 2 for 30min showed that the vacuolating factor(s) was acid sensitive, as the vacuolating activity was significantly reduced in ES preparations. The slight increase in vacuolation in the control cells could be potentially caused by slight increases in the osmolarity (max. +31.9mOsM) of the sample after the acid-treatment. In patients with intracerebral hemorrhage, agents which reduce intracerebral osmotic pressure were shown to be effective at only 10mOsM (Kalita *et al.*, 2003).

Although some proteins or peptides are heat or acid stable (Grütter *et al.*, 1988; Ingebritsen, 1989; Jacobsen and Shaw, 1989), together these experiments demonstrate that it is very likely that the vacuolating factor(s) is a protein, as proteins usually denature at extreme conditions like high temperature or low pH. The vacuolating activity being minimised or abolished by increasing temperatures and low pH indicate that this factor(s) is probably denatured, impairing its function. However, as already discussed (3.4.1) parietal cell vacuolation *in vivo* appears to be different and other factors may be involved, or due to the different environment in the abomasum (compared with *in vitro* incubation conditions) the ES composition may be different as well. ES products *in vivo* are at least partly exposed to lower pH, although the pH in close vicinity to the parasites may be different from the overall abomasal pH.

Experiments with ES preparations that had been digested by proteinase K or inhibited by protease and phosphatase inhibitor cocktails could have further confirmed the proteinaceous origin, or even more the protein class. Unfortunately, all treatments were detrimental to the HeLa or AGS cell test system. With proteinase K, the cells died at all concentrations used, as well as after pre-incubation with proteinase K, which should have autodigested the enzyme. After treatment with phosphatase inhibitor cocktail, most of the cells died using the recommended dosage and even lower concentrations. Protease inhibitor cocktail treatment did not kill the cells, but at the recommended concentration as well as lower concentrations, cells were already vacuolated. Further experiments with single inhibitors (e.g. cysteine protease inhibitor, serine protease inhibitor) might be an alternative. 4-(2-Aminoethyl)-benzenesulfonyl fluoride (AEBSF, a serine protease inhibitor), which is stated to have a relatively low toxicity towards eucaryotic cells (supplier data sheet, Roche), appeared to have no detrimental effect itself on CaCo-2 cells at low concentrations of 0.25mM (unpublished observations, L. R. Walker).

In summary, the experiments described in this chapter revealed some further characteristics of the vacuolation as well as the vacuolating factor: vacuoles were observed as early as 1h after application of ES preparations; vacuolation was partly reversible, but recovery of the cells was slow; products of dead and degrading worms were able to induce similar vacuoles as do routine ES preparations; lipids were detected in ES preparations, but neither lipids nor prostaglandins appear to play a role in vacuolation and the vacuolating factor is likely to be a protein. However, the identification of the vacuolating factor(s) in ES products was not possible. Identification of the vacuolating factor(s) *in vitro*, which may not be the same *in vivo* or additional factors may be involved *in vivo*, is probably difficult to achieve.

Chapter 4

EFFECT OF *H. CONTORTUS* ES PRODUCTS *IN VITRO*: CELL DETACHMENT

4.1 Introduction

ES products typically cause vacuolation *in vitro*, visualised by NR uptake (chapter 3). However, using the NR uptake assay to examine ES-induced vacuolation in HeLa cells, reduced NR uptake was observed after application of ES products of L_3 and adult worms of *T. circumcincta* or *H. contortus*. This occurred at greater relative ES concentrations, which were derived from higher parasite densities or longer incubation periods for the generation of ES preparations (Przemeck, 2003; Przemeck *et al.*, 2005). A parallel microscopic study revealed marked detachment of cells from the coverslip, which led to the suggestion that the decreased NR uptake was due to decreased cell numbers (Przemeck *et al.*, 2005). Huber *et al.* (2005) also observed an increased rate of cell detachment in cells treated with ES products from L_3 and adult *H. contortus* or *H. pylori* outer membrane vesicles (OMV). Decreased cell numbers after exposure to *H. pylori* supernatants *in vitro* had previously been reported (Cover *et al.*, 1991), as well as ulceration and gastric lesions *in vivo* (Telford *et al.*,

1994), and later attributed to VacA induced apoptosis (Kuck *et al.*, 2001; Cover *et al.*, 2003). Furthermore, VacA bound to several cell surface components, one of which is receptor tyrosine phosphatase β (RPTPβ) (Cover and Blanke, 2005). Binding of VacA to RPTPβ resulted in detachment of primary murine gastric epithelilal cells and tissue damage *in vivo* only occurred in mice which possess the receptor (Fujikawa *et al.*, 2003).

As described in 1.3.3 and 3.1, several of the released ES products are either known to or suggested to have detrimental effects on abomasal tissue and cells. Possible candidates that could be involved in tissue damage, as well as the observed cell detachment after ES exposure *in vitro*, include the proteases, phosphatase, enolase, calreticulin and galectins. Proteases may play a role by degrading the extracellular matrix (Rhoads and Fetterer, 1996). Phosphatase may interfere with host intracellular signalling pathways, resulting in the disruption of the cytoskeleton as has been demonstrated for bacterial and protozoan phosphatase (Hueck, 1998, Aguirre-García *et al.*, 2003; Anaya-Ruiz *et al.*, 2003). Enolase could be involved by interfering with the plasminogen/plasmin system resulting in plasmin-mediated proteolysis such as degradation of extracellular matrix (Jolodar *et al.*, 2003; Marcilla *et al.*, 2007). Calreticulin could also play a role in cell detachment because it is able to complex with integrins and thereby mediate thrombospondin-induced focal adhesion disassembly (Johnson *et al.*, 2001). The calcium binding properties of calreticulin may also play a role, as Ca^{2+} is an important factor in the adhesion process. Galectins, which were identified as eosinophil chemotractants in *H. contortus* ES products (Turner *et al.*, 2008), could also be involved. In this context, particularly galectin-8 was shown to bind to integrins and inhibit adhesion (Hadari *et al.*, 2000; Zick *et al.*, 2004).

The aim of the experiments described in this chapter was the characterisation of cell detachment, which has been previously observed (Huber *et al.*, 2005; Przemeck *et al.*, 2005), by staining of the actin cytoskeleton and its quantification using an assay, which measures fluorescence of DNA to determine cell numbers.

4.2 Materials and Methods

4.2.1 ES Preparations of Adult *H. contortus*

Adult worms of *H. contortus* were obtained 21d after the infection of the sheep as described in Appendix I. Worms were incubated for 12h in CEM or F12-Hams in 15ml and 50ml tubes in an incubator in an atmosphere containing 5% CO_2 and 95% humidified air at 37°C. CEM and F12-Hams were also incubated under the same conditions to serve as negative controls. The supernatants of the ES preparations and the negative controls (CEM or F12-Hams) were sterile filtered through 0.2µm filters into new tubes. The pH of each preparation was readjusted to 7.4 if necessary. The preparations were stored at 4°C if being used immediately or frozen at -20°C in small aliquots, which were used only once (used for the assay determining cell numbers).

4.2.2 Cell Culture

HeLa cells, which had been passaged between 9 and 15 times (p9 to p15), and AGS cells passaged 45 times (p45) were used for experiments. Cells were grown on coverslips for staining the actin cytoskeleton or on 24 and 96 well plates for the assay determining cell numbers. Cell culture techniques for both cell lines are described in detail in Appendix II.

4.2.3 Incubations with ES Preparations on Cells

To test the effects of ES preparations on cells, the culture medium of the cells (HeLa or AGS) was discarded and replaced with either ES preparations or negative control and incubated for 24h in an incubator in an atmosphere containing 5% CO_2 and 95% humidified air at 37°C. HeLa cells were also incubated for 48h under similar conditions.

4.2.4 Actin Staining Using Alexa Fluor® Phalloidin

The actin cytoskeleton was stained using Alexa Fluor® Phalloidin, following a protocol slightly modified from the supplier's manual. After incubation, the supernatant (ES preparation or control) in the petri dishes (2ml) was discarded and the cells were washed once with PBS (500µl) before they were fixed with 4% paraformaldehyde (Appendix II) for 30min. After washing twice with PBS, cells were permeabilised with 0.1 or 0.2% Triton-X-100 for 15min. Another wash with PBS was followed by 1h incubation with the filamentous actin stain Alexa Fluor® Phalloidin as a 1:100 dilution (Appendix II; blue laser/488 excitation with emission maximum of ~530nm/green fluorescence) and DNA stain Hoechst 33258 at a concentration of 15µg/ml (Appendix II; UV laser/405nm excitation with emission maximum at ~460nm/blue fluorescence). Cells were incubated in a mixture of both stains diluted in PBS. After a final wash with PBS, cells were examined using an inverted confocal microscope (40x or 60x/water immersion objective). All images were processed with Adobe Photoshop.

Following Alexa Fluor® Phalloidin and Hoechst 33258 staining, two of the incubations of HeLa cells with ES preparation or negative control for each 24h or 48h were also examined as a single blind study.

4.2.5 Determination of Cell Numbers Using the CyQUANT® NF Assay

For the assay using CyQUANT® NF, HeLa cells were counted in a hemocytometer (Neubauer counting chamber) and seeded at 10,000 and 15,000 cells/well (in 500µl CEM) on a 24 well plate and incubated for 6h in an incubator in an atmosphere containing 5% CO_2 and 95% humidified air at 37°C to allow adhesion. The assay was also performed using 96 well plates and HeLa cells at 50,000 and 100,000 cells/well and AGS cells at 80,000 and 100,000 cells/well were used (in 100µl either CEM for HeLa cells or F12-Hams for AGS cells). Medium of the cells was discarded and replaced for 24h by different preparations (100µl for the 96 well plate and 500µl for the 24 well plate) of ES and control

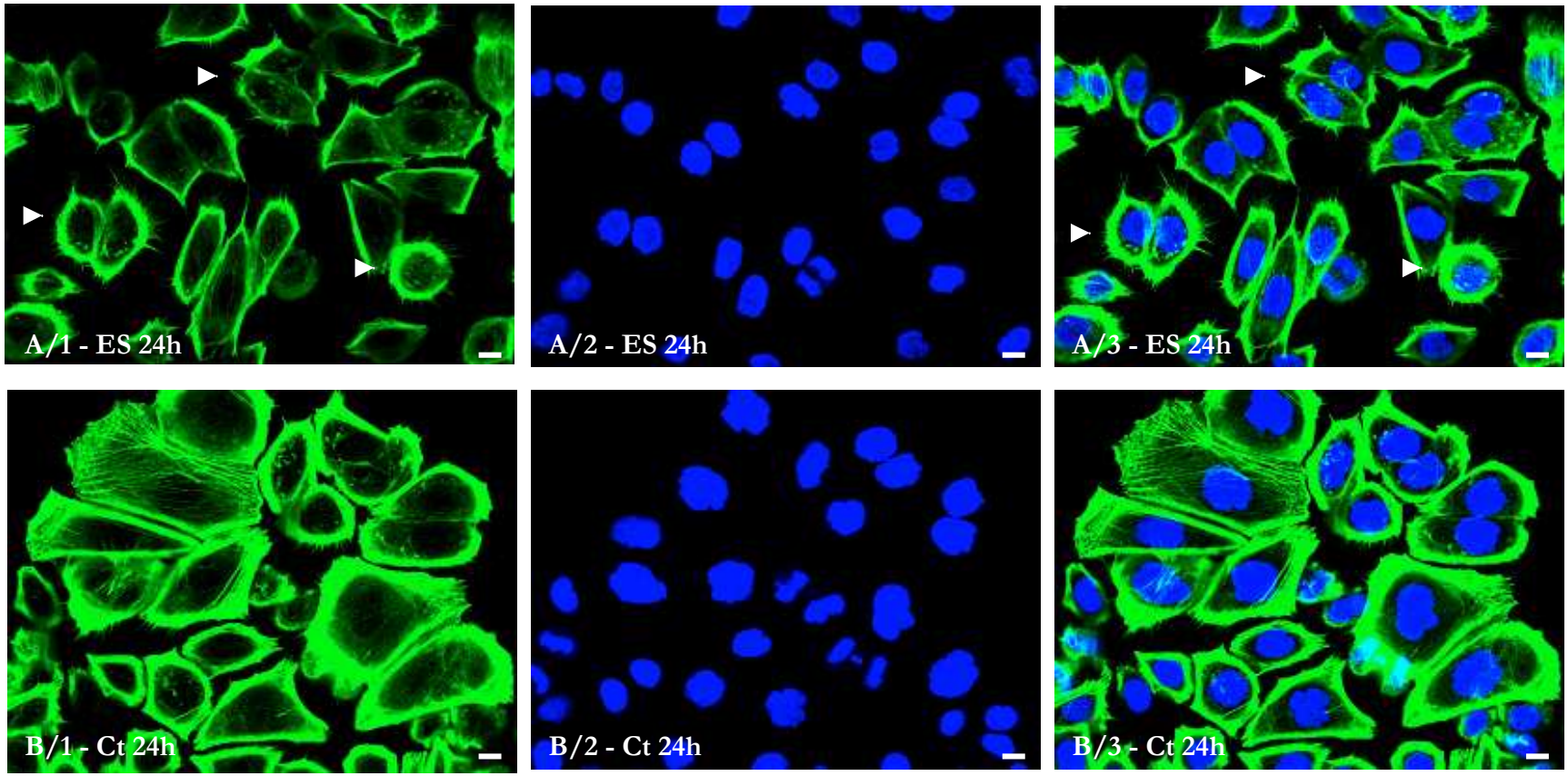

Figure 4.3: ES-induced detachment of AGS cells 24h after exposure to *H. contortus* ES products. A. and B. Fluorescent imaging. A. ES incubation 24h, A/1 Actin cytoskeleton (Alexa Fluor® Phalloidin 488; 488nm excitation), A/2 Nuclei (Hoechst 33258; 405nm exciation), A/3 Merge A/1 and A/2, B. Control incubation 24h (F12-Hams), B/1 Actin cytoskeleton, B/2 Nuclei, B/3 Merge B/1 and B/2. Some of the detaching cells are marked by arrowheads. Original magnification 600x, bars 10μm.

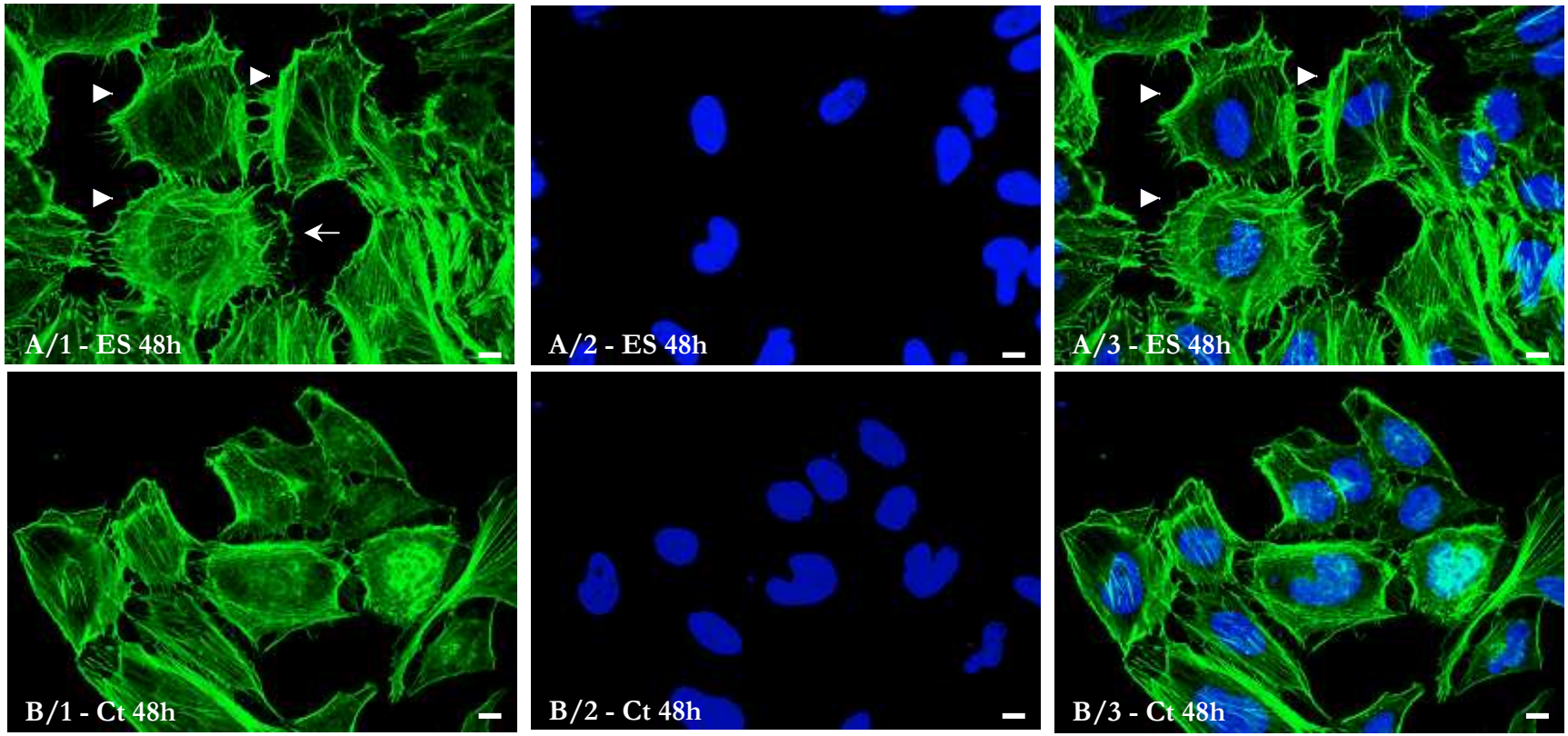

Figure 4.2: ES-induced detachment of HeLa cells 48h after exposure to *H. contortus* ES products. A. and B. Fluorescent imaging. A. ES incubation 48h, A/1 Actin cytoskeleton (Alexa Fluor® Phalloidin 488; 488nm excitation), A/2 Nuclei (Hoechst 33258; 405nm excitation), A/3 Merge A/1 and A/2, B. Control incubation 48h (CEM), B/1 Actin cytoskeleton, B/2 Nuclei, B/3 Merge B/1 and B/3. Some of the detaching cells are marked by arrowheads, also note the actin "footprint" that is left behind from the cell in the centre in A (arrow). Original magnification 600x, bars 10µm.

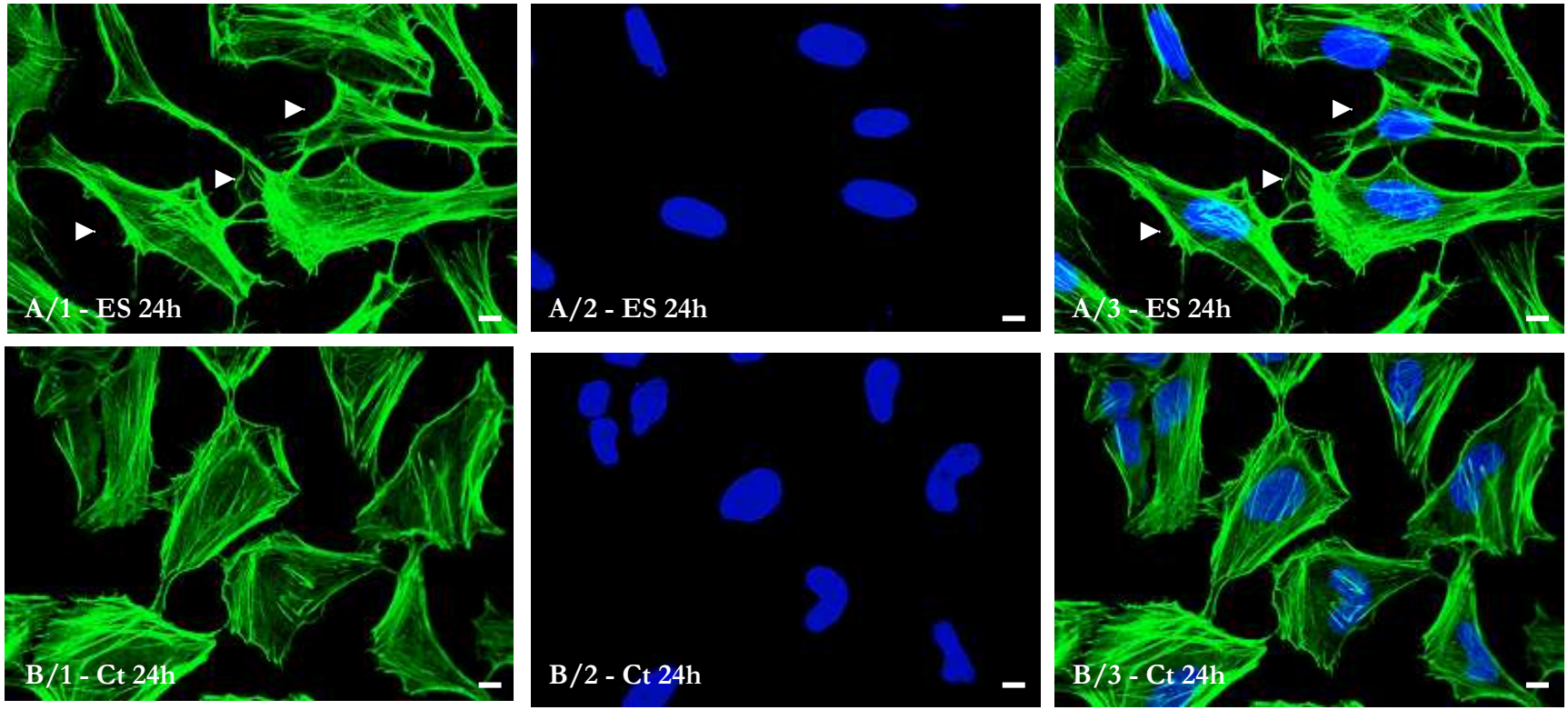

Figure 4.1: ES-induced detachment of HeLa cells 24h after exposure to *H. contortus* ES products. A. and B. Fluorescent imaging. A. ES incubation 24h, A/1 Actin cytoskeleton (Alexa Fluor® Phalloidin 488; 488nm excitation), A/2 Nuclei (Hoechst 33258; 405nm excitation), A/3 Merge A/1 and A/2, B. Control incubation 24h (CEM), B/1 Actin cytoskeleton, B/2 Nuclei, B/3 Merge B/1 and B/2 Some of the detaching cells are marked by arrowheads. Original magnification 600x, bars 10µm.

media. Wells with no cells added were used as a negative control for the assay. All applications were set up in triplicate.

The CyQUANT® NF assay is based on measuring the fluorescence of cellular DNA to determine cell numbers. DNA dye binding is achieved by using the dye binding solution, which also contains a plasma membrane permeabilisation reagent. The assay was used following the suppliers protocol. Briefly, the different preparations of ES and control media were removed from the cells and replaced by dye binding solution: 50µl/well for the 96 well plate or 250µl/well for the 24 well plate. The plate was incubated for 60min in an incubator in an atmosphere containing 5% CO_2 and 95% humidified air at 37°C in the dark before fluorescence of the DNA was read in a plate reader (Wallac 1420 multilabel counter VICTOR^3, Perkin Elmer) with excitation at 485nm and emission detection at 530nm.

4.2.6 Statistical Analysis

Data for the quantification of cell detachment are presented as mean ± SEM. Two-way ANOVA with Bonferroni *post hoc* tests was used to compare cell numbers after application of control media or ES preparations.

4.3 Results

4.3.1 Staining of the Actin Cytoskeleton

H. contortus ES products applied for 24h to HeLa or AGS cells induced detachment in some cells after the application of ES preparations compared with the controls. 24h incubations of ES preparations and control media on HeLa cells were performed five times with three different ES and control batches and 48h incubations three times with two different batches. 24h incubations on AGS cells were performed three times with the same ES and control batch. Results of the detachment study are shown in Figures 4.1 to 4.3. Staining of

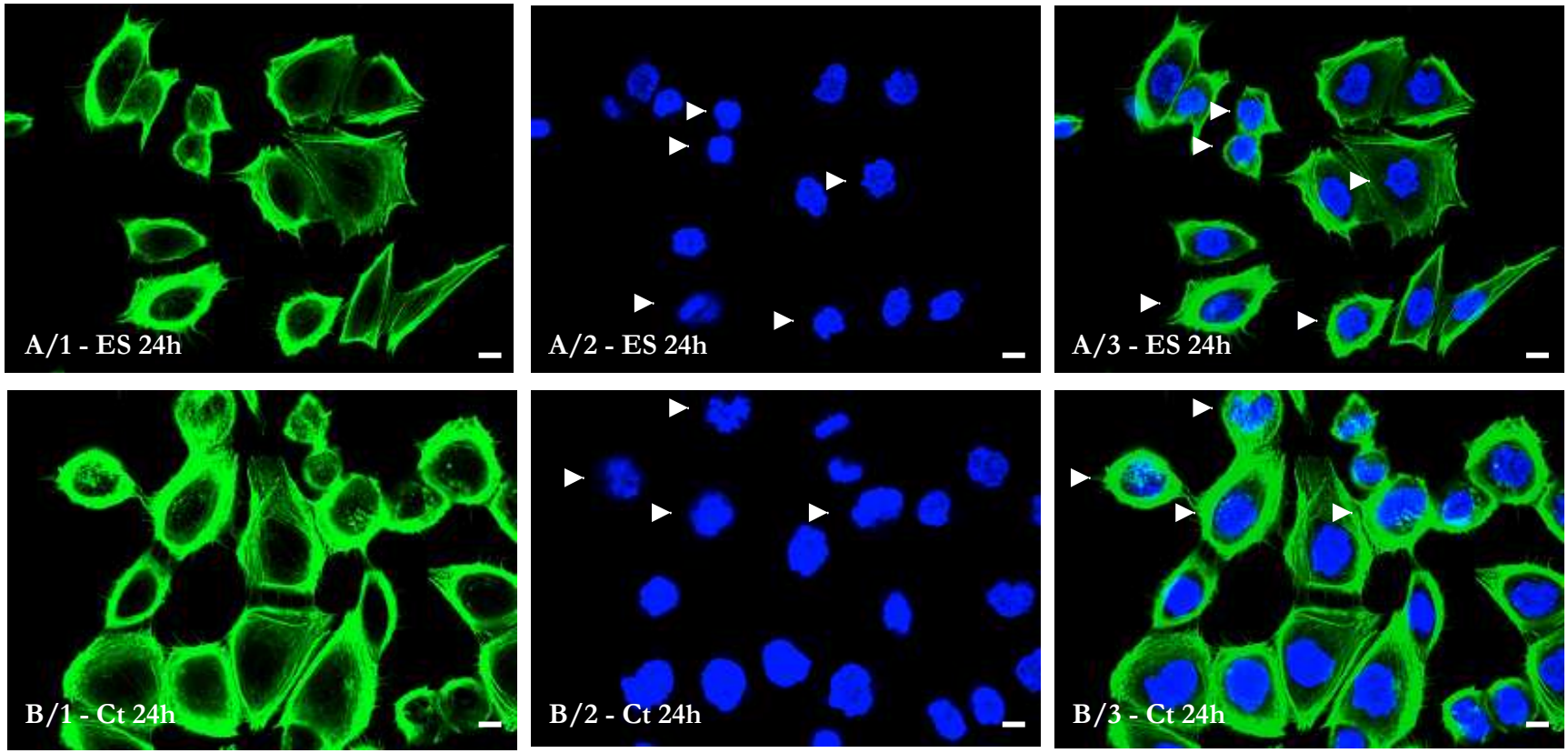

Figure 4.7: ES-induced detachment of AGS cells 24h after exposure to *H. contortus* ES products - apoptotic processes. Fluorescent imaging. A. ES incubation 24h, A/1 Actin cytoskeleton (Alexa Fluor® Phalloidin 488; 488nm excitation), A/2 Nuclei (Hoechst 33258; UV/405nm excitation), A/3 Merge A/1 and A/2, B. Control incubation 24h (F12-Hams), B/1 Actin cytoskeleton, B/2 Nuclei, B/3 Merge B/1 and B/2. Original magnification 600x, bars 10µm.

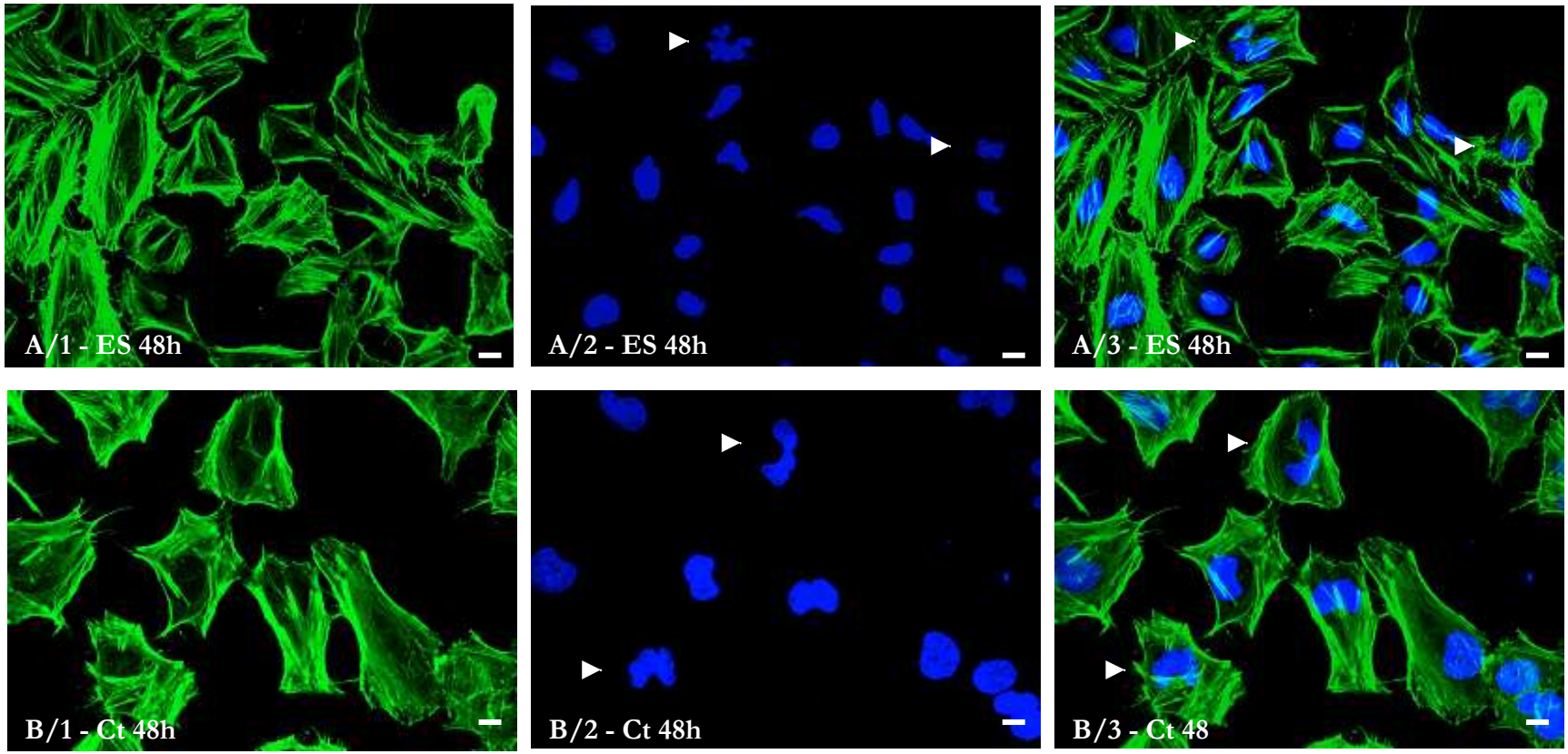

Figure 4.6: ES-induced detachment of HeLa cells 48h after exposure to *H. contortus* ES products - apoptotic processes. A. and B. Fluorescent imaging. A. ES incubation 48h, A/1 Actin cytoskeleton (Alexa Fluor® Phalloidin 488; 488nm excitation), A/2 Nuclei (Hoechst 33258; 405nm exciation), A/3 Merge A/1 and A/2, B. Control incubation 48h (CEM), B/1 Actin cytoskeleton, B/2 Nuclei, B/3 Merge B/1 and B/2. A. Original magnification 400x, bars 20µm, B. Original magnification 600x, bars 10µm.

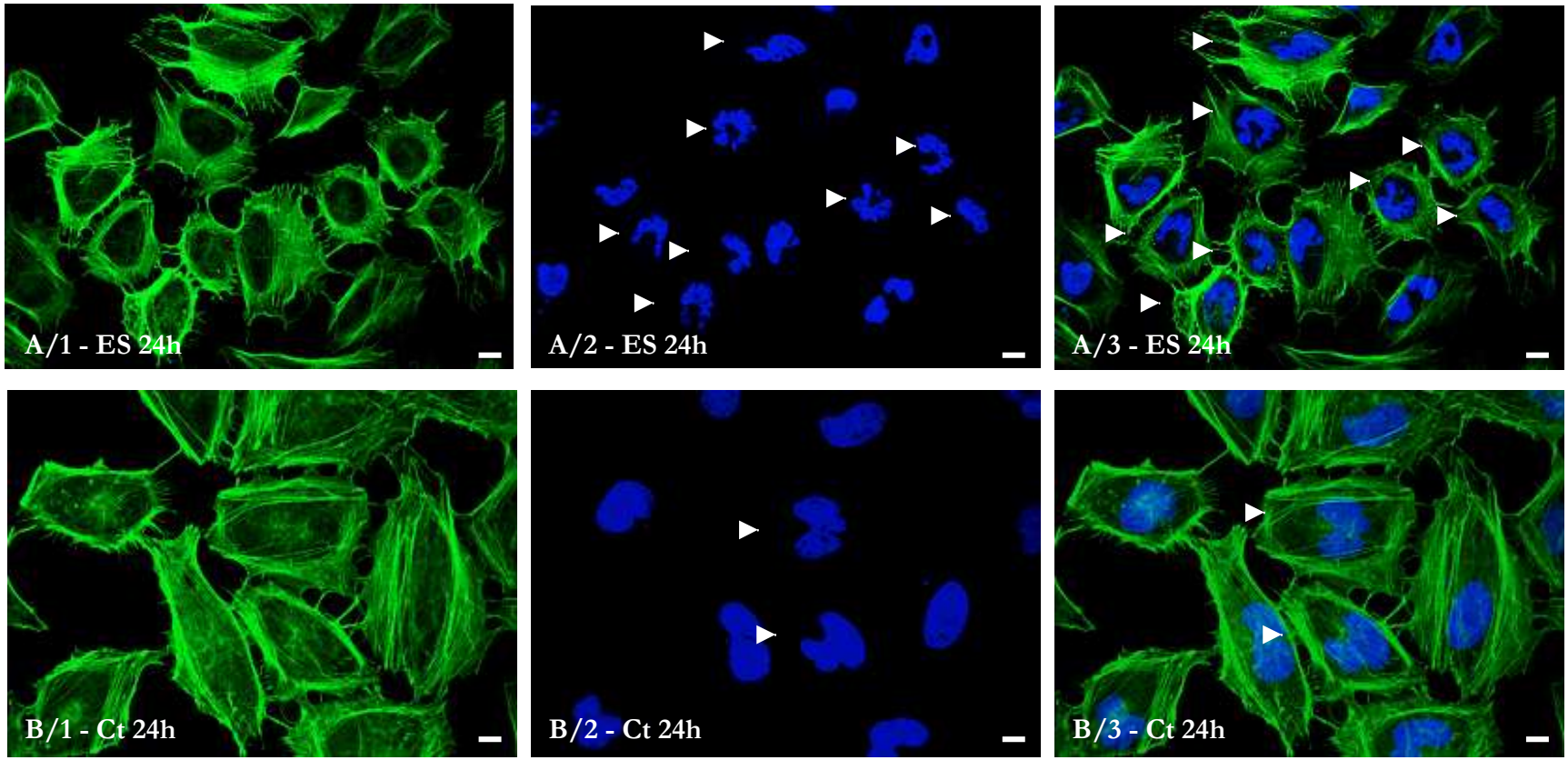

Figure 4.5: ES-induced detachment of HeLa cells 24h after exposure to *H. contortus* ES products - apoptotic processes. A. and B. Fluorescent imaging. A. ES incubation 24h, A/1 Actin cytoskeleton (Alexa Fluor® Phalloidin 488; 488nm exciation), A/2 Nuclei (Hoechst 33258; 405nm exciation), A/3 Merge A/1 and A/2, B. Control incubation 24h (CEM), B/1 Actin cytoskeleton, B/2 Nuclei, B/3 Merge B/1 and B/2. A. Original magnification 400x, bars 20µm, B. Original magnification 600x, bars 10µm.

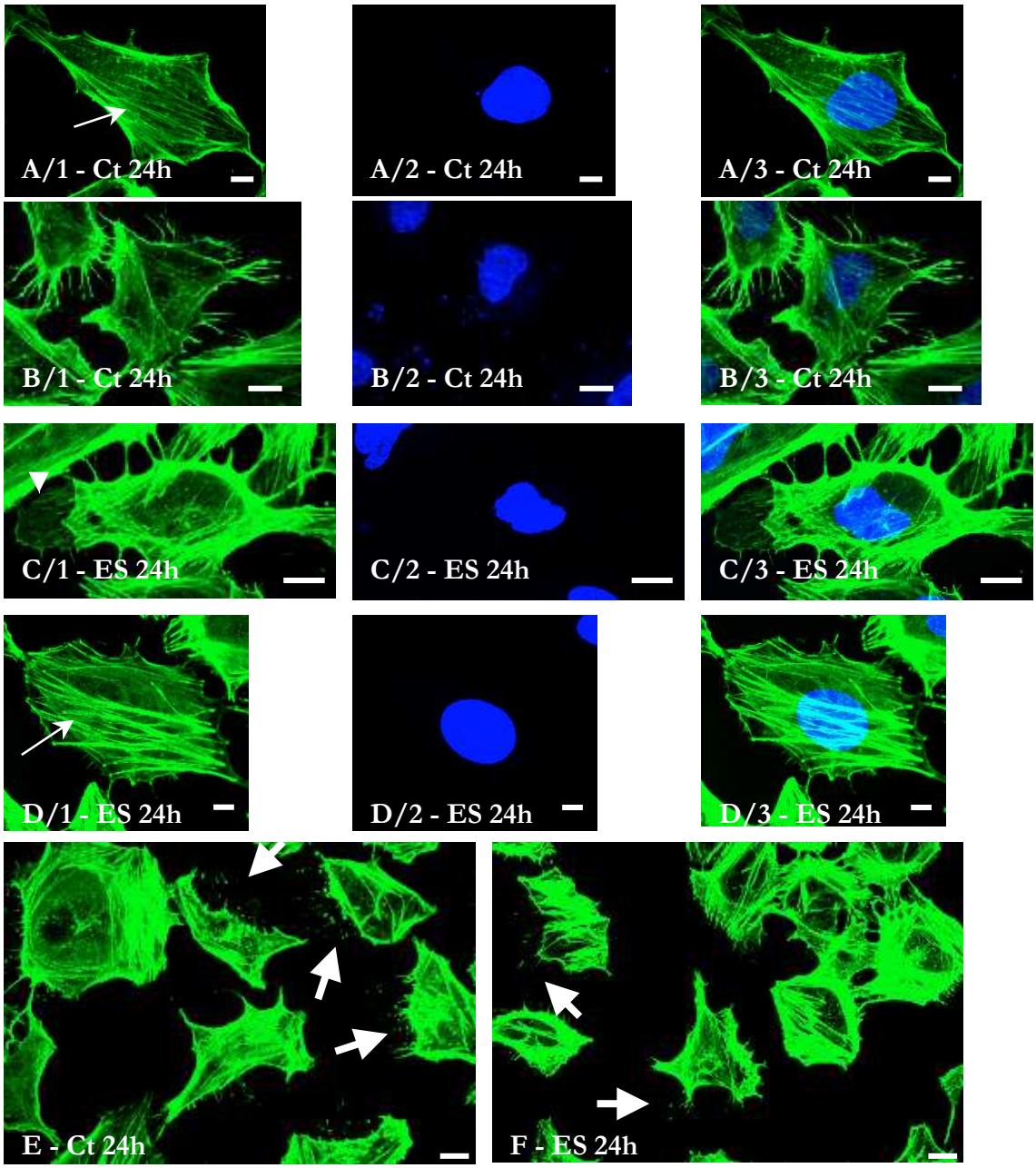

Figure 4.4: Detachment of HeLa cells - Control incubations vs. exposure to *H. contortus* ES. Fluorescent imaging. A/1 to A/3 Control incubation 24h (CEM) - normal cell appearance, A/1 Actin cytoskeleton (Alexa Fluor® Phalloidin 488; 488nm excitation), A/2 Nuclei (Hoechst 33258; 405nm excitation), A/3 Merge, B/1 to B/3 Control incubation 24h (CEM) - detaching cell, B/1 Actin cytoskeleton, B/2 Nuclei, B/3 Merge, C/1 to C/3 ES incubation 24h - detaching cell, C/1 Actin cytoskeleton, C/2 Nuclei, C/3 Merge, D/1 to D/3 ES incubation 24h - normal cell appearance, D/1 Actin cytoskeleton, D/2 Nuclei, D/3 Merge. E. Control incubation 24h (CEM), actin cytoskeleton, F. ES incubation 24h. Stressfibres are marked with arrows, also note the probably temporary actin "footprint" that is left behind in C/1 (arrowhead) and the "footprints" in E. and F. (bold arrows). Original magnification 600x, bars 10µm.

the actin cytoskeleton resulted in similar patterns in most cells, including stress fibres, but this was also dependent on the cell section photographed (Figure 4.4 A/1 and D/1). This pattern of actin staining was different in detaching cells, particularly in cells which appeared to be at more advanced stages of detachment, containing fewer or less pronounced stress fibres, for example comparing the cells in Figure 4.4 A. and B. Cellular rounding increased in detaching cells and resulted in most cases in fibrillar actin structures on the cell edges. In some cases this appeared as actin "footprints" (Figure 4.4 C/1, E. and F.). In addition, increased numbers of degenerating nuclei and apoptotic bodies were seen in ES-exposed cells, HeLa and AGS, compared with the control cells (Figures 4.5 to 4.7).

However, for all applications, the difference between control medium and ES preparation was not always obvious. More cells of both, HeLa or AGS, were detaching in some applications of the ES preparations compared with the controls, but the single blind study of a total of eight applications (four control and four ES) highlighted the difficulty in determining the state of detachment. Only half of the applications were assigned to the right group, ES or control. It was also not possible to identify a difference between 24 and 48h applications as to whether longer incubations caused more cell detachment compared with 24h ES applications. Figure 4.4 shows the problem of identifying the right application group showing strongly attached and detaching cells of both ES-exposed and control cells.

4.3.2 Quantification of Detachment

H. contortus ES products applied to HeLa and AGS cells in order to quantitate cell detachment due to ES products using the CyQUANT® NF assay (4.2.5) showed a trend that cell numbers were generally decreased after ES-exposure compared with control medium, however, the overall variation between wells was high.

HeLa and AGS cells were incubated with different batches of ES and compared with cells exposed to corresponding control medium, with the number of cells per well being measured after 24h exposure. The assay was first run several times using 96 well plates, but these results were all unsatisfactory, showing very high variations between wells and/or

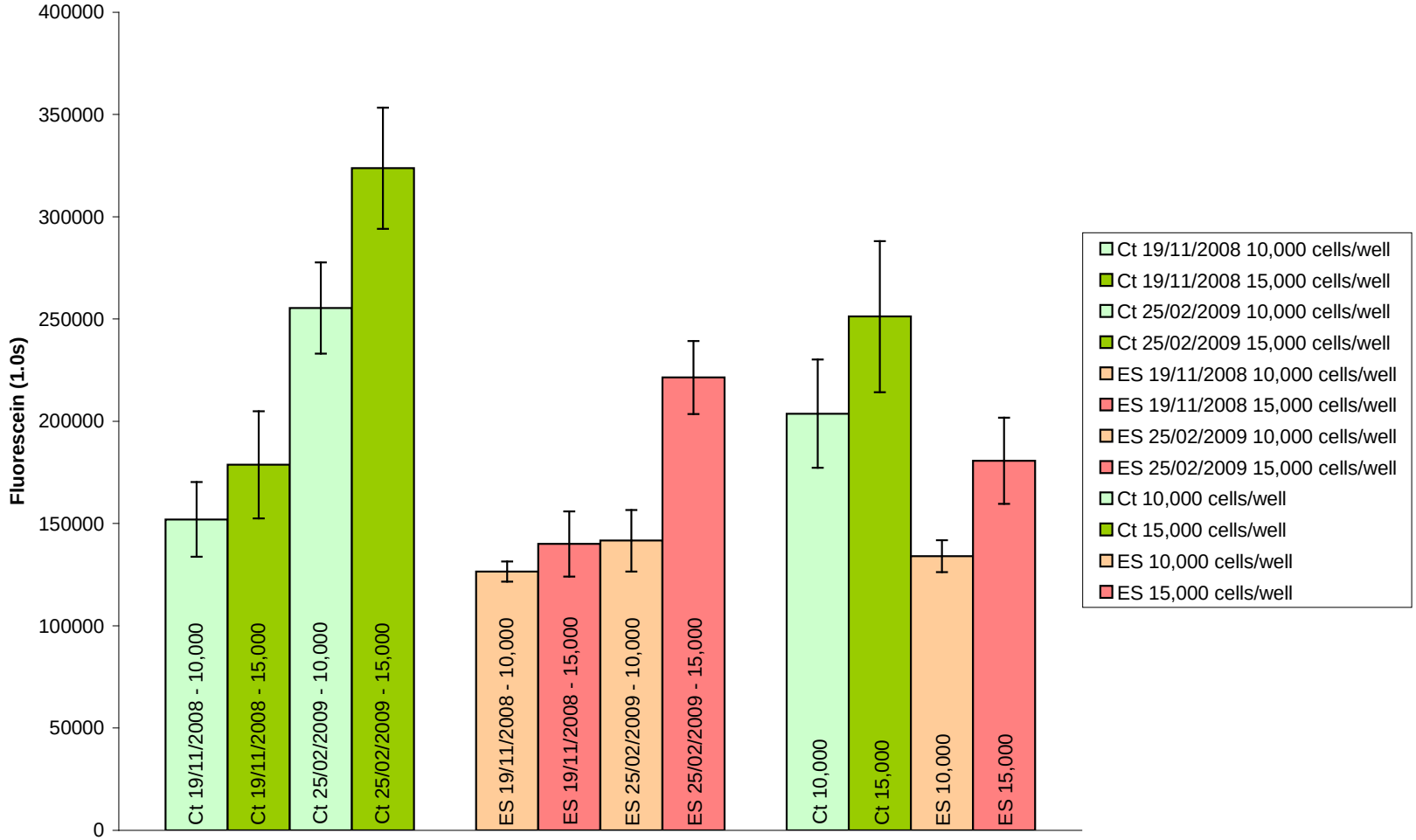

Figure 4.8: Cell Detachment due to exposure to *H. contortus* ES products - Quantification. Two different batches of ES (19/11/2008 and 25/02/2009) were tested and the number of cells per well determined after 24h exposure by measuring the fluorescence of cellular DNA.

samples. To reduce this inherent variation the assay was performed instead using 24 well plates. For the final assay, two different batches of ES preparation and control media were used. For both batches, wells containing ES preparations had comparably lower fluorescence values than wells which contained the corresponding control sample; the difference was statistically significant only for batch 25/02/2009 ($p<0.05$). Overall, comparison between ES-treated and control samples showed a similar trend: cell numbers (fluorescence) were decreased after exposure to ES preparations. For most applications, variation between wells containing the same number of cells was high, for example comparing wells containing 10,000 cells exposed to control samples from the two different batches. These results are shown in Figure 4.8.

4.4 Discussion

Experiments were undertaken to characterise and quantify cell detachment in response to adult *H. contortus* ES products. In general, it appeared that the number of cells detaching from the coverslip was increased in some wells after the application of ES preparations, as was previously reported by Huber *et al.*, 2005 and Przemeck *et al.*, 2005. However, it was difficult to determine the state of detachment, which was particularly highlighted by the single blind study, where only half of the applications were assigned to the right group. This can be explained by the fact that cell detachment is not an all or none effect and cells that were beginning to detach may not have been recognised.

Results of the CyQUANT® NF assay, determining cell numbers, confirmed the observations from the cytoskeletal staining. However, the variation between wells was high, even when comparing wells containing either the same cell number and sample or after application of different batches of control media or ES preparations to the same cell number/well. This problem was slightly reduced by using 24 well instead of 96 well plates. Using a different assay method, where the cell number in each well could be determined before and after the application, could reduce the inherent variability and improve this quantification.

Similar patterns of the actin cytoskeleton were observed in most cells, including stress fibres, but this pattern of actin staining was notably different in detaching cells, particularly in cells with advanced detachment. These detaching cells contained fewer or less pronounced stress fibres, suggesting the degradation of actin fibres. This can be seen by comparing the cells in Figure 4.4 A. and B. The actin rearrangements led to cellular rounding (also comparable to the cells at the top in Figure 1.23) until the cells detached from the coverslip. The contraction of the cytoskeleton in detaching cells resulted in most cases in fibrillar actin structures on the cell edges. In some cases this appeared as actin "footprints". These might be temporary until the cell completely detached (Figure 4.1 G. and 4.3 C.) as generally no actin staining was observed in areas without cells, but in rare cases it appeared that some cell material was permanently left behind (Figure 4.3 E. and F.). Permanent "footprints" have been shown for a number of cell lines, mainly in migrating cells leaving a migration track (Kirfel *et al.*, 2004), but were also detected in detaching rat liver epithelial cells (Britch and Allen, 1980) and mesangial cells (Hartner *et al.*, 1999). Antibody staining for integrins and/or some of the focal adhesion plaque proteins could further clarify whether cell material is left behind in detaching HeLa and AGS cells in response to ES products and its origin.

The ability to alter the actin cytoskeleton, by a yet unidentified factor, was also shown for mermithid nematodes (Li *et al.*, 2009), although these alterations of the cytoskeleton appear to be different from the observed ES-induced alterations. *Ovomermis sinensis* changed the spreading behaviour of hemocytes of its host *Helicoverpa armigera* (cotton bollworm) to a more round morphology with less organised actin cytoskeleton. In addition, "hot spots" of intense actin staining were detected. This was proposed to be part of an active mechanism by *O. sinensis* to suppress the cellular immune response and avoid encapsulation in the host.

The increased number of degenerating nuclei and apoptotic bodies after exposure to ES products (Figure 4.5 to 4.7) suggests that the increased rate of cell detachment could be a result of an increased rate of apoptosis. Similar observations have been made for *H. pylori*, which was shown to induce apoptosis in AGS cells (Jones, N. L. *et al.*, 1999; Kuck *et al.*, 2001; Cover *et al.*, 2003). Frisch and Francis (1994) demonstrated that apoptosis could also be induced by the disruption of epithelial cell-matrix interactions, which was termed anoikis. This could also be a possible mechanism for the observed parietal cell loss during

abomasal parasitism (Scott *et al.*, 1998a; 2000; Przemeck, 2003). Cysteine proteases in adult *H. contortus* ES products and live L_4 and adult worms were shown to degrade a model extracellular matrix consisting of glycoproteins, elastin and collagen (Rhoads and Fetterer, 1996). In addition, serine and metalloproteases of *T. vitrinus* ES products were able to degrade the extracellular matrix glycoprotein fibronectin (Maclennan *et al.*, 1997) and the serine protease Sat from uropathogenic *E. coli*, which was shown to induce vacuolation (see 3.1), was also able to detach different cell lines (Guyer *et al.*, 2000). These proteases could also be responsible for the observed *in vitro* cell detachment, acting in a similar manner to trypsin, which is commonly used in cell culture to detach adherent cells. Recently, Toubarro *et al.* (2009) demonstrated that a serine protease in the ES products from the parasitic stage of *Steinernema carpocapsae*, an insect nematode, was able to degrade extracellular matrix proteins and also induced apoptosis. Overall, it is not clear whether cell detachment is a result of apoptosis or if apoptosis follows cell detachment (anoikis). Experiments with apoptosis markers could clarify this, but the relative contribution of apoptosis followed by detachment versus anoikis may be difficult to assess. Furthermore, the use of protease inhibitors could determine whether proteases play a role in the observed cell detachment, but possible cell toxicity of the inhibitor(s) needs to be considered (see also 3.4.2.5). However, it seems more likely that cells detach due to apoptosis because of the increase in degenerating nuclei/apoptotic bodies after ES exposure and, in addition, the process of cell detachment/loss of cells from the coverslip appeared to be slow compared with cell vacuolation, where ~90% of the cells were affected after just 2h exposure (3.3.4). Similarly, if proteases are involved, acting in a similar manner to trypsin, more rapid detachment would be expected, although it may be dependent on the concentration of the proteases.

ES products may interfere with the host proteolytic plasminogen/plasmin system *in vivo*. Enolase has been detected in ES products of several parasites (reviewed in 1.3.3.4) as well as on the surface of bacteria, both pathogenic and normal gastro-intestinal microbiota (Bergmann *et al.*, 2001; Hurmalainen *et al.*, 2007; Esgleas *et al.*, 2008). The glycolytic enzyme enolase has additional functions, one of which is binding to plasminogen (Pancholi, 2001). Plasminogen is mainly produced in the liver (Raum *et al.*, 1980), but was recently also found to be expressed in several other tissues including the gut (Zhang *et al.*, 2002). After conversion to plasmin by its activators, tissue type (tPA) and urokinase plasminogen

activator (uPA), it plays a central role in fibrinolysis (Parry *et al.*, 2000) and degradation of the extracellular matrix (Vassalli *et al.*, 1991). Furthermore, it was demonstrated that plasmin activates several matrix metalloproteases (MMP), each degrading different matrix proteins (Davis *et al.*, 2001; Lijnen, 2001). Some bacteria also possess plasminogen activators, but most rely on the presence of host plasminogen activators during infection (Bergmann *et al.*, 2001; Candela *et al.*, 2008). In particular for bacteria, it has been shown that the plasminogen/plasmin system is hijacked for tissue invasion and dissemination by recruiting plasminogen to the cell surface to gain surface-associated proteolytic activity (Lähteenmäki *et al.*, 2005). In the case of normal gastrointestinal microbiota, which possess plasminogen binding properties, it was suggested that the plasminogen/plasmin system is used to colonise the mucosal surface. Other additional factors may be involved for pathogenic bacteria which invade the tissue (Lähteenmäki *et al.*, 2005; Candela *et al.*, 2008). Secretion of enolase by *H. contortus* and *T. circumcincta* could also play a role during infection, causing tissue damage. Further experiments would be required to assess whether the enolase of *H. contortus* and *T. circumcincta* is capable of binding plasminogen. The use of plasminogen/plasmin was also demonstrated as an alternative to trypsin for the detachment of adherent cells in culture (Muranova *et al.*, 1998).

Acid phosphatase, which is present in adult *H. contortus* ES products (Fetterer and Rhoads, 2000), could also be involved in the disruption of the actin cytoskeleton, as does the enzyme from bacteria (*Yersina* spp. and *Salmonella* spp.) and protozoa (*Entamoeba histolytica*) (Hueck, 1998; Aguirre-García *et al.*, 2003; Anaya-Ruiz *et al.*, 2003). *Yersinia* tyrosine phosphatases were shown to catalyse the dephosphorylation of several macrophage proteins, including paxillin, and in HeLa cells FAK and p120CAS, proteins of the focal adhesion plaque and adherens junction, as well as causing a collapse of the cytoskeleton via the disruption of the actin microfilaments, probably by an indirect mechanism (Hueck, 1998). Cell adhesion is reviewed in detail in 1.1.1.2 and focal adhesions in 1.1.1.1.2. It has been suggested that the dephosphorylation of host proteins, which caused the disruption of the actin cytoskeleton and cellular detachment in HeLa cells, mediated by *E. histolytica* acid phosphatase (secreted and membrane-bound) interferes with host signalling (Aguirre-García *et al.*, 2003; Anaya-Ruiz *et al.*, 2003). Acid phosphatase would be expected to be active at raised pH of the parasitised abomasum, as the optimum pH for *H. contortus* acid phosphatase is 4.5 (Fetterer and Rhoads, 2000). Further experiments with purified acid

phosphatase from ES products, as well as the use of specific inhibitors, could determine whether *H. contortus* acid phosphatase is a possible detachment factor. A limitation to the use of protease and phosphatase inhibitors is potential toxicity to cells, as was seen in experiments to evaluate HeLa cell vacuolation (chapter 3), even at low concentrations.

Galectins are present in *H. contortus* and *T. circumcincta* ES products (reviewed in 1.3.3.7.2) and could also play a role in the observed cell detachment, as mammalian galectins -1, -3 and -8 were also shown to have a role in regulating adhesion. Depending on the cell type and concentration of galectin, galectin-1 and -3 can either inhibit or promote adhesion by binding to extracellular matrix proteins. In the case of inhibition, galectin binding was suggested to sterically prevent the adhesion to cell surface integrins (Hughes, 2001). Galectin-8 was shown to bind to different integrins thus inhibiting cell adhesion (Hadari *et al.*, 2000). It was suggested that galectin-8 binding to integrins might stabilise integrins in a low-affinity conformation, inhibiting binding to extracellular matrix proteins. It was also proposed that intracellular signalling following galectin-8-integrin binding leads to the suppression of integrin activation (Hadari *et al.*, 2000). Another possibility is the endocytosis of integrins, which can be mediated by galectin-3, and was potentially suggested for galectin-8 as well (Zick *et al.*, 2004). Furthermore, galectin-8 was able to induce apoptosis (Hadari *et al.*, 2000).

Another possible mediator of cell detachment could be secreted calreticulin. In general, calreticulin is a multifunctional protein in eucaryotic cells. Interesting in the context of infection, it also plays a role in cellular adhesion. Calreticulin has been demonstrated to bind to integrin and mediate thrombospondin-induced rearrangement of stress fibres and disassembly of focal adhesions (Johnson *et al.*, 2001; Goicoechea *et al.*, 2002). Calreticulin uses the low density lipoprotein receptor-related protein as a co-receptor to mediate intracellular signalling in response to thrompospondin-calreticulin binding that leads to focal adhesion disassembly (Orr *et al.*, 2003). Thrompospondin interaction stimulates PI3 kinase, increasing intracellular PI3 phosphate, which binds to α-actinin (actin crosslinking protein) unbundling the actin stress fibres. In addition, vinculin is lost from the focal adhesion plaque, but not talin or integrin (Murphy-Ullrich, 2001; Orr *et al.*, 2003). Secreted nematode calreticulin may play a role in such a de-adhesive scenario, however, additional factor(s) may be involved since the intermediate adhesive state, resulting from signalling,

has been proposed to support cell survival (Murphy-Ullrich, 2001). Matricellular proteins like thrombospondin are expressed in response to injury. Maintaining a spread, extended morphology in the intermediate state has been suggested to support cell survival and repair by promoting cell motility (Murphy-Ullrich, 2001).

A second mode of action of calreticulin in the detachment of cells may be through its calcium binding properties, as integrin binding to ligands is dependent on divalent cations. Integrins possess multiple Ca^{2+}- and/or divalent cation-binding sites. Ligand binding depends on the formation of a ligand carboxyl-divalent cation coordination complex at the metal ion dependent adhesion site (MIDAS) of the integrin. It was proposed that the other cation binding sites play a role in integrin structure stabilisation, but the precise role of cations on integrin conformation and ligand binding is still unclear (Humphries *et al.*, 2003). Kirchhofer *et al.* (1991) demonstrated that Ca^{2+} in the presence of Mg^{2+} had inhibiting or enhancing effects on binding affinity of different integrin receptors. Similar results were shown for Mn^{2+} and Ca^{2+}, with Ca^{2+} inhibiting adhesion (Smith, J. W. *et al.*, 1994). Mould *et al.* (1995) confirmed previous studies and proposed that ligand binding is regulated by binding of divalent cations at different binding sites. It may be a possibility that the high affinity of calreticulin for Ca^{2+} is affecting integrin binding, although it was proposed that Mn^{2+} and Mg^{2+} generally promote binding and Ca^{2+} has inhibitory effects (Humphries *et al.*, 2003). Furthermore, integrin-mediated cell spreading induces a transient increase in $[Ca^{2+}]_i$, released from intracelleular stores and/or influx of extracellular Ca^{2+}, which appears to play a regulatory role in adhesion (Schwartz, 1993; Sjaastad *et al.*, 1996; Sjaastad and Nelson, 1997; Belusa *et al.*, 2002). Inhibition of Ca^{2+} channels (Sjaastad *et al.*, 1996) as well as chelation of Ca^{2+} (Britch and Ellen, 1980; Rowin *et al.*, 1998) was shown to reduce adhesion. Chelation of Ca^{2+} by calreticulin could also be a possible factor in the observed cell detachment. The role of calreticulin will also be discussed in chapter 5, since it may also play a role in disruption of cell-cell adhesion. Experiments with calreticulin antibodies to neutralise calreticulin or the use of calreticulin that has been purified from ES products, which would additionally clarify if other factors are involved, could clarify whether it is involved in the observed cell detachment.

Since ES products appear to be involved in the inhibition of acid secretion (Simpson *et al.*, 1999; Hertzberg *et al.*, 2000; Merkelbach *et al.*, 2002) it could also be a possibility that the

sodium/potassium pump (Na^+/K^+-ATPase), which shows high sequence homology to the H^+/K^+-ATPase, is affected by ES products. Contreras *et al.* (1999) and Belusa *et al.* (2002) demonstrated that Na^+/K^+-ATPase inhibition with ouabain resulted in cell detachment. Both studies showed an increase in $[Ca^{2+}]_i$ following the inhibition of the pump which was suggested to override physiological Ca^{2+} signalling pathways. In addition, the inhibition of the Na^+/K^+-ATPase resulted in modifications in the distribution of several cell attachment related proteins including vinculin and α-actinin, but also tight and adherens junctional as well as desmosomal proteins (also discussed in chapter 5) (Contreras *et al.*, 1999). Further experiments would have to clarify whether the Na^+/K^+-ATPase could be inhibited or somehow else affected by ES products.

Several possible candidates responsible for cell detachment have been identified in ES products, including proteases, enolase, acid phosphatase, galectins and calreticulin. The actin cytoskeletal rearrangements and detachment seen in epithelial cell cultures resemble actions of virulence factors of microorganisms. As discussed above, all appear capable of interfering with cell adhesion, which is very relevant to the host-parasite interaction. Parietal cells cannot tolerate breaking of their cell junctions during isolation as this limits their ability to secrete acid (Chew, 1994). ES products may also penetrate the gastric barrier by increasing permeability. This latter possibility is examined using CaCo-2 cells (chapter 5).

Table 5.1: Selection of diseases related to dysfunctional tight junctions.

Disease	TJ or TJ-associated protein(s) affected	Reference (Reviews)
Cancer		
Breast cancer: invasive ductal cancer	Claudin-1 and ZO-1	Förster, 2008
Prostate cancer: prostatic adenocarcinomas	Claudin-1, -3, -4 and -7	Förster, 2008, Krause *et al.*, 2008
Inflammation		
Multiple sclerosis	Occludin, claudin-5	Förster, 2008
Inflammatory bowl disease: Morbus Crohn	Claudin-2, -3, -5 and -8, ZO-1	Förster 2008, Krause *et al.*, 2008
Hereditary diseases		
Herediatary deafness	Claudin-14	Tsukita *et al.*, 2001; Förster, 2008, Krause *et al.*, 2008
Herediatary hypomagnesemia	Claudin-16	Tsukita *et al.*, 2001; Förster, 2008, Krause *et al.*, 2008
Viral Infections		
Reovirus	JAM-1	Schneeberger and Lynch, 2004; Förster, 2008
Coxsackie B Virus	CAR	Schneeberger and Lynch, 2004
Adenovirus	TJ plaque proteins including MUPP-1, MAGI-1 and ZO-2	Schneeberger and Lynch, 2004
Papillomavirus	TJ plaque proteins including MUPP-1 and MAGI-1	Schneeberger and Lynch, 2004
Bacterial Infections		
Clostridium perfringens enterotoxin	Claudin-3 and -4	Schneeberger and Lynch, 2004; Förster, 2008
H. pylori	ZO-1 and JAM-1	Schneeberger and Lynch, 2004
E. coli (enteropathogenic)	MLCK	Clayburgh *et al.*, 2004
Parasitic Infections		
Dermatophagoides pteronyssinus (mite)	Occludin and ZO-1	Schneeberger and Lynch, 2004

Chapter 5

TIGHT JUNCTION PERMEABILITY

5.1 Introduction

The dysfunction of tight junctions (tight junctions are reviewed in 1.2.3.2.1.1) plays a crucial role in numerous diseases, including gastrointestinal diseases, infections with viruses, bacteria or parasites and the host inflammatory response (Tsukita *et al.*, 2001; Clayburgh *et al.*, 2004; Schneeberger and Lynch, 2004; Aktorius and Brabieri, 2005; Van Itallie and Anderson, 2006; Förster, 2008). Some of these diseases are summarised in Table 5.1.

The mechanisms of the tight junction dysfunctions vary and include functional changes in tight junction proteins through direct interactions with the pathogen or a pathogenic factor. Some tight junction proteins have a reported receptor function for pathogens, for example JAM is a receptor for reovirus, CAR even named after its receptor function for coxsackie- and adenovirus, whereas others interact with pathogenic factors (Sawada *et al.*, 2003). The latter includes *Clostridium perfringens* enterotoxin interaction with claudins, reportedly affecting tight junction structure and function leading to diarrhoea, and *Dermatophagoides*

pteronyssinus (house dust mite) allergen (Der p 1; present in their faecal pellets), which has protease activity and upon inhalation results in cleavage of occludin and ZO-1 leading to tight junction opening with the loss of the barrier function to inhaled allergens, causing asthma (Sawada *et al.*, 2003; Schneeberger and Lynch, 2004).

Other mechanisms of action include changes in cellular actin organisation involving Rho and MLCK. For example, tight junction morphology is disrupted by enteropathogenic *E. coli*, including actin cytoskeleton reorganisation, tight junction protein redistribution and increase in myosin light chain (MLC) phosphorylation by MLCK, resulting in diarrhoea (Sawada *et al.*, 2003; Clayburgh *et al.*, 2004). One mode of action of *H. pylori* also includes increased MLC phosphorylation, which is independent of the virulence factors VacA and CagA (encoded by cytotoxin-associated gene A) (Fedwick *et al.*, 2005; Wroblewski *et al.*, 2009). MLCK and Rho kinase are involved in MLC phosphorylation.

In addition, *H. pylori* is able to increase permeability by disrupting claudin-4 and -5 (Fedwick *et al.*, 2005) and internalising occludin from an insoluble (membrane-associated) fraction to a soluble (cytosolic) fraction (Wroblewski *et al.*, 2009). Internalisation of occludin and the expression of a low molecular weight form of occludin is reportedly linked to *H. pylori* urease activity and the production of ammonium (Lytton *et al.*, 2005; Wroblewski *et al.*, 2009). Ammonium-dependent increase in permeability has also been shown to be reversible (Lytton *et al.*, 2005). *H. pylori* is also able to disrupt epithelial cell polarity by CagA interaction with partitioning defective 1 (PAR1) kinase, which in turn prevents PAR1 phosphorylation by aPKC, resulting in dissociation of PAR1 from the membrane (Saadat *et al.*, 2007) (for an overview see also Figure 1.19, Table 1.2 and 1.3). Several other interaction partners for CagA have been identified, including ZO-1, which are suggested to lead to the disruption of tight junctions as well as adherens junctions and focal adhesions (Wessler and Backert, 2008).

Many cytokines and growth factors, which are usually produced during pathological conditions, are able to decrease the barrier function (Sawada *et al.*, 2003; Förster, 2008). This is especially important in diseases such as inflammatory bowl disease (including Crohn's disease). In Crohn's disease, the barrier dysfunction precedes the inflammatory response. This can be due to genetic predisposition or environmental factors including

infection, as intestinal permeability is also increased in many relatives of Crohn's disease patients, who do not show clinical symptoms (Förster, 2008). An abnormal immune response including the overproduction of TNF-α, interferon-γ (IFN-γ) and IL-1β, especially, acts then to further disrupt the barrier (Clayburgh *et al.*, 2004; Al-Sadi and Ma, 2007; Förster, 2008). IFN-γ has been shown to promote endocytosis of occludin, JAM-1 and claudin-1 and TNF-α to downregulate ZO-1 expression through activation of NFκB and to redistribute ZO-1 away from the tight junction (Förster, 2008). IL-1β downregulates occludin expression, which is also regulated by NFκB activation (Al-Sadi and Ma, 2007).

Protein is lost and serum pepsinogen increases during abomasal parasitism due to a more permeable epithelium (Holmes and MacLean, 1971; McLeay *et al.*, 1973; McKellar, 1993) (1.3.1), which possibly results from a loss of tight junction integrity. Experiments described in this chapter were designed to examine a possible role of ES products of *H. contortus* and *T. circumcincta* in tight junctional damage. CaCo-2 cells, which form a monolayer with cell-cell junctions including tight junctions, were used as a model system for the epithelial barrier, as well as tissue from infected animals. The tight junction proteins occludin and ZO-1 were immunohistochemically stained in both CaCo-2 cells and tissue. In addition, possible changes in permeability of the CaCo-2 cell monolayers were also monitored by transepithelial electrical resistance (TEER) measurements.

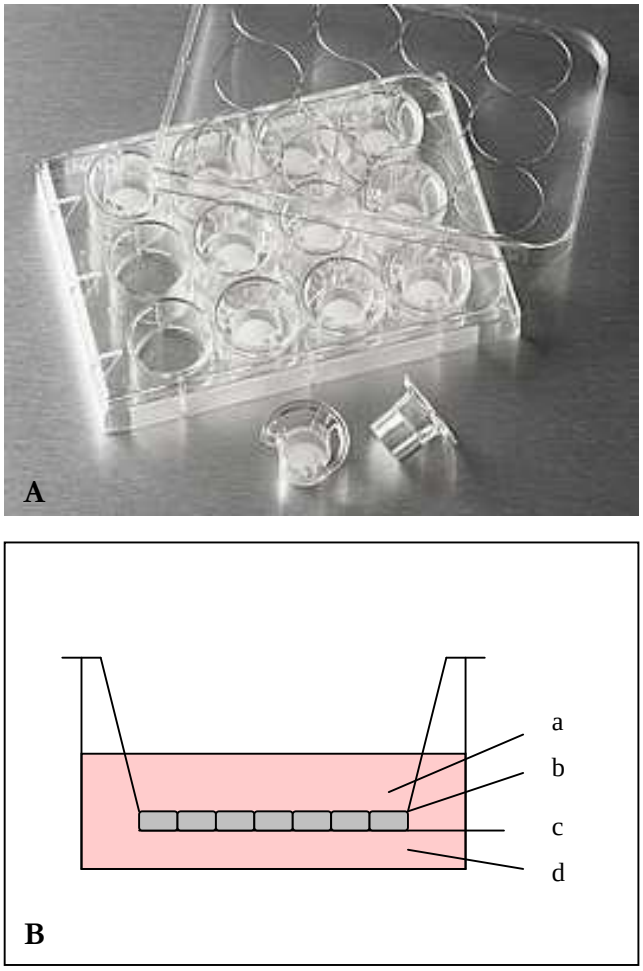

Figure 5.1: Transwell® system. A. 12 well plate with transwell inserts (Corning), B. Schematic setup of a single transwell, a apical compartment, b cell monolayer, c polycarbonate membrane, d basolateral compartment.

5.2 Materials and Methods

5.2.1 ES Preparations of Adult *H. contortus* and *T. circumcincta*

Adult worms of *H. contortus* and *T. circumcincta* were obtained 21d and 28d, respectively, after the infection of the sheep as described in Appendix I. They were incubated for 12h in D10 medium (composition listed in Appendix II) in 15ml tubes in an incubator in an atmosphere containing 5% CO_2 and 95% humidified air at 37°C. D10 medium was also incubated under the same conditions to serve as a negative control. The supernatants of the ES preparations and the negative controls were sterile filtered through 0.2µm filters into new tubes. The pH of each preparation was readjusted to 7.4 if necessary. The preparations were stored at 4°C until direct use.

5.2.2 Preparation of Sheep Gastric Mucosa

Fundic tissue folds from sheep infected with *H. contortus* (21d p.i.) and from uninfected control sheep were fixed using 4% paraformaldehyde as described in chapter 2, 2.2.1.5.

5.2.3 Cell Culture

CaCo-2 cells were grown as described in detail in Appendix II. For experiments, they were seeded on transwell plates (Corning; 12 well plates, Figure 5.1), 200,000 cells in 0.4ml cell culture medium per transwell insert (apical side), where they grew on polycarbonate membranes. 1.5ml medium was applied to the basolateral side. The medium was changed three times per week in the apical compartment and once per week in the basolateral compartment. A differentiated cell monolayer was formed ~21d after confluence was reached, which was then used for experiments. The integrity of the confluent cell monolayer was monitored by TEER measurements (5.2.5).

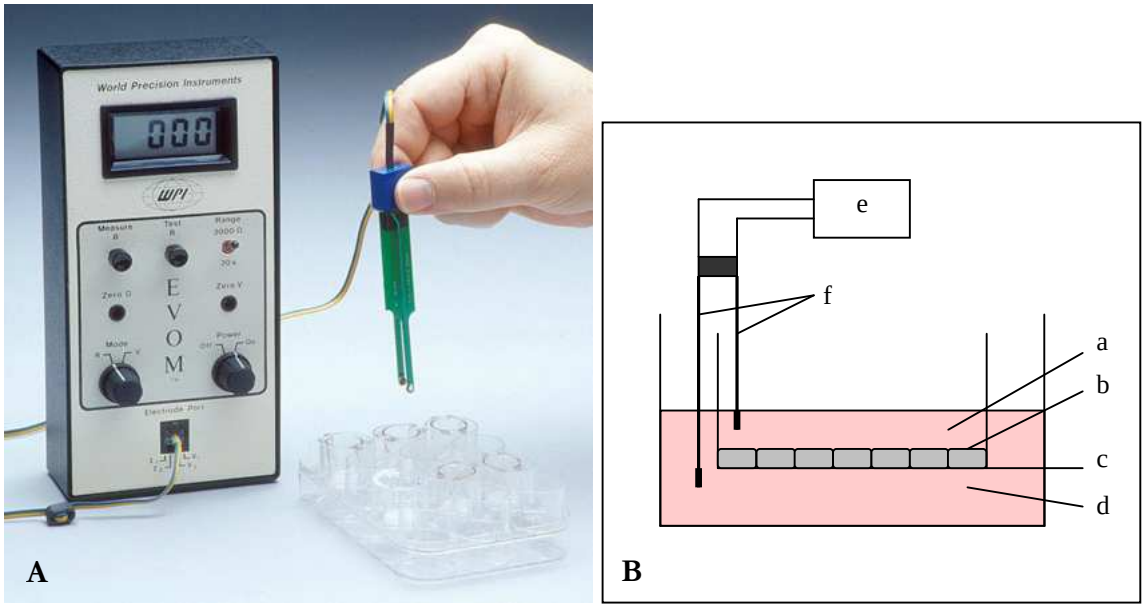

Figure 5.2: Set-up for TEER measurements of cell monolayers growing on transwells with the volt-ohm meter. A. Epithelial volt-ohm meter (EVOM™, World Precision Instruments) with „chopstick“ electrodes, B. Schematic setup of TEER measurements in a single transwell, a apical compartment, b cell monolayer, c polycarbonate membrane, d basolateral compartment, e volt-ohm meter, f electrodes.

5.2.4 Incubations with ES Preparations on Cells

The culture medium of the cells was discarded and replaced by either ES preparations or control media (negative controls) on the apical side and cell culture medium in the basolateral compartment. Cells were incubated for 24h in an incubator in an atmosphere containing 5% CO_2 and 95% humidified air at 37°C.

5.2.5 TEER Measurements

The transepithelial electrical resistance was measured (volt-ohm meter EVOM™, World Precision Instruments) before each experiment to ensure the integrity of confluent cell monolayers (Figure 5.2). For CaCo-2 cells that should exceed 300Ω (Buesen *et al.*, 2002; Troutman and Thakker, 2003; Lim and Lim, 2006). Once confluence was reached, ES preparations and control samples were applied and TEER was measured after 6h and 24h. The electrodes were sterilised with 96% ethanol before the measurements. All TEER values were corrected by subtracting the TEER of control blank wells (≙ TEER of the filter membrane). To obtain the unit area resistance [Ω cm^2], the TEER readings were multiplied by the effective surface area of the filter membrane (1.12cm^2).

5.2.6 Antibody Staining of Tight Junction Proteins (Occludin and ZO-1)

The polycarbonate membrane with the CaCo-2 monolayer attached was carefully removed from the transwell and cut in half for the staining procedure. The cell monolayer on the membrane was fixed with 4% paraformaldehyde (30min at room temperature), then washed three times with PBS. Filter membranes were either stored at 4°C until use or stained immediately. Cells on the filter membrane were first exposed to acetone (-20°C) for 3min before they were permeabilised with 0.2% Triton-X-100 in PBS for 15min at room temperature. After washing three times for 1min with PBS, they were incubated with blocking buffer (Appendix V) for 60min. The antibodies (diluted in blocking buffer) were applied in the following order, each for 60min and followed by washing three times with

Table 5.2: TEER values (mean ± SEM) of CaCo-2 cell monolayers before (0h) and after 6 and 24h exposure to ES preparations of *H. contortus* adults (n=12) and corresponding controls (n=17). Means with the same superscript are significantly different ($p<0.05$).

	0h	6h	24h
Control			
TEER [Ω cm^2]	421.7 ± 16.8	400.9 ± 13.6	394.5 ± 13.0
TEER decrease [Ω cm^2]	-	20.8 ± 4.3	27.2 ± 5.2
Percentage values	100 ± 4.0	95.1 ± 3.2	93.5 ± 3.1
Percentage decrease	-	4.9 ± 0.7	6.5 ± 0.9
ES			
TEER [Ω cm^2]	532.28 ± 10.0$^{a, b}$	380.2 ± 7.8^{a}	422.9 ± 7.8^{b}
TEER decrease [Ω cm^2]	-	152.0 ± 4.7	109.4 ± 4.0
Percentage values	100 ± 1.9	71.4 ± 1.5	79.4 ± 1.5
Percentage decrease	-	28.6 ± 0.6	20.6 ± 0.5

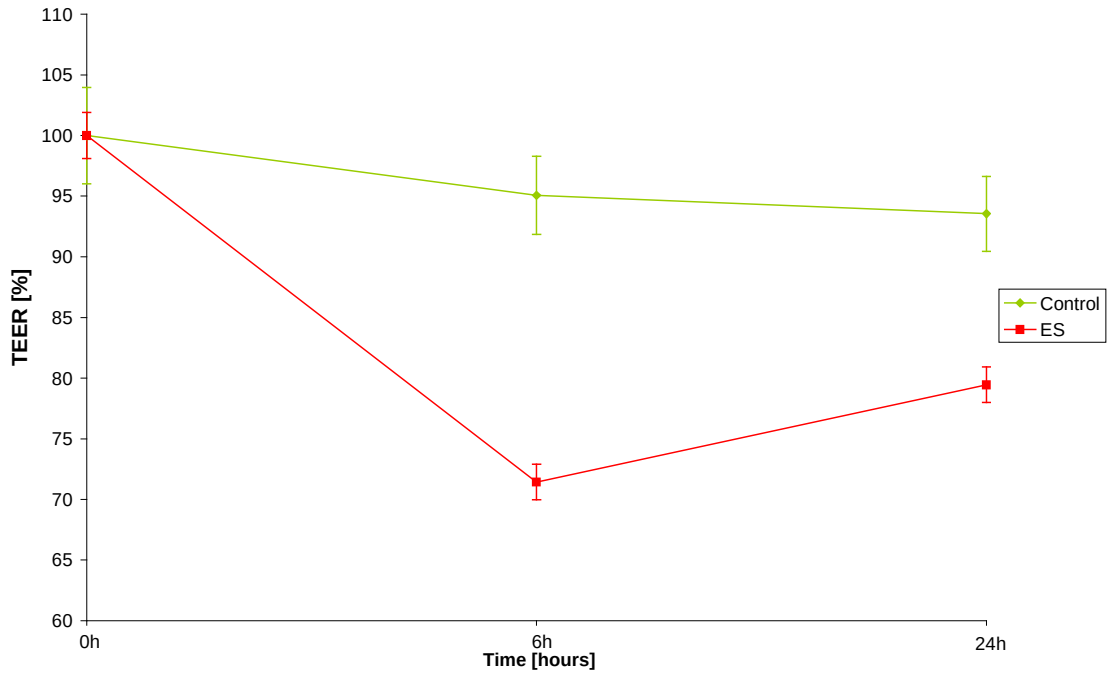

Figure 5.3: TEER of CaCo-2 cell monolayers after 6 and 24h exposure to ES preparations of *H. contortus* adults (n=12) and corresponding controls (n=17). Expressed as percentage of zero time values.

blocking buffer: 1:200 dilution of mouse anti-occludin; 1:100 dilution of biotin-XX goat anti-mouse IgG; 1:100 dilution of rabbit anti-ZO-1; 1:100 dilution of Alexa Fluor® 488 goat anti-rabbit IgG (blue laser/488 excitation with emission maximum of ~530nm/green fluorescence) and finally 1:100 dilution of streptavidin, Alexa Fluor® 546 conjugate (green laser/546nm excitation with emission maxiumum of 573nm/red fluorescence). The stained cell monolayer on the membrane was kept in PBS at 4°C. All relevant solutions for the antibody staining are listed in Appendix V.

5.2.7 Microscopic Examination of Cells and Tissue

After staining the tight junction proteins occludin and ZO-1, cells and tissue were examined using an inverted confocal microscope with 40x or 60x/water immersion objectives. All images were processed with Adobe Photoshop.

5.2.8 Statistical Analysis

Data for TEER values are presented as mean ± SEM. Two-way ANOVA with Bonferroni *post hoc* tests was used to compare TEER values after application of control media or ES preparations.

5.3 Results

5.3.1 Changes in Tight Junction Permeability Shown by TEER Measurements

TEER measurements of CaCo-2 cell monolayers immediately before (0h) and 6h and 24h after application of ES preparations of *H. contortus* adults (n=12) and of corresponding controls (n=17) are shown in Table 5.2 and Figure 5.3. Mean TEER slightly decreased in

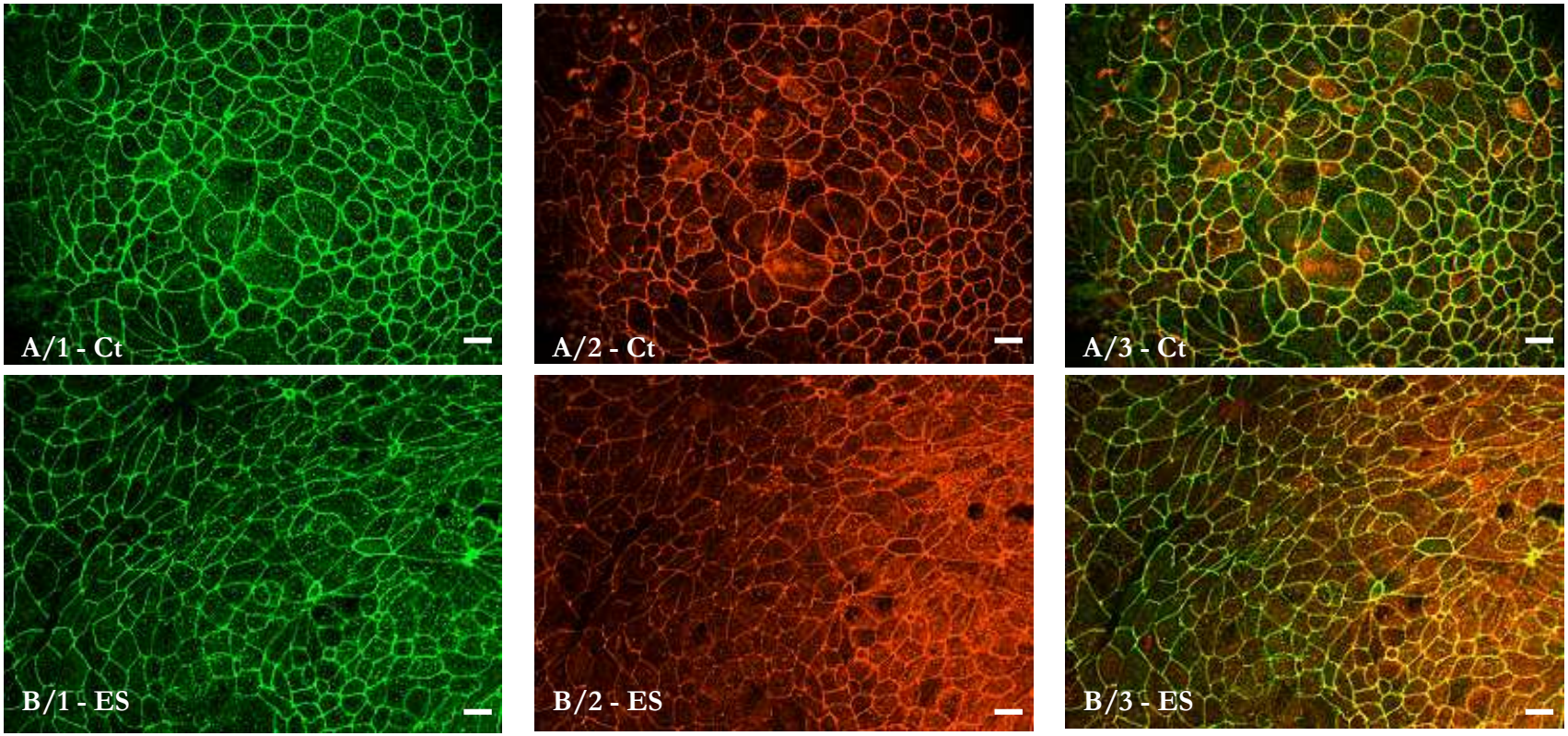

Figure 5.5: Effect of *T. circumcincta* ES on the tight junctional structure of CaCo-2 cell monolayers. A/1 to A/3 CaCo-2 cell monolayers control (D10 medium), B/1 to B/3 CaCo-2 cell monolayers exposed to *T. circumcincta* ES for 24h. A/1 and B/1 ZO-1 localisation, A/2 and B/2 Occludin localisation, A/3 and B/3 Merged A/1 and A/2 or B/1 and B/2, respectively, showing the co-localisation as yellow. Original magnification 400x, bars 20µm.

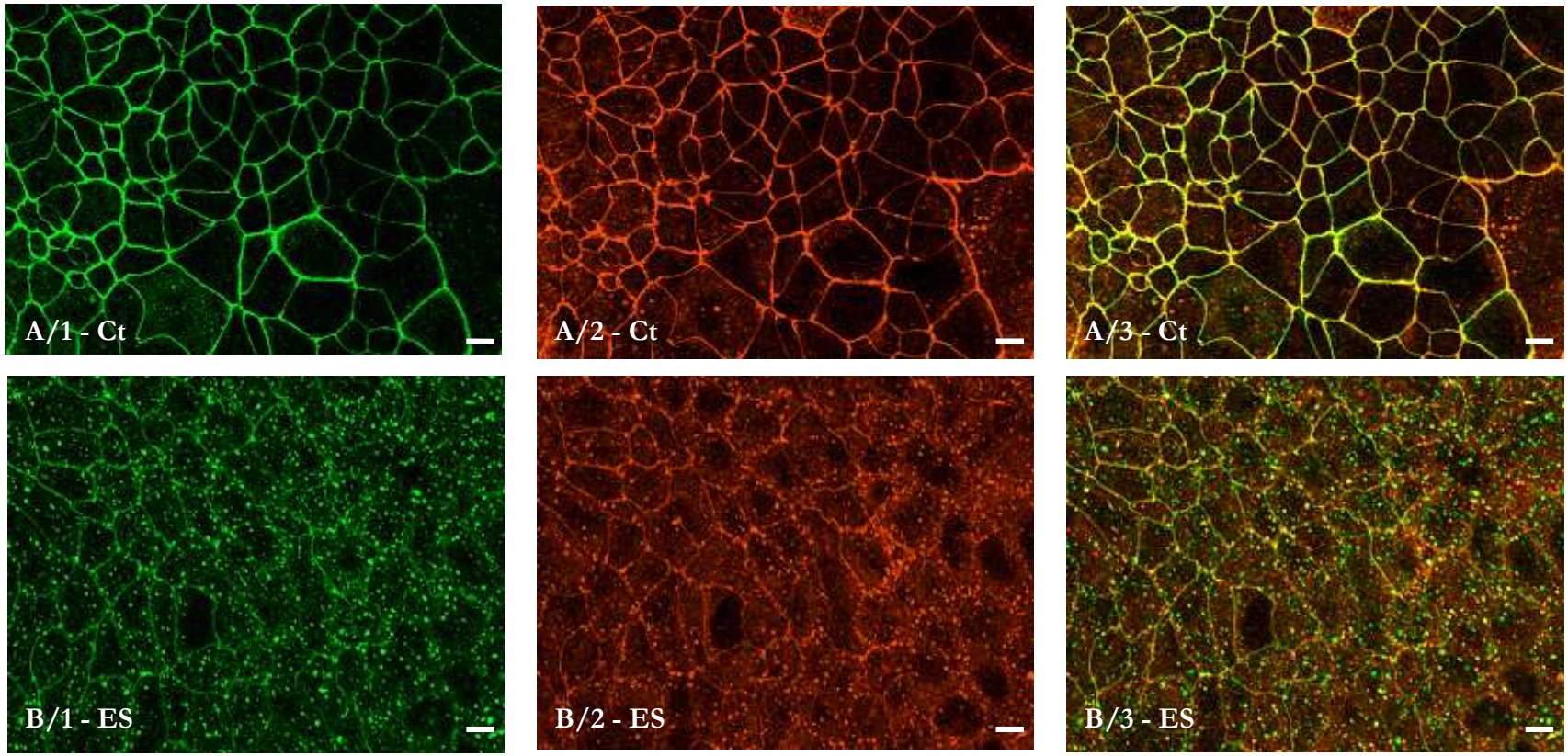

Figure 5.4: Effect of *H. contortus* ES on the tight junctional structure of CaCo-2 cell monolayers. A/1 to A/3 CaCo-2 cell monolayers control (D10 medium), B/1 to B/3 CaCo-2 cell monolayers exposed to *H. contortus* ES for 24h. A/1 and B/1 ZO-1 localisation, A/2 and B/2 Occludin localisation, A/3 and B/3 Merged A/1 and A/2 or B/1 and B/2, respectively, showing the co-localisation as yellow. Original magnification 400x, bars 10µm.

control cell monolayers (20.8 ± 4.3 after 6h and 27.2 ± 5.2 after 24h). In comparison, exposure to ES products led to a decrease of 152.0 ± 4.7 after 6h and 109.4 ± 4.0 after 24h, equivalent to a decrease of 28.6% ± 0.6 and 20.6% ± 0.5, respectively. Statistical Analysis showed that there was a significant difference at later time points ($p=<0.0001$) as well as for the treatment ($p=0.0005$) and interaction between these factors ($p<0.0001$).

5.3.2 Changes in Tight Junction Permeability Shown by Tight Junction Protein Staining

5.3.2.1 CaCo-2 Cells

Decreased membrane-associated staining of the tight junction proteins occludin and ZO-1 was shown after 24h ES exposure with *H. contortus* and *T. circumcincta* ES products to CaCo-2 cell monolayers.

Incubations of CaCo-2 cells with ES preparations and control media followed by immunhistochemistry for occludin and ZO-1 were performed three times using one batch of ES preparations for *H. contortus* and *T. circumcincta* and control media each. Results are shown in Figure 5.4 for application of *H. contortus* ES products and in Figure 5.5 for *T. circumcincta* ES products. In control cells, both occludin and ZO-1 staining was mainly cell membrane-associated with low level intracellular punctate staining. Merged images showed almost uniform colocalisation of occludin and ZO-1, which appeared as yellow. The distribution of both occludin and ZO-1 changed after exposure to ES products: membrane-associated staining was decreased with a simultaneous marked increase in intracellular punctate staining. This effect was more prominent after exposure to *H. contortus* ES products compared with *T. circumcincta* ES products. Merged images also showed a different distribution of the intracellular punctate staining with mainly single-molecule-type vesicles (either ZO-1- or occludin-type vesicles) rather than a colocalisation inside vesicles.

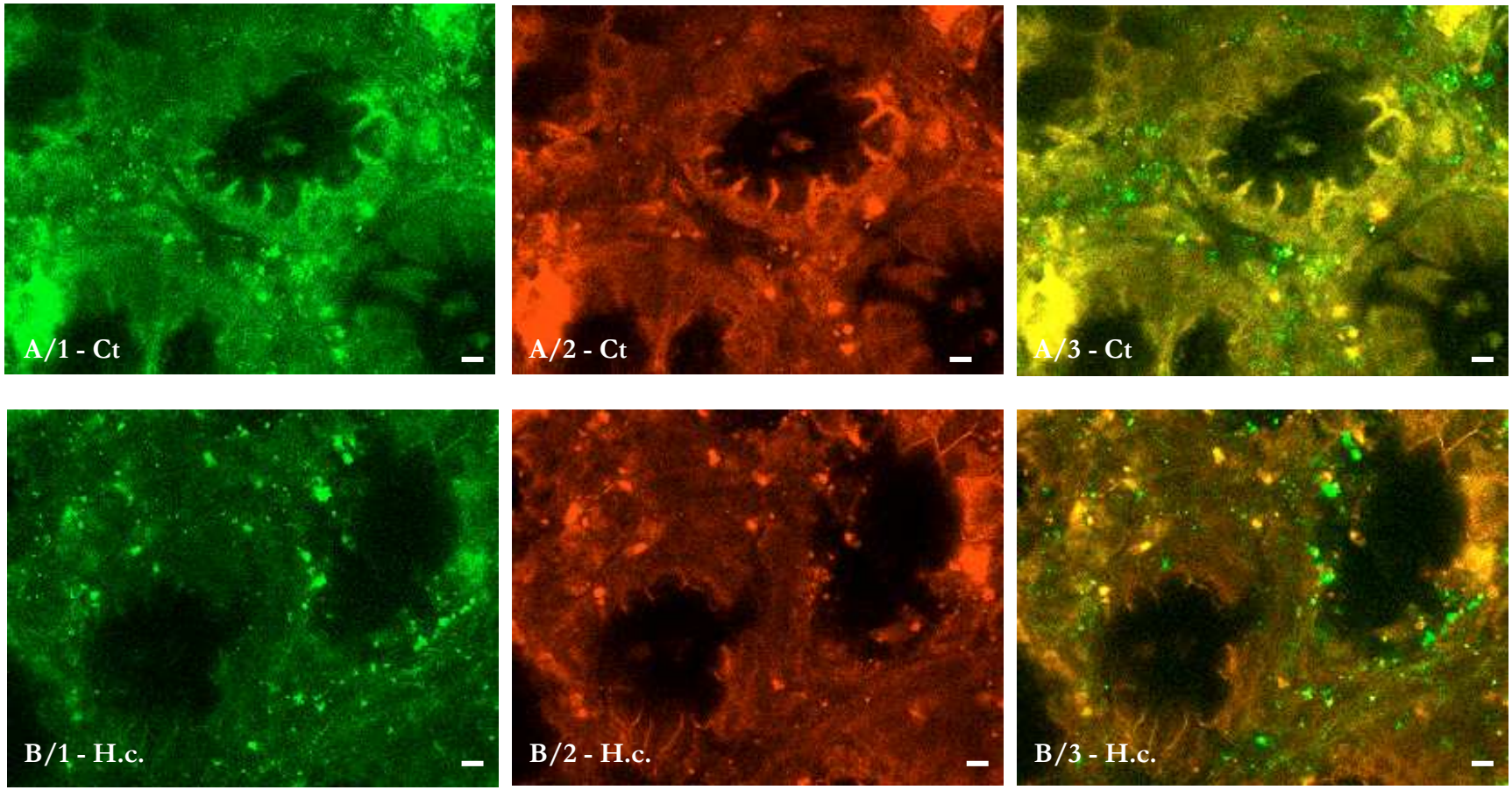

Figure 5.7: Effect of *H. contortus* infection on the tight junctional structure of abomasal mucosa - close-up. A/1 to A/3 Fundic abomasal tissue folds of uninfected control sheep, B/1 to B/3 Fundic abomasal tissue folds of *H. contortus* infected sheep 21d p.i.. A/1 and B/1 ZO-1 localisation, A/2 and B/2 Occludin localisation, A/3 and B/3 Merged A/1 and A/2 or B/1 and B/2, respectively, showing the co-localisation as yellow. Original magnification 600x, bars 5µm.

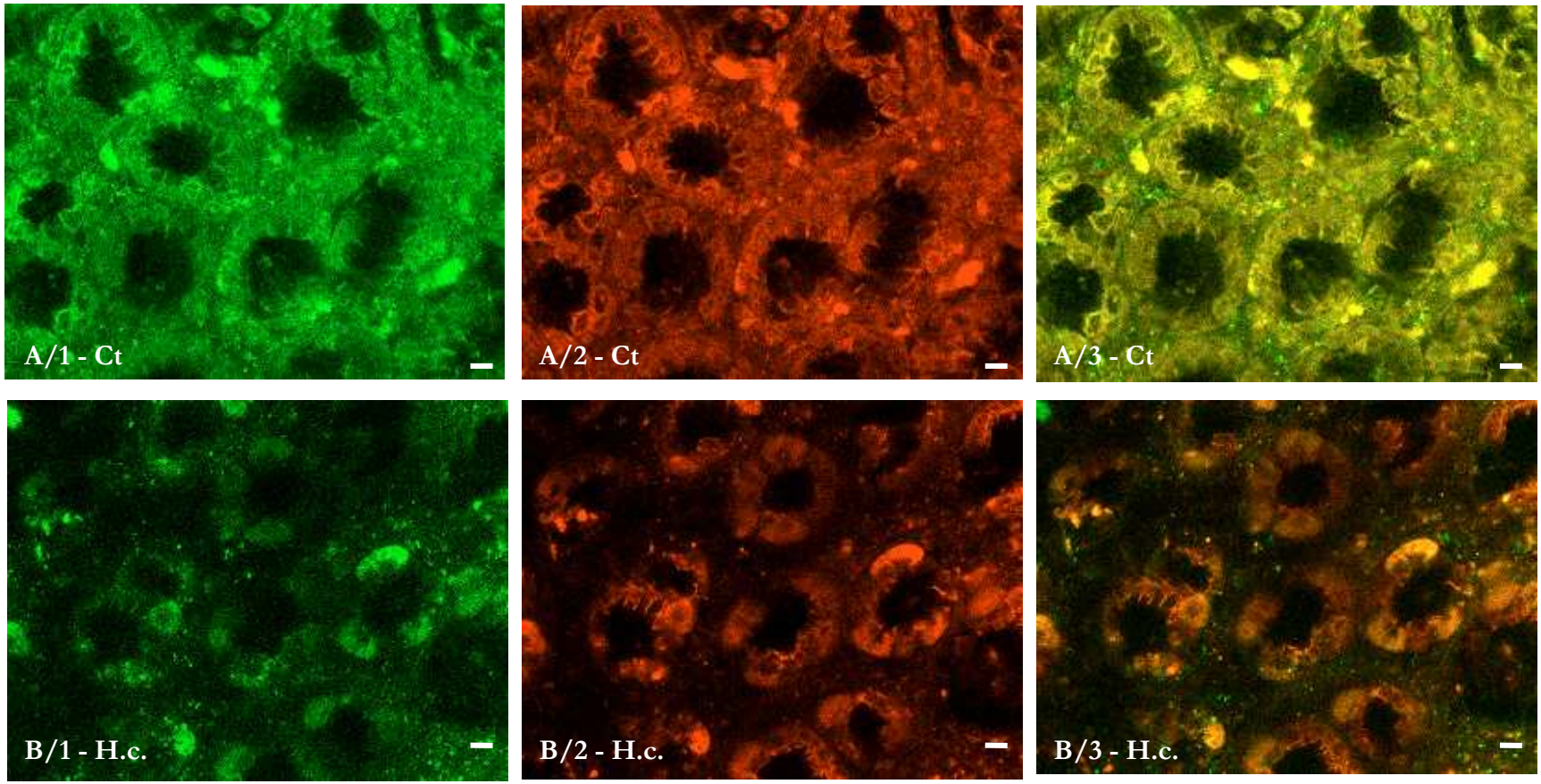

Figure 5.6: Effect of *H. contortus* infection on the tight junctional structure of abomasal mucosa. A/1 to A/3 Fundic abomasal tissue folds of uninfected control sheep, B/1 to B/3 Fundic abomasal tissue folds of *H. contortus* infected sheep 21d p.i.. (H.c.) A/1 and B/1 ZO-1 localisation, A/2 and B/2 Occludin localisation, A/3 and B/3 Merged A/1 and A/2 or B/1 and B/2, respectively, showing the co-localisation as yellow. Original magnification 600x, bars 10µm.

5.3.2.2 Fixed Abomasal Tissue Folds

Pieces of fundic tissue collected from sheep 21d after infection with *H. contortus* and from uninfected control sheep were stained immunohistochemically for the tight junction proteins occludin and ZO-1 and infected abomasal tissue appeared to show less intense membrane-associated staining for both proteins.

Figures 5.6 and 5.7 show the gland openings of the luminal abomasal surface. Parts of pit cells/surface mucous cells can be seen, but the tissue is not as flat as a cell layer. In control tissue, cell membrane-associated occludin and ZO-1 staining appeared more intense and thicker than in tissue from infected sheep. This was more prominent for ZO-1 staining. Intracellular staining, as seen in CaCo-2 cells, was not observed.

5.4 Discussion

Experiments described in this chapter were aimed at investigating a possible role of ES products in the disruption of tight junctions. Both *H. contortus* and *T. circumcincta* ES products were able to modify the structural organisation of tight junctions, demonstrated by the relocation of occludin and ZO-1 in CaCo-2 cells (Figure 5.4 and 5.5). Furthermore, the CaCo-2 cell monolayer became leaky after ES exposure, shown by decreased TEER, with a maximum drop of 26.6% after 6h (Table 5.2 and Figure 5.3). *H. contortus* ES products appear to be more effective than those of *T. circumcincta*, as was similarly seen in vacuolation studies (Przemeck, 2003). This was shown by less severe tight junctional structure rearrangements after exposure to *T. circumcinta* ES preparation compared with *H. contortus* (Figure 5.4 and 5.5). Structural rearrangements appeared as decreased membrane-associated staining with a concomitant increase in intracellular punctate staining in CaCo-2 cells, consistent with endocytosis of tight junction proteins.

Internalisation of apical junctional proteins, including tight junction proteins, by endocytosis may occur both under normal physiological conditions and in pathological conditions (Ivanov *et al.*, 2005; Shen *et al.*, 2008; Yu and Turner, 2008). Suggested

physiological functions include constitutive remodelling, accelerated internalisation at certain stages of the cell cycle (cell division and apoptosis) or in conditions which require transient opening of the epithelial barrier without loss of integrity (Ivanov *et al.*, 2005; Shen *et al.*, 2008). Low level punctate staining of occludin and ZO-1, which was observed in control cells, could be indicative of constitutive remodeling.

The response to pathogenic stimuli is usually accompanied by dramatic relocations of tight junctional proteins, as shown for infection with Rotavirus (Obert *et al.*, 2000), *Clostridium difficile* (Nusrat *et al.*, 2001) or *H. pylori* (Wroblewski *et al.*, 2009). Similarly, exposure to ES preparations resulted in marked increases in intracellular vesicles, but the distribution of occludin and ZO-1 inside the vesicles was mainly different. A quantitative test of colocalisation by intensity correlation analysis (Li *et al.*, 2004) showed that occludin and ZO-1 were differently distributed (unpublished data K. C. Pedley). In contrast, Ivanov *et al.* (2004) reported significant colocalisation of ZO-1 with occludin, JAM-1 and claudin-4 after induced endocytosis by calcium depletion. Further staining with markers for different intracellular compartments (e.g. early endosome markers Rab5 and EEA1, recycling endosome markers Rab4 and Rab11, lysosome marker LAMP1) could both clarify the origin of the vesicles observed after ES exposure and may provide an indication why occludin and ZO-1 were not colocalised after internalisation.

As well as in the CaCo-2 model system, structural changes in the organisation of tight junctions appear to occur also in tissue of infected sheep, but were less prominent. In general, cell membrane-associated occludin and ZO-1 staining appeared weaker in tissue from infected sheep. However, for this staining, the thickness and uneven nature of the tissue was challenging, with only parts of pit cells visible in most cases. In addition, small pieces of abomasal contents, which were sticking to the mucus, showed high levels of autofluorescence. To further investigate the distribution of occludin and ZO-1 in infected sheep *in vivo*, tissue sections were also stained, but staining was unsuccessful despite several attempts (not shown). Alternatively, tissue could be analysed by freeze-fracture electron microscopy, revealing tight junctional strand organisation (as seen in Figure 1.18).

This is the first reported study demonstrating that ES products are capable of disrupting tight junctions. Mechanisms of tight junctional disruption can be diverse and could involve

proteases of ES products, suggested from studies with other pathogens. The bacterial protease gelatinase E of *Enterococcus faecalis* was found to impair barrier function demonstrated by TEER reductions of ~75% (Steck *et al.*, 2009). Additional secreted bacterial components were shown to be required, since purified gelatinase E failed to reduce TEER. Furthermore, exposure to the *D. pteronyssinus* allergen Der p 1, which has protease activity, was shown to result in cleavage of occludin and ZO-1 (Wan *et al.*, 1999; 2000). For the intracellular located ZO-1, this might happen indirectly and was proposed to be the result of tight junction disassembly. In addition, degradation of JAM-1 and occludin after exposure of cell monolayers to trypsin or chymotrypsin, respectively, was shown by Ivanov *et al.* (2004). The degradation of extracellular matrix proteins by proteases of *H. contortus* have been shown in *in vitro* experiments (reviewed in 1.3.3.1) and, relating to the observed detrimental effects of other pathogenic proteases on tight junctions, it could be a possibility that the proteases present in ES products are also able to degrade tight junctional proteins. The use of different protease inhibitors could clarify whether a certain class of ES proteases is involved. Experiments with the serine protease inhibitor AEBSF were conducted (not shown), but were unsuccessful. TEER measurements increased for all applications (Ct, Ct + AEBSF, ES, ES + AEBSF) and were inconclusive as well as occludin and ZO-1 staining, which did not differ between exposure to ES preparations and control samples.

Another involvement of secreted proteases could be indirect through protease activated receptors (PAR). Four different receptors have been identified (PAR1 to 4) and, depending on cell type and receptor, their activation result in a variety of effects. In the gastrointestinal tract, these include for example neuropeptide release, cytokine release, muscle contraction or relaxation (Vergnolle, 2005; 2008; Ramachandran and Hollenberg, 2008). Important in the context of barrier function, activation of PAR1 and PAR2 was reported to increase intestinal permeability. For PAR1, this was shown to be due to apoptosis *in vitro* and similarly *in vivo* dependent on caspase-3 activation. PAR2 activation was reported to lead to rearrangements of the cytoskeleton dependent on MLCK (Vergnolle, 2005; 2008). As both receptors are also expressed on CaCo-2 cells (Darmoul *et al.*, 2003; Fyfe *et al.*, 2005), this could be a possible mechanism *in vivo* and *in vitro* by which parasite secreted proteases impair barrier function.

Parasite-secreted calreticulin, with its Ca^{2+} binding properties, could also be involved in the disruption of the epithelial barrier, in addition to a possible role in cellular detachment (chapter 4). It has been reported that extracellular depletion of Ca^{2+} (max. for 2h) results in decreased TEER, increased paracellular permeability and disassembly of tight junctions and adherens junctions (Shasby and Shasby *et al.*, 1986; Klingler *et al.*, 2000; Ma *et al.*, 2000; Ivanov *et al.*, 2004). These effects could be reversed by repletion of Ca^{2+}. PKA and MLCK were involved in the disruption as inhibition of PKA or MLCK prevented tight junction disruption (Klingler *et al.*, 2000; Ma *et al.*, 2000). It was proposed that Ca^{2+} depletion leads to activation of both enzymes. For MLCK, it was suggested that its activation promotes the contraction of the cytoskeleton leading to the opening of the tight junction barrier (Ma *et al.*, 2000). Similarly, activation of PKA was proposed to affect the cytoskeletal organisation (Klingler *et al.*, 2000). Similar experiments as already stated in chapter 4 (neutralisation of secreted calreticulin, use of purified calreticulin) could clarify a possible role of calreticulin in the disruption of tight junctions *in vitro*. However, the question still remains whether calcium chelation by calreticulin *in vivo* would be sufficient to induce tight junction disruption.

The involvement of MLCK was also shown for *H. pylori*. MLC phosphorylation was increased in a MLCK- and Rho kinase-dependent manner. Functional urease activity resulting in ammonium production was required for this process. Moreover, ammonium chloride (10mM) itself reduced the TEER significantly (Wroblewski *et al.*, 2009). It would be interesting to examine the minimum concentration of ammonia required to disrupt the barrier function. Although the ammonia concentration in ES product may be too low to be involved in the induction of vacuoles (chapter 3), excreted ammonia could play a role in the disruption of tight junctions.

Inhibition of the Na^+/K^+-ATPase (also discussed in chapter 4), which shares a high sequence homology to the H^+/K^+-ATPase, by ES products could also be a possible mechanism. The inhibition of Na^+/K^+-ATPase was shown to affect the distribution of ZO-1 and occludin (Contreras *et al.*, 1999). In addition, the possible inhibition of the H^+/K^+-ATPase by ES products (Simpson *et al.*, 1999; Hertzberg *et al.*, 2000; Merkelbach *et al.*, 2002) could also be involved in the disruption of the barrier *in vivo*. It was demonstrated that chronic inhibition (5d) of the H^+/K^+-ATPase by omeprazole in rabbit gastric mucosa

enhanced parietal cell degeneration, which was accompanied by macrophage invasion (Karam and Forte, 1994). Macrophage invasion was proposed as a mechanism to eliminate degenerated parietal cells. Moreover, Mullin *et al.* (2007) reported that an eight-week course of the proton pump inhibitor esomeprazole in gastroesophageal reflux disease patients induced a transepithelilal leak in the upper gastrointestinal tract.

The immune system may also be involved in tight junction opening *in vivo*. McDermott *et al.* (2003) showed that mast cells are involved in increasing epithelial paracellular permeability. Permeability was increased and occludin translocated and degraded in *T. spiralis* infection of the small intestine. In the absence of mast cells or mast cell protease I, permeability did not increase. Previously, using an *ex vivo* perfusion model Scudamore *et al.* (1995) demonstrated that soluble adult *N. brasiliensis* antigen triggered the release of mast cell protease II and moreover, purified mast cell protease II was able to increase permeabilty. Mast cell tryptase is also an activating protease for PAR2 (see above) (Vergnolle, 2005). Increased mucosal mast cell responses are also observed in *T. circumcincta* infections and are suggested as a mechanism for regulating worm numbers (Stear *et al.*, 2003).

Increased expression of cytokines and MMPs during the host inflammatory response could also be a possible factor. Several cytokines, including IFN-γ, TNF-α, HGF, TGF-α and several interleukins (IL-1, -4, -6, -13) , were reported to increase paracellular permeability in a variety of mechanisms, but this also depends on the context (Sawada *et al.*, 2003; González-Marsical *et al.*, 2007; Yu and Turner, 2008; Capaldo and Nusrat, 2009), for example, IFN-γ, TNF-α and HGF increased permeability in some cell lines, but decreased permeability in others (Capaldo and Nusrat, 2009). Mechanisms to increase permeability include downregulation of tight junction proteins, MLC posphorylation and actin reorganisation (Yu and Turner, 2008; Capaldo and Nusrat, 2009). Additionally, it was demonstrated that MMPs were able to degrade claudin-5 and occludin (Rosenberg and Yang, 2007) and translocate occludin and ZO-1 (Tan *et al.*, 2005). Epithelial cells also produce cytokines and MMPs. Secretion of IL-6 and -8 (Hosoi *et al.*, 2003) and MMP-2 and -9 (Li and Shan, 2005) was shown in CaCo-2 cells in response to pathogenic and non-pathogenic bacteria or HGF, respectively. This could also be a possible mechanism of tight junction disruption in the *in vitro* model. Apart from direct effects of ES products on tight

junctions, exposure to ES products might also trigger the release of cytokines and/or MMPs, which in turn have an effect. Determination of cytokine and MMP secretion of CaCo-2 cells in response to ES products could clarify whether this is a possible mechanism.

In summary, the experiments described in this chapter clearly demonstrate that ES products of *H. contortus* are able to reduce the TEER and ES products of both *H. contortus* and *T. circumcincta* to disrupt the distribution of the tight junctional proteins occludin and ZO-1 in CaCo-2 cells. This could also be a possible mechanism *in vivo*. Occludin and ZO-1 also appeared to be differently distributed in infected tissue compared with uninfected tissue. However, further experiments would be needed to assess the effects and mechanisms *in vitro* and *in vivo* and the nature of the responsible factor(s).

Chapter 6

GENERAL DISCUSSION

The work presented in this thesis was aimed at investigating host-parasite interactions during abomasal parasitism with *H. contortus* or *T. circumcincta*. An important aspect was the mechanism by which these abomasal nematodes might disrupt the normal function of the parietal cell resulting in the development of hypoacidity. A major focus was on investigating potential roles of ES products, which was conducted *in vitro* and may relate to *in vivo* observations. The examination included possible roles for ES products in the induction of vacuolation and cell loss, which is observed in parietal cells *in vivo*. In addition, effects of ES products on the tight junctional barrier were investigated as a possible mechanism for protein loss and pepsinogenaemia during parasitism.

In vivo, the fate of the parietal cell was examined via histological studies of tissue derived from sheep after transplantation of adult *T. circumcincta*, using TGF-α and H^+/K^+-ATPase antibodies. Lectin staining as an additional marker for parietal cells was not successful, although parietal cell staining with lectins has been reported (Malchiodi Albedi *et al.*, 1985; Kessiman *et al.*, 1986; Callaghan *et al.*, 1990; 1992). Staining parietal cells for TGF-α and

H^+/K^+-ATPase, parietal cell numbers were decreased 12h and 72h after the transplant compared with the control, which was similar to previous studies (Scott *et al.*, 2000; Przemeck, 2003). The main finding of the experiments presented here was that 72h after the transplant, numbers of TGF-α positive and H^+/K^+-ATPase positive parietal cells differed markedly with the population of H^+/K^+-ATPase positive parietal cells being decreased compared with TGF-α positive parietal cells. This could indicate that a sequence of events might lead to hypoacidity with the H^+/K^+-ATPase being lost first before parietal cells are lost. Loss of the H^+/K^+-ATPase might be sufficient to initially increase abomasal pH without a major change in parietal cell numbers, which are then lost later in infection. Similarly, increases in H^+/K^+-ATPase expression without increase in parietal cell numbers might be involved in the fast recovery of acid secretion after drenching, before parietal cell numbers recover. Parietal cell numbers in sheep infected with adult *T. circumcincta* did not recover within seven days after drenching (Scott *et al.*, 2000).

Vacuolation of parietal cells was observed previously in abomasal tissue sections of sheep infected with *T. circumcincta* larvae and after adult worm transfer (Scott *et al.*, 1998a; 2000; Przemeck, 2003) and was also observed in the presented study. Various studies, *in vivo* and *in vitro*, have now been conducted which suggested that a parasite-derived factor could be involved with the decreased parietal function (Eiler *et al.*, 1981; Simpson *et al.*, 1997; 1999; Merkelbach *et al.*, 2002). However, the involvement of a parasite-factor is only presumed and it has to be noted that for all *in vitro* experiments, reported previously and presented in this thesis, the concentration of ES products, which originate from incubations of huge densities of worms, is very likely much higher compared with ES concentrations present in the abomasum. *In vitro* experiments presented here have also shown that the vacuolating ability of ES preparations starts to decrease with 4-fold dilution of the *in vitro* incubations and ES concentrations are likely to be even lower *in vivo*. Alternatively to a parasite-derived factor, there is also evidence that the inflammatory response of the host might be involved in parietal cell loss (Scott *et al.*, 1998a; 2000). However, an association between cellular vacuolation and inflammation has not yet been evident. Moreover, ES products were shown to induce vacuolation in HeLa cells *in vitro* (Huber *et al.*, 2005; Przemeck *et al.*, 2005).

These *in vitro* experiments of Huber *et al.* (2005) and Przemeck *et al.* (2005) also demonstrated that larval ES preparations of *H. contortus* or *T. circumcincta* induce less severe effects than adult ES preparations. However, *in vivo* ES products are released from a larva inside a gland to a very confined area and the ES concentration in direct vicinity to the cells might be very high.

Experiments presented here further characterised the vacuolation *in vitro* as well as the vacuolating factor(s). ES products were able to induce vacuolation in different epithelial cell lines with vacuolation taking place in the first two hours after exposure to ES products, which demonstrated that cell damage due to ES products can occur very quickly and could be a possible factor in the rapid changes observed in abomasal function and morphology due to adult parasites (Lawton *et al.*, 1996; Simpson *et al.*, 1997; 1999; Scott *et al.*, 2000). ES-induced vacuolation was also partly reversible, but with ~30% of the cells still vacuolated 48h after the withdrawal of ES preparations. It is not clear whether vacuolation was reduced because of increasing cell numbers due to normal cell proliferation, but this seemed likely. Some of the vacuolated cells could also possibly have been detached and lost, although this seems not been linked to the observed vacuolation as vacuolated cells usually appeared viable (also see below). However, vacuolation *in vitro* appears to be different from that observed in parietal cells *in vivo* and it remains speculative whether ES products are involved *in vivo*. ES products generated *in vivo* might also be different in composition and amounts released compared with *in vitro* generated ES preparations since *in vitro* conditions are very different from the natural environment of the worms. Furthermore, differences in ES preparations were even noted in successive *in vitro* incubations.

An interesting result from the experiments characterising the vacuolating factor present in *H. contortus* ES products was the finding that the ability to induce vacuolation in HeLa cells differed markedly for ES preparations generated via successive incubation periods, reflecting changes in the release of ES products during *in vitro* incubations. Vacuolating ability dropped notably after the first incubation periods, followed by a gradual increase in

vacuolating ability concomitant with loss of worm viability. The vacuolating activity was highest in samples collected after all worms had died, indicating that either increased amounts of ES products or other worm constituents, which were also able to induce vacuolation, were released from dying and degrading worms. If ES products are involved in inducing parietal cell vacuolation *in vivo*, this could indicate that not only alive worms contribute to the observed histopathology, but components released by dying and degrading worms may also partly contribute. Although, dying worms will detach from the mucosa and be removed from the abomasum.

Low concentrations of lipids were detected in ES products via SDS-PAGE and TLC, however extracted lipids from the TLC were not able to induce vacuolation demonstrating that it is very unlikely that the lipid compounds detected are involved in vacuole formation in HeLa cells. Another interesting finding from the experiments characterising the vacuolating factor was that the vacuolating factor(s) is most likely a protein as it was heat and acid sensitive, reducing vacuolation ability markedly after the respective treatment of the ES preparation. The acid sensitivity to pH 2 is of special interest as abomasal pH of uninfected control sheep averaged between pH 2 and 3 (Simpson *et al.*, 1997; 1999; Scott *et al.*, 2000). After infection with *T. circumcincta*, which were shown to induce similar vacuoles *in vitro* (Przemeck *et al.*, 2005), increased vacuolation of parietal cells *in vivo* occurred as early as 5d after larval infection (Przemeck, 2003), around the time the parasites emerge into the lumen after development for 5-6 days (Armour *et al.*, 1966; 1981; Anderson *et al.*, 1976; Lawton *et al.*, 1996), or 12h after adult transplant, which was reported by Przemeck (2003) and observed in the experiments presented here. The abomasal pH might not represent the pH in the vicinity of the worms and a vacuolating factor in ES products might still be active and responsible for the vacuolation. Alternatively, this could also suggest that vacuoles are not directly induced by ES products. Vacuoles observed in parasitised tissues appear to be different from those *in vitro* and were suggested to be due to necrosis (Scott *et al.*, 2000).

ES products were further analysed *in vitro* for their ability to induce cell detachment or cell loss. The loss of parietal cells during abomasal parasitism has been observed *in vivo* (Scott *et*

al., 1998a; 2000; Przemeck, 2003), which could possibly be mediated by ES products. Huber *et al.* (2005) and Przemeck *et al.* (2005) noted that exposure of HeLa cells to ES preparations appeared to increase the rate of cell detachment. *In vitro* experiments described in this thesis to quantify the rate of cell detachment showed a similar trend in the results with decreased cell numbers after exposure to ES preparations compared with control cells, however, the variation was high. Staining of the actin cytoskeleton revealed a decreased content of stress fibres or less conspicuous stress fibre staining. Fibrillar actin structures were also often visible on the edges of detaching cells. Simultaneous staining of the nuclei showed an increased number of degenerating nuclei and apoptotic bodies after exposure to ES products, which could indicate that an increased rate of apoptosis is responsible for the increased rate of cell detachment. Another possibility is that apoptosis follows cell detachment, a process which in anchorage-dependent cells is termed anoikis. *In vivo* and *in vitro*, both apoptosis and anoikis are possible mechanisms of cell detachment or cell loss and it needs to be further examined how cells are lost.

It is also not clear whether it is the same factor that is causing vacuolation and cell detachment or whether cell detachment might be a result of the vacuolation. Karam *et al.* (2003) reported that *in vivo* parietal cells occasionally degenerate with extensive dissolution of canaliculi and intermitochondrial cytoplasm with the formation of vacuoles. Although, *in vitro* it seems that cell detachment and cell loss may not be a result of vacuolation. Very often cells were heavily vacuolated but appeared otherwise normal and showed no signs of cell detachment, which can also be seen as fibrillar structures on the cell edges in bright field images. This is consistent with results from Huber *et al.* (2005). They demonstrated that HeLa cells exposed to *H. pylori* OMV or adult *H. contortus* ES products were viable despite being heavily vacuolated.

Furthermore, *in vitro* experiments undertaken to investigate the ability of ES products to disrupt the tight junctional barrier clearly showed that ES products of both *H. contortus* and *T. circumcincta* were able to do so, but ES products from *T. circumcincta* were less effective. Staining of the tight junction proteins occludin and ZO-1 changed markedly after exposure to ES products, with decreases in membrane-associated staining and simultaneously

increasing intracellular punctate staining. In addition, for *H. contortus* ES products, it was shown that ES exposure resulted in significant decreases in TEER.

Taken together with the other experiments with HeLa and AGS cells, these results suggest that it seems very unlikely that the disruption of the tight junctions leads to the observed cell detachment since both HeLa and AGS cells detached, but do not form tight junctions. However, this might also be different *in vivo*, where opening of tight junctions might lead to other events including vacuolation, cell loss and leakage of proteins such as pepsinogen into serum, but also leakage of proteins into the gastrointestinal tract.

Tight junctions might also play a role in the development of other pathological changes observed during abomasal parasitism. Opening of the tight junctions increases the exposure to bacteria, toxins and luminal antigens potentially present in abomasal contents, which could also be a factor in increased inflammatory responses as seen in inflammatory bowl disease (Clayburgh *et al.*, 2004). Furthermore, Suzuki *et al.* (2000) demonstrated that the serosal side of fundic mucosa was more sensitive to ammonia than the luminal side. Ammonia applied *in vitro* to the serosal side resulted in comparably greater decreases of TEER and more severe vacuolation in all cell types of the gland with numerous small vacuoles in surface mucous cells and large vacuoles in parietal cells, which was also the case when applied on the luminal side of injured mucosa. Similarly, it has been previously shown by Boron *et al.* (1994) that gastric gland cells are unaffected by 2.7mM ammonia applied to the apical but not basolateral membrane. Although it was shown in previous studies (Huber *et al.*, 2005; Przemeck *et al.*, 2005) and in experiments described here that the ammonia concentrations in ES products were very low and are therefore unlikely to be involved in the observed pathology, it is possible that other ES products might have more detrimental effects on the serosal/basolateral side of the epithelium, which is exposed after disruption of the tight junctions.

Stear *et al.* (2003) hypothesised that a key event in the pathogenesis in *T. circumcincta* infected sheep is the destruction of cell junctions, which was suggested to apply also to *O. ostertagi*

infected cattle and might also explain some of the pathology of *H. contortus* infected sheep. It was proposed that parasite derived molecules trigger mast cell degranulation releasing mast cell proteases, which have been shown to increase epithelial paracellular permeability (Scudamore *et al.,* 1995; McDermott *et al.,* 2003). However, experiments presented here clearly demonstrated for the first time that parasite ES products of both *H. contortus* and *T. circumcincta* are also capable of directly targeting tight junctions and possibly might act together with the inflammatory response *in vivo*. In addition to mast cell proteases, several cytokines have been shown to increase paracellular permeability (Sawada *et al.*, 2003; González-Marsical *et al.*, 2007; Yu and Turner, 2008; Capaldo and Nusrat, 2009), some of which are also able to interfere with acid secretion (Lord *et al.*, 1991; Robert *et al.*, 1991; Prinz *et al.*, 1997; Yasunaga *et al.*, 1997).

In vivo, it seems likely that parasite-derived factors and the inflammatory response potentiate each other leading to the observed pathophysiology and histopathology. The opening of the tight junctions seems likely to be a key event as previously hypothesised (Stear *et al.*; 2003), which then leads to further damage by ES products penetrating the mucosal barrier but also other noxious components potentially present in abomasal contents. It is possible that opening of the tight junctions also allows inhibition of parietal cells deeper in the glands, which is possibly also linked to the disruption of cell-cell and cell-matrix adhesion as parietal cells cannot function when separated from adjacent cells.

References

Abe, S., Sasano, H., Katoh, K., Ohara, S., Arikawa, T., Noguchi, T., Asaki, S., Yasui, W., Tahara, E., Nagura, H. and Toyota, T. (1997) Immunohistochemical studies on EGF family growth factors in normal and ulcerated human gastric mucosa. *Digestive Diseases and Science* **42**, 1199-1209.

Abner, S. R., Hill, D. E., Turner, J. R., Black, E. D., Bartlett P., Urban, J. F. and Mansfield, L. S. (2002) Response of intestinal epithelial cells to *Trichuris suis* excretory-secretory products and the influence on *Campylobacter jejuni* invasion under *in vitro* conditions. *Journal of Parasitology* **88** (4), 738-745.

Aguirre-García, M. M., Anaya-Ruiz, M. and Talamás-Rohana, P. (2003) Membrane-bound acid phosphatase (MAP) from *Entamoeba histolytica* has phosphotyrosine phosphatase activity and disrupts the actin cytoskeleton of host cells. *Parasitology* **126**, 195-202.

Akagi, K., Nagao, T. and Urushidani, T. (2001) Reconstitution of acid secretion in digitonin-permeabilized rabbit gastric glands - Identification of cytosolic regulatory factors. *Journal of Biological Chemistry* **276** (30), 28171-28178.

Aktories, K. and Barbieri, J. T. (2005) Bacterial cytotoxins: targeting eukaryotic switches. *Nature Reviews Microbiology* **3**, 397-410.

Alberts, B., Bray, D., Lewis, J., Raff, M., Roberts, K. and Watson, J. D. (1995) *Molekularbiologie der Zelle, 3. Auflage*. Wiley-VCH.

Al-Sadi, R. M. and Ma, T. Y. (2007) IL-1beta causes an increase in intestinal epithelial tight junction permeability. *The Journal of Immunology* **178**, 4641-4649.

Anaya-Ruiz, M., Pérez-Santos, J. L. M., Talamás-Rohana, P. (2003) An ecto-protein tyrosine phosphatase of *Entamoeba histolytica* induces cellular detachment by disruption of actin filaments in HeLa cells. *International Journal for Parasitology* **33**, 663-670.

Anderson, N. G. and Hanson, P. J. (1985) Involvement of calcium-sensitive phospholipid-dependent protein-kinase in control of acid-secretion by isolated rat parietal cells. *Biochemical Journal* **232** (2), 609-611.

Anderson, N., Armour, J., Jennings, F. W., Ritchie, J. S. D. and Urquhart, G. M. (1965) Inhibited development of *Ostertagia ostertagi*. Veterinary Record 77, 146-147, in *Nematode parasites of vertebrates: their development and transmission* (2000), Chapter 3 Order Strongylida (the Bursate Nematodes), pp 41-229. CABI Publishing.

Anderson, N., Blake, R. and Titchen, D. A. (1976) Effects of a series of infections of *Ostertagia circumcincta* on gastric secretion of the sheep. *Parasitology* **72**, 1-12.

Anderson, N., Hansky, J. and Titchen, D. A. (1985) Effects on plasma pepsinogen, gastrin and pancreatic polypeptide of *Ostertagia* spp. transferred directly into the abomasum of sheep. *International Journal for Parasitology* **15**, 159-165.

Anderson, R. C. (2000) Chapter 3 Order Strongylida (the Bursate Nematodes). In *Nematode parasites of vertebrates: their development and transmission*, pp 41-229. CABI Publishing.

Andrews, S. J., Hole, N. J. K., Munn, E. A. and Rolph, T. P. (1995) Vaccination of sheep against haemonchosis with H11, a gut membrane-derived protective antigen from the adult parasite: prevention of the periparturient rise and colostral transfer of protective immunity. *International Journal for Parasitology* **25** (7), 839-846.

Armour, J., Jarrett, W. F. H. and Jennings, F. W. (1966) Experimental *Ostertagia circumcincta* infections in sheep: development and pathogenesis of a single infection. *American Journal of Veterinary Research* **27**, 1267-1278.

Armour, J., Jennings, F. W., Kirkpatrick, K. S., Malezewski, A., Murray, M. and Urquhart, G. M. (1967) The use of thiabendazole in bovine ostertagiasis: treatment of experimental Type I disease. *Veterinary Record* **80**, 510-514.

Asahara, M., Mushiake, S., Shimada, S., Fukui, H., Kinoshita, Y., Kawanami, C., Watanabe, T., Tanaka, S., Ichikawa, A., Uchiyama, Y., Narushima, Y., Takasawa, S., Okamoto, H., Tohyama, M. and Chiba, T. (1996) Reg gene expression is increased in rat gastric enterochromaffin-like cells following water immersion stress. *Gastroenterology* **111**, 45-55.

Asano, S., Kawada, K., Kimura, T., Grishin, A. V., Caplan, M. J. and Takeguchi, N. (2000) The roles of carbohydrate chains of the beta-subunit on the functional expression of gastric H^+,K^+-ATPase. *Journal of Biological Chemistry* **275** (12), 8324-8330.

Athmann, C., Zeng, N., Scott, D. R. and Sachs, G. (2000) Regulation of parietal cell calcium signaling in gastric glands. *American Journal of Physiology Gastrointestinal and Liver Physiology* **279**, G1048-G1058.

Bado, A., Moizo, L., Laigneau, J. P., Delwaide, J. and Lewin, M. J. (1994) H3-receptor regulation of vascular gastrin and somatostatin releases by the isolated rat stomach. *Yale Journal of Biology and Medicine* **67**, 113-121.

Baermann, G. (1917) Eine einfache Methode zur Auffindung von *Ancylostomum* (Nematoden) Larven in Erdproben. *Geneeskundig Tijdschrift voor Nederlandsch Indie* **57**, 131-137.

Bakker, N., Velverde, L., Kanobana, K., Knox, D. P., Cornelissen, A. W. C. A., de Vries, E. and Yatsuda A. P. (2004) Vaccination against the nematode *Haemonchus contortus* with a thiol-binding fraction from the excretory/secretory products (ES). *Vaccine* **22**, 618-628.

Balic, A., Bowles, V. M., Liu, Y. S. and Meeusen M. T. (2003) Local immune responses in sensitized sheep foloowing challenge infection with *Teladorsagia circumcincta*. *Parasite Immunology* **25**, 375-381.

Barker, I. K., Van Dreumal, A. A., Palmer, N. (1993) The alimentary system. Infectious diseases of the gastrointestinal tract. Gastrointestinal helminthosis. In *Pathology of domestic animals (4th ed.)* Eds. Jubb, K. V. F., Kennedy, P.C. and Palmer, N., pp258-295. San Diego, Academic Press.

Beales, I. L. P. (2000) Acid secretion in *H. pylori* associated enlarged fold gastritis. *Gut* **47**, 313-315.

Beales, I. L. P. (2004) Gastrin and interleukin-1beta stimulate growth factor secretion from cultured rabbit gastric parietal cells. *Life Sciences* **75**, 2983-2995.

Beauchamp, R. D., Barnard, J. A., McCutchen, C. M., Cherner, J. A. and Coffey, R. J. Jr. (1989) Localization of transforming growth factor alpha and its receptor in gastric mucosal cells. *Journal of Clinical Investigation* **84**, 1017-1023.

Becker, H. D., Reeder, D. D. and Thompson, J. C. (1973) The effect of changes in antral pH on the basal release of gastrin. *Proceedings of the Society of Experimental Biology and Medicine* **143**, 238-240

Beglinger, C., Hildebrand, P., Meier, R., Bauerfeind, P., Hasslocher, H., Urscheler, N., Delco, F., Eberle, A. and Gyr, K. (1992) A physiological role for cholecystokinin as a regulator of gastrin secretion. *Gastroenterology* **103** (2), 490-495.

Beil, W., Mannschedel, W. and Sewing, K. F. (1987) Protein kinase C and parietal cell function. *Biochemical and Biophysical Research Communications* **149** (2), 720-728.

Belusa, R., Aizman, O., Andersson, R. M. and Aperia, A. (2002) Changes in Na^+-K^+-ATPase activity influence cell attachment to fibronectin. *American Journal of Physiology Cell Physiology* **282**, C302-309.

Bergmann, S., Rohde, M., Chhatwal, G. S. and Hammerschmidt, S. (2001) Alpha-enolase of *Streptococcus pneumoniae* is a plasmin(ogen)-binding protein displayed on the bacterial cell surface. *Molecular Microbiology* **40** (6), 1273-1287.

Bernal, D., de la Rubia, J. E., Carrasco-Abad, A. M., Toledo, R., Mas-Coma, S. and Marcilla. A. (2004) Identification of enolase as a plasminogen-binding protein in excretory–secretory products of *Fasciola hepatica*. *FEBS Letters* **563** (1-3), 203-206.

Berrier, A. L. and Yamada, K. M. (2007) Cell-matrix adhesion. *Journal of Cellular Physiology* **213** (3), 565-573.

Bhaskar, K. R., Garik, P., Turner, B. S., Bradley, J. D., Bansil, R., Stanley, H. E. and LaMont, J. T. (1992) Viscous fingering of HCI through gastric mucin. *Nature* **360** (6403), 458-461.

Billadeau, D. D., Nolz, J. C. and Gomez, T. S. (2007) Regulation of T-cell activation by the cytoskeleton. *Nature Reviews Immunology* **7**, 131-143.

Blair, A. J. III, Richardson, C. T., Walsh, J. H. and Feldman, M. (1987) Variable contribution of gastrin to gastric acid secretion after a meal in humans. *Gastroenterology* **92**, 944-949.

Blitz, N. M. and Gibbs, H. C. (1972a) Studies on the arrested development of *Haemonchus contortus* in sheep I. The induction of arrested development. International Journal for Parasitology 2, 5-12, in *Nematode parasites of vertebrates: their development and transmission* (2000), Chapter 3 Order Strongylida (the Bursate Nematodes), pp 41-229. CABI Publishing.

Blitz, N. M. and Gibbs, H. C. (1972b) Studies on the arrested development of *Haemonchus contortus* in sheep II. Termination of arrested development and the spring rise phenomenon. International Journal for Parasitology 2, 13-22, in *Nematode parasites of vertebrates: their development and transmission* (2000), Chapter 3 Order Strongylida (the Bursate Nematodes), pp 41-229. CABI Publishing.

Blonder, J., Terunuma, A., Conrads, T. P., Chan, K. C., Yee, C., Lucas, D. A., Schaefer, C. F., Yu, L.-R., Issaq, H. J., Veenstra, T. D. and Vogel, J. C. (2004) A proteomic characterization of the plasma membrane of human epidermis by high-throughput mass spectrometry. The *Journal of Investigative Dermatology* **123**, 691-699.

Bolleter, W. T., Bushman, C. J and Tidwell, P. W. (1961) Spectrophotometric determination of ammonia as indophenol. *Analytical Chemistry* **33** (4), 592-594.

Bordi, C., D'Adda, T., Azzoni, C. and Ferraro, G. (2000) Classification of gastric endocrine cells at the light and electron microscopical levels. *Microscopy Research and Technique* **48**, 258-271.

Boron, W. F., Waisbren, S. J., Modlin, I. M. and Geibel, J. P. (1994) Unique permeability barrier of the apical surface of parietal and chief cells in isolated perfused gastric glands. *The Journal of experimental Biology* **196**, 347-360.

Bowman, D. D. (2003) *Georgis' parasitology for veterinarians*, 8th edition. Saunders.

Bradford, M. M. (1976) A rapid and sensitive method for the quantitation of microgram quantities of protein utilizing the principle of protein-dye binding. *Analytical Biochemistry* **72**, 248-254.

Brattig, N. W., Büttner, D. W. and Hoerauf, A. (2001) Neutrophil accumulation around *Onchocerca* worms and chemotaxis of neutrophils are dependent on *Wolbachia* endobacteria. *Microbes and Infection* **3** (6), 439-46.

Brindley, P. J., Kalinna, B. H., Wong, J. Y. M., Bogitsh, B. J., King, L. T., Smyth, D. J., Verity, C. K., Abbenante, G., Brinkworth, R. I., Fairlie, D. P., Smythe, M. L., Milburn, P. J., Bielefeldt-Ohmann, H., Zheng, Y. and McManus, D. P. (2001) Proteolysis of human hemoglobin by schistosome cathepsin D. *Molecular and Biochemical Parasitology* **112** (1), 103-112.

Britch, M. and Allen, T. D. (1980) The modulation of cellular contractility and adhesion by trypsin and EGTA. *Experimental Cell Research* **125**, 221-231.

Brown, E. M. and MacLeod, R. J. (2001) Extracellular calcium sensing and extracellular calcium signaling. *Physiological Reviews* **81** (1), 239-297.

Brown, M. R. and Chew, C. S. (1987) Multiple effects of phorbol ester on secretory activity in rabbit gastric glands and parietal cells. *Canadian Journal of Physiology and Pharmacology* **65** (9), 1840-1847.

Buchan, A. M. J., Sikora, L. K. J., Levy, J. G., McIntosh, C. H. S., Dyck, I. and Brown, J. C. (1985) An immunocytochemical investigation with monoclonal antibodies to somastatin. *Histochemistry and Cell Biology* **83** (2), 175-180.

Buesen, R., Mock, M., Seidel, A., Jacob, J. and Lampen, A. (2002) Interaction between metabolism and transport of benzo[*a*]pyrene and its metabolites in enterocytes. *Toxicology and Applied Pharmacology* **183**, 168-178.

Calafat, J., Janssen, H., Ståhle-Bäckdahl, M., Zuurbier, A. E., Knol, E. F. and Egesten, A. (1997) Human monocytes and neutrophils store transforming growth factor-alpha in a subpopulation of cytoplasmic granules. *Blood* **90** (3), 1255-66.

Callaghan, J. M., Toh, B.-H., Pettitt, J. M., Humphris, D. C. and Gleeson, P. A. (1990) Poly-N-acetyllactosamine-specific tomato lectin interacts with gastric parietal cells. *Journal of Cell Science* **95**, 563-576.

Callaghan, J. M., Toh, B.-H., Simpson, R. J., Baldwin, G. S. and Gleeson, P. A. (1992) Rapid purification of the gastric H^+/K^+-ATPase complex by tomato-tectin affinity chromatography. *The Biochemical Journal* **283**, 63-68.

Cancela, M., Carmona, C., Rossi, S., Frangione, B., Goñi, F. and Berasain, P. (2004) Purification, characterization, and immunolocalization of paramyosin from the adult stage of *Fasciola hepatica*. *Parasitology Research* **92**, 441-448.

Candela, M., Miccoli, G., Bergmann, S., Turroni, S., Vitali, B., Hammerschnidt, S. and Brigidi, P. (2008) Plasminogen-dependent proteolytic activity in *Bifidobacterium lactis*. *Microbiology* **154**, 2457-2462.

Canfield V., West A. B., Goldenring J. R. and Levenson, R. (1996) Genetic ablation of parietal cells in transgenic mice: A new model for analyzing cell lineage relationships in the gastric mucosa *Proceedings of the National Academy of Sciences of the United States of America* **93**, 2431-2435.

Canfield, V. A., Okamoto, C. T., Chow, D., Dorfman, J., Gros, P., Forte, J. G, and Levenson, R. (1990) Cloning of the H,K-ATPase beta subunit. Tissue-specific expression, chromosamal assignment, and relationship to Na,K-ATPase beta subunits. *Journal of Biological Chemistry* **265** (32), 19878-19884.

Capaldo, C. T. and Nusrat, A. (2009) Cytokine regulation of tight junctions. *Biochimica et Biophysica Acta* **1788**, 864-871.

Carragher, N. O. and Frame, M. C. (2004) Focal adhesion and actin dynamics: a place where kinases and proteases meet to promote invasion. *Trends in Cell Biology* **14** (5), 241-249.

Černý, H., Mazánek, S. and Černá, E. (1991) Immunohistochemical localization of endocrine G-cells in the epithelium of the pars pylorica mucosa of the cat and mouse stomach. *Acta Veterinaria Brno* **60** (4), 317-322.

Chen, D., Zhao, C. M., Dockray, G. J., Varro, A., Van Hoek, A., Sinclair, N. F., Wang, T. C. and Koh, T. J. (2000) Glycine-extended gastrin synergizes with gastrin 17 to stimulate acid secretion in gastrin deficient mice. *Gastroenterology* **119** (3), 756-765.

Chen, M. C., Goliger, J., Bunnett, N. and Soll, A. H. (2001) Apical and basolateral EGF receptors regulate gastric mucosal paracellular permeability. *American Journal of Physiology Gastrointestinal and Liver Physiology* **280**, G264-G272.

Cheng, I., Qureshi, I., Chattopadhyay, N., Qyreshi, A., Butters, R. R., Hall, A. E., Cima, R. R., Rogers, K. V., Hebert, S. C., Geibel, J. P., Brown, E. M. and Soybel, D. I. (1999) Expression of an extracellular calcuim-sensing receptor in rat stomach. *Gastroenterology* **116**, 118-126.

Chew, C. S. (1994) Parietal cell culture: new models and directions. *Annual Review of Physiology* **56**, 445-461.

Chew, C. S. and Brown, M. R. (1986) Release of intracellular Ca^{2+} and elevation of inositol triphophate by secretagogues in parietal and chief cells isolated from rabbit gastric mucosa. *Biochemica et Biophysica Acta* **888**, 116-125.

Chew, C. S. and Brown, M. R. (1987) Histamine increases phosphorylation of 27- and 40-kDa parietal cell proteins. *American Journal of Physiology Gastrointestinal and Liver Physiology* **253** (6), G823-829.

Chew, C. S., Nakamura, K. and Petropoulos, A. C. (1994) Multiple actions of epidermal growth factor and TGF-alpha on rabbit gastric parietal cell function. *American Journal of Physiology Gastrointestinal and Liver Physiology* **267**, G818-G826.

Chew, C. S., Parente, J. A. Jr., Zhou, C.-J., Baranco, E. and Chen, X. (1998) Lasp-1 is a regulated phosphoprotein within the cAMP signaling pathway in the gastric parietal cell. *American Journal of Physiology Cell Physiology* **275** (1), C56-67.

Chew, C. S., Parente, J. A., Chen, X., Chaponnier, C. andCameron, R. S. (2000) The LIM and SH3 domain-containing protein, lasp-1, may link the cAMP signaling pathway with dynamic membrane restructuring activities in ion transporting epithelia. *Journal of Cell Science* **113** (11), 2035-2045.

Chiba, T., Fisher, S. K., Agranoff, B. W. and Yamada, T. (1989) Autoregulation of muscarinic and gastrin receptors on gastric parietal cells. *American Journal of Physiology Gastrointestinal and Liver Physiology* **256** (2), G356-363.

Chilton, N. B., Huby-Chilton, F., Gasser, R. B. and Beveridge, I. (2006) The evolutionary origins of nematodes within the order strongylida are related to predilection sites within hosts. *Molecular Phylogenetics and Evolution* **40**, 118-128.

Chow, D. C. and Forte, J. G. (1995) Functional significance of the beta-subunit for heterodimeric P-type ATPases. *Journal of Experimental Biology* **198**, 1-17.

Chow, D. C., Browning, C. M. and Forte, J. G. (1992) Gastric H(+)-K(+)-ATPase activity is inhibited by reduction of difulfide bonds in beta-subunit. *American Journal of Physiology Cell Physiology* **263**, C39-46.

Christie, M. G. (1970) The fate of very large doses of *Haemonchus contortus* and their effect on conditions in the ovine abomasum. *Journal of Comparative Pathology* **80**, 89-100.

Chuang, C. N., Chen, M. C. and Soll, A. H. (1991) Gatsrin-histamine interactions: direct and paracrine elements. *Scandinavian Journal of Gastroenterology* **26 (suppl. 180)**, 95-103.

Clark, E. A. and Brugget, J. S. (1995) Integrins and signal transduction pathways: the road taken. *Science* **268**, 233-239.

Clayburgh, D. R., Shen, L. and Turner, J. R. (2004) A porous defense: the leaky epithelial barrier in intestinal disease. *Laboratory Investigation* **84**, 282-291.

Cliffe, L. J., Potten, C. S., Booth, C. E. and Grencis, R. K. (2007) An increase in epithelial cell apoptosis is associated with chronic intestinal nematode infection. *Infection and Immunity* **75** (4), 1556-1564.

Contreras, R. G., Shoshani, L., Flores-Maldonado, C., Lázaro, A. and Cereijido, M. (1999) Relationship between Na^+-K^+-ATPase and cell attachment. *Journal of Cell Science* **112**, 4223-4232.

Coop, R. L. and Kyriazakis, I. (1999) Nutrition-parasite interaction. *Veterinary Parasitology* **84**, 187-204.

Coulton, G. R. and Firth, J. A. (1983) Cytochemical evidence for functional zonation of parietal cells within the gastric glands of the mouse. *Histochemical Journal* **15**, 1141-1150.

Cover , T. L. and Blanke, S. R. (2005) *Helicobacter pylori* VacA, a paradigm for toxin multifunctionality. *Nature Reviews Microbiology* **3** (4), 320-332.

Cover, T. L. (1996) The vacuolating cytotoxin of *Helicobacter pylori*. *Molecular Microbiology* **20** (2), 241-246.

Cover, T. L., Krishna, U. S., Israel, D. A. and Peek, R. M. Jr. (2003) Induction of gastric epithelial cell apoptosis by *Helicobacter pylori* vacuolating cytotoxin. *Cancer Research* **63**, 951-957.

Cover, T. L., Puryear, W., Perez -Perez, G. I. and Blaser, M. J. (1991) Effect of urease on HeLa cell vacuolation induced by *Helicobacter pylori* cytotoxin. *Infection and Immunity* **59**, 1264-1270.

Cox, K. H., Adair-Kirk, T. L. and Cox, J. V. (1996) Variant AE2 anion exchanger transcripts accumulate in multiple cell types in the chicken gastric epithelium. *Journal of Biological Chemistry* **271** (15), 8895-8902.

Craig, H., Wastling, J. M. and Knox, D. P. (2006) A preliminary proteomic survey of the in vitro excretory/secretory products of fourth-stage larval and adult *Teladorsagia circumcincta*. *Parasitology* **132**, 535-543.

Creutzfeldt, W., Arnold, R., Creutzfeldt, C., Feurle, G. and Ketterer, H. (1971) Gastrin and G-cells in the antral mucosa of patients with pernicious anaemia. Acromegaly and hyperparathyroidism and in a Zollinger-Ellison tumour of the pancreas. *European Journal of Clinical Investigation* **1**, 461-479.

Crothers, J. M. Jr., Asano, S., Kimura, T., Yoshida, A., Wong, A., Kang, J. W. and Forte, J. G. (2004) Contribution of oligosaccharides to protection of the H,K-ATPase beta-subunit against trypsinolysis. *Electrophoresis* **25**, 2586-2592.

Crothers, J. M. Jr., Chow, D. C. and Forte, J. G. (1993) Omeprazole decreases H(+)-K(+)-ATPase protein and increases permeability of oxyntic secretory membranes in rabbits. *American Journal of Physiology Gastrointestinal and Liver Physiology* **265**, G231-G241.

Cui, G., Takaishi, S., Ai, W., Betz, K. S., Florholmen, J., Koh, T. J., Houghton, J., Pritchard, D. M. and Wang, T. C. (2006) Gastrin-induced apoptosis contributes to carcinogenesis in the stomach. *Laboratory Investigation* **86**, 1037-1051.

Cybulski, W. and Andren, A. (1990) Immunohistochemical studies on the development of cells containing progastricsin (minor pepsinogen) in comparison to prochymosin and pepsinogen in bovine abomasal mucosa. *Anatomical Record* **227**, 458-463.

Darmoul, D., Gratio, V., Devaud, H., Lehy, T. and Laburthe, M. (2003) Aberrant expression and activation of the thrombin receptor protease-activated receptor-1 induces cell proliferation and motility in human colon cancer cells. *American Journal of Pathology* **162**, 1503-1513.

daSilva, R. G. and Minomo, F. R. (1995) Circadian and seasonal variation of the body temperature of sheep in a tropical environment. *International journal of biometeorology* **39**, 69-73.

Daugschies, A. and Joachim, A. (2000) Eicosanoids in parasites and parasitic infections. *Advances in Parasitology* **46**, 181-240.

Davis, G. E., Pintar Allen, K. A., Salazar, R. and Maxwell, S. A. (2001) Matrix metalloproteinase-1 and -9 activation by plasmin regulates a novel endothelial cell-mediated mechanism of collagen gel contraction and capillary tube regression in three-dimensional collagen matrices. *Journal of Cell Science* **114**, 917-930.

De Giorgio, R., Su, D., Peter, D., Edwards, R. H., Brecha, N. C. and Sternini C. (1996) Vesicular monoamine transporter 2 expression in enteric neurons and enterochromaffin-like cells of the rat. *Neuroscience Letters* **217** (2-3), 77-80.

Debas, H. and Carvajal, S. H. (1994) Vagal regulation of acid secretion and gastrin release. *Yale Journal of Biology and Medicine* **67**, 145-151.

Debas, H. T., Walsh, J. H. and Grossman, M. I. (1975) Evidence for oxyntopyloric reflex for release of antral gastrin. *Gastroenterology* **68**, 687-690.

Delvalle, J., Tsunoda, Y., Williams, J. A. and Yamada, T. (1992) Regulation of [Ca2+]i by secretagogue stimulation of canine gastric parietal cells. *American Journal of Physiology Gastrointestinal and Liver Physiology* **262**, G420-G426.

Dempsey, P. J., Goldenring, J. R., Soroka, C. J., Modlin, I. M., McClure, R. W., Lind, C. D., Ahlquist, D. A., Pittelkow, M. R., Lee, D. C., Sandgren, E. P., Page, D. L. and Coffey, R. J. (1992) Possible role of transforming growth factor alpha in the pathogenesis of Ménétrier's disease: supportive evidence from humans and transgenic mice. *Gastroenterology* **103**, 1950-1963.

Derynck, R. (1988) Transforming growth factor-alpha. *Cell* **54**, 593-595.

Deutzmann, R. (2008/2009) Zell-Matrix-Interaktion, Einführung, in *Extrazelluläre Matrix und Zell-Matrix-Interaktion*, Wintersemester 2008/2009 Zellbiologie- Vorlesung: Zell-Zell- und Zell-Matrix-Interaktion - Folien, Vorlesungen, accessed 21 June 2009, from http://www.biologie.uni-regensburg.de/Biochemie/Deutzmann/mainframe.htm.

DiDonato, J. A., Hayakawa, M., Rothwarf, D. M., Zandi, E. and Karin, M. (1997) A cytokine-responsive I kappa B kinase that activates the transcription factor NF-kappa B. *Nature* **388** (6642), 548-554.

Dockray, G. J. and Gregory, R. A. (1989) Gastrin. In *Handbook of Physiology, Section 6*, Vol. 2 (ed. G. M. Makhlouf), pp. 311-336. American Physiological Society, Bethseda.

Dockray, G. J. and Tracy, H. J. (1980a) Atropine does not abolish cephalic vagal stimulation of gastrin release in dogs. *Journal of Physiology* **306**, 473-480.

Dockray, G. J. and Tracy, H. J. (1980b) Atropine-resistant cephalic stimulation of gastrin release in dogs. *Journal of Physiology* **298**, 46P.

Dockray, G. J., Varro, A. and Dimaline, R. (1996) Gastric endocrine cells: gene expression, processing, and targeting of active products. *Physiological Reviews* **76**, 767-798.

Dufner, M. M., Kirchhoff, P., Remy, C., Hafner, P., Müller, M. K., Cheng, S. X., Tang, L.-Q., Hebert, S. C., Geibel, J. P. and Wagner, C. A. (2005) The calcium-sensing receptor acts as a modulator of gastric acid secretion in freshly isolated human gastric glands. *American Journal of Physiology Gastrointestinal and Liver Physiology* **289**, G1084-G1090.

Duman, J. G., Pathak, N. J., Ladinsky, M. S., McDonald, K. L. and Forte, J. G. (2002) Three-dimensional reconstruction of cytoplasmic membrane networks in parietal cells. *Journal of Cell Science* **115** (6), 1251-1258.

Dunsmore, J. D. (1960) Retarded development of *Ostertagia* species in sheep. *Nature* **186**, 986-987.

Durette-Desset, M. C., Hugot, J. P., Darlu, P. and Chabaud, A. G. (1999) A cladistic analysis of the Trichostrongyloidea (Nematoda). *International Journal for Parasitology* **29**, 1065-1086.

Durham, P. J. K. and Elliott, D. C. (1976) Experimental *Ostertagia* spp. infection of sheep: development of worm populations and lesions resulting from different dose-levels of larvae. *Veterinary Parasitology* **2**, 157-166.

DuVal, J. W., Saffouri, B., Wier, G. C., Walsh, J. H., Arimura, A. and Makhlouf G. M. (1981) Stimulation of gastrin and somatostatin secretion from the isolated rat stomach by bombesin. *American Journal of Physiology Gastrointestinal and Liver Physiology* **241**, G242-G247.

Eiler, H., Baber, W., Lyke, W. A. and Scholtens, R. (1981) Inhibition of gastric hydrochloric acid secretions in the rat given *Ostertagia ostertagi* (a gastric parasite of cattle) extract. *American Journal of Veterinary Research* **42**, 498-502.

Elliott, D. C. (1974a) Experimental *Ostertagia* infection of sheep: worm populations resulting from single and multiple larval doses. *New Zealand Journal of Experimental Agriculture* **2**, 109-113.

Elliott, D. C. (1974b) Experimental *Ostertagia* infection of sheep: worm populations resulting from single larval doses. *New Zealand Journal of Experimental Agriculture* **2**, 103-107.

Elovic, A., Galli, S. J., Weller, P. F., Chang, A. L., Chiang, T., Chou, M. Y., Donoff, R. B., Gallagher, G. T., Matossian, K. and McBride, J. (1990) Production of transforming growth factor alpha by hamster eosinophils. *American Journal of Pathology* **13**,1425-1434.

Esgleas, M., Li, Y., Hancock, M. A., Harel, J., Dubreuil, J. D. and Gottschalk, M. (2008) Isolation and characterization of alpha-enolase, a novel fibronectin-binding protein from *Staphylococcus suis*. *Microbiology* **154**, 2668-2679.

Eubel, H., Braun, H.-P. and Millar, A. H. (2005) Blue-native PAGE in plants: a tool in analysis of protein-protein interactions. *Plant Methods* **1** (1), 11.

Fabry, T. L. (1990) How the parietal secretion crosses the gastric mucus without being neutralized. *Gastroenterology* **98**, A42.

Fedwick, J. P., Lapointe, T. K., Meddings, J. B., Sherman, P. M. and Buret, A. G. (2005) *Helicobacter pylori* activates Myosin Light-Chain kinase to disrupt claudin-4 and claudin-5 and increase epithelial permeability. *Infection and Immunity* **72** (12), 7844-7852.

Ferreira, V., Valck, C., Sánchez, G., Gingras, A., Tzima, S., Molina, M. C., Sim, R., Schwaeble, W. and Ferreira, A. (2004) The classical activation pathway of the human complement system is specifically inhibited by calreticulin from *Trypanosoma cruzi*. *Journal of Immunology* **172** (5), 3042-3050.

Fetterer, R. H. and Rhoads, M. L. (2000) Characterization of acid phosphatase and phosphorylcholine hydrolase in adult *Haemonchus contortus*. *Journal of Parasitology* **86** (1), 1-6.

Figarella, K., Rawer, M., Uzcategui, N. L., Kubata, B. K., Lauber, K., Madeo, F., Wesselborg, S. and Duszenko, M. (2005) Prostaglandin D2 induces programmed cell death in *Trypanosoma brucei* bloodstream form. *Cell Death and Differentiation* **12**, 335-346.

Figarella, K., Uzcategui, N. L., Beck, A., Schoenfeld, C., Kubata, B. K., Lang, F. and Duszenko, M. (2006) Prostaglandin-induced programmed cell death in *Trypanosoma brucei* involves oxidative stress. *Cell Death and Differentiation* **13**, 1802-1814.

Fiorucci, S., Lanfrancome, L., Santucci, L., Calabro, A., Orsini, B., Federici, B. and Morelli, A. (1996) Epidermal growth factor modulates pepsinogen secretion in guinea pig gastric chief cells. *Gastroenterology* **111** (4), 945-58.

Flemstrom, G. (1994) Gastric and duodenal mucosal bicarbonate secretion. In *Physiology of the Gatrointestinal Tract (3rd ed.)* (ed. L.R. Johnson), pp1285-1309. Raven press, Inc, New York.

Forgac, M. (1999) Structure and Properties of the Vacuolar (H^+)-ATPases. *Journal of Biological Chemistry* **274** (19), 12951-12954.

Förster, C. (2008) Tight junctions and the modulation of barrier function in disease. *Histochemistry and Cell Biology* **130**, 55-70.

Forte, J. G. and Lee, H. C. (1977) Gastric adenosine triphosphatase: a review of their possible role in HCl secretion. *Gastroenterology* **73**, 921-926.

Forte, J. G. and Soll, A. H. (1989) Cell biology of hydrochloric acid secretion. In *Handbook of Physiology*, Chapter 11 (Sect. 6), pp207-228. American Physiological Society, Oxford University Press.

Forte, J. G. and Wolosin, J. M. (1987) HCl secretion by the gastric oxyntic cell. In *Physiology of the Gatrointestinal Tract(2nd ed.)* (ed. L.R. Johnson), pp853-863. Raven Press, Inc., New York.

Forte, J. G. and Yao, X. (1996) The membrane-recruitment-and-recycling hypothesis of gastric HCl secretion. *Trends in Cell Biology* **6**, 45-48.

Fox, J. G., Li, X., Cahill, R. J., Andrutis, K., Rustgi, A. K., Odze, R. and Wang, T. C. (1996) Hypertrophic gastropathy in Helicobacter felis - Infected wild-type C57BL/6 mice and p53 hemizygous transgenic mice. *Gastroenterology* **110** (1), 155-166.

Fox, M. T. (1997) Pathophysiology of infection with gastrointestinal nematodes in domestic ruminants: recent developments. *Veterinary Parasitology* **72**, 285-308.

Fox, M. T., Carroll, A. P., Hughes, S. A., Uche, U. E., Jacobs, D. E. and Vaillant, C. (1993) Gastrin and gastrin-related responses to infection with *Ostertagia ostertagi* in the calf. *Research In Veterinary Science* **54**, 384-391.

Fox, M. T., Gerrelli, D., Pitt, S. R., Jacobs, D. E., Gill, M. and Gale, D. L. (1989a) *Ostertagia ostertagi* infection in the calf: effects of a trickle challenge on appetite, digestibility, rate of passage of digesta and liveweight gain. *Research In Veterinary Science* **47**, 294-298.

Fox, M. T., Gerrelli, D., Pitt, S. R., Jacobs, D. E., Gill, M. and Simmonds, A. D. (1989b) *Ostertagia ostertagi* infection in the calf: effects of a trickle challenge on the hormonal control of digestive and metabolic function. *Research In Veterinary Science* **47**, 299-304.

Fox, M. T., Pitt, S. R., Gerrelli, D., Jacobs, D. E., Adhikari, D. R. and Goddard, P. J. (1988) Use of blood gastrin assay in the diagnosis of ovine haemonchiasis. *Veterinary Record* **122**, 136-137.

Friis-Hansen, L., Sundler, F., Li, Y., Gillespie, P. J., Saunders, T. L., Greenson, J. K., Owyang, C., Rehfeld, J. F. and Samuelson, L. C. (1998) Impaired gastric acid secretion in gastrin-deficient mice. *American Journal of Physiology Gastrointestinal and Liver Physiology* **274**, G561-G568.

Frisch, S. M. and Francis, H. (1994) Disruption of epithelial cell-matrix interactions induces apoptosis. *The Journal of Cell Biology* **124** (4), 619-626.

Fuchs, E. and Raghavan, S. (2002) Getting under the skin of epidermal morphogenesis. *Nature Reviews Genetics* **3**, 199-209.

Fujikawa, A., Shirasaka, D., Yamamoto, S., Ota, H., Yahiro, K., Fukada, M., Shintani, T., Wada, A., Aoyama, N., Hirayama, T., Fukamachi, H. and Noda, M. (2001) Mice deficient in protein tyrosine phosphatase receptor type Z are resistant to gastric ulcer induction by VacA of *Helicobacter pylori*. *Nature Genetics* **33**, 375-381.

Fujita, A., Horio, Y., Nielsen, S., Nagelhus, E. A., Hata, F., Ottersen, O. P. and Kurachi,Y. (1999) High-resolution immunogold cytochemistry indicates that AQP4 is concentrated along the basal membrane of parietal cell in rat stomach. *FEBS Letters* **459**, 305-309.

Fukui, H., Kinoshita, Y., Maekawa, T., Okada, A., Waki, S., Hassan, M. D. S., Okamoto, H. and Chiba, T. (1998) Regenerating gene protein may mediate gastric mucosal proliferation induced by hypergastrinemia in rats. *Gastroenterology* **115**, 1483-1493.

Furuta, T., Baba, S., Takashima, M., Shirai, F., Xiao, F., Futami, H., Arai, H., Hanai, H. and Kaneko, E. (1999) H+/K+-adenosine triphosphatase mRNA in gastric fundic gland mucosa in patients intfected with *Helicobacter pylori*. *Scandinavian Journal of Gastroenterology* **34**, (4), 384-390.

Fyfe, M., Bergström, M., Aspengren, S. and Peterson, A. (2005) PAR-2 activation in intestinal epithelial cells potentiates interleukin-1beta-induced chemokine secretion via MAP kinase signaling pathways. *Cytokine* **31** (5), 358-367.

Gamble, H. R. and Mansfield, L. S. (1996) Characterisation of excretory-secretory products from larval stages of *Haemonchus contortus* cultured in vitro. *Veterinary Parasitology* **62**, 291-305.

Ganser, A. L. and Forte, J. G. (1973) K^+-stimulated ATPase in purified microsomes of bullfrog oxyntic cells. *Biochimica et Biophysica Acta* **307**, 169-180.

Garner, A., Flemstrom, G., Allen, A., Heylings, J. R. and McQueen, S. (1984) Gastric mucosal protective mechanisms: roles of epithelial bicarbonate and mucus secretions. *Scandinavian Journal of Gastroenterology* **101 (suppl.)**, 79-86.

Garner, J. A. and Cover, T. L. (1996) Binding and internalization of the *Helicobacter pylori* vacuolating cytotoxin by epithelial cells. *Infection and Immunity* **64** (10), 4197-4203.

Geldorf, P. and Knox, D. P. (2008) The intestinal concortin structure in *Haemonchus contortus*: an immobilised anticoagulant? *International Journal for Parasitology* **38**, 1579-1588.

Giancotti, F. G. and Ruoslahti, E. (2001) Integrin signaling. *Science* **285**, 1028-1032.

Giaume, C. and McCarthy, K. D. (1996) Control of gap-junctional communication in astrocytic networks. *Trends in Neurosciences* **19** (8), 319-325.

Gibbs, H. C. (1986) Hypobiosis in parasitic nematodes - an update. Advances in Parasitology 25, 129-174, in *Nematode parasites of vertebrates: their development and transmission* (2000), Chapter 3 Order Strongylida (the Bursate Nematodes), pp 41-229. CABI Publishing.

Gibson, S., Tu, S., Oyer, R., Anderson, S. M. and Johnson, G. L. (1999) Epidermal growth factor protects epithelial cells against Fas-induced apoptosis. *The Journal of Biological Chemistry* **274** (25), 17612-17618.

Gobert, G. N. and McManus, D. P. (2005) Update on paramyosin in parasitic worms. *Parasitology International* **54**, 101-107.

Goicoechea, S., Pallero, M. A., Eggleton, P., Michalak, M. and Murphy-Ullrich, J. E. (2002) The anti-adhesive activity of thrombospondin is mediated by the N-terminal domain of cell surface calreticulin. *The Journal of Biological Chemistry* **277** (40), 37219-37228.

Gonzáles-Mariscal, L., Lechuga, S. and Garay, E. (2007) Role of tight junctions in cell proliferation and cancer. *Progress in Histochemistry and Cytochemistry* **42**, 1-57.

Gonzáles-Marsical, L., Tapia, R. and Chamorro, D. (2008) Crosstalk of tight junction components with signaling pathways. *Biochimica et Biophysica Acta* **1778**, 729-756.

Gounaris, K., Thomas, S., Najarro, P. and Selkirk, M. E. (2001) Secreted variant of nucleoside diphosphate kinase from the intracellular parasitic nematode *Trichinella spiralis*. *Infection and Immunity* **69** (6), 3658-3662.

Greenhalgh, C. J., Loukas, A., Donald, D., Nikolaou, S. and Newton, S. E. (2000) A family of galectins from *Haemonchus contortus*. *Molecular and Biochemical Parasitology* **107**, 117-121.

Grütter, M. G., Fendrich, G., Huber, R. and Bode, W. (1988) The 2.5 Å X-ray crystal structure of the acid-stable proteinase inhibitor from human mucous secretions analysed in its complex with bovine alpha-chymotrypsin. *The EMBO Journal* **7** (2), 345-351.

Guillemot, L., Paschoud, S., Pulimeno, P., Foglia, A. and Citi, S. (2008) The cytoplasmic plaque of tight junctions: a scaffolding and signalling center. *Biochimica et Biophysica Acta* **1178**, 601-613.

Guyer, D. M., Henderson, I. R., Nataro, J. P. and Mobley, H. L. T. (2000) Identification of Sat, an autotransporter toxin produced by uropathogenic *Escherichia coli*. *Molecular Microbiology* **38** (1), 53-66.

Guyer, D. M., Radulovic, S., Jones, F.-E. and Mobley, H. T. L. (2002) Sat, the secreted autotransporter toxin of uropathogenic *Escherichia coli,* is a vacuolating cytotoxin for bladder and kidney epithelial cells. *Infection and Immunity* **70** (8), 4539-4546.

Haag, E., Lawton, D. and Simpson H. V. (2005) The failure of *Haemonchus contortus* excretory/secretory products to stimulate gastrin secretion *in vitro*. *Parasitology Research* **95**, 155-160.

Hadari, Y. R., Arbel-Goren, R., Levy, Y., Amsterdam, A., Alon, R., Zakut, R. and Zick, Y. (2000) Galectin-8 binding to integrins inhibits cell adhesion and induces apoptosis. *Journal of Cell Science* **113**, 2385-2397.

Hadás, E., Rabel, B. and Stankiewicz, M. (1998) The isolation and identification of prostaglandins of *Trichostrongylus colubriformis* and *Haemonchus contortus*. *Acta Parasitologica* **43** (3), 167-170.

Håkanson, R., Chen, D., Andersson, K., Monstein, H.-J., Zhao, C. M., Ryberg, B., Sundler, F. and Mattsson, H. (1994) The biology and physiology of the ECL cell. *Yale Journal of Biology and Medicine* **67**, 123-134.

Hanson, P. J. and Hatt, J. F. (1989) Intracellular signalling and regulation of gastric acid secretion. Quarterly Journal of *Experimental Physiology* **74** (5), 607-34.

Hanzel, D. K., Urushidani, T., Usinger, W. R., Smolka, A. and Forte, J. G. (1989) Immunological localization of an 80-kDa phosphoprotein to the apical membrane of gastric parietal cells. *American Journal of Physiology Gastrointestinal and Liver Physiology* **256** (6), G1082-1089.

Hanzel, D., Reggio, H., Bretscher, A., Forte, J. G. and Mangeat, P. (1991) The secretion-stimulated 80K phosphoprotein of parietal cells is ezrin, and has properties of a membrane cytoskeletal linker in the induced apical microvilli. *The EMBO Journal* **10** (9), 2363-2373.

Harburger, D. S. and Calderwood, D. A. (2009) Integrin signalling at a glance. *Journal of Cell Science* **122**, 159-163.

Harlan, J. M. (1985) Leukocyte-endothelial interactions. *Blood* **65**, 513-525.

Harrison, G. B. L., Pulford, H. D., Hein, W. R., Severn, W. B. and Shoemaker, C. B. (2003) Characterization of a 35-kDa carbohydrate larval antigen (CarLA) from *Trichostrongylus colubriformis*; a potential target for host immunity. *Parasite Immunology* **25**, 79-86.

Hartner, A., Schöcklmann, H., Pröls, F., Müller, U. and Sterzel, R. B. (1999) Alpha8 integrin in glomerular mesangial cells and in experimental glomerulonephritis. *Kidney International* **56**, 1468-1480.

Helander, H. F. and Hirschowitz, B. I. (1972) Quantitative ultrastructural studies on gastric parietal cells. *Gastroenterology* **63**, 951-961.

Helander, H. F. and Hirschowitz, B. I. (1974) Quantitative ultrastructural studies on inhibited and on partly stimulated gastric parietal cells. *Gastroenterology* **67,** 447-452.

Helenius, A. and Simons, K. (1975) Solubilization of membranes by detergents. *Biochimica et Biophysica Acta* **415**, 29-79.

Henkle-Dührsen, K. and Kampkötter, A. (2001) Antioxidant enzyme families in parasitic nematodes. *Molecular and Biochemical Parasitology* **114**, 129-142.

Herbert, S., Cheng, S. and Geibel, J. (2004) Functions and roles of the extracellular Ca^{2+}-sensing receptor in the gastrointestinal tract. *Cell Calcium* **35**, 239-247.

Hersey, S. J. (1989) Cellular basis of pepsinogen secretion. In *Handbook of Physiology, section 6. The Gastrointestinal System*, Vol. III (eds. Schultz, S. G. and Makhlouf, G. M.), pp. 267-278. American Physiological Society, Bethesda.

Hersey, S. J. and Sachs, G. (1995) Gastric acid secretion. *Physiological Reviews* **75**, 155-189.

Hertzberg, H., Guscetti, F., Lischer, C., Kohler, L., Neiger, R. and Eckert, J. (2000) Evidence for a parasite-mediated inhibition of abomasal acid secretion in sheep infected with *Ostertagia leptospicularis*. *Veterinary Journal* **159**, 238-251.

Hertzberg, H., Kohler, H., Deplazes, P., Häcki, W. H. and Eckert, J. (1995) Pathophysiological studies of sheep during the build-up of immunity against *Ostertagia leptospicularis* and after a challenge infection. *Research In Veterinary Science* **58**, 14-19.

Hertzberg, H., Lindström, E., Chen, D. and Håkanson, R. (1999a) Excretory/secretory products of *Haemonchus contortus* suppress stimulation of parietal cells by inhibiting secretory activity of enterochromaffine-like (ECL) cells. In *Proceedings of the 17th International Conference of the World Association for the Advancement of Veterinary Parasitology*, pp. a.2.02, Copenhagen.

Hertzberg, H., Schallig, H. D. F. H. and Deplazes, P. (1999b) Development of a protective immunity against *Ostertagia leptospicularis* in trickle-infected sheep and parallel changes of serum gastrin, pepsinogen and antibody levels. *Veterinary Journal* **157**, 148-159.

Hewitson, J. P., Harcus, Y. M., Curwen, R. S., Dowle, A. A., Atmadja, A. K., Wilson, A. and Maizels R. M. (2008) The secretome of the filarial parasite, *Brugia malayi*: proteomic profile of adult excretory-secretory products. *Molecular and Biochemical Parasitology* **160**, 8-21.

Hewitt, K. J., Agarwal, R. and Morin, P. J. (2006) The claudin gene family: expression in normal and neoplastic tissues. *BMC Cancer* **6**, 186.

Higham, A. D., Bishop, L. A., Dimaline, R., Blackmore, C. G., Dobbins, A. C., Varro, A., Thompson, D. G. and Dockray, G. J. (1999) Mutations of *Reg*Ialpha are associated with enterochromaffin-like cell tumor development in patients with hypergastrinemia. *Gastroenterology* **116**, 1310-1318.

Hill, K. L. and L'Hernault, S. W. (2001) Analyses of Reproductive Interactions That Occur after Heterospecific Matings within the Genus *Caenorhabditis*. Developmental Biology, 232 (1), 105-114.

Hirashima, M. (2000) Ecalectin/Galectin-9, a novel eosinophil chemoattractant: its function and production. *International Archives of Allergy and Immunology* **122 (suppl. 1)**, 6-9.

Hirschowitz, B. I. (1984) Pepsinogen. *Postgraduate Medical Journal* **60,** 743-750.

Hirschowitz, B. I. (1989) Neural and hormonal control of gastric secretion. In *Handbook of Physiology, sect. 6*, vol. III (ed. S. G. Schultz), pp. 127-157. American Physiology Society, Bethseda.

Hirschowitz, B. I. and Fong, J. (1990) Effects of antral vagotomy in dogs on gastrin and gastric secretion with various stimuli. *American Journal of Physiology Gastrointestinal and Liver Physiology* **258**, G919-G925.

Holmes, P. H. (1985) Pathogenesis of trichostrongylosis. *Veterinary Parasitology* **18** (2), 89-101.

Holmes, P. H. (1993) Interactions between parasites and animal nutrition: the veterinary consequences. *Proceedings of the Nutrition Society* **52**, 113-120.

Holmes, P. H. and MacLean, J. M. (1971) The pathophysiology of ovine ostertagiasis: a study of the changes in plasma protein metabolism following single infections. *Research In Veterinary Science* **12**, 265-271.

Honde, C. B. L. and Bueno L. (1982) *Haemonchus contortus*: Egg laying influenced by abomasal pH in lambs. *Experimental Parasitology* **54**, 371-378.

Hosoi, T., Hirose, R., Saegusa, S., Ametani, A., Kiuchi, K. and Kaminogawa, S. (2003) Cytokine responses of human intestinal epithelial-like Caco-2 cells to the nonpathogenic bacterium *Bacillus subtilis* (natto). *International Journal of Food Microbiology* **82**, 255-264.

Hoste, H., Nano, J. L., Mallet, S., Huby, F., Fournel, S. and Rampal, P. (1995) Stimulation of HT29-D4 cell growth by excretory/secretory products of the parasite nematode *Trichostrongylus colubriformis*. *Epithelial Cell Biology* **4**(2), 87-92.

Huber, A., Prosl, H., Joachim, A., Simpson, H. V. and Pedley, K. C. (2005) Effects of excretory/secretory products of *Haemonchus contortus* on cell vacuolation. *Parasitology Research* **96**, 290-295.

Huby, F., Hoste, H., Mallet, S., Fournel, S. and Nano, J. L. (1995) Effects of the excretory/secretory products of six nematode species, parasites of the digestive tract, on the proliferation of HT29-D4 and HGT-1 cell lines. *Epithelial Cell Biology* **4** (4), 156-162.

Huby, F., Nano, J. L., Mallet, S. and Hoste, H. (1999) Effects of the excretory/secretory products of *Trichostrongylus colubriformis* on the growth of different cell lines. *International Journal for Parasitology* **29**, 697-702.

Hueck, C. H. (1998) Type III protein secretion systems in bacterial pathogens of animals and plants. *Microbiology and Molecular Biology Reviews* **62** (2), 379-433.

Hughes, R. C. (2001) Galectins as modulators of cell adhesion. *Biochimie* **83**, 667-676.

Humphries, M. J., McEwan, P. A., Barton, S. J., Buckley, P. A., Bella, J. and Mould, A. P. (2003) Integrin structure: heady advances in ligand binding, but activation still makes the knees wobble. *Trends in Biochemical Science* **28** (6), 313-320.

Hurmalainen, V., Edelman, S., Antikainen, J., Baumann, M., Lähteenmäki, K. and Korhonen, T. K. (2007) Extracellular proteins of *Lactobacillus crispatus* enhance activation of human plasminogen. *Microbiology* **153**, 1112-1122.

Hüsken, R. (2007) *Identifikation, Expression und Antigencharakterisierung von Paramyosin des Hakenwurms Ancylostoma caninum*. Dissertation, Tierärztliche Hochschule Hannover, Germany.

Ichikawa, T., Endoh, H., Hotta, K. and Ishihara, K. (2000) The mucin biosynthesis stimulated by epidermal growth factor occurs in surface mucus cells, but not in gland mucus cells, of rat stomach. *Life Sciences* **67** (9), 1095-101.

Ingebritsen, T. S. (1989) Phosphotyrosyl-Protein Phosphatases II. Identification and characterization of two heat-stable protein inhibitors. *The Journal of Biological Chemistry* **264** (13), 7754-7759.

International Federation for Animal Health IFAH (2007) Animal health market - 2007 animal health industry. In *IFAH Representing the Animal Health Industry*, accessed 18 June 2009, from http://www.ifahsec.org/Industry/animal_health_market.htm#

Ito, S. (1981) Functional gastric morphology. In *Physiology of the Gastrointestinal Tract* (ed. L.R. Johnson), pp517-550. Raven Press, Inc., New York.

Ito, S. (1987) Functional gastric morphology. In *Physiology of the Gatrointestinal Tract (2nd ed.)* (ed. L.R. Johnson), pp817-851. Raven Press, Inc, New York.

Ito, S. and Schofield, G. C. (1974) Studies on the depletion and accumulation of microvilli and changes in the tubulovesicular compartment of mouse parietal cells in relation to gastric acid secretion. *Journal of Cell Biology* **63**, 364-382.

Ivanov, A. I., Nusrat, A. and Parkos, C. A. (2004) Endocytosis of epithelial apical junctional proteins by a clathrin-mediated pathway into a unique storage compartment. *Molecular Biology of the Cell* **15**, 176-188.

Ivanov, A. I., Nusrat, A. and Parkos, C. A. (2005) Endocytosis of the apical junctional complex: mechanisms and possible roles in regulation of epithelial barriers. *BioEssays* **27**, 356-365.

Jacobsen, J. V. and Shaw, D. C. (1989) Heat-stable proteins and abscisic acid action in barley aleurone cells. *Plant Physiology* **91**, 1520-1526.

Jasmer, D. P., Roth, J. and Myler, P. J. (2001) Cathepsin B-like cysteine proteases and *Caenorhabditis elegans* homologues dominate gene products expressed in adult *Haemonchus contortus* intestine. *Molecular and Biochemical Parasitology* **116**, 159-169.

Jenkins, R. E., Taylor, M. J., Gilvary, N. J. and Bianco, A. E. (1998) Tropomyosin implicated in host protective responses to microfilariae in onchocerciasis. *Proceedings of the National Academy of Sciences of the United States of America* **93**, 7550-7555.

Jennings, F. W., Armour, J., Lawson, D. D. and Roberts, R. (1966) Experimental *Ostertagia ostertagi* infections in calves: studies with abomasal cannulas. *American Journal of Veterinary Research* **27**, 1249-1257.

Johnson, L. R. (1976) The trophic action of gastrointestinal hormones. *Gastroenterology* **70**, 278-288.

Johnson, L. R. (1988) Regulation of gastrointestinal mucosal growth. *Physiological Reviews* **68**, 456-502.

Johnson, S., Michalak, M., Opas, M. and Eggleton, P. (2001) The ins and outs of calreticulin: from the ER lumen to the extracellular space. *Trends in Cell Biology* **11** (3), 122-129.

Johnston, M. J. G., MacDonald, J. A. and McKay, D. M. (2009) Parasitic helminths: a pharmacopeia of anti-inflammatory molecules. *Parasitology* **136**, 125-147.

Jolodar, A., Fischer, P., Bergmann, S., Büttner, D. W., Hammerschmidt, S. and Brattig, N. W. (2003) Molecular cloning of an alpha-enolase from the human filarial parasite *Onchocerca volvulus* that binds human plasminogen. *Biochimica et Biophysica Acta* **1627** (2-3), 111-120.

Jones, M. K., Tomikawa, M., Mohajer, B. and Tarnawski, A. S. (1999) Gastrointestinal mucosal regeneration: Role of growth factors. *Frontiers in Bioscience* **4**, d303-309.

Jones, N. L., Day, A. S., Jennings, H. A. and Sherman, P. M. (1999) *Helicobacter pylori* induces gastric epithelial cell apoptosis in association with increased Fas receptor expression. *Infectiona and Immunity* **67** (8), 4237-4242.

Jons, T. and Drenckhahn, D. (1998) Anion exchanger 2 (AE2) binds to erythrocyte ankyrin and is colocalised with ankyrin along the basolateral plasma membrane of human gastric parietal cells. *European Journal of Cell Biology* **75** (3), 232-236.

Joshi, P. and Singh, B. P. (2000) Purification and characterization of a cholinesterase from *Haemonchus contortus*. *Indian Journal of Biochemistry and Biophysics* **37** (3), 192-197.

Kalita, J., Ranjan, P. and. Misra, U. K (2003) Current status of osmotherapy in intracerebral hemorrhage. *Neurology India* **51** (1), 104-109.

Kaminsky, R., Gauvry, N., Schorderet Weber, S., Skripsky, T., Bouvier, J., Wenger, A., Schroeder, F., Desaules, Y., Hotz, R., Goebel, T., Hosking, B. C., Pautrat, F., Wieland-Berghausen, S. and Ducray, P. (2008) Identification of the amino-acetonitrile derivative monepantel (AAD 1566) as a new anthelmintic drug development candidate. *Parasitology Research* **103**, 931-939.

Kaminsky, R., Mosimann, D., Sager, H., Stein, P. and Hosking, B. (2009) Determination of the effective dose rate for monepantel (AAD 1566) against adult gastro-intestinal nematodes in sheep. *International Journal for Parasitology* **39**, 443-446.

Kanai, M., Konda, Y., Nakajima, T., Izumi, Y., Takeuchi, T. and Chiba, T. (2001) TGF-alpha inhibits apoptosis of murine gastric pit cells through an NF-kappaB-dependent pathway. *Gatroenterology* **121**, 56-67.

Kaplan, R. M. (2004) Drug resistance in nematodes of veterinary importance: a status report. *Trends in Parasitology* **20** (10), 477-481.

Kaplan, R. M. (2008) Emerging research fronts - 2008, April 2008, Ray M. Kaplan interview with ScienceWatch.com. In *ScienceWatch.com*, accessed 07 June 2009, from http://sciencewatch.com/dr/erf/2008/08aprerf/08/aprerfKap1/

Kapur, S. P. (1982) An ultrastructural and cytochemical study of enteroendocrine cells of the pyloric antrum in the gerbil, *Meriones unguiculatus*. *Acta Anatomica* **112** (3), 220-232.

Karam, S. M. (1993) Dynamics of epithelial cells in the corpus of the mouse stomach. IV. Bidirectional migration of parietal cells ending in their gradual degeneration and loss. *The Anatomical Record* **236**, 314-332.

Karam, S. M. (1999) Lineage commitment and maturation of epithelial cells in the gut. *Frontiers in Bioscience* **4**, d286-298.

Karam, S. M. and Alexander, G. (2001) Blocking of histamine H2 receptors enhances parietal cell degeneration in the mouse stomach. *Histology and Histopathology* **16** (2), 469-480.

Karam, S. M. and Forte, J. G. (1994) Inhibiting gastric H^+-K^+-ATPase activity by omeprazole promotes degeneration and production of parietal cells. *American Journal of Physiology Gastrointestinal and Liver Physiology* **266** (4), G745-G758.

Karam, S. M. and Leblond, C. P. (1992) Identifying and counting epithelial cell types in the "corpus" of the mouse stomach. *The Anatomical Record* **232**, 231-246.

Karam, S. M. and Leblond, C. P. (1993a) Dynamics of epithelial cells in the corpus of the mouse stomach. I. Identification of proliferative cell types and pinpointing of the stem cell. *The Anatomical Record* **236**, 259-279.

Karam, S. M. and Leblond, C. P. (1993b) Dynamics of epithelial cells in the corpus of the mouse stomach. II. Outward migration of pit cells. *The Anatomical Record* **236**, 280-296.

Karam, S. M. and Leblond, C. P. (1993c) Dynamics of epithelial cells in the corpus of the mouse stomach. III. Inward migration of neck cells followed by progressive transformation into zymogenic cells. *The Anatomical Record* **236**, 297-313.

Karam, S. M. and Leblond, C. P. (1993d) Dynamics of epithelial cells in the corpus of the mouse stomach. V. Behavior of entero-endocrine and caveolated cells: general conclusions on cell kinetics in the oxyntic epithelium. *The Anatomical Record* **236**, 333-340.

Karam, S. M., Straiton, T., Hassan, W. M. and Leblond, C. P. (2003) Defining epithelial progenitors in the human oxyntic mucosa. *Stem Cells* **21**, 322-336.

Karam, S. M., Yao, X. and Forte, J. G. (1997) Functional heterogeneity of parietal cells along the pit-gland axis. *American Journal of Physiology Gastrointestinal and Liver Physiology* **272**, G161-G171.

Kasper, G., Brown, A., Eberl, M., Vallar, L., Kieffer, N., Berry, C., Girdwood, K., Eggleton, P., Quinnell, R. and Pritchard, D. I. (2001) A calreticulin-like molecule from the human hookworm *Necator americanus* interacts with C1q and the cytoplasmic signalling domains of some integrins. *Parasite Immunology* **23** (3), 141-152.

Kaunitz, J. D. (1999) Barrier function of gastric mucus. *The KeioJournal of Medicine* **48** (2), 63-68.

Kazumori, H., Ishihara, S., Fukuda, R. and Kinoshita, Y. (2002) Localization of Reg receptor in rat fundic mucosa. *The Journal of Laboratory and Clinical Medicine* **139** (2), 101-108.

Kessiman, N., Langner, B. J., McMillan, P. N. and Jauregui, H. O. (1986) Lectin binding to parietal cells of human gastric mucosa. *The Journal of Histochemistry and Cytochemistry* **34** (2), 237-243.

Kimura, T., Yoshida, A., Tabuchi, Y., Ikari, A., Takeguchi, N. and Asano, S. (2002) Stable expression of gastric proton pump activity at the cell surface. *The Journal of Biochemistry* **131** (6), 923-932.

Kirchhofer, D., Grzesiak, J. and Pierschbacher, M. D. (1991) Calcium as a potential physiological regulator of integrin-mediated cell adhesion. *The Journal of Biological Chemistry* **266** (7), 4471-4477.

Kirfel, G., Rigort, A., Borm, B. and Herzog, V. (2004) Cell migration: mechanisms of rear detachment and the formation of migration tracks. *European Journal of Cell Biology* **83**, 717-724.

Kirton, C. M., Wang, T. and Dockray, G. J. (2002) Regulation of parietal cell migration by gastrin in the mouse. *American Journal of Physiology Gastrointestinal and Liver Physiology* **283**, G787-G793.

Kittelberger, R. and Hilbink, F. (1993) Sensitive silver-staining detection of bacterial lipopolysaccharides in polyacrylamide gels. *Journal of Biochemical and Biophysical Methods* **26**, 81-86.

Klaassen, C. H., Fransen, J. A., Swarts, H. G. and De Pont, J. J. (1997) Glycosylation is essential for biosynthesis of functional gastric H+,K+-ATPase in insect cells. *Biochemical Journal* **321**, 419-424.

Klesius, P. H. (1993) Regulation of immunity to *Ostertagia ostertagi*. *Veterinary Parasitology* **46**, 63-79.

Klingler, C., Kniesel, U., Bamforth, S. D., Wolburg, H., Engelhardt, B. and Risau, W. (2000) Disruption of epithelial tight junctions is prevented by cyclic nucleotide-dependent protein kinase inhibitors. *Histochemistry and Cell Biology* **113**, 349-361.

Knox, D. P. (2000) Development of vaccines against gastrointestinal nematodes. *Parasitology* **120**, S43-S61.

Knox, D. P. (2007) Proteinase inhibitors and helminth parasite infection. *Parasite Immunology* **29**, 57-71.

Knox, D. P. and Jones, D. G. (1990) Studies on the presence and release of proteolytic enzymes (proteinases) in gastro-intestinal nematodes of ruminants. *International Journal for Parasitology* **20**, 243-249.

Koh, T. J., Goldenring, J. R., Ito, S., Mashimo, H., Kopin, A. S., Varro, A., Dockray, G. J. and Wang, T. C. (1997) Gastrin deficiency results in altered gastric differentiation and decreased colonic proliferation in mice. *Gastroenterology* **113**, 1015-1025.

Köhler, K. and Zahraoui, A. (2005) Tight junction: a co-ordinator of cell signalling and membrane trafficking. *Biology of the Cell* **97**, 659-665.

Konda, Y., Kamimura, H., Yokota, H., Hayashi, N., Sugano, K., and Takeuchi, T. (1999) Gastrin stimulates the growth of gastric pit with less-differentiated features. *American Journal of Physiology Gastrointestinal and Liver Physiology* **277**, G773-G784.

Konturek, J. W., Konturek, S. J. and Domschke, W. (1995) Cholecystokinin in the control of gastric acid secretion and gastrin release in response to a meal at low and high pH in healthy and duodenal ulcer patients. *Scandinavian Journal of Gastroenterology* **30**, 738-744.

Koski, K. G. and Scott, M. E. (2001) Gastrointestinal nematodes, nutrition and immunity: breaking the negative spiral. *Annual Review of Nutrition* **21**, 297-321.

Koski, K. G. and Scott, M. E. (2003) Gastrointestinal nematodes, trace elements, and immunity. *The Journal of Trace Elements in Experimental Medicine* **16**, 237-251.

Kovacs, T. O. G., Walsh, J. H., Maxwell, V., Wong, H. C., Azuma, T. and Katt, E. (1989) Gastrin is a major mediator of the gastric phase of acid secretion in dogs: proof by monoclonal antibody neutralization. *Gastroenterology* **97**, 1406-1413.

Krause, G., Winkler, L., Mueller, S. L., Haseloff, R. F., Piontek, J. and Blasig, I. E. (2008) Structure and function of claudins. *Biochimica et Biophysica Acta* **1778**, 631-645.

Kubata, B. K., Duszenko, M., Martin, K. S. and Urade, Y. (2007) Molecular basis for prostaglandin production in hosts and parasites. *Trends in Parasitology* **23** (7), 325-331.

Kuck, D., Kolmerer, B., Iking-Konert, C., Krammer, P. H., Stremmel, W. and Rudi, J. (2001) Vacuolating cytotoxin of *Helicobacter pylori* induces apoptosis in the human gastric epithelial cell line AGS. *Infection and Immunity* **69** (8), 5080-5087.

Kurbel, S., Kurbel, B., Dmitrović and Včev, A. (2001) A model of the gastric gland ejection cycle: low ejection fractions require reduction of the glandular dead space. *Journal of theoretical Biology* **210**, 337-343.

Lacy, E. R., Cowart, K. S., King, J. S., DelValle, J. and Smolka, A. J. (1996) Epithelial response of the rat gastric mucosa to chronic superficial injury. *Yale Journal of Biology and Medicine* **69** (2), 105-118.

Lähteenmäki, K., Edelman, S. and Korhonen, T. K. (2005) Bacterial metastasis: the host plasminogen system in bacterial invasion. *Trends in Microbiology* **13** (2), 79-85.

Larsson, L. I. (2000) Development biology of gastrin and somatostatin cells in the antropyloric mucosa of the stomach. *Microscopy Research and Technique* **48**, 272-281.

Larsson, L. I., Goltermann, N., de Magistris, L., Rehfeld, J. F. and Schwartz, T. W. (1979) Somatostatin cell processes as pathways for paracrine secretion. *Science* **205**, 1393-1395.

Lawton, D. E. B., Reynolds, G. W., Hodgkinson, S. M., Pomroy, W. E. and Simpson, H. V. (1996) Infection of sheep with adult and larval *Ostertagia circumcincta*: effects on abomasal pH and serum gastrin and pepsinogen. *International Journal for Parasitology* **26**, 1063-1074.

Lawton, D. E. B., Simcock, D. C., Candy, E. J. and Simpson, H. V. (2000) Gastrin secretion by ovine antral mucosa in vitro. *Comparative Biochemistry and Physiology - Part A: Molecular and Integrative Physiology* **126** (2), 233-243.

Lawton, D. E. B., Wigger, H., Simcock, D. C. and Simpson, H. V. (2002) Effect of *Ostertagia circumcincta* excretory/secretory products on gastrin release in vitro. *Veterinary Parasitology* **104**, 243-255.

Lee, E. R. (1985) Stomach: I. Architecture of antral units. *The American Journal of Anatomy* **172**, 187-204.

Lees, C., Howie, S., Sartor, R. B. and Satsangi, J. (2005) The hedgehog signalling pathway in the gastrointestinal tract: implications for development, homeostasis, and disease. *Gastroenterology* **129**, 1696-1710.

Lehmann, F. S., Golodner, E. H., Wang, J., Chen, M. C. Y., Avedian, D., Calam, J., Walsh, J. H., Dubinett, S. and Soll, A. H. (1996) Mononuclear cells and cytokines stimulate gastrin release from canine antral cells in primary culture. *American Journal of Physiology Gastrointestinal and Liver Physiology* **270**, G783-G788.

Levy, A. M. and Kita, K. (1996) The eosinophil in gut inflammation: Effector or director? *Gastroenterology* **110** (5), 952-954.

Li, H.-W. and Shan, J.-X. (2005) Effects of hepatocyte growth factor/scatter factor on the invasion of colorectal cancer cells *in vitro*. *World Journal of Gastroenterology* **11** (25), 3877-3881.

Li, Q., Karam, S. M. and Gordon, J. I. (1996) Diphtheria toxin-mediated ablation of parietal cells in the stomach of transgenic mice. *The Journal of Biological Chemistry* **271** (7), 3671-3676.

Li, Q., Lau, A., Morris, T. J., Guo, L., Fordyce, C. B. and Stanley, E. F. (2004) A syntaxin 1, $G\alpha_o$, and N-type calcium channel complex at a presynaptic nerve terminal: analysis by quantitative immunocolocalization. *The Journal of Neuroscience* **24** (16), 4070-4081.

Li, Q., Sun, Y., Wang, G. and Liu, X. (2009) Effects of the mermithid nematode *Ovomermis sinensis* on the hemocytes of its host *Helicoverpa armigera*. *Journal of Insect Physiology* **55**, 47-50.

Li, Z. Q., Cabero, J. L. and Mardh, S. (1995) Gastrin and carbachol require cAMP to elicit aminopyrine accumulation in isolated pig and rat parietal cells. *American Journal of Physiology Gastrointestinal and Liver Physiology* **268**, G82-89.

Lichtenfels, J. R., Hoberg, E. P. and Zarlenga, D. S. (1997) Systematics of gastrointestinal nematodes of domestic ruminants: advances between 1992 and 1995 and proposals for future research. *Veterinary Parasitology* **72**, 225-245.

Liebich, H.-G. (1993) *Funktionelle Histologie*, 2nd edition. Verlag Schattauer.

Lijnen, H. R. (2001) Plasmin and matrix metalloproteinases in vascular remodeling. *Thrombosis and Haemostasis* **86** (1), 324-33.

Lim, S.-L. and Lim, L.-Y. (2006) Effects of citrus fruit juices on cytotoxicity and drug transport pathways of Caco-2 cell monolayers. *International Journal of Pharmaceutics* **307**, 42-50.

Longbottom, D., Redmond, D. L., Russell, M., Liddell, S., Smith, W. D. and Knox, D. P. (1997) Molecular cloning and characterisation of a putative aspartate proteinase associated with a gut membrane protein complex from adult *Haemonchus contortus*. *Molecular and Biochemical Parasitology* **88** (1-2), 63-72.

Lorenz, R. G. and Gordon, J. I. (1993) Use of transgenic mice to study regulation of gene expression in the parietal cell lineage of gastric units. *Journal of Biological Chemistry* **268**, 26559-26570.

Lottspeich, F. and Zorbas, H. (eds.) (1998) *Bioanalytik*. p37. Spektrum.

Lytton, S. D., Fischer, W., Nagel, W., Haas, R. and Beck, F. X. (2005) Production of ammonium by *Helicobacter pylori* mediates occludin processing and disruption of tight junctions in CaCo-2 cells. *Microbiology* **151**, 3267-3276.

Ma, T. Y., Tran, D., Hoa, N., Nguyen, D., Merryfield, M. and Tarnawski, A. (2000) Mechanism of extracellular calcium regulation of intestinal epithelial tight junction permeability: role of cytoskeletal involvement. *Microscopy Research and Technique* **51**, 156–168.

Ma, W., Rogers, K., Zbar, B. and Schmidt, L. (2002) Effects of different fixatives of different fixatives on β-galactosidase activity. *The Journal of Histochemistry and Cytochemistry* **50** (10), 1421-1424.

Maclennan, K., Gallagher, M. P. and Knox, D. P. (1997) Stage-specific serine and metallo-proteinase release by adult and larval *Trichostrongylus vitrinus*. *International Journal for Parasitology* **27** (9), 1031-1036.

MacLennan, K., McLean, K. and Knox, D. P. (2005) Serpin expression in the parasitic stages of *Trichostrongylus vitrinus*, an ovine intestinal nematode. *Parasitology* **130**, 349-357.

Malchiodi Albedi, F., Barsotti, P., Mingazzini, P. and Marinozzi, V. (1985) Visualization of the secretory canaliculi of human parietal cells with a peroxidase-labelled peanut lectin. *Cell and Tissue Research* **239**, 447-450.

Mallery, C. (2009) Intercellular Junctions... Desmosome, in Major Eukaryotic Cell Organelles, accessed 21 June 2009, from http://www.bio.miami.edu/~cmallery/150/cells/organelle.htm.

Mallet, S., Huby, F.and Hoste, H. (1997) Characterization of acetylcholinesterase secreted by the trichostrongyle nematode parasites of ruminants. *Veterinary Research* **28**, 287-293.

Manela, F. D., Ren, J., Gao, J., McGuigan, J. E. and Harty, R. F. (1995) Calcitonin gene-related peptide modulates acid-mediated regulation of somatostatin and gastrin release from rat antrum. *Gastroenterology* **109,** 701-706.

Marcilla, A., Pérez-García, A., Espert, A., Bernal, D., Muñoz-Antolí, C., Esteban, J. G. and Toledo, R. (2007) *Echinostoma caproni*: identification of enolase in excretory/secretory products, molecular cloning, and functional expression. *Experimental Parasitology* **117**, 57-64.

Martins, E., Martins, V. M. V., Marques Júnior, A. P., Vasconcelos, A. C., Chiarini-Garcia, H. and Malard, P. F. (2000) Bovine placentome preservation for light microscopy evaluation. *Arquivo Brasileiro de Medicina Veterinária e Zootecnia* **52** (2), 117-124.

McDermott, J. R., Bartram, R. E., Knight, P. A., Miller, H. R. P. and Garrod, D. R. (2003) Mast cells disrupt epithelial barrier function during enteric nematode infection. *Proceedings of the National Academy of Sciences of the United States of America* **100** (13), 7761-7766.

McKay, E. J. and McLeay, L. M. (1981) Location and secretion of gastric intrinsic factor in the sheep. *Research In Veterinary Science* **30**, 261-265.

McKellar, Q. A. (1993) Interactions of *Ostertagia* species with their bovine and ovine hosts. *Internation Journal for Parasitology* **23**, 451-462.

McKellar, Q. A., Duncan, J. L., Armour, J. and McWilliam, P. (1986) Response to transplanted adult *Ostertagia ostertagi* in calves. *Research In Veterinary Science* **40**, 367-371.

McKellar, Q. A., Duncan, J. L., Armour, J., Linsay, F. E. F. and McWilliam, P. (1987) Further studies on the response to transplanted adult *Ostertagia ostertagi* in calves. *Research In Veterinary Science* **42**, 29-34.

McKerrow, J. H., Caffrey, C., Kelly, B., Loke, P. and Sajid, M. (2006) Proteases in parasitic diseases. *The Annual Review of Pathology: Mechanisms of Disease* **1**, 497-536.

McLeay, L. M., Anderson, N., Bingley, J. B. and Titchen, D. A. (1973) Effects on abomasal function of *Ostertagia circumcincta* infections in sheep. *Parasitology* **66**, 241-257.

Meeusen, E. N. T. (1999) Immunology of helminth infections, with special reference to immunopathology. *Veterinary Parasitology* **84**, 259–273.

Mégraud, F., Neman-Simha, V. and Brügmann, D. (1992) Further evidence of the toxic effect of ammonia produced by *Helicobacter pylori* urease on human epithelial cells. *Infection and Immunity* **60**, 1858-1863.

Mehlhorn, H. (ed.) (2001) *Encyclopedic Reference of Parasitology*, 2nd edition. parasitology.informatik.uni-wuerzburg.de, accessed 07 June 2009, from http://parasitology.informatik.uni-wuerzburg.de/login/frame.php

Merkelbach, P., Scott, I., Khalaf, S. and Simpson, H. V. (2002) Excretory/secretory products of *Haemonchus contortus* inhibit aminopyrine accumulation by rabbit gastric glands *in vitro*. *Veterinary Parasitology* **104**, 217-228.

Michel, J. F. (1970) The regulation of populations of *Ostertagia ostertagi* in calves. *Parasitology* **61**, 435-447.

Michel, J. F. (1971) Adult worms as a factor in the inhibition of development of *Ostertagia ostertagi* in the host. *International Journal for Parasitology* **1**, 31-36.

Michel, J. F. (1974) Arrested development of nematodes and some related phenomena. Advances in Parasitology 12, 279-366, in *Nematode parasites of vertebrates: their development and transmission* (2000), Chapter 3 Order Strongylida (the Bursate Nematodes), pp 41-229. CABI Publishing.

Milani, S. and Calabrò, A. (2001) Role of growth factors and their receptors in gastric ulcer healing. *Microscopy Research and Technique* **53** (5), 360-71.

Miller, J. E., Horohov, D. W. (2006) Immunological aspects of nematode parasite control in sheep. *Journal of Animal Science* **84 (E. suppl.)**, E124-E132.

Miyaoka, Y., Kadowaki, Y., Ishihara, S., Ose, T., Fukuhara, H., Kazumori, H., Takasawa, S., Okamoto, H., Chiba, T. and Kinoshita, Y. (2004) Transgenic overexpression of Reg protein caused gastric cell proliferation and differentiation along parietal and chief cell lineages. *Oncogene* **23**, 3572-3579.

Miyazaki, Y., Shinomura, Y., Tsutsui, S., Zushi, S., Higashimoto, Y., Kanayama, S., Higashiyama, S., Taniguchi, N., and Matsuzawa, Y. (1999) Gastrin induces heparin-binding epidermal growth factor-like growth factor in rat gastric epithelial cells transfected with gastrin receptor. *Gastroenterology* **116**, 78-89.

Mizukawa, Y., Nishizawa, T., Nagao, T., Kitamura, K. and Urushidani, T. (2002) Cellular distribution of parchorin, a chloride intracellular channel-related protein, in various tissues. *American Journal of Physiology Cell Physiology* **282** (4), C786-795.

Montecucco, C. and de Bernard, M. (2003) Molecular and cellular mechanisms of action of the vacuolating cytotoxin (VacA) and neutrophil-activating protein (HP-NAP) virulence factors of *Helicobacter pylori*. *Microbes and Infection* **5**, 715-721.

Moreno, Y. and Geary, T. G. (2008) Stage- and gender-specific proteomic analysis of *Brugia malayi* excretory-secretory products. *PloS Neglected Tropical Diseases* **2** (10), e262.

Mori, S., Morishita, Y., Sakai, K., Kurimoto, S., Okamoto, M., Kawamoto, T. and Kuroki, T. (1987) Electron microscopic evidence for epidermal growth factor receptor (EGF-R)-like immunoreactivity associated with the basolateral surface of gastric parietal cells. *Pathology International* **37** (12), 1907-1917.

Mould, A. P., Akiyama, S. K. and Humphries, M. J. (1995) Regulation of integrin alpha5beta1-fibronectin interactions by divalent cations. *The Journal of Biological Chemistry* **270** (44), 26270-26277.

Mullin, J. M., Schmidt, J. D., Allegretti, P., Valenzano, M. C., Whitby, M., Lurie, D., Tully, J. O., Jain, V., Lazowick, D., Mercogliano, G. and Thornton, J. J. (2007) Esomeprazole induces a transepithelial gastroesophageal mucosal leak in GERD patients. *Gastrointestinal Endoscopy* **65** (5), AB140.

Munn, E. A. (1977) A helical, polymeric extracellular protein associated with the luminal surface of *Haemonchus contortus* intestinal cells. *Tissue and Cell* **9** (1), 23-34.

Muranova, T., Shvyrkova, I., Arkhipov, V. and Rykunova, A. (1998) Anti-adhesive property of plasmin/plasminogen system: the use of plamin(ogen) for cell detachment and disaggregation in cell culture technique. *Fibrinolysis and Proteolysis* **12** (1), 23-32.

Murayama, Y., Miyagawa, J., Higashiyama, S., Kondo, S., Yabu, M., Isozaki, K., Kayanoki, Y., Kanayama, S., Shinomura, Y., Taniguchi, N., and Matsuzawa, Y. (1995) Localization of heparin-binding epidermal growth factor-like growth factor in human gastric mucosa. *Gastroenterology* **109**, 1051-105.

Murayama, Y., Miyagawa, J., Shinomura, Y., Kanayama, S., Yasunaga, Y., Nishibayashi, H., Yamamori, K., Higashimoto, Y. and Matsuzawa, Y. (1999) Morphological and functional restoration of parietal cells in *Helicobacter pylori* associated enlarged fold gastritis after erradication. *Gut* **45**, 653-661.

Muresan, Z., Paul, D. L. and Goodenough, D. A. (2000) Occludin 1B, a variant of the tight junction protein occludin. *Molecular Biology of the Cell* **11**, 627-634.

Murphy-Ullrich, J. E. (2001) The de-adhesive activity of matricellular proteins: is intermediate cell adhesion an adaptive state? *The Journal of Clinical Investigation* **107** (7), 785-790.

Nagata, A., Ito, M., Iwata, N., Kuno, J., Takano, H., Minowa, O., Chihara, K., Matsui, T. and Noda, T. (1996) G protein-coupled cholecystokinin-B/gastrin receptors are responsible for physiological cell growth of the stomach mucosa *in vivo*. *Proceedings of the National Academy of Sciences of the United States of America* **93**, 11825-11830.

Nagata, H., Akiba, Y., Suzuki, H., Okano, H. and Hibi, T. (2006) Expression of Musashi-1 in the rat stomach and changes during mucosal injury and restitution. *FEBS Letters* **580** (1), 27-33.

Nakajima, T., Konda, Y., Izumi, Y., Kanai, M., Hayashi, N., Chiba, T. and Takeuchi, T. (2002) Gastrin stimulates the growth of gastric pit cell precursors by inducing its own receptors. *American Journal of Physiology Gastrointestinal and Liver Physiology* **282** (2), G359-366.

Nakamura, M., Oda, M., Kaneko, K., Yonei, Y., Tsukada, N., Komatsu, H., Tsugu, M. and Tsuchiya, M. (1987) Autoradiographic demonstration of gastrin binding sites in rat gastric mucosa. *Peptides* **8**, 391-398.

Nakamura, M., Okano, H., Blendy, J. A. and Montell, C. (1994) Musashi, a neural RNA-binding protein required for drosophila adult external sensory organ development. *Neuron* **13** (1), 67-81.

Negulescu, P. A., Reenstra, W. W. and Machen, T. E. (1989) Intracellular Ca requirements for stimulus-secretion coupling in parietal cell. *American Journal of Physiology Cell Physiology* **256**, C241-C251.

Neu, B., Puschmann, A. J., Mayerhofer, A., Hutzler, P., Grossmann, J., Lippl, F., Schepp, W. and Prinz, C. (2003) TNF-a induces apoptosis of parietal cells. *Biochemical Pharmacology* **65**, 1755-1760.

Newlands, G. F. J., Skuce, P. J., Nisbet, A. J., Redmond, D. L. and Smith, S. K. (2006) Molecular characterization of a family of metalloendopeptidases from the intestinal brush border of *Haemonchus contortus*. *Parasitology* **133**, 357-368.

Newton, S. E. and Munn, E. A. (1999) The development of vaccines against gastrointestinal nematode parasites, particularly *Haemonchus contortus*. *Parasitology Today* **15** (3), 116-122.

Nguyen, V. Q., Caprioli, R. M. and Cover, T. L. (2001) Carboxy-terminal proteolytic processing of *Helicobacter pylori* vacuolating toxin. *Infection and Immunity* **69** (1), 543-546.

Nicholls, C. D., Hayes, P. R. and Lee, D. L. (1987) Physiological and microbiological changes in the abomasum of sheep infected with large doses of *Haemonchus contortus*. *Journal of Comparative Pathology* **97**, 299-308.

Nicholls, C. D., Lee, D. L., Adrian, T. E., Bloom, S. R. and Care, A. D. (1988) Hypergastrinaemia of sheep infected with *Haemonchus contortus*. *Research In Veterinary Science* **45**, 124-126.

Niessen, C. M. (2007) Tight junctions/adherens junctions: basic structure and function. *Journal of Investigative Dermatology* **127**, 2525-2532.

Nijtmans, L. G. J., Henderson, N. S. and Holt, I. J. (2002) Blue Native electrophoresis to study mitochondrial and other protein complexes. *Methods* **26**, 327-334.

Nishi, T. and Forgac, M. (2002) The vacuolar (H+)-ATPases - Nature's most versatile proton pumps. *Nature Reviews Molecular Cell Biology* **3** (2), 94-103.

Nishizawa, T., Nagao, T., Iwatsubo, T., Forte, J. G. and Urushidani, T. (2000) Molecular cloning and characterization of a novel chloride intracellular channel-related protein, parchorin, expressed in water-secreting cells. *Journal of Biological Chemistry* **275** (15), 11164-11173.

Noffsinger, T. L., Otagaki, K. K. and Furukawa, C. T. (1961) Effect of feed and water intake on rumen and body temperatures of sheep under subtropical conditions. *Journal of Animal Science* **20**, 718-722.

Nusrat, A., von Eichel-Streiber, C., Turner, J. R., Verkade, P., Madara, J. L. and Parkos, C. A. (2001) *Clostridium difficile* toxins disrupt epithelial barrier function by altering membrane microdomain localization of tight junction proteins. *Infection and Immunity* **69** (3), 1329-1336.

O'Donnell, I. J., Dineen, J. K., Wagland, B. M., Letho, S., Werkmeister, J. A. and Ward, C. W. (1989) A novel hosr-protective antigen from *Trichostrongylus colubriformis*. *International Journal for Parasitology* **19** (3), 327-335.

Obert, G., Peiffer, I. and Servin, A. L. (2000) Rotavirus-induced structural and functional alterations in tight junctions of polarized intestinal Caco-2 cell monolayers. *Journal of Virology* **74** (10), 4645-4651.

Ogata, T. and Yamasaki, Y. (2000) Morphological studies on the translocation of tubulovesicular system toward the intracellular canaliculus during stimulation of the gastric parietal cell. *Microscopy Research and Technique* **48**, 282-292.

Okamoto, C. T. and Forte, J. G. (2001) Vesicular trafficking machinery, the actin cytoskeleton, and H^+-K^+-ATPase recycling in the gastric parietal cell. *The Journal of Physiology* **532**, 287-296.

Okamoto, C. T., Karpilow, J. M., Smolka, A. and Forte, J. G. (1990) Isolation and characterization of gastric microsomal glycoproteins. Evidence for a glycosylated beta-subunit of the H+/K(+)-ATPase. *Biochimica et Biophysica Acta* **1037** (3), 360-72.

Okano, H., Imai, T. and Okabe, M. (2002) Musashi: a translational regulatoer of cell fate. *Journal of Cell Science* **115**, 1355-1359.

Oliver, E. M., Skuce, P. J., McNair, C. M. and Knox, D. P. (2006) Identification and characterization of an asparaginyl proteinase (legumain) from the parasitic nematode, *Haemonchus contortus*. *Parasitology* **133**, 237-244.

Opperman, C. H. and Chang, S. (1992) Nematode acetylcholinesterases: molecular forms and their potential role in nematode behavior. *Parasitology Today* **8**, 406-411.

Orr, A. W., Pedraza, C. E., Pallero, M. A., Elzie, C. A., Goicoechea, S., Strickland, D. K. and Murphy-Ullrich, J. E. (2003) Low density lipoprotein receptor-related protein is a calreticulin coreceptor that signals focal adhesion disassembly. *The Journal of Cell Biology* **161** (6), 1179-1189.

Osawa, H., Kita, H., Ohnishi, H., Hoshino, H., Mutoh, H., Ishino, Y., Watanabe, E., Satoh, K. and Sugano, K. (2006) *Helicobacter pylori* eradication induces marked increase in H^+/K^+-adenosine triphosphatase expression without altering parietal cell number in human gastric mucosa. *Gut* **55**, 152-157.

Pahl, H. L. (1999) Activators and traget genes of Rel/NF-kappaB transcription factors.*Oncogene* **18** (49), 6853-6866.

Pancholi, V. (2001) Multifunctional alpha-enolase: its role in diseases. *Cellular and Molecular Life Sciences* **58**, 902-920.

Paradiso, A. M., Townsley, M. C., Wenzl, E. and Machen, T. E. (1989) Regulation of intracellular pH in resting and in stimulated parietal cells. *American Journal of Physiology Cell Physiology* **257** (3), C554-561.

Park, J., Chiba, T. and Yamada, T. (1987) Mechanisms for direct inhibition of canine gastric parietal cells by somatostatin. *Journal of Biological Chemistry* **262** (29), 14190-14196.

Parker, P. (2006) Gap Junctions, in *Great Controversies in Neurobiology Brown University Neur 1930E*, accessed 21 June 2009, from https://wiki.brown.edu/confluence/display/BN0193S04/gap+junctions.

Parkin, C. A. and Ingham, P. W. (2008) The adventures of sonic hedgehog in development and repair. I. Hedgehog signaling in gastrointestinal development and disease. *American Journal of Physiology Gastrointestinal and Liver Physiology* **294**, G363-G367.

Parkins, J. J. and Holmes, P. H. (1989) Effects of gastrointestinal helminth parasites on ruminant nutrition. *Nutrition Research Reviews* **2**, 227-246.

Parry, M. A. A., Zhang, X. C. and Bode, W. (2000) Molecular mechanisms of plasminogen activation: bacterial cofactors provide clues. *Trends in Biochemical Sciences* **25** (2), 53-59.

Pérez-Sánchez, R., Ramajo-Hernández, A., Ramajo-Martín, V. and Oleaga, A. (2006) Proteomic analysis of the tegument and excretory-secretory products of adult *Schistosoma bovis* worms. *Proteomics* **6**, S226-S236.

Philipp, M. (1984) Acetylcholinesterase secreted by intestinal nematodes: a reinterpretation of its putative role of "biochemical holdfast". *Transactions of the Royal Society of Tropical Medicine and Hygiene* **78**, 139-139.

Pomroy, W. E. and Adlington, B. A. (2006) Efficacy of short-term feeding of sulla (*Hedysarum coronarium*) to young goats against a mixed burden of gaastrointestinal nematodes. *Veterinary Parasitology* **136**, 363-366.

Poulsen, S. S., Nexø, E., Olsen, P. S., Hess, J. and Kirrkegaard, P. (1986) Immunohistochemical localisation of epidermal growth factor in rat and man. *Histochemistry* **85**, 389-394.

Prasad, K. N., La Rosa, F. G. and Prasad, J. E. (1998) Prostaglandins act as a neurotoxin for differentiated neuroblastoma cells in culture and increase levels of ubiquitin and beta-amyloid. *In vitro Cellular and Developmental Biology, Animal* **34**, 265-274.

Prinz, C., Neumayer, N., Mahr, S., Classen, M. and Schepp, W. (1997) Functional impairment of rat enterochromaffin-like cells by Interleukin 1beta. *Gastroenterology* **112**, 364-375.

Prinz, C., Zanner, R., Gerhard, M., Mahr, S., Neumayer, N., Hohne-Zell, B. and Gratzl, M. (1999) The mechanism of histamine secretion from gastric enterochromaffin-like cells. *American Journal of Physiology Cell Physiology* **277** (5), C845-855.

Prusch, R. D., Goette, S.-M. and Haberman, P. (1989) Prostaglandins may play a signal-coupling role during phagocytosis in *Amoeba proteus*. *Cell and Tissue Research* **255**, 553-557.

Przemeck, S. M. C. (2003) *Effects of Abomasal Nematode Parasites in vivo and in vitro*. PhD Thesis, Massey Universitiy Palmerston North, New Zealand.

Przemeck, S., Huber, A., Brown, S., Pedley, K. C. and Simpson, H. V. (2005) Excretory/secretory products of sheep abomasal nematode parasites cause vacuolation and increased neutral red uptake by HeLa cells. *Parasitology Research* **95**, 213-217.

Punj, V., Zaborina, O., Dhiman, N., Falzari, K., Bagdasarian, M., and Chakrabarty, A. M. (2000) Phagocytic cell killing mediated by secreted cytotoxic factors of *Vibrio cholerae*. *Infection and Immunity* **68** (9), 4930-4937.

Radebold, K., Horakova, E., Gloeckner, J., Ortega, G., Spray, D. C., Vieweger, H., Siebert, K., Manuelidis, L. and Geibel, J. P. (2001) Gap junctional channels regulate acid secretion in the mammalian gastric gland. *Journal of Membrane Biology* **183** (3), 147-153.

Ramachandran, R. and Hollenberg, M. D. (2008) Proteinases and signalling: pathophysiological and therapeutic implications via PARs and more. *British Journal of Pharmacology* **153**, S263-S282.

Rathore, D. K., Suchitra, S., Saini, M., Singh, B. P. and Joshi, P. (2006) Identification of a 66kDa *Haemonchus contortus* excretory/secretory antigen that inhibits host monocytes. *Veterinary Parasitology* **138**, 291-300.

Raum, D., Marcus, D., Alper, C. A., Levey, R., Taylor, P. D. and Starzl, T. E. (1980) Synthesis of human plasminogen by the liver. *Science* **208**, 1036-1037.

Reenstra, W. W. and Forte, J. G. (1990) Characterization of K^+ and Cl^- conductances in apical membrane vesicles from stimulated rabbit oxyntic cells. *American Journal of Physiology Gastrointestinal and Liver Physiology* **259**, G850-G858.

Reinhardt, S. (2004) *Chemoattractants produced by abomasal nematodes in sheep*. Dissertation, Tierärztliche Hochschule Hannover, Germany.

Remy, C., Kirchhoff, P., Hafner, P., Busque, S. M., Müller, M. K., Geibel, J. P. and Wagner, C. A. (2007) Stimulatory pathways of the calcium-sensing receptor on acid secretion in freshly isolated human gastric glands. *Cellular Physiology and Biochemistry* **19**, 33-42.

Ren, J., Young, R. L., Lassiter, D. C., Rings, M. C. and Harty, R. F. (1992) Calcitonin gene-related peptide: mechanisms of modulation of antral endocrine cells and cholinergic neurons. *American Journal of Physiology Gastrointestinal and Liver Physiology* **262**, G732-G739.

Reynolds, G. W., Simpson, H. V., Carr, D. H. and McLeay, L. M. (1991) Gastrin: its molecular forms and secretion in sheep. In *Physiological aspects of digestion and metabolism in ruminants* (eds. Tsuda, T., Sasaki, Y. and Kawashima, R.), pp. 63-87. Academic Press, Inc., San Diego.

Rhoads, M. L. (1984) Secretory cholinesterases of nematodes: possible functions in the host-parasite relationship. *Tropical Veterinarian* **2**, 3-10.

Rhoads, M. L. and Fetterer, R. H. (1996) Extracellular matrix degradation by *Haemonchus contortus*. *The Journal of Parasitology* **82** (3), 379-383.

Rhodes, J. M. and Milton, J. D. (1997) *Lectin Methods and Protocols, Methods in Molecular Medicine*, Vol. 9. Humana Press.

Richardson, C. T., Walsh, J. H., Hicks, M. I. and Fordtran, J. S. (1976) Studies on the mechanisms of food-stimulated gastric acid secretion in normal human subjects. *Journal of Clinical Investigation* **58**, 623-631.

Richelsen, B., Rehfeld, J. F. and Larsson, L. I. (1983) Antral gland cell column: a method for studying release of gastric hormones. *American Journal of Physiology Gastrointestinal and Liver Physiology* **245**, G463-G469.

Robert, A., Olafsson, A. S., Lancaster, C. and Zhang, W. (1991) Interleukin-1 is cytoprotective, antisecretory, stimulates PGE2 synthesis by the stomach, and retards gastric emptying. *Life Sciences* **48**, 123-134.

Rogers, W. P. and Somerville, R. I. (1963) The infective stage of nematode parasites and its significance in parasitism. Advances in Parasitology 1, 109-177, in *Nematode parasites of vertebrates: their development and transmission* (2000), Chapter 3 Order Strongylida (the Bursate Nematodes), pp 41-229. CABI Publishing.

Rogers, W. P. and Somerville, R. I. (1968) The infectious process, and its relation to the development of early parasitic stages of nematodes. Advances in Parasitology 6, 327-348, in *Nematode parasites of vertebrates: their development and transmission* (2000), Chapter 3 Order Strongylida (the Bursate Nematodes), pp 41-229. CABI Publishing.

Rosenberg, G. A. and Yang, Y. (2007) Vasogenic edema due to tight junction disruption by matrix metalloproteinases in cerebral ischemia. *Neurosurgical Focus* **22** (5), E4.

Rossetto, O., de Bernard, M., Pellizzari, R., Vitale, G., Caccin, P., Schiavo, G. and Montecucco, C. (2000) Bacterial toxins with intracellular protease activity. *Clinical Chimica Acta* **291**, 189-199.

Rossmann, H., Bachmann, O., Wang, Z., Shull, G. E., Obermaier, B., Stuart-Tilley, A., Alper, S. L. and Seidler, U. (2001) Differential expression and regulation of AE2 anion exchanger subtypes in rabbit parietal and mucous cells. *Journal of Physiology* **534** (3), 837-848.

Rowin, M. E., Whatley, R. E., Yednock, T. and Bohnsack, J. F. (1998) Intracellular calcium requirements for beta1 integrin activation. *Journal of Cellular Physiology* **175**, 193-202.

Saadat, I., Higashi, H., Obuse, C., Umeda, M., Murata-Kamiya, N., Saito, Y., Lu, H., Ohnishi, N., Azuma, T., Suzuki, A., Ohno, S. and Hatakeyama, M. (2007) *Helicobacter pylori* CagA targets PAR1/MARK kinase to disrupt epithelial cell polarity. *Nature* **44**, 330-334.

Sachs, G., Chang, H. H., Rabon, E., Schackman, R., Lewin, M. and Saccomani, G. (1976) A nonelectrogenic H^+ pump in plasma membranes of hog stomach. *Journal of Biological Chemistry* **251**, 7690-7698.

Sáez, J. C., Berthoud, V. M., Moreno, A. P. and Spray, D. C. (1993) Gap junctions. Multiplicity of controls in differentiated and undifferentiated cells and possible functional implications. *Advances in Second Messenger Phosphoprotein Research* **27**, 163-198.

Saffouri, B., DuVal, J. W. and Makhlouf, G. M. (1984) Stimulation of gastrin secretion in vitro by intraluminal chemicals: regulation by intramural cholinergic and noncholinergic neurons. *Gastroenterology* **87**, 557-561.

Saffouri, B., Weir, G. C., Bitar, K. N. and Makhlouf, G. M. (1980) Gastrin and somatostatin secretion by perfused rat stomach: functional linkage of antral peptides. *American Journal of Physiology Gastrointestinal and Liver Physiology* **238** (6), G495-G501.

Saha, A., Hammond, C. E., Trojanowska, M. and Smolka, A. J. (2008) *Helicobacter pylori*-induced H,K-ATPase alpha-subunit gene repression is mediated by NF-kappaB p50 homodimer promoter binding. *American Journal of Physiology Gastrointestinal and Liver Physiology* **294**, G795-G807.

Sajid, M., McKerrow, J. H., Hansell, E., Mathieu, M. A., Lucas, K. D., Hsieh, I., Greenbaum, D., Bogyo, M., Salter, J. P., Lim, K. C., Franklin, C., Kim, J. H. and Caffrey, C. R. (2003) Functional expression and characterization of *Schistosoma mansoni* cathepsin B and its trans-activation by an endogenous asparaginyl endopeptidase. *Molecular and Biochemical Parasitology* **131** (1), 65-75.

Samloff, I. M. (1989) Peptic ulcer: the many proteinases of aggression. *Gastroenterology* **96**, 586-595.

Sawada, N., Murata, M., Kikuchi, K., Osanai, M., Tobioka, H., Kojima, T. and Chiba, H. (2003) Tight junctions and human diseases. *Medical Electron Microscopy* **36**, 147-156.

Schallig, H. D. F. H. and Van Leeuwen, M. A. W. (1997) Protective immunity to the blood-feeding nematode *Haemonchus contortus* induced by vaccination with parasite low molecular weight antigens. *Parasitology* **114**, 293-299.

Schallig, H. D. F. H., Van Leeuwen, A. W. and Cornelissen, A. W. C. A. (1997) Protective immunity induced by vaccination with two *Haemonchus contortus* excretory secretory proteins in sheep. *Parasite Immunology* **19**, 447-453.

Schiller, L. R., Walsh, J. H. and Feldman, M. (1980) Distention-induced gastrin release. Effects of luminal acidification and intravenous atropine. *Gastroenterology* **78**, 912-917.

Schneeberger, E. E. and Lynch, R. D. (2004) The tight junction: a multifunctional complex. *American Journal of Physiology Cell Physiology* **286**, C1213-C1228.

Schubert, M. L. and Makhlouf, G. M. (1993) Gastrin secretion induced by distention is mediated by gastric cholinergic and vasoactive intestinal peptide neurons in rats. *Gastroenterology* **104**, 834-839.

Schubert, M. L. and Makhlouf, G. M. (1996) Neural and paracrine regulation of gastrin and gastric acid secretion. *Gastroenterology* **111** (3), 837-838.

Schubert, M. L., Coy, D. H. and Makhlouf, G. M. (1992) Peptone stimulates gastrin from the stomach by activating bombesin/GRP and cholinergic neurons. *American Journal of Physiology Gastrointestinal and Liver Physiology* **262**, G685-G689.

Schubert, M. L., Edwards, N. F. and Makhlouf, G. M. (1988) Regulation of gastric somatostatin secretion in the mouse by luminal acidity: a local feedback mechanism. *Gastroenterology* **94,** 317-322.

Schubert, M. L., Saffouri, B., Walsh, J. H. and Makhlouf, G. M. (1985) Inhibition of neurally mediated gastrin secretion by bombesin antiserum. *American Journal of Physiology Gastrointestinal and Liver Physiology* **248**, G456-G462.

Schusdziarra, V., Harris, V., Conlon, J. M., Arimura, A. and Unger, R. (1978) Pancreatic and gastric somatostatin release in response to intragastric and intraduodenal nutrients and HCl in the dog. *Journal of Clinical Investigation* **62**, 509-518.

Scott, I. and McKellar, Q. A. (1998) The effects of excretions/secretions of *Ostertagia circumcincta* on ovine abomasal tissues *in vitro*. *International Journal for Parasitology* **28**, 451-460.

Scott, I., Dick, A., Irvine, J., Stear, M. J. and McKellar, Q. A. (1999) The distribution of pepsinogen within the abomasa of cattle and sheep infected with *Ostertagia* spp. and sheep infected with *Haemonchus contortus*. *Veterinary Pathology* **82**, 145-159.

Scott, I., Hodgkinson, S. M., Khalaf, S., Lawton, D. E. B., Collett, M. G., Reynolds, G. W., Pomroy, W. E. and Simpson, H. V. (1998a) Infection of sheep with adult and larval *Ostertagia circumcincta*: abomasal morphology. *International Journal for Parasitology* **28**, 1383-1392.

Scott, I., Hodgkinson, S. M., Lawton, D. E. B., Khalaf, S., Reynolds, G. W., Pomroy, W. E. and Simpson, H. V. (1998b) Infection of sheep with adult and larval *Ostertagia circumcincta*: gastrin. *International Journal for Parasitology* **28**, 1393-1401.

Scott, I., Khalaf, S., Simcock, D. C., Knight, C. G., Reynolds, G. W., Pomroy, W. E. and Simpson, H. V. (2000) A sequential study of the pathology associated with the infection of sheep with adult and larval *Ostertagia circumcincta*. *Veterinary Parasitology* **89**, 79-94.

Scott, I., McKellar, Q. A., Irvine, J. and Dick, A. (1995) The role of the mucosal growth factors, transforming growth factor-alpha and epidermal growth factor in the pathogenesis of infection of sheep with *Ostertagia circumcincta*. *Proceedings 15th International Conference of the WAAVP*, p. 122.

Scott, I., Stear, M. J., Irvine, J. I., Dick, A. and Wallace, D. S. (1998c) Changes in the zymogenic cell populations of the abomasa of sheep infected with *Haemonchus contortus*. *Parasitology* **116**, 569-577.

Scrimshaw, N. S. and SanGiovanni, J. P. (1997) Synergism of nutrition, infection and immunity: an overview. *The American Journal of Clinical Nutrition* **66**, 464-77.

Scudamore, C. L., Thornton, E. M., McMillan, L., Newlands, G. F. J. and Miller, H. R. P. (1995) Release of the mucosal mast cell granule chymase, rat mast cell protease-II, during anaphylaxis is accociated with the rapid development of paracellular permeability to macromolecules in rat jejunum. *The Journal of Experimental Medicine* **182**, 1871-1881.

Shafee, N. and AbuBakar, S. (2003) Dengue virus type 2 NS3 protease and NS2BNS3 protease precursor incduce apoptosis. *Journal of General Virology* **84**, 2191-2195.

Sharp, R., Babyatsky, M. W., Takagi, H., Tågerud, S., Wang, T. C., Bockman, D. E., Brand, S. J. and Merlino, G. (1995) Transforming growth factor alpha disrupts the normal program of cellular differentiation in the gastric mucosa of transgenic mice. *Development* **121**, 149-161.

Shasby, D. M. and Shasby, S. S. (1986) Effects of calcium on transendothelial albumin transfer and electrical resistance. *Journal of Applied Physiology* **60** (1), 71-79.

Shen, L., Weber, C. R. and Turner, J. R. (2008) The tight junction protein complex undergoes rapid and continous molecular remodeling at steady state. *Journal of Cell Biology* **181** (4), 683-695.

Shi, Q. and Jackowski, G. (1998) Blue native polyacrylamide gel electrophoresis, in *Gel Electrophoresis of Proteins, A practical Approach 3rd edition* (ed. Hames, E. D.), p40-41. Oxford University Press.

Shull, G. E. (1990) cDNA cloning of the beta-subunit of the rat gastric H,K-ATPase. *Journal of Biological Chemistry* **265** (21), 12123-12126.

Shull, G. E. and Lingrel, J. L. (1986) Molecular cloning of the rat stomach (H+ + K+)-ATPase. *Journal of Biological Chemistry* **261** (36), 16788-16791.

Simcock, D. C., Lawton, D. E. B., Scott, I. and Simpson, H. V. (2006b) Abomasal bacteria produce an inhibitor of gastrin secretion in vitro. *Research in Veterinary Science* **81**, 152-157.

Simcock, D. C., Scott, I., Przemeck, S. and Simpson, H. V. (2006a) Abomasal contents of parasitised sheep contain an inhibitor of gastrin secretion in vitro. *Research in Veterinary Science* **81**, 225-230.

Simpson, H. V. (2000) Pathophysiology of abomasal parasitism: is the host or parasite responsible? *The Veterianary Journal* **160**, 177-191.

Simpson, H. V., Lawton, D. E. B., Simcock, D. C., Reynolds, G. W. and Pomroy, W. E. (1997) Effects of adult and larval *Haemonchus contortus* on abomasal secretion. *International Journal for Parasitology* **27,** 825-831.

Simpson, H. V., Reynolds, G. W. and Carr, D. H. (1993) Low tissue gastrin content in the ovine distal duodenum is associated with increased percentage of G34. *Comparative Biochemistry and Physiology* **104A**, 461-468.

Simpson, H. V., Simpson, B. H., Simcock, D. C., Reynolds, G. W. and Pomroy, W. E. (1999) Abomasal secretion in sheep receiving adult *Ostertagia circumcincta* that are prevented from contact with the mucosa. *New Zealand Veterinary Journal* **47**, 20-24.

Sjaastad, M. D. and Nelson, W. J. (1997) Integrin-mediated calcium signaling and regulation of cell adhesion by intracellular calcium. *BioEssays* **19** (1), 47-55.

Sjaastad, M. D., Lewis, R. S. and Nelson, W. J. (1996) Mechanisms of integrin-mediated calcium signaling in MDCK Cells: regulation of adhesion by IP_3- and store-independent calcium influx. *Molecular Biology of the Cell* **7**, 1025-1041.

Skuce, P. J., Steward, E. M., Smith, W. D. and Knox, D. P. (1999) Cloning and characterization of glutamate dehydrogenase (GDH) from the gut of *Haemonchus contortus*. Parasitology **118,** 297-304.

Smith, J. W., Piotrowiczg, R. S. and Mathis, D. (1994) A mechanism for divalent cation regulation of beta3-integrins. *The Journal of Biological Chemistry* **269** (2), 960-967.

Smith, P. R., Bradford, A. L., Joe, E. H., Angelides, K. J., Benos, D. J. and Saccomani, G. (1993) Gastric parietal cell H(+)-K(+)-ATPase microsomes are associated with isoforms of ankyrin and spectrin. *American Journal of Physiology Cell Physiology* **264** (1), C63-70.

Smith, S. K., Nisbet, A. J., Meikle, L. I., Inglis, N. F., Sales, J., Beynon, R. J. and Matthews, J. B. (2009) Proteomic analysis of excretory/secretory products released by *Teladorsagia circumcincta* larvae early post-infection. *Parasite Immunology* **31**, 10-19.

Smith, W. D., Smith, S. K. and Murray, J. M. (1994) Protection studies with integral membrane fractions of *Haemonchus contortus*. *Parasite Immunology* **16**, 231-241.

Soll, A. H. (1982) Potentiating interactions of gastric stimulants on [^{14}C]aminopyrine accumulation by isolated canine parietal cells. *Gastroenterology* **83**, 216-223.

Sommerville, R. I. (1953) Development of *Ostertagia circumcincta* in the abomasal mucosa of the sheep. *Nature* **171** (4350), 482-3.

Sommerville, R. I. (1954) The histotropic phase of the nematode parasite, *Ostertagia circumcincta*. *Australian Journal of Agricultural Research* **5**, 130-140.

Sommerville, R. I. (1957) The exsheathing mechanism of nematode infective larvae. Experimental Prasitology 6, 18-30, in *Nematode parasites of vertebrates: their development and transmission* (2000), Chapter 3 Order Strongylida (the Bursate Nematodes), pp 41-229. CABI Publishing.

Stafford, K. J., West, D. M. and Pomroy, W. E. (1994) Nematode worm egg output by ewes. *New Zealand Veterinary Journal* **42***,* 30-32.

Stear, M. J., Bishop, S. C., Doligalska, M., Duncan, J. L., Holmes, P. H., Irvine, J., McCririe, L., McKellar, Q. A., Sinski, E. and Murray, M. (1995) Regulation of egg production, worm burden, worm length and worm fecundity by host responses in sheep infected with *Ostertagia circumcincta*. *Parasite Immunology* **17**, 643-652.

Stear, M. J., Bishop, S. C., Henderson, N. G. and Scott, I. (2003) A key mechanism of pathogenesis in sheep infected with the nematode *Teladorsagia circumcincta*. *Animal Health Research Reviews* **4** (1), 45-52.

Steck, N., Hoffmann, M., Hew Ferstl, C. M., Kim, S. C., Liu, B., Vogel, R. F., Sartor, R. B. and Haller, D. (2009) Bacterial proteases contribute to the development of chronic intestinal inflammation by impairing epithelial barrier function. *Gastroenterology* **136 (suppl.)** (5), A21-A22.

Stepan, V., Ramamoorthy, S., Pausawasdi, N., Logsdon, C. D., Askari, F. K. and Todisco, A. (2004) Role of small GTP binding proteins in the growth-promoting and antiapoptotic actions of gastrin. *Am J Physiol Gastrointest Liver Physiol* **287** (3), G715-725.

Stevenson, L. A., Robin, B. G. and Chilton, N. B. (1996) The IST-2 rDNA of *Teladorsagia circumcincta*, *T. trifurcata* and *T. davtiani* (Nematoda: Trichostrongylidae) indicates that these taxa are one species. *International Journal for Parasitology* **26** (10), 1123-1126.

Strunz, U. T., Walsh, J. H. and Grossman, M. I. (1978) Stimulation of gastrin release in dogs by individual amino acids. *Proceedings of the Society for Experimental Biology and Medicine* **157** (3), 440-441.

Suarez, V. H. and Cabaret, J. (1992) Interbreeding in the subfamily Ostertagiinae (Nematoda: Trichostrongylidae) of ruminants. *Journal of Parasitology* **78** (3), 402-405.

Suarez, V. H., Cabaret, J., and Gruner, L. (1995) Morphological polymorphism in the nematode *Teladorsagia circumcincta* in relation to age of larvae, infection mode and lamb characteristics in experimental conditions. *International Journal for Parasitology* **25** (10), 1173-1177.

Suchitra, S. and Joshi, P. (2005) Characterization of *Haemonchus contortus* calreticulin suggests its role in feeding and immune evasion by the parasite. *Biochimica et Biophysica Acta* **1722**, 293-303.

Suchitra, S., Anbu, K. A., Rathore, D. K., Mahawar, M., Singh, B. P. and Joshi P. (2008) *Haemonchus contortus* calreticulin binds to C-reactive protein of its host, a novel survival strategy of the parasite. *Parasite Immunology* **30**, 371-374.

Suzuki, H., Yanaka, A. and Muto, H. (2000) Luminal ammonia retards restitution of guinea pig injured gastric mucosa in vitro. *American Journal of Physiology Gastrointestinal and Liver Physiology* **279**, G107-G117.

Takagi, H., Jhappan, C., Sharp, R. and Merlino, G. (1992) Hypertrophic gastropathy resembling Ménétrier's disease in transgenic mice overexpressing transforming growth factor alpha in the stomach. *Journal of Clinical Investigation* **90**, 1161-1167.

Takeuchi, K., Speir, G. R. and Johnson, L. R. (1980) Mucosal gastrin receptor. III. Regulation by gastrin. *American Journal of Physiology Gastrointestinal and Liver Physiology* **238**, G135-140.

Takeuchi, Y., Pausawasdi, N. and Todisco, A. (1999) Carbachol activates ERK2 in isolated gastric parietal cells via multiple signaling pathways. *American Journal of Physiology Gastrointestinal and Liver Physiology* **276** (6), G1484-G1492.

Takeuchi, Y., Yamada, J., Yamada, T. and Todisco, A. (1997) Functional role of extracellular signal-regulated protein kinases in gastric acid secretion. *American Journal of Physiology Gastrointestinal and Liver Physiology* **36** (6), G1263-G1272.

Tan, X., Egami, H., Abe, M., Nozawa, F., Hirota, M. and Ogawa, M. (2005) Involvement of MMP-7 in invasion of pancreatic cancer cells through activation of the EGFR mediated MEK-ERK signal transduction pathway. *Journal of Clinical Pathology* **58** (12), 1242-1248.

Tanaka, J., Baba, T. and Torisu, M. (1979) Ascaris and eosinophil. II. Isolation and characterization of eosinophil chemotactic factor and neutrophil chemotactic factor of parasite in Ascaris antigen. *Journal of Immunology* **122**, 302-308.

Tarasova, N. I., Romanov, V. I., Da Silva, P. P. and Michejda, C. J. (1996) Numerous cell targets for gastrin in the guinea pig stomach revealed by gastrin/CCKB receptor localisation. *Cell and Tissue Research* **283**, 1-6.

Tari, A., Wu, V., Sumii, M., Sachs G. and Walsh, J. H. (1991) Regulation of rat gastric H^+/K^+-ATPase α-subunit mRNA by omeprazole. *Biochimica et Biophysica Acta Gene Structure and Expression* **1129** (1), 49-56.

Tashima, K., Zhang, S., Ragasa, R., Nakamura, E., Seo, J. H., Muvaffak, A. and Hagen, S. J. (2009) Hepatocyte growth factor regulates the development of highly pure cultured chief cells from rat stomach by stimulating cell proliferation in vitro. *American Journal of Physiology Gastrointestinal and Liver Physiology* **296**, G319-G329.

Taupin, D. and Podolsky, D. K. (2003) Trefoil factors: initiators of mucosal healing. *Nature Reviews Molecular Cell Biology* **4**, 721-732.

Telford, J. L., Ghiara, P., Dell'Orco, M., Comanducci, M., Burroni, D., Bugnoli, M., Tecce, M. F., Censini, S., Covacci, A., Xiang, Z., Papini, E., Montecucco, C., Parente, L. and Rappuoli, R. (1994) Gene structure of the *Helicobacter pylori* cytotoxin and evidence of its key role in gastric disease. *The Journal of Experimental Medicine* **179**, 1653-1658.

Thangarajah, H., Wong, A., Chow, D. C., Crothers, J. M. Jr. and Forte, J. G. (2002) Gastric H-K-ATPase and acid-resistant surface proteins. *American Journal of Physiology Gastrointestinal and Liver Physiology* **282** (6), G953-961.

Thomas, D. M., Nasim, M. M., Gullick, W. J. and Alison, M. R. (1992) Immunoreactivity of transforming growth factor-alpha in the normal adult gastrointestinal tract. *Gut* **33**, 628-631.

Todisco, A., Pausawasdi, N., Ramamoorthy, S., Del Valle, J., Van Dyke, R. W. and Askari, F. K. (2001) Functional role of protein kinase B/Akt in gastric acid secretion. *Journal of Biological Chemistry* **276** (49), 46436-46444.

Todisco, A., Ramamoorthy, S., Pausawasdi, N. and Tacey, K. (1999) Carbachol activates I kappa B kinase in isolated canine gastric parietal cells. *Biochemical and Biophysical Research Communications* **261** (3), 877-884.

Tortora, G. J. and Grabowski, S. R. (1996) Stomach, in *rivm National Institute for Public Health and the Environment, Interspeciesinfo*, accessed 08 June 2009, from http://www.rivm.nl/interspeciesinfo/intra/human/stomach/

Toubarro, D., Lucena-Robles, M., Nascimento, G., Costa, G., Montiel, R., Coelho, A. V. and Simões, N. (2009) An apoptosis-inducing serine protease secreted by the entomopathogenic nematode *Steinernema carpocapsae*. *International Journal for Parasitology* **39** (12), 1319-1330.

Troutman, M. D. and Thakker, D. R. (2003) Efflux ratio cannot assess P-glycoprotein-mediated attenuation of absorptive transport: asymmetric effect of P-glycoprotein on absorptive and secretory transport across Caco-2 cell monolayers. *Pharmaceutical Research* **20** (8), 1200-1209.

Tsukita, S. and Furuse, M. (1999) Occludin and claudin in tight-junction strands: leading or supporting players? *Trends in Cell Biology* **9**, 268-273.

Tsukita, S., Furuse, M. and Itoh, M. (2001) Multifunctional strands in tight junctions. *Nature Reviews Molecular Cell Biology* **2**, 285-293.

Tsunoda, Y. Funasaka, M., Modlin, I. M., Hidaka, H., Fox, L. M. and Goldenring, J. R. (1992) An inhibitor of Ca2+/calmodulin-dependent protein kinase II, KN-62, inhibits cholinergic-stimulated parietal cell secretion. *American Journal of Physiology Gastrointestinal and Liver Physiology* **262**, 118-122.

Turner, D. G., Wildblood, L. A., Inglis, N. F. and Jones, D. G. (2008) Characterization of a galectin-like activity from the parasitic nematode, *Haemonchus contortus*, which modulates ovine eosinophil migration *in vitro*. *Veterinary Immunology and Immunopathology* **122**, 138-145.

Tyagarajan, K., Forte, J. G. and Townsend, R. R. (1996) Topology of membrane proteins in native membranes using matrix-assisted laser desorption ionisation/mass spectrometry. In *Techniques in protein Chemistry VIII*. (ed. Marshak, D. R.), pp533-542. New York Academic Press.

Tzimas, G. N., Afshar, M., Emadali, A., Chevet, E., Vali, H. and Metrakos, P. P. (2004) Correlation of cell necrosis and tissue calcification with ischemia/reperfusion injury after liver transplantation. *Transplantation Proceedings,* **36**, 1766-1768.

Urushidani, T. and Forte, J. G. (1987) Stimulation-associated redistribution of H^+-K^+-ATPase activity in isolated gastric glands. *American Journal of Physiology Gastrointestinal and Liver Physiology* **252**, G458-G465.

Urushidani, T. and Forte, J. G. (1997) Signal transduction and activation of acid secretion in the parietal cell. *Journal of Membrane Biology* **159**, 99-111.

van Houtert, M. F. J. and Sykes, A. R. (1996) Implications of nutrition for the ability of ruminants to withstand gastrointestinal nematode infections. *International Journal for Parasitology* **26**, 1151-1168.

Van Itallie, C. M. and Anderson, J. M. (2004) The molecular physiology of tight junction pores. *Physiology* **19**, 331-338.

van Wyk, J. A. and Gerber, H. M. (1978) Recovery of nematodes from ruminants by migration from gastrointestinal ingesta and mucosa gelled in agar: preliminary report. *Journal of Veterinary Research* **45**, 29-38.

Vassalli, J.-D., Sappino, A.-P. and Bein, D. (1991) The plasminogen activator/plasmin system. *The Journal of Clinical Investigation* **88**, 1067-1072.

Vergnolle, N. (2005) Clinical relevance of proteinase activated receptors (PARs) in the gut. *Gut* **54**, 867-874.

Vergnolle, N. (2008) Proteinase-activated receptors (PARs) in infection and inflammation in the gut. *The International Journal of Biochemistry and Cell Biology* **40**, 1219–1227.

Vial, J. D., Garrido, J. and González, A. (1985) The early changes of parietal cell structure in the course of secretory activity in the rat. *American Journal of Anatomy* **172**, 291-306.

Viguera, E., Trelles, O., Urdiales, J. L., Matés, J. M., Sánchez-Jiménez, F. (1994) Mammalian L-amino-acid decarboxylases producing 1,4-diamines: analogies among differences. *Trends in Biochemical Sciences* **19** (8), 318-319.

von Herbay, A. and Rudi, J. (2000) Role of apoptosis in gastric epthelial turnover. *Microscopy Research and Technique* **48**, 303-311.

von Samson-Himmelstjerna, G. (2006) Molecular diagnosis of anthelmintic resistance. *Veterinary Parasitology* **136**, 99-107.

Wagner, R. C. and Hossler, F. E. (2009) Tight Junctions, in *Epithelium Ultrastructure*, accessed 21 June 2009, from http://www.udel.edu/biology/Wags/histopage/empage/eep/eep.htm.

Waisbren, S. J., Geibel, J. P., Modlin, I. M., Boron, W. F. (1994) Unusual permeability properties of gastric gland-cells. *Nature* **368** (6469), 332-335.

Walsh, J. H. (1988) Peptides as regulators of gastric acid secretion. *Annual Review of Physiology* **50**, 41-63.

Wan, H., Winton, H. L., Soeller, C., Gruenert, D. C., Thompson, P. J., Cannell, M. B., Stewart, G. A., Garrod, D. R. and Robinson, C. (2000) Quantitative structural and biochemical analysis of tight junction dynamics following exposure of epithelial cells to house dust mite allergen Der p 1. *Clinical and Experimental Allergy* **30**, 385-398.

Wan, H., Winton, H. L., Soeller, C., Tovey, E. R., Gruenert, D. C., Thompson, P. J., Stewart, G. A., Taylor, G. W., Garrod, D. R., Cannell, M. B. and Robinson, C. (1999) Der p 1 facilitates transepithelial allergen delivery by disruption of tight junctions. *The Journal of Clinical Investigation* **104**, 123-133.

Wang, K. S., Komar, A, R., Ma, T., Filiz, F., McLeroy, J., Hoda, K., Verkman, A. S. and Bastidas, J., A. (2000a) Gastric acid secretion in aquaporin-4 knockout mice. *American Journal of Physiology Gastrointestinal and Liver Physiology* **279** (2), G448-G453.

Wang, T. C. and G. J. Dockray (1999) Lessons from genetically engineered animal models. I. Physiological studies with gastrin in transgenic mice. *American Journal of Physiology Gastrointestinal and Liver Physiology* **277**, G6-G11.

Wang, T. C., Dangler, C. A., Chen, D., Goldenring, J. R., Koh, T., Raychowdhury, R., Coffey, R. J., Ito, S., Varro, A., Dockray, G. J. and Fox, J. G. (2000b) Synergistic interaction between hypergastrinemia and *Helicobacter* infection in a mouse model of gastric cancer. *Gastroenterology* **118** (1), 36-47.

Wang, Z., Schultheis, P. J. and Shull, G. E. (1996) Three N-terminal variants of the AE2 Cl^-/HCO_3^- exchanger are encoded by mRNAs transcribed from alternative promoters. *Journal of Biological Chemistry* **271** (13), 7835-7843.

Ward, P. F. V. and Huskisson, N. S. (1978) The energy metabolism of adult *Haemonchus contortus*, *in vitro*. *Parasitology* **77**, 255-271.

Ward, P. F. V., Coadwell, W. J. and Huskisson, N. S. (1981) The glucose metabolism of adult *Ostertagia circumcincta in-vitro*. *Parasitology* **82**, 17-22.

Watson, F., Kiernan, R. S., Deavall, D. G., Varro, A. and Dimaline, R. (2001) Transcriptional activation of the rat vesicular monoamine transporter 2 promoter in gastric epithelial cells. Regulation by gastrin. *Journal of Biological Chemistry* **276** (10), 7661-7671.

Weigert, N., Madaus, S., Alexiou, C., Schepp, W., Li, Y., Coy, D. H., Classen, M. and Schusdziarra, V. (1993) Effect of bombesin antagonist D-Phe6-BN(6-13)OMe on vagally induced gastrin release from perfused rat stomach. *Life Sciences* **52** (8), 725-32.

Weigert, N., Schaffer, K., Schusdziarra, V., Classen, M. and Schepp, W. (1996) Gastrin secretion from primary cultures of rabbit antral G cells: stimulation of inflammatory cytokines. *Gastroenterology* **110**, 147-154.

Weigert, N., Schaffer, K., Wegner, U., Schusdziarra, V., Classen, M. and Schepp, W (1994) Functional characterization of a muscarinic receptor stimulating gastrin release from rabbit antral G-cells in primary culture. *European Journal of Pharmacology* **264** (3), 337-344.

Werther, J. L. (2000) The gastric mucosal barrier. *The Mount Sinai Journal of Medicine* **67** (1), 41-53.

Wessler, S. and Backert, S. (2008) Molecular mechanisms of epithelial-barrier disruption by *Helicobacter pylori*. *Trends in Microbiology* **16** (8), 397-405.

Wildblood, L. A., Kerr, K., Clark, D. A. S., Cameron, A., Turner, D. G. and Jones, D. G. (2005) Production of eosinophil chemotracttant activity by ovine gastrointestinal nematodes. *Veterinary Immunology and Immunopathology* **107**, 57-65.

Williamson, A. L., Brindley, P. J., Knox, D. P., Hotez, P. J. and Loukas, A. (2003) Digestive proteases of blood-feeding nematodes. *Trends in Parasitology* **19** (9), 417-423.

Williamson, A. L., Lecchi, P., Turk, B. E., Choe, Y., Hotez, P. J., McKerrow, J. H., Cantley, L. C., Sajid, M., Craik, C. S. and Loukas, A. (2004) A Multi-enzyme cascade of hemoglobin proteolysis in the intestine of blood-feeding hookworms. *The Journal of Biological Chemistry* **279** (34), 35950-35957.

Wolfe, M. M. and Reel, G. M. (1986) Inhibition of gastrin release by gastric inhibitory peptide mediated by somatostatin. *American Journal of Physiology Gastrointestinal and Liver Physiology* **250**, G331-G335.

Wolfe, M. M., Reel, G. M. and McGuigan, J. E. (1983) Inhibition of gastrin release by secretin is mediated by somatostatin in cultured rat antral mucosa. *Journal of Clinical Investigation* **72** (5), 1586-1593.

Wolstenholme, A. J., Fairweather, I., Prichard, R., von Samson-Himmelstjerna, G. and Sangster, N. C. (2004) Drug resistance in veterinary helminths. *Trends in Parasitology* **20** (10), 469-476.

Wong, D. T., Weller, P. F., Galli, S. J., Elovic, A., Rand, T. H., Gallagher, G. T., Chiang, T., Chou, M. Y., Matossian, K. and McBride, J. (1990) Human eosinophils express transforming growth factor alpha. *Journal of Experimental Medicine* **172**, 673-681.

Wroblewski, L. E., Shen, L., Ogden, S., Romero-Gallo, J., Lapierre, L. A., Israel, D. A., Turner, J. R. and Peek, R. M. Jr. (2009) *Helicobacter pylori* dysregulation of gastric epithelial tight junctions by urease-mediated myosin II activation. *Gastroenterology* **136**, 236-246.

Yamada, J., Andrén, A., Kitamura, N. and Yamashita, T. (1988) Electron immunocytochemical co-localization of prochymosin and pepsinogen in chief cells, mucous neck cells and transitional mucous neck/chief cells of the calf fundic glands. *Acta Anatomica* **132**, 246-252.

Yao, X. and Forte, J. G. (2003) Cell biology of acid secretion by the parietal cell. *Annual Review of Physiology* **65**, 103-131.

Yasunaga, Y., Shinomura, Y., Kanayama, S., Higashimoto, Y., Yabu, M., Miyazaki, Y., Murayama, Y., Nishibayashi, H., Kitamura, S. and Matsuzawa, Y. (1997) Mucosal interleukin-1 beta production and acid secretion in enlarged fold gastritis. *Alimentary Pharmacology and Therapeutics* **11** (4), 801-809.

Yasunaga, Y., Shinomura, Y., Kanayama, S., Higashimoto, Y., Yabu, M., Miyazaki, Y., Kondo, S., Murayama, Y., Nishibayashi, H., Kitamura, S. and Matsuzawa, Y. (1996) Increased production of interleukin 1 beta and hepatocyte growth factor may contribute to foveolar hyperplasia in enlarged fold gastritis. *Gut* **39** (6), 787-794.

Yatsuda, A. P., Bakker, N., Krijgsveld, J., Knox, D. P., Heck, A. J. R. and de Vries, E. (2006) Identification of secreted cysteine proteases from the parasitic nematode *Haemonchus contortus* detected by biotinylated inhibitors. *Infection and Immunity* **74** (3), 1989-1993.

Yatsuda, A. P., Krijgsveld, J., Cornelissen, A. W. C. A., Heck, A. J. R. and de Vries, E. (2003) Comprehensive analysis of the secreted proteins of the parasite *Haemonchus contortus* reveals extensive sequence variation and differential immune recognition. *The Journal of Biological Chemistry* **278** (19), 16941-16951.

Yepiz-Plascencia, G., Jiménez-Vega, F., Romo-Figueroa, M. G., Sotelo-Mundo, R. R. and Vargas-Albores, F. (2002) Molecular characterization of the bifunctional VHDL-CP from the hemolymph of white shrimp *Penaeus vannamei*. *Comparative Biochemistry and Physiology* **Part B 132**, 585-592.

Yu, D. and Turner, R. (2008) Stimulus-induced reorganization of tight junction structure: the role of membrane traffic. *Biochimica et Biophysica Acta* **1778**, 709-716.

Zaborina, O., Misra, N., Kostal, J., Kamath, S., Kapatral, V., El-Azami El-Idrissi, M., Prabhakar, B. S. and Chakrabarty, A. M. (1999) P2Z-independent and P2Z receptor-mediated macrophage killing by *Pseudomonas aeruginosa* isolated from cystic fibrosis patients. *Infection and Immunity* **67** (10), 5231-5242.

Zeng, N., Walsh, J. H., Kang, T., Helander, K. G., Helander, H. F. and Sachs, G. (1996) Selective ligand-induced intracellular calcium changes in a population of rat isolated gastric endocrine cells. *Gastroenterology* **110** (6), 1835-1846.

Zhang, L., Seiffert, D., Fowler, B. J., Jenkins, G. R., Thinnes, T. C., Loskutoff, D. J., Parmer, R. J. and Miles, L. A. (2002) Plasminogen has a broad extrahepatic distribution. *Thrombosis and Haemostasis* **8** (3), 493-501.

Zick, Y., Eisenstein, M., Goren, R. A., Hadari, Y. R., Levy, Y. and Ronen, D. (2004) Role of galectin-8 as a modulator of cell adhesion and cell growth. *Glycoconjugate Journal* **19**, 517-526.

Appendix I: Parasitology

1.1 Animals

Between two and four month of age male sheep (Romney and Romney-cross; Massey sheep farm) were brought inside a shed and kept in pens of up to six animals, fed chaff and water *ad libitum* and cleaned once daily. A parasite-free stage (before experimental single infections) was reached by a double dose (1ml/5kg, calculated with the weight of the heaviest animal in the group) of Matrix (Ancare, New Zealand) followed by a single dose (1ml/10kg) of Matrix two days later. The parasite-free stage was controlled via faecal egg count (FEC) (1.2).

1.2 FEC

A modification of the McMaster technique (modified by Stafford *et al.*, 1994) was used. The collected faecal sample from the sheep (2g for quantification) was placed in a small sieve in a scale pan. 30ml saturated sodium chloride (universal glass filled) was poured over the faecal sample, which was mashed, submerged in the salt solution, with a pestle. The sieve with the large detritus left behind was discarded then. For qualification, the float method was used: the salt solution/faecal mix was poured back into the universal glass and a coverslip placed on top on which any eggs present in the faecal sample will stick to after floatation. After 10min, the coverslip was placed onto a slide and the sample examined for any eggs. For quantification, both sides of the McMaster slide were filled with the salt solution/faecal mix and the number of eggs within the grids was counted. The total number was multiplied by 50 to get the eggs per gram of faeces (e.p.g.).

1.3 Infections

Once the sheep were parasite-free and free of drench residues (five weeks after drench with Matrix for *H. contortus* infection and four weeks for *T. circumcincta*) they were infected. After counting (100µl in 0.5ml iodine), the desired number was taken out from the *H. contortus* (approximately 10,000 L_3) or *T. circumcincta* (approximately 50,000 L_3) larval culture stock and sheep were infected orally via syringe.

1.4 Labelling of *H. contortus*

1.4.1 Solutions

Hoechst 33258 (stock solution 2mM)

1.068mg/ml were diluted in MilliQ water. The stock solution was stored in 1ml aliquots at -20°C.

Nile Red

For a stock solution 0.5mg/ml Nile Red was dissolved in Acetone. The working solution was a 1:100 dilution in PBS.

1.5 ES Preparations of Adult *H. contortus* and *T. circumcincta*

1.5.1 Solutions

Saline 0.9%

18g NaCl were diluted in a final Volume of 2l in MilliQ water. The solution was warmed to 37°C and used directly.

Agar 3%

3% agar was made up in 0.9% saline. 1l was heated for 8min in the microwave (high power) and kept warm in a water bath at 45°C (prior to use).

Phosphate Buffered Saline (PBS)

4.0g NaCl

0.2g KCl

0.575g Na_2HPO_4

0.1g KH_2PO_4

Made up in 500ml of MilliQ water and adjusted to pH 7.2 before sterilised by autoclaving. PBS in use was kept at 4°C for a maximum of four weeks.

1.5.2 Method

Sheep were killed 21 (*H. contortus*) or 28 days (*T. circumcincta*) after infection with L_3 using a captive bolt pistol followed by exsanguination. The abdomen was opened and the abomasum tied off at both ends and removed from the animal. Adult worms were collected from the abomasum using a slightly altered technique described by Simpson *et al.* (1999), which was modified from van Wyk and Gerber (1978). The abomasum was cut open along its greater curvature and washed with 0.9% saline (37°C). The abomasal contents and washings were collected and mixed 2:1 (v/v) with 3% agar (37°C). This mixture was poured in a thin layer (~1cm high) into plastic trays and after the agar set overlaid with 0.9% saline (37°C) and incubated 10-30min in a 37°C room in the dark until the worms migrated out of the agar into the saline.

Worms, most of them aggregated, were then carefully picked with forceps. 53mg/ml (Huber *et al.*, 2005) *H. contortus* were incubated for 12h in cell culture media (CEM, F12-Hams, D10; composition see Appendix II/Cell Culture) or PBS (15ml and 50ml tubes or T75 cell culture flask) in an incubator in an atmosphere containing 5% CO_2 and 95% humidified air at 37°C.

1.6 Larval Culture Stock

For the maintenance of larval culture stocks, sheep were regularly infected with either *H. contortus* or *T. circumcincta*. Their faeces were collected each into a bag that was attached to a harness. The presence of nematode eggs in the faeces was monitored from day 18 p.i for both *H. contortus* and *T. circumcincta* infections by FEC (qualification/float method, 1.2). Once present, FECs (quantification/McMaster slide, 1.2) were carried out and feaces collected once there were more than 200 e.p.g present. Feaces were placed in trays, moistened and mixed with vermiculite. The trays were covered with glass plates and incubated in a warm room (27 to 28°C) for 10 to 14 days for both *H. contortus* and *T. circumcincta*. The mixture was kept moist and turned over twice during the incubation. Larvae were harvested using a modified Baermann technique (Baermann, 1917): the faeces mixture was placed into a sieve lined with tissue and the sieve was put into a tray filled with RO water leading to L_3 entering the RO water. After 24h, the RO water containing the larvae was placed into another sieve lined with tissue on top of a funnel attached to a short tube with a closable end where the larvae were collected after another 24h. *H. contortus* larvae were stored at 10°C, and *T. circumcincta* at 4°C, in RO water in culture flasks.

Appendix II: Cell Culture

2.1 Cell Culture Media and Solutions

Complete Essential Medium (CEM)

74ml autoclaved MilliQ water
10ml FBS
10ml MEM 10x liquid
3ml $NaHCO_3$
1ml PSN 100x liquid
1ml Non-essential amino acids solution 100x liquid
1ml Glutamax

The pH was adjusted with 1M HCl or 0.1M NaOH to 7.4 if it was necessary. CEM was kept for a maximum of 10 days at 4°C.

F12-Hams

100ml F12-Hams media were supplemented with 10ml FBS and 1ml PSN 100x liquid. The pH was adjusted with 1M HCl or 0.1M NaOH to 7.4 if it was necessary. F12-Hams was kept for a maximum of 10 days at 4°C.

D10 (DMEM + 10%FBS)

84ml DMEM 1x liquid
10ml FBS
3ml $NaHCO_3$
1ml PSN 100x liquid
1ml Non-essential amino acids solution 100x liquid
1ml Glutamax

The pH was adjusted with 1M HCl or 0.1M NaOH to 7.4 if it was necessary. D10 was kept for a maximum of 10 days at 4°C.

PSN (Penicillin-Streptomycin-Neomycin)

PSN 100x liquid was divided into 1ml aliquots, which were stored at -20°C.

FBS

FBS was thawed at 37°C, aliquot at 10ml and stored at -20°C then.

Sodium Bicarbonate (7.5%)

15g $NaHCO_3$ were diluted in 200ml MilliQ water and sterilised by filtration through a 0.2µm filter. The solution was stored at 4°C.

HCl 1M

Concentrated HCl was diluted with MilliQ water and sterilised by filtration through a 0.2µm filter.

NaOH 0.1M

0.4g were diluted in 100ml MilliQ water, sterilised by filtration through a 0.2µm filter.

Trypsin-Versene

0.02% EDTA

0.25% Trypsin

The solution was made up in 0.9% saline and sterilised by filtration through a 0.2µm filter and was stored at -20°C in 10ml aliquots.

Ammonium chloride 1M

0.53g was diluted in a final volume of 10ml in MilliQ water. The solution was kept at 4°C.

Prostaglandins

PGA_2 and PGB_2 were delivered as 1mg in 100ml methylacetate. PGD_2, $PGF_{2\alpha}$ and PGE_2 were dissolved as 1mg/ml in ethanol.

Proteinase K

A 1mg/ml stock solution was prepared in MilliQ water and sterile filtered (0.2µm syringe filter). The solution was stored at 4°C.

Paraformaldehyde 4%

4g paraformaldehyde were diluted in 80ml MilliQ water and carefully heated at ~60°C for 30-60min. 10µl aliquots of 1M NaOH were added with stirring until the solution cleared. After cooling to room temperature, the solution was filtered through a 0.2µm filter and was made up to the final volume of 100ml. The pH was adjusted to 7.4 to 7.6. The solution was kept for a maximum of two weeks at 4°C or stored in aliquots at -20°C.

Hoechst 33258 (stock solution 2mM)

1.068mg/ml were diluted in MilliQ water. The stock solution was stored in 1ml aliquots at -20°C.

Alexa Fluor Phalloidin (stock solution 200units/ml)

The vial contents were dissolved in 1.5ml methanol. The stock solution was stored at -20°C.

2.2 HeLa Cell Passage

Cells were grown in 75cm^2 cell culture flasks and split every two to five days when they reached ~80% confluency. The supernatant of CEM was removed and the cells were washed twice with 10ml PBS. 2ml of Trypsin-versene was added and the cells were incubated for 2 to 5min in an incubator in an atmosphere containing 5% CO_2 and 95% humidified air at 37°C until the cells were detaching from the cell culture flask (sometimes supported by gently rocking the flask if it was necessary). After that, 8ml CEM was added to neutralise the trypsin. For normal culture, the desired amount (split ratio 1:5 to 1:10) were then placed into the new flask containing 15ml CEM and cultivated in an incubator in an atmosphere containing 5% CO_2 and 95% humidified air at 37°C.

For experiments, the cell solution was centrifuged (20°C, 5min, 1000rpm) and the medium discarded to a volume of 1ml. Then, the cells were counted in a hemocytometer (Neubauer counting chamber), seeded at 10,000 cells/ml on autoclaved coverslips (in a petri dish) and incubated for 48h in an incubator in an atmosphere containing 5% CO_2 and 95% humidified air at 37°C before they were used for experimental incubations.

For the cell proliferation assay, cells were seeded in wells of 24 and 96 well plates and allowed to attach for 6h before they were used for experimental incubations.

2.3 AGS Cell Passage

AGS cell passage was followed the same protocol as for HeLa cells (2.2). Instead of CEM, F12-Hams medium was used and the cells were usually split at a ratio of 1:5 to 1:10 every 2 to 5 days.

For experiments, cells were counted and seeded at 20,000 cells/ml on autoclaved coverslips and for the cell proliferation assay in wells of a 96 well plate with the same attaching periods like HeLa cells.

2.4 CaCo-2 Cell Passage

CaCo-2 cell passage followed the same protocol as for HeLa cells (2.2) but D10 medium was used. Cells were split at a ratio of 1:5 to 1:10 when they were ~80% confluent (~6-10days). The medium was changed once per week for the longer incubation periods. For experiments, they were seeded in transwell plates (12 wells per plate).

2.5 Cryopreservation of Cells

The same protocol as for the cell passage was used. After counting, the cells they were resuspended at $2x10^6$ cells/ml in adequate medium containing 5% DMSO. The cryocups were placed in "Mr. Frosty" (Nalgene) for 2 days at -80°C before they were put into liquid nitrogen.

2.6 Thawing of Cryopreserved Cells

After warming the cryocup (out of the liquid nitrogen tank) in a 37°C water bath, the cell suspension was transferred to a final volume of 10ml in cell culture medium and centrifuged for 5min at 1000rpm (at 20°C), the supernatant was discarded. The cell pellet was resuspended in 10ml cell culture medium and transferred into a cell culture flask with a final volume of 15ml medium. Cell culture medium was changed after 24h and the cells were split the next time at ~80% confluence.

Appendix III: Gel Electrophoresis

3.1 SDS-PAGE

3.1.1 Solutions

All solutions were kept at 4°C unless stated otherwise.

Acrylogel 30%

40% acrylogel was diluted to 30% by diluting 15ml of 40% solution with 5ml MilliQ water.

Tris 1.5M, pH 8.8

100ml were made up of 18.165g Tris in MilliQ water and the pH was adjusted to 8.8 then; filtered through Whatman No.1 filter.

SDS 10% (w/v)

3.5g SDS were diluted to a final volume of 35ml MilliQ water. The solution was filtered through a 0.2µm filter and stored at room temperature.

Tris 1M, pH 6.8

10ml were made up of 1.211g Tris in MilliQ water and the pH was adjusted to 6.8; filtered through Whatman No.1 filter.

Ammonium persulfate 10% (w/v)

0.1g was dissolved in 1ml MilliQ water (prior to use), kept for a maximum time of five days.

SDS Gel Loading Buffer (4x)

200mM	≙	6.055g	Tris HCl
8%	≙	2g	SDS
24%	≙	6ml	Glycerol
4%	≙	1ml	β-Mercaptoethanol
0.016%	≙	0.004g	Bromphenolblue

The solution was made up to 25ml of MilliQ water, filtered through a 0.2µm filter and the pH adjusted to 6.8. The solution was stored at room temperature.

Tris-Glycine Electrophoresis Buffer (5x)

125mM	≙	7.5686g	Tris
1250mM	≙	46.9375g	Glycine
0.5% SDS	≙	25ml	SDS 10% solution

Made up to a final volume of 500ml. The pH was adjusted to 8.3; filtered through Whatman No.1 filter.

3.1.2 Gel Composition

5-20% Gradient-Gels (size range ~10-200kDa) were prepared (using gel electrophoresis device 73.1010V, Apollo; gradient mixer GM-40, C.B.S. Scientific; peristaltic pump Mini Pulse 3, Gilson):

	5% [ml]	20% [ml]
MilliQ water	2.8	0.3
30% Acrylogel	0.8	3.3
1.5M Tris (pH 8.8)	1.3	1.3
10% SDS	0.05	0.05
10 % Ammoniumpersulfate	0.05	0.05
TEMED	0.004	0.001

On top of the resolving gel a 4% stacking gel was poured:

	4% [ml]
MilliQ water	1.178
30% Acrylogel	0.53
1M Tris (pH 6.8)	0.25
10% SDS	0.02
10 % Ammoniumpersulfate	0.02
TEMED	0.002

For the detection of lipids with Sudan Black staining 20% gels were also used:

	20% [ml]
MilliQ water	0.6
30% Acrylogel	6.6
1.5M Tris (pH 8.8)	2.6
10% SDS	0.1
TEMED	0.1
10 % Ammoniumpersulfate	0.002

3.2 BN-PAGE

3.2.1 Solutions

All solutions were kept at 4°C unless stated otherwise.

Acrylogel 30%

See above (3.1.1)

Ammonium persulfate 10% (w/v)

See above (3.1.1)

Resolving-Gel Buffer (4x)

2M ≙ 26.236g 6-Aminocaproic acid

200mM ≙ 2.422g Tris

Made up to 100ml of MilliQ water and adjusted to pH 7, filtered through Whatman No.1 filter.

Cathode Buffer (5x)

50mM ≙ 44.7925g Tricine

15mM ≙ 9.0825g Tris

0.02% ≙ 1g Coomassie Brilliant Blue G250

Made up to 1l of MilliQ water, adjusted to pH 7 with 6M HCl and filtered through a Whatman No.1 filter.

Anode Buffer (5x)

50mM ≙ 24.22g Tris

Made up to 1l of MilliQ water and adjusted to pH 7 with 6M HCl, filtered through Whatman No.1 filter.

Sample Buffer (3.5x)

750mM ≙ 1.9677g 6-Aminocaproic acid

50mM ≙ 0.1211g Tris

1.25% ≙ 0.25g Dodecylmaltoside

0.35% ≙ 0.07g Coomassie Brilliant Blue G250

Made up in 6ml of MilliQ water, adjusted to pH 7 and filtered through a 0.2µm syringe filter.

3.2.2 Gel Composition

5-20% gradients gels were prepared:

	5% [ml]	20% [ml]
MilliQ water	2.85	0.35
30% Acrylogel	0.8	3.3
4x Resolving Gel Buffer	1.3	1.3
10 % Ammoniumpersulfate	0.05	0.05
TEMED	0.004	0.001

On top of the resolving gel a 4% stacking gel was poured:

	4% [ml]
MilliQ water	1.198
30% Acrylogel	0.53
4x Resolving Gel Buffer	0.25
10 % Ammoniumpersulfate	0.02
TEMED	0.002

Gels were stained after a complete destain in destaining solution.

Destaining Solution

45% Methanol/10% acetic acid in MilliQ water (prior to use).

3.3 Gel Staining Methods

3.3.1 Coomassie Brilliant Blue

3.3.1.1 Solutions

Staining Solution

100ml were made up of 0.25g Coomassie Brilliant Blue G250 dissolved in 90ml of methanol : MilliQ water (1:1 v/v) and 10ml acetic acid. The solution was filtered through a Whatman No. 1 filter.

Destaining Solution

100ml were made up of 90ml methanol : MilliQ water (1:1 v/v) and 10ml acetic acid. The solutions were made up prior to use.

3.3.1.2 Method

The gels were stained in staining solution containing Coomassie Brilliant Blue G250 for 4h at room temperature before they were destained in destaining solution with several solution changes, kept in MilliQ water and photographed with a Canon Power Shot G1 digital camera on a light box.

3.3.2 Silver Staining

3.3.2.1 Solutions

Fixative I

45% ethanol/10% acetic acid made up in MilliQ water (prior to use).

Fixative II

40% ethanol/10% acetic acid made up in MilliQ water (prior to use).

0.1% Silver Nitrate

The solution was made up prior to use in MilliQ water

3% Sodium Carbonate/0.5% Formaldehyde

The solution was made up prior to use in MilliQ water.

Stop solution

1% acetic acid in MilliQ water made up prior to use.

Farmer's Reducer

0.3% sodium thiosulfate, 0.15% potassium ferricyanide, 0.05% sodium carbonate made up in MilliQ water (prior to use).

3.3.2.2 Method

Alternatively, for a more sensitive stain gels were stained with silver. They were fixed in fixative I (1h) and II (2x 30min) followed by a 2x 20min wash in MilliQ water. Then, the gels were stained with silvernitrate for 30min, washed for 2x 20s before they were developed in sodium carbonate/formaldehyde. This process was stopped with 1% acetic acid. After a 5min wash in MilliQ water, Farmers Reducer was added to clear the background. This was stopped again with 1% acetic acid. Gels were stored in MilliQ water until photographing.

3.3.3 Modified Carbohydrate Silver Staining

3.3.3.1 Solutions

Fixative

30% ethanol/10% acetic acid made up in MilliQ water (prior to use).

0.7% Periodic Acid in Fixative

The solution was made up prior to use.

0.1% Silver Nitrate

see above (3.3.2)

3% Sodium Carbonate/0.02% Formaldehyde

The solution was made up prior to use in MilliQ water.

Farmer's Reducer

See above (3.3.2)

Stop solution

See above (3.3.2)

3.3.3.2 Method

Gels were also stained with a modified silver stain, staining proteins and carbohydrates (Kittelberger and Hilbink, 1993; Harrison *et al.*, 2003): the gel was fixed overnight in 30% ethanol/10% acetic acid, then oxidised in 0.7% periodic acid in fixative (30% ethanol/10% acetic acid) for 10min, followed by a three times wash in MilliQ water for 10min each. Then, the gel was stained with 0.1% silver nitrate for 30min, washed one time in MilliQ water (10s) and the staining developed with 3% sodium carbonate/0.002% formaldehyde for 20min. This reaction was stopped by a five minute incubation with 1% acetic acid. The gel was washed again three times for 10min with MilliQ water, reduced for 10 to 30s with Farmer's reducer and then washed another three times for 10min with MilliQ water. The staining/developing/reduction cycle was repeated a second time and the gel was then stored in 7% acetic acid until photographing.

3.3.4 Sudan Black

3.3.4.1 Solutions

Sudan Black Staining Solution

500mg Sudan Black were dissolved in 20ml acetone. This was added to 15ml of acetic acid, and then added to 85ml of MilliQ water. This mixture was stirred for 30min and then centrifuged to remove any precipitate.

Destaining Solution

37.5ml	Acetic acid
50ml	Acetone
162.5ml	MilliQ water

3.3.4.2 Method

Sudan Black staining was performed for detecting lipids following the suppliers protocol. The gels were placed overnight in Sudan Black staining solution and destained in three changes of Sudan Black destaining solution, kept at 4°C in MilliQ water until photographing. For a pre-stain of the samples 6µl of a sudan black staining solution (20% in ethylene glycol) were added and the samples were incubated for 1½h before loading onto the gel (Yepiz-Plascencia *et al.*, 2002).

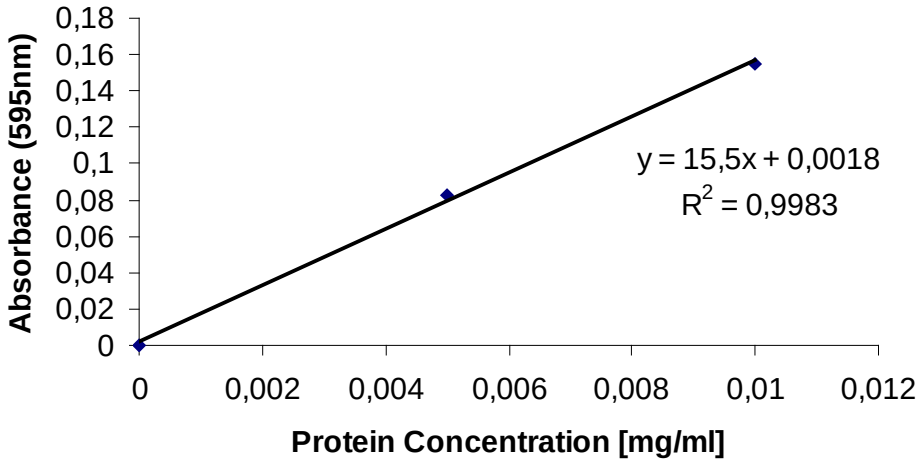

Figure IV.1: Bradford assay standard curve with BSA.

Appendix IV: Assays

4.1 Bradford Assay

The samples were set up in triplicate and measured (6505 UV/Vis Spectrophotometer, Jenway) in acryl cuvettes against the blank:

Blank	0.4ml MilliQ water
Standard solutions	0.4ml 0.005mg/ml to 0.1mg/ml BSA in MilliQ water
Samples	0.4ml ES/Ct preparation (undiluted or dilutions in MilliQ water)

1.6ml Bradford reagent were added to each sample including the blank, mixed and incubated for 10min. The absorbance was read at 595nm against the blank. To estimate the protein concentration a standard curve was constructed (Figure IV.1).

4.2 Ammonia Assay

4.2.1 Solutions

Phenol Nitroprusside Reagent

0.017g nitroprusside was diluted in 25ml MilliQ water, 3.5g phenol were added and the solution was made up to 50ml. The solution was stored at room temperature in the dark.

Hypochlorite Reagent

1.48g NaOH were diluted in 70ml MilliQ water, 14.87g Na_2HPO_4•12 H_2O were added and 8.3ml of a 5% NaOCl solution. The volume was made up to 100ml. The solution was stored at room temperature in the dark.

Facing page 206

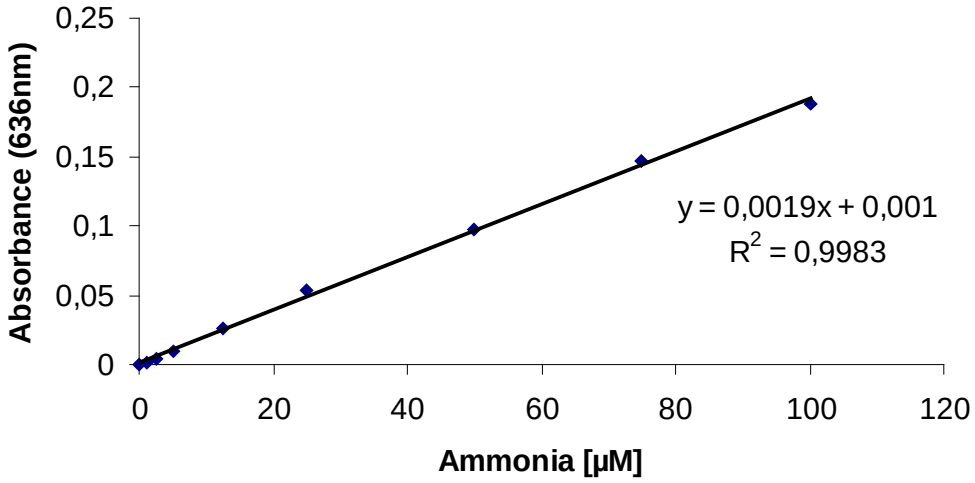

Figure IV.2: Ammonia assay standard curve.

4.2.2 Method

A standard curve was produced using NH_4Cl standard solutions of 0, 1.25, 2.5, 5, 12.5, 25, 50, 75 and 100µM in MilliQ water (Figure IV.2). If necessary the pH of the samples was adjusted to near 7. Then, 50µl phenol nitroprusside reagent and 100µl hypochlorite reagent were added to 0.5ml sample and the tube mixed immediately. The samples were heated in a 50°C water bath for 30min and the absorbance read at 636nm against an appropriate blank.

Appendix V: Histochemistry

5.1 Solutions

2% Calcium acetate

The 2% calcium acetate solution was made up in MilliQ water and stored at 4°C.

Carnoy's Fluid

Carnoy's fluid was made up of ethanol, chloroform and acetic acid in a ratio 6:3:1 and was kept at room temperature in the fume hood.

Ethanol

The different ethanol concentrations (90%, 70%, 40%) were made up by diluting 95% ethanol with MilliQ water.

Blocking Buffer

1g BSA was diluted in 100ml PBS, aliquot at 5ml and stored at -20°C. Goat serum at a concentration of 2% was added prior to use.

Sodiumborohydride

1mg/ml made up in MilliQ water (on ice, prior to use).

H^+/K^+-ATPase

A stock of a 1:100 dilution in PBS was stored in aliquots at -20°C. This stock solution was diluted with blocking buffer to a working concentration of 1:2000 every time prior to use.

Label

The H^+/K^+-ATPase antibody was labelled with the Zenon® Alexa Fluor® 488 Mouse IgG_1 labelling Kit following the suppliers protocol every time prior to use. As the

concentration of the H^+/K^+-ATPase antibody was not available, the best ratio for the label was found to be 10µl of the 1:100 solution of H^+/K^+-ATPase antibody labelled with 5µl of the label (for 5min); the reaction was then stopped by adding 5µl of the blocking solution. To get a final concentration of 1:2000 of H^+/K^+-ATPase antibody 180µl blocking buffer were added.

TGF-α

The antibody was stored at 4°C and was diluted 1:100 (≙ 1µg/ml) with blocking buffer every time prior to use .

Occludin

The antibody (0.5mg/ml) was aliquoted at 5µl and stored at -20°C. Before use 995µl blocking buffer were added to get a final concentration of 1:200 (2.5µg/ml).

ZO-1

The antibody (0.25mg/ml) was aliquoted at 10µl and stored at -20°C. Before use 990µl blocking buffer were added to get a final concentration of 1:100 (2.5µg/ml).

2nd Antibody, fluorescent

The biotinylated goat anti-mouse IgG [2mg/ml] was diluted 1:20 and then stored in 100µl aliquots at -20°C. For use, it was diluted with blocking buffer to a final concentration of 1µg/ml.

Streptavidin

The streptavidin Alexa Fluor® 546 conjugate was dissolved in PBS at a concentration of 1mg/ml. A 1:10 stock solution was prepared and stored in 100µl aliquots at -20°C. For use, it was diluted with blocking buffer to a final concentration of 1 µg/ml.

Lectins: DBA, SBA, PNA, UEA

A 1mg/ml stock solution of each lectin was prepared with sterilised MilliQ water and they were stored at 4°C. Stock solutions were diluted with PBS to a final concentration of 7.5µg/ml.

Appendix VI: Chemicals

6-Aminocaproic acid	Sigma
Acetic acid	Riedel de-Haën
Acetone	Merck
Acrylogel (40% Acrylamide)	BDH
Agar	Sigma
Alexa Fluor® 488 goat anti-rabbit IgG	Invitrogen (Molecular Probes)
Alexa Fluor® Phalloidin 488	Invitrogen (Molecular Probes)
Ammonium chloride	BDH
Ammonium persulfate	Sigma
Anti-H^+/ K^+-ATPase β Antibody (host: mouse)	Affinity BioReagents
Anti-Occludin Antibody (host: mouse; Zymed®)	Invitrogen (Molecular Probes)
Anti-TGF-α Antibody (host: mouse)	Calbiochem
Anti-ZO-1 Antibody (host: rabbit; Zymed®)	Invitrogen (Molecular Probes)
Aprotonin from bovine lung	Sigma-Aldrich
Biotin-XX goat anti-mouse Antibody	Invitrogen (Molecular Probes)
Bradford Reagent	Sigma
Bromphenolblue	Sigma
BSA liquid	New England Biolabs
BSA powder	Boehringer
Calcium acetate	Aldrich
Calcium chloride	BDH
Chloroform	Univar
Coomassie Brilliant Blue G250	Fluka
CyQUANT® NF Cell Proliferation Assay Kit	Invitrogen
DMSO	Sigma
DMEM	Gibco
Dodecylmaltoside	Sigma
EDTA	Sigma

Entellan	Merck
Ethanol 95%	Massey Chem Store
absolute	Merck
Ethyl acetate	Fluka
F12-Hams media	Sigma, Gibco
FBS	Gibco
Formaldehyde	Aldrich
Glutamax™ (100x)	Gibco
Glycerol	Sigma
Glycine	Sigma
Goat serum	Invitrogen
HCl	BDH
Hoechst 33258	Sigma
Iodine	Sigma
Isopropanol	BDH
KCl	Sigma
KH_2PO_4	Ajax Chemicals
Lectins (DBA, SBA, PNA, UEA)	Vector Laboratories
Mayer's Hematoxylin	Sigma
MEM	Gibco
MEM Non-essential amino acids solution	Gibco
Methanol	Massey Chem Store
Na_2HPO_4	Pancreac Quimica
NaCl	Sigma
$NaHCO_3$	Merck
NaOH	BDH
Neutral red	Sigma
Nile Red	Sigma
Nitroprusside	Sigma
Pre-stained protein molecular weight standard (Novex Sharp)	Invitrogen
Paraformaldehyde	BDH
Penicillin-Streptomycin-Neomycin (PSN)	Gibco

Periodic acid	Sigma
pH standards (IUPAC, pH 10.012/7.00/4.00)	Radiometer analytical
Phosphatase inhibitor cocktail	Sigma
Phosphomolybdic acid	Sigma-Aldrich
Potasium ferricyanide	Sigma
Prostaglandins	Cayman Chemical
Protease inhibitor cocktail	Sigma
Protein molecular weight marker, broad range	Sigma
Proteinase K	Sigma
SDS	BDH
Silica gel 60 ADAMANT on TLC plates (glass)	Fluka
Silver nitrate	Sigma
Sodium borohydride	Sigma-Aldrich
Sodium carbonate	BDH
Sodium hypochloride	Sigma-Aldrich
Sodium thiosulfate	M&B Laboratory Chemicals
Streptavidin Alexa Fluor® 546 conjugate	Invitrogen (Molecular Probes)
Sudan Black	Sigma
Syto® 17	Invitrogen (Molecular Probes)
TEMED	Sigma
Tricine	Sigma
Triton-X-100	BDH, Sigma
Trizma Base (Tris)	Sigma
Trypsin	Sigma
Trypsin inhibitor from *Glycine max* (soybean)	Sigma
Xylene	Merck
Zenon® Mouse IgG labelling Kit	Invitrogen (Molecular Probes)
β-Galactosidase from *Escherichia coli*	Sigma
β-Mercaptoethanol	Merck